

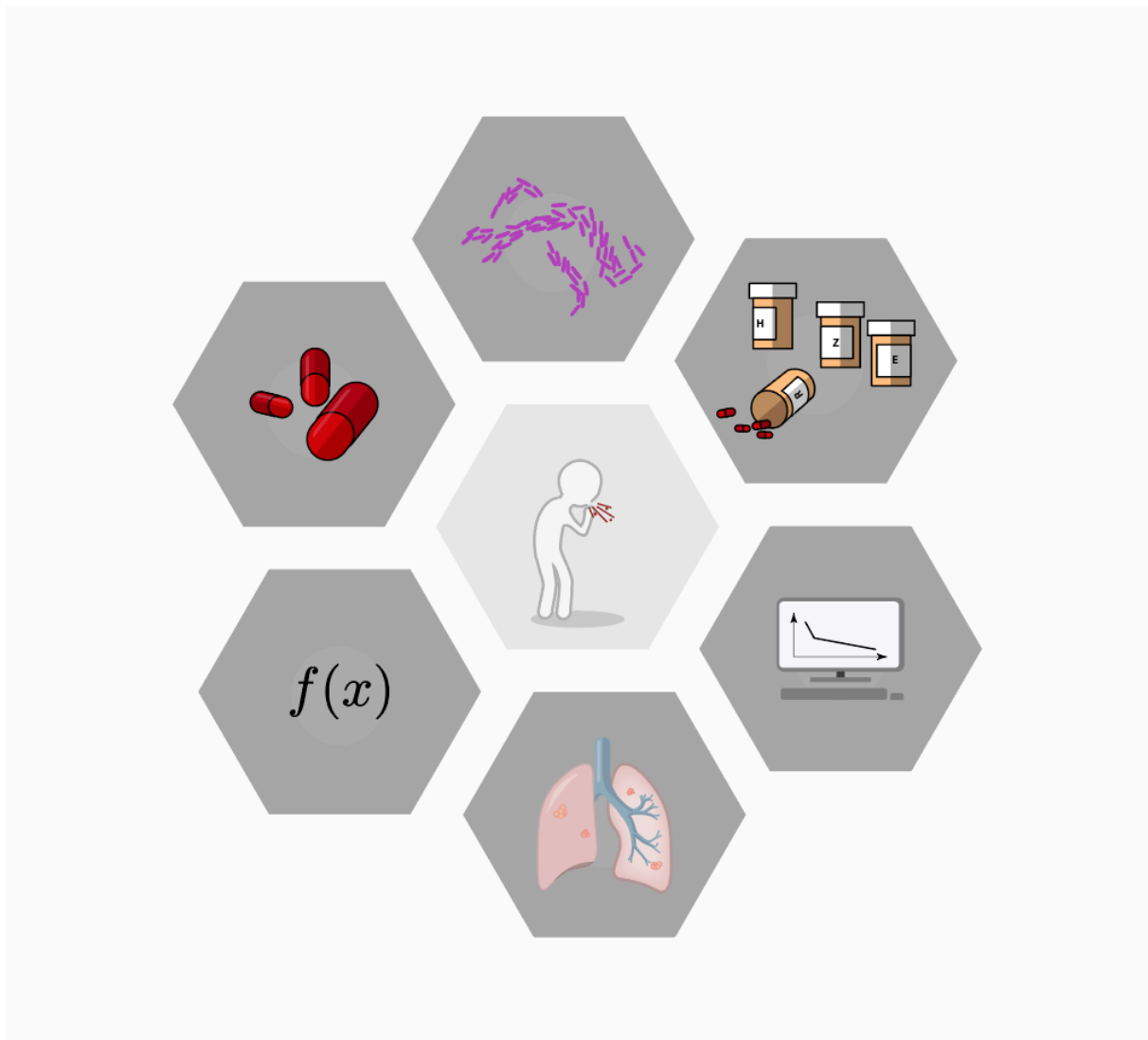


Faculty of Health Sciences, Department of Pharmacy

Mathematical Models of Optimal Antibiotic Treatment

Antal Martinecz

A dissertation for the degree of Philosophiae Doctor, May 2020



Acknowledgements

First and foremost I would like to express my deepest gratitude towards Pia Abel zur Wiesch, my main supervisor. Her mentoring me in research, her support, as well as her guidance in my early career as a researcher helped me tremendously in my PhD. Furthermore, I would like to thank Roland Regoes, my co-supervisor, for hosting me in Zurich. Him coaching me on developing projects led me to find my style in research. This has impacted almost all the works presented in this thesis. I would also like to thank Fabrizio Clarelli, my other co-supervisor for his advices on mathematical approaches, as well as for the numerous discussions on science, projects, life, and food.

During the course of my PhD, I have formed numerous connections (both personal and professional) at my home department(s), as well as during my extensive travels abroad. These travels would not have been possible without funding from the Faculty of Health sciences at the University of Tromsø, the PhD schools of NFIF, IBA, and NORBIS. Without any particular order, I am grateful for all the memories to my friends and colleagues: Vidar Sørum, Klaus Harms, Julia Kloos, Balint Csoboz, Garri Fagerbakk, Marie Lindberg, Annika Koumans Lily Hsieh, Colin Hemez, Santiago Ramon Garcia, Vi Ngoc-Nha Tran, Anup Shrestha, Iren Wu, Theresa Wagner, Giacomo Tartari, Moa Nyamwathi Lønning, Kristian Svendsen, Elisabeth Pedersen, Elizabeth Fredheim, Marcin Wojewodzic, Peter Ashcroft, Daniel Angst, Sebastian Bonhoeffer, Desiree Bader, Ryuta Yoshimatsu, Balazs Bogos, Bonnie Qian, Richard Allen, Alex Hall, Yi Min Ko, Laura Kaminsky, Tina Lasisi, and many others in Norway, Switzerland, the US, and the TBNet group. I may have forgotten to include some that should be mentioned here, if so, it is not intentional.

Because of my journeys, I now have close friends all around the world. Special thanks goes to all of them as they have been the source of my strength at the various stages of my life and PhD:

Without my friends in Tokyo – Avelyn Deckard, Haris Christodoulou, Audun Sanderud, and Keita Suzuki it would have not been possible to start my path in research and making the decision to pursue PhD. Additionally, without Prof. Mihoko Niitsuma supporting my passion for research, I would not have considered pursuing PhD.

Thanks to my “Tromsø family” – Christopher Fröhlich, Jónína Sæunn Guðmundsdóttir, Margherita Falavigna, Jennifer Cauzzo, Selenia Ternullo, João Gama, and Alex Rosenberg, the polar night and cold never bothered me. The countless experiences, dinners, coffee, your company, and friendship have made so that I feel the most at home in the arctic circle despite my preference for large cities.

At the same time, I always looked forward to moving back to Zurich and reunite with Imre Majer. Thanks to our oddly parallel lives, our friendship has now spanned many years, countries, and continents. I am looking forward to our next set of mischievous adventures.

After having moved to the US in the final stages of my PhD, the support and friendship of Jingyi Liang, Edelio Bazan, Ciara Newton, and Xalli Zuniga made writing this thesis a breeze. Having you around made my stress melt away.

Many thanks to those that I have left back in Hungary, particularly Matyas Bukva and most importantly my family: Miklos, Dina, and Oliver Martinecz. While I rarely got to visit, your remote support have made a difference for me over the years.

Finally, I would like to thank Christoph Lange and Roger Kouyos for evaluating my thesis and taking the time to make the trip to Tromsø to do that.

Table of Contents

Acknowledgements	I
Abbreviations	III
List of publications	IV
Scientific abstract	V
Abstract.....	V
1 Introduction.....	1
1.1 Tuberculosis, and the current standard of care	1
1.2 The search for shorter tuberculosis treatments	1
1.3 Rational treatment design and its challenges	2
1.3.1 How do antibiotics actually work: modelling antibiotic action.....	2
1.3.2 Bacteria are not all the same: bacterial heterogeneity	3
1.3.3 Change in scenery: going from the ideal <i>in vitro</i> environment to <i>in vivo</i> environments....	4
1.3.4 Design, evaluation, and challenges posed by tuberculosis clinical trials	6
1.3.5 Aims.....	7
2 Materials and Methods.....	7
2.1 Mathematical models	7
2.2 Datasets	8
3 Results.....	8
3.1 Paper 1: Review on state of the art in modelling antibiotic action	8
3.2 Characterizing heteroresistance	8
3.2.1 Paper 2: Estimating treatment length in mathematical models of slowdown in bacterial elimination	8
3.2.2 Paper 3: Modeling the effects of heterogeneity in multi-step antibiotic action using Gillespie simulations.....	9
3.3 Tuberculosis treatments	10
3.3.1 Paper 4: Characterizing a slowdown in bacterial elimination and its effects on the treatment in a clinical trial on tuberculosis patients.	10
3.3.2 Paper 5: Modeling the effects of heteroresistance with multiple infected sites	10
4 Discussion.....	11
5 References.....	14

Abbreviations

EBA trial – early bactericidal activity trial

MAMS trial – multi-arm multi-stage trial

MIC – minimum inhibitory concentration

M.tb – *Mycobacterium tuberculosis*

TB – tuberculosis

TSCC – time to sputum culture conversion

List of publications

- Paper 1:** Clarelli F, Liang J, Martinecz A, Heiland I, Abel zur Wiesch P. Multi-scale modeling of drug binding kinetics to predict drug efficacy. *Cell Mol Life Sci* **2019**;
- Paper 2:** Martinecz A, Abel zur Wiesch P. Estimating treatment prolongation for persistent infections. *Pathogens and Disease* **2018**;
- Paper 3:** Martinecz A, Clarelli F, Abel S, Abel zur Wiesch P. Reaction Kinetic Models of Antibiotic Heteroresistance. *IJMS* **2019**; 20:3965.
- Paper 4:** Martinecz A, Boeree M, Diacon A, Dawson R, Aarnoutse R, Abel zur Wiesch P. High peak rifampicin plasma concentrations accelerate the slow phase of bacterial elimination in tuberculosis patients: evidence for heteroresistance. (Manuscript)
- Paper 5:** Martinecz A, Abel zur Wiesch P, Regoes R. Heteroresistance increases the necessary treatment length in a within-host metapopulation model (Manuscript)

Scientific abstract

When bacteria are exposed to antibiotics, the rate of killing can slow down dramatically over time. This phenomenon can be observed both *in vitro* and *in vivo*. *In vitro*, the mechanistic explanations for this can be divided into two main categories: antibiotic persistence and heteroresistance. *In vivo*, both mechanisms thought to contribute to observed slowdowns in the elimination and as a result may prolong the necessary treatment lengths. Therefore, by mitigating the slowdown it might be possible to shorten antibiotic treatments, however this is yet to be shown conclusively. This is also the case in tuberculosis when treatment regimens take at least 6 months.

This thesis focuses on heteroresistance and its effects on the treatments lengths necessary to eliminate bacteria, particularly in the treatment of tuberculosis. To do so, I expand the mathematical toolbox of modeling heteroresistance on different scales, ranging from modeling chemical reaction kinetics to modeling multiple bacterial colonies within the tissues of patients. In addition, I analyzed clinical trials on high rifampicin doses in tuberculosis patients to show that heteroresistance the likely cause of the observed slowdown in elimination within the trial.

Abstract

Tuberculosis (TB) is a deadly disease that results in 1.5 million related deaths worldwide each year [1]. Due to the complexities of the disease, even for the drug susceptible form, the treatment takes six months and requires a cocktail of four different antibiotics. For those who are infected with drug resistant strains, or cases where the bacteria developed drug resistance to the key drugs during and after (unsuccessful) treatments, the treatment regimens take even longer. In the drug resistant case, the length of treatment, the perceived and real stigma associated with the disease [2], and the side-effects of treatment itself on top of the disease makes it a miserable experience [3]. As one patient summed up in a study: “I cry every day” [4]. Arguably, by improving the treatment success rates and effectiveness of the for the drug susceptible tuberculosis treatments, the prevalence of drug resistant cases can also be reduced.

Improving treatments however is a complex issue. This problem is well illustrated by the fact that even though one of the current key drugs, rifampicin, has been introduced for the treatment of tuberculosis in the late 1960s [5], its use still not optimized. As a result, there are still clinical trials aimed at finding optimal treatment regimens, strategies, or dosing [5–7].

Optimizing the use of antibiotics faces multiple challenges, one of which is the apparent slowdown in elimination rates of bacteria. When bacteria are exposed to antibiotics, the majority of bacteria can often be killed rapidly, however the remaining bacteria may take a long time to be killed. It is often assumed that this slowdown can affect the treatment of patients, however has not been proven conclusively. This is partly because during treatments the immune system eliminates bacteria as well in addition to antibiotics. The impact of the immune system is well illustrated by the fact that bacteriostatic antibiotics (antibiotics that only prevent the replication of bacteria) often work just as well for treatments as bactericidal antibiotics (antibiotics that kill bacteria) [8]. In tuberculosis it has been shown that in “successful treatments” (no relapse after the termination of treatment), viable bacteria may still exist in the patients [9]. In addition to knowledge gaps in modeling the immune system, and the behavior of bacteria *in vivo* in general, our ability to evaluate and analyze these problems is hindered by our ability to measure the amount of bacteria (bacterial loads) in patients. In tuberculosis for example, bacterial loads in patients are assessed via sputum bacterial count measurements which only offer an incomplete picture [10–12]. This is well illustrated by the fact that even though there are no bacteria detected in the sputum after the first 2-3 months of the treatment, it is necessary to treat for the full 6 months in order to avoid relapse [13,14]. In cases where direct measurements are not possible, mathematical modeling approaches have been shown to be useful in the decision making processes. As a result, in recent years theoretical and modeling approaches have been on the rise in tuberculosis clinical trials as well, complementing the traditionally empirical approaches in the field in order to further optimize treatments [15].

In this thesis I expand the mathematical toolbox of modeling the slowdown in elimination. I use these methods to analyze a clinical trial on high rifampicin doses in tuberculosis treatments in order to assess the impact and possible mechanical causes of the observed slowdown in bacterial elimination within the trial. Ultimately, these results and approaches contribute to our understanding why certain treatment approaches are more effective than others and as a result aid in optimizing current and future treatment regimens.

1 Introduction

Note: One of the papers in this thesis is a review on mathematical modeling of antibiotic action by Clarelli et al. (I am the third author). There, we describe modeling approaches in detail, therefore in this introduction I mainly focus on tuberculosis and the impact of heteroresistance on its treatment in order to complement the review paper.

1.1 Tuberculosis, and the current standard of care

Tuberculosis (TB) is a deadly disease that results in 1.5 million related deaths worldwide each year [1]. It is believed that a third of the world's population is latently infected with TB, however only a fraction of cases may result in an infection. A recent analysis suggests that the overwhelming majority of TB activation cases happen within two years of infection with TB, after this period the probability of activation drops dramatically [16].

The current standard of care involves a cocktail of four different drugs for the first two months (isoniazid, rifampicin, pyrazinamide, and ethambutol) followed by taking two of these drugs (isoniazid and rifampicin) for an additional four months. This treatment is still carries a significant risk of relapse: up to 15% [13,14]. Rifampicin is one of the key drugs in this treatment and is the also the focus of this thesis. Particularly, the effectiveness of high versus low rifampicin doses.

Rifampicin was discovered in 1957 [17], followed by nearly a decade of *in vitro* and animal studies before its first human use in 1966 [5,18]. The necessity for multi drug combination was discovered at the early stages during the animal studies, where they have found that rifampicin monotherapy only resulted in a subset of animals being cured [5,19]. The current dosing recommendation is 10mg/kg bodyweight that has been unchanged since the 1970s [5]. At the time, the 10 mg/kg dose as decided based on concerns regarding adverse reactions [5,6,20], cost of treatments [21–25], peak serum concentrations being sufficiently above MIC [26], and the assumption that high doses may cause the emergence or resistance [5]. Since then however, costs of rifampicin have significantly decreased [6], and high rifampicin doses seem to be well tolerated in both historical and current trials [6,27–32]. Current evidence does not support the idea that higher doses would facilitate resistance emergence more than low doses [33]. Finally, according to current *in vitro* and *in vivo* studies, drug serum concentrations are at the lower end of the dose-response curves due to the distribution characteristics of the drug as well as pharmacodynamic characteristics [6,34–37].

As the current regimen was based on considerations other than the effectiveness of treatment, currently there are efforts to establish high rifampicin dosing regimens to improve the efficiency of tuberculosis treatments. As a result, there is accumulating evidence supporting the recommendation for higher rifampicin doses [27,37–39]. Even though high dose rifampicin is already occasionally used in treating high-risk patients, it is yet to be endorsed by the WHO guidelines [5].

1.2 The search for shorter tuberculosis treatments

Ideally, after an antibiotic treatment, patients should be cured as fast as possible without the possibility of relapse. Longer treatments are not only more expensive and uncomfortable for the patients, but are also associated with problems in patient adherence to the regimen [40]. Imperfect adherence to tuberculosis treatments is not uncommon [41,42], which is highly problematic as even 10% of missed doses pose a significant risk of unfavorable treatment outcomes in the current standard of care [43]. Additionally, the longer bacteria are exposed to antibiotics (without completely eliminating them), the higher the risk of resistance emergence. This can happen either by selecting for preexisting resistant mutants with antibiotic pressure or increasing the probability of encountering a resistant mutants and selecting for those. This issue is illustrated by a recent case study that has shown the emergence of “micro-heteroresistance” against the new tuberculosis drug, bedaquiline, after 6 months of treatment [44]. Finally, the human elements of the treatments cannot be neglected when considering the effects of a long tuberculosis therapy where patients centeredness has an important role [3,45].

Currently, there are multiple clinical trials aimed at improving tuberculosis treatments which can be done in various ways. For instance, by shortening treatments, decreasing side-effects, or increasing the robustness against resistance emergence. These are often conflicting goals, and improving one aspect may decrease the other [46]. Additionally, properties of treatments (length, risk of relapse, probability of resistance emergence) have impacts beyond a single patient and can affect epidemiological characteristics of tuberculosis differently as shown recently via mathematical modelling [47].

The trade-off between the different aspects of treatments can be illustrated with the trade-off between the length of treatments and the probability of relapse. Using data from an early tuberculosis trial [48], Nunn et al in [49] showed that the expected increase in relapse rates was 9-10% when shortening the streptomycin, isoniazid, rifampicin, and pyrazinamide regimen from 6 months to 4 months [50]. A different study demonstrated that the cure rates for latent tuberculosis (treated with isoniazid) were heavily affected by treatment length: cure rates were 31%, 69%, 93% for 3, 6, and 12 months of treatments respectively [51].

In general, finding and introducing new treatment regimens for any disease is a difficult, costly, and time consuming. Due to the knowledge gaps, and difficulties, optimal treatments may not be found immediately and therefore established treatments may be suboptimal and can be improved after reevaluation [28,52,53]. This is also the case for tuberculosis, where it has been argued that the current approach for clinical trial design (and proving non-inferiority) is not sustainable and there is an increasing need for using quantitative and translational approaches in drug design [46]. These approaches have been successfully used for drug development in other diseases, and have been slowly gaining traction in tuberculosis research as well [54–56].

1.3 Rational treatment design and its challenges

1.3.1 How do antibiotics actually work: modelling antibiotic action

Antibiotics were discovered by Alexander Fleming in 1928 and since then they have become one of the cornerstones of modern medicine. Antibiotics work by binding to and inhibiting the intracellular machinery of bacteria, thereby preventing replication (bacteriostatic action), killing the bacterium (bactericidal action), or both. The details on how specific antibiotics work is still poorly understood. This is partly because the processes that result in a cidal or static action may be further downstream from the processes affected by antibiotics (target molecules that the antibiotic molecules bind to). As there are thousands of processes in bacteria, our ability to predict effects further downstream is limited. Out of the hundreds of possible targets, there are only a few dozen targets for the current antibiotics. In most cases, these are part of the growth or replications processes i.e. heavily energy dependent processes [57,58]. This shows the disconnect between antibiotics affecting a process in bacteria and the resulting bactericidal action: the targets of antibiotics may only be indirectly involved in the process that eventually leads to the cell's death. As a result, antibiotic action is often seemingly unpredictable. This is further illustrated by the fact that the combined use of antibiotics is not necessarily additive, and the two effects may interfere with each other [59,60]. For now, there is no reliable method to accurately predict the interaction between two or more antibiotics.

Antibiotic action is often quantified using pharmacodynamic curves. These curves show the net growth rates of a bacterial population at different antibiotic concentrations for a given bacterium, antibiotic, and environment combination (see Figure 1). Closely related to this is the concept of “minimum inhibitory concentration” (MIC): the concentration where the net growth of a bacterial population is zero. The MIC is often used in microbiology to characterize an antibiotic-bacterium pairing as well as to describe changes in susceptibility to antibiotics (via the changes in the MIC). It is highly standardized, relatively easy to determine experimentally. It represents susceptibility with only a single number which keeps comparisons between drugs straightforward. However, the MIC also has its limitations, therefore in computational approaches and when comparing simulations to experimental data, it has to be kept in mind that changes in MIC, do not provide information on whether the shape of the pharmacodynamic curve changed. Additionally, when experimentally determined, there can be substantial variation of MICs depending on the manufacturer of media, technique used by the experimentalist, or strain used

[61]. Finally, the MIC only gives information on the concentrations at which bacterial replication and elimination is in balance, this does not necessarily mean that there is no replication within the bacterial population.

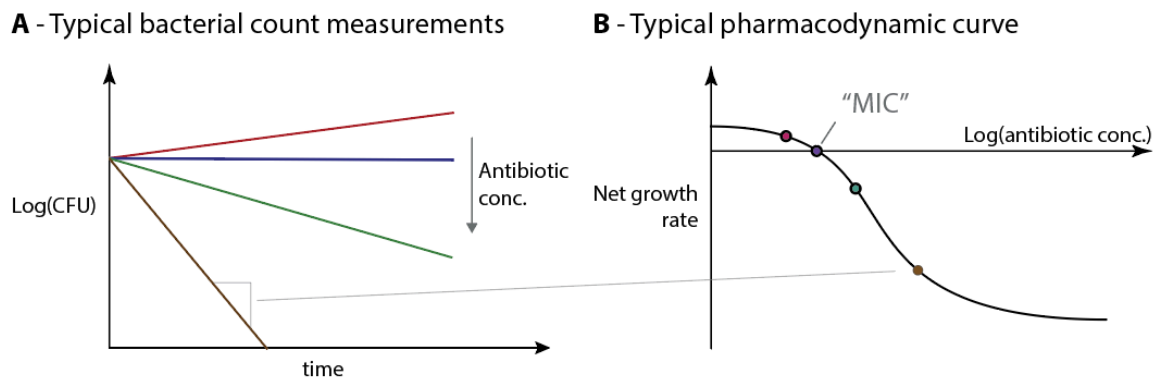


Figure 1 **Pharmacodynamic curves.** Figure A illustrates typical bacterial count measurements over time used to estimate the pharmacodynamic functions (Figure B). Pharmacodynamic functions describe the relationship between the net growth rates of the bacterial populations over time. Here the minimum inhibitory concentration (MIC) is defined as the concentration at which the net growth rate predicted by the pharmacodynamic function is zero.

Susceptibility to bactericidal antibiotics can depend on replication rates, for instance in: beta-lactams [62], fluoroquinolones [63], glycopeptides [64] and lipopeptides [65]. This is thought to be a contribution factor to the observation that interactions between bacteriostatic and cidal antibiotics are often antagonistic [66]. The relationship between susceptibility to bactericidal antibiotics and altered replication rates both depend on the antibiotic class, and the mechanism that alters replication rates [67]. Recent evidence suggests, that the metabolic state has a major impact on both the susceptibility to antibiotics and replication rates rather than the replication rates affecting antibiotic susceptibility directly [57,58].

Bacteria not only mutate and change over time, but also respond to their environments: different genes are expressed in different environments which can affect the susceptibility to antibiotics. This is well illustrated in studies comparing gene expressions between *in vitro* studies and *in vivo* studies [68] as well as studies investigating the disparity between antibiotic susceptibility of bacteria residing intracellularly and extracellularly [69]. To be able to better predict the differences in antibiotic action *in vivo* and *in vitro*, modelling approaches connecting molecular level phenomena to bacterial population level phenomena have been gaining traction. Such approaches have been successfully used to predict the bacteriostatic activity of a FabI inhibitor in *Staphylococcus Aureus* both *in vivo* (mice) and *in vitro* [70] or the bactericidal effects of an LpxC enzyme inhibitor for *Pseudomonas aeruginosa* both *in vivo* (mice) and *in vitro* [71]. The approach of using chemical reaction kinetics to predict the effectiveness of drugs is not exclusive to antibiotics: the effects of the Bruton's tyrosine kinase inhibitor have been successfully used to predict to the ankle swelling size in a rat model of rheumatoid arthritis [72]. These approaches are further reviewed in paper #1 of this thesis.

1.3.2 Bacteria are not all the same: bacterial heterogeneity

Antibiotic exposure may fail to eliminate small fractions of bacterial populations as the elimination rates of bacteria may slow down over time. This observation was first made by Joseph Bigger in 1944 and has been termed “persistence” [73]. It is thought to allow bacteria to survive antibiotic exposure over time, despite being genetically sensitive. In Joseph Bigger’s words:

“ So far we have considered only experiments in vitro, but it is believed that these are of importance because persisters are no mere laboratory artefacts. Clinical evidence strongly suggests that they also occur in the body. Every bacteriologist with experience of the control of penicillin treatment has probably examined specimens of pus from lesions treated locally with penicillin which on direct plating yield no growth, but which after treatment with penicillinase

give extensive growths of the causative bacteria. If cultures of these organisms are tested, they will usually be found just as sensitive to the action of penicillin and just as easily killed by it as was the strain isolated before treatment was commenced. Such organisms are 'persisters' and not 'resisters'." [73]

One of the first and most influential mechanistic/mathematical investigation of this phenomenon was done by Natalie Balaban et al. in 2004. There, they have concluded that the slowdown in elimination can be caused by a switch between the actively replicating (susceptible) and a dormant (entirely non-susceptible) states [74]. The entirely non-susceptible state is a "tolerant" state in which the same antibiotic concentrations can still eliminate all the bacteria, however a longer exposure is necessary until the bacteria switch back to a replicating state and can be eliminated. There are other mechanistic explanations for the slowdown in elimination that do not include tolerant or dormant states. These models almost always describe the coexistence of bacterial subpopulations that show a range of susceptibilities to antibiotics. As a result, higher antibiotic concentrations are necessary to kill the less susceptible subpopulations of bacteria. The possible mechanisms include: cell to cell variations in the number of efflux pumps [75,76], variations in the sizes of bacteria and therefore the intracellular target concentrations [77,78], mutations [79] and gene amplification [80]. Due to the diverse nature of the possible mechanistic explanations, over the next 15 years there have been heated discussions in the field behind the nature of persistence which at the time was synonymous with the dormant state model [81]. This was settled in 2019, in a consensus statement by the major groups working in the field [82]. They have decided that mechanisms that include a tolerant state will be termed persistence (an alternative name, heterotolerance was also considered), and mechanisms that include the coexistence of bacteria with a range of susceptibilities will be termed heteroresistance [82]. While this cleared up controversies behind the term "persistence", the term "heteroresistance" itself has been problematic as well to begin with. Depending on the field, heteroresistance can mean the coexistence of susceptible and resistant strains (stable resistance mutations) as well, most notably in tuberculosis research [79,83]. According to the current definitions, both stable and unstable resistance mutations as well as other mechanisms are all "heteroresistance". The stable resistance mutation case is often referred to as "polyclonal" heteroresistance, while the unstable case is often referred to as "monoclonal" heteroresistance [84,85]. Finally, the current definitions do not draw a clear boundary on what is a resistant subpopulation. In the 2019 consensus statement, heteroresistance was defined as having subpopulations with at least 8x the MIC of the majority of the bacterial population [82,84,86]. However, the definition of 8x MIC mainly has experimental reasons behind it [61,80], therefore in this work we are applying it as a guideline and not as a breakpoint to differentiate between heteroresistance and non-heteroresistance.

1.3.3 Change in scenery: going from the ideal *in vitro* environment to *in vivo* environments

1.3.3.1 Pharmacokinetics and environmental effects

Bacteria are living organisms and therefore they respond to their environments. As a result, different environments can affect the genes expressed which in turn can affect the susceptibility to antibiotics. The simplest example is the efflux pumps that are only expressed in abscesses [87]. The dependence of susceptibility on the environment is also illustrated in [69], where they have exposed bacteria hiding intracellularly to antibiotics and shown that correcting for the antibiotic penetration into the cells is not sufficient to be able to calculate their bactericidal activity.

Differential susceptibility in response to different environments also plays a role when assessing and modelling antibiotic action in tuberculosis where there can be a wide variation in the types infected sites [42,88]. This may be a contributing factor to the observation that there is a high diversity in the *Mycobacterium tuberculosis* (*M.tb*) genome within hosts, especially when it comes to bacteria found at different foci within the same host [89–91]. So far, it is not clear whether this diversity in the genome affects treatments as well and it is only speculated [89]. It is assumed that spatial heterogeneity affects treatments as drug gradients within host can facilitate the evolution of resistance due to functional monotherapy [92] (i.e. one drug being above MIC at a given site in a given timeframe). This functional monotherapy was demonstrated in a recent work that obtained pharmacokinetic data from lesion specific

tissues on seven major TB drugs (including rifampicin) from TB patients undergoing lung resection surgery [93]. There, they have also shown that different sites will have different drug exposure profiles, and there may be a wide variance of drug distribution patterns among similar lesions within a single patient. This was true for rifampicin as well which normally shows an excellent penetration into tissues [94].

Taken together, the uncertainty in how *in vivo* environments affect bacterial susceptibility as well as uncertainty in drug distribution patterns pose a challenge in modeling: parameter estimates based on *in vitro* models may do not readily translate into predictions in *in vivo* and other environments. As a consequence, currently results obtained from PK-PD (pharmacokinetic and pharmacodynamic) models can be important guides but may not reflect the total bacterial burden in a patient. This highlights the need to develop approaches that can allow modelling antibiotic action in detail.

1.3.3.2 Evidence for bacterial heterogeneity *in vivo*

Both persistence and heteroresistance has been shown to exist *in vivo* and there is mounting evidence that both affect treatments [82,84–86]. Progress in this field is slow due to the transient nature of both phenomena and as result evidence often indirect. In case of persistence, in clinical isolates it has been shown that prolonged antibiotic treatments select for high persister mutants [95–97]. Furthermore, in mice infected with *Staphylococcus aureus*, disease pathology and treatment outcomes can be different when the mice were infected with bacteria from stationary phase cultures (enriched with persisters) rather than bacteria from exponential phase cultures [98]. In tuberculosis, it is often assumed that persistence contributes to relapse, thereby necessitating longer treatments in tuberculosis treatments and therefore has been a subject of interest in the field [99–102]. The rationale for this is that persister *M.tb* cells have been observed in macrophages, biofilms and granulomas [99–101,103] and most TB drugs (excluding pyrazinamide) only affect actively growing cells [51,102]. Most of these works were published prior to the new definitions separating heteroresistance and persistence, and as a result, assumptions in the field on the effects of persistence are also related to heteroresistance.

Heteroresistance has been shown to increase treatment failure in mice infected with *Enterobacter cloacae* [104], and a case study has shown the emergence of “micro-heteroresistance” against bedaquiline, after 6 months of treatment in a tuberculosis patient [44]. Additionally, Band et al. [105] have demonstrated that *in vitro* “multiple heteroresistances” can exist, i.e. multiple subpopulations with different resistance profiles. As a result, different subpopulations may emerge during monotherapy depending on the drug used. They have also repeated these experiments in animal models and shown that drug combinations work well against multi-heteroresistance (one drug eliminates one population but not the other and the other way around as well). However, drug combinations were ineffective when there was homogeneous resistance to one drug and heteroresistance to the other.

1.3.3.3 The role of the immune system and spatial distribution of bacteria

While the phenomenon of the slowdown in elimination has been commonly thought to complicate antibiotic treatments by prolonging the necessary treatment length, it is difficult to quantify how much of an impact it may have. The immune system can also often eliminate bacteria and therefore extrapolating based on the slow phase may overestimate the necessary treatment length. An extreme example of this is the observation that treatments with bacteriostatic antibiotics can be just as effective as treatments with bactericidal drugs [8,106].

The immune system itself is highly complex and acts on different timescales with different effectors, therefore its mathematical modeling is also a challenging task [107–110]. This results in a difficulty in applying mathematical modeling approaches to *in vivo* environments as efforts to include immune effectors to models are hampered by the lack of our understanding of the immune system. Approaches on modeling the interplay between the immune system and antibiotic treatments (also when modeling persistence or heteroresistance *in vivo*) usually rely on modeling only one infected site, occasionally with an additional reservoir of bacteria at a different site/organ [8,106,111–114].

As result, models aimed at assessing the impact of persistence of heteroresistance *in vivo* often focus on the possibility of bacterial regrowth at one site of infection, rather than within a patient as a whole. In some diseases, such as *Staphylococcus aureus* infections, salmonella, or tuberculosis, bacteria infect multiple sites. Therefore the spread of bacteria from site-to-site is thought to be an overlooked but contributing factor to the failure of the immune system to clear the infection from the body, even though most if not all individual sites may be cleared by the immune system [115,115–118].

This is the case in tuberculosis as well, where local immune responses have been shown to play an important role in controlling the progression of the disease [56,88,119]. The fate of individual sites of infection (i.e. granulomas) show a great variation, and the clearance of individual sites may be common [120,121]. Furthermore, it has been shown that after a curative treatment, viable *M.tb* bacteria may still remain in patients and are contained or cleared by the immune system eventually [9].

Finally, the interaction between the immune system, persistence, and heteroresistance is also poorly understood and may be dependent on the mechanisms, bacteria, and immune effectors [122–125]. Conversely, immune responses can also facilitate the formation of persisters or affect susceptibility to antibiotics by altering the environment around the bacteria [87,123,126].

1.3.4 Design, evaluation, and challenges posed by tuberculosis clinical trials

Similarly to the transition of modelling approaches from *in vitro* to *in vivo*, transitioning from approaches using animal models to approaches for evaluating clinical trials require different considerations. First and foremost, animal models only capture specific parts of human diseases (for example, latency, progression in tuberculosis). Therefore while they are useful in investigating the effects of treatments [88], results cannot be directly translated into the effects of drugs on human diseases. To resolve this, there is ongoing research aimed at improving our ability to translate results (PK and PD for example) from animal studies to predictions in human therapy [55].

Additionally, while *in vitro* and animal models it is common to investigate drugs given as monotherapy, in tuberculosis clinical trials monotherapy is less common. This is not only because that different drugs may affect each other in various ways, but due to the substantial risk of developing resistance to the given drug. As a result, currently the 14 days is the accepted ethical maximum for monotherapy studies [15]. This can be even shorter, for example the trial analyzed in this thesis only had 7 days of monotherapy [28]. The magnitude of this risk can be demonstrated by the 1968 rifampicin clinical trial when it was introduced to tuberculosis treatments. There, patients have received rifampicin monotherapy for 45 days and a combination therapy for another 45. After the initial 45 days, 3 out of 11 patients (27%) developed resistance to rifampicin. After the second 45 days, this has gone up to 5 patients out of 11 patients (45%, additionally, 2 drug sensitive patients remained culture positive i.e. not cured) [127]. At the time of this trial, the introduction of rifampicin (and other drugs) shortened treatments from 18-24 months to 9 months, however this became unavailable for the patients who developed resistance to rifampicin during the trials with long monotherapy [128].

In clinical trials, treatments also have to be assessed in indirect ways as it is not possible to accurately measure the total bacterial burden in patients. For instance, in tuberculosis trials, bacterial burden is estimated via the sputum [15]. The use of sputum to estimate bacterial burden is supported by the observation that baseline bacterial counts (both colony counts and smear) have been shown to be indicative of disease state (cavitary vs non cavitary) [129]. In this work we rely on two types of bacteriological assessments using the sputum: sputum colony counts (mainly phase 2A, EBA trials) and the time to sputum culture conversion (TSCC), i.e. the time until sputum cultures are repeatedly negative (mainly phase 2B trials and later) [15,54]. Late culture conversion has been shown to be associated with adverse events after treatments [130]. Historically, the 8 week culture conversion has been a reliable endpoint for TB trials, however it is imperfect. As it is a binary measure, it requires large population sizes to be able to distinguish between the effectiveness of treatments. For shorter studies such as EBA trials (that last for 2 weeks), it is also problematic as it takes place multiple weeks after the trial itself. To solve these issues, quantitative methods have been gaining traction in TB clinical trials [15].

While the bacterial burden in sputum is thought to be correlated with the total bacterial burden in a patient, the sputum paints an incomplete picture. First, cultures may not represent of the full diversity of bacteria within the sputum [10–12]. Second, bacteria in the sputum originate from a subset of infected sites within the lungs, for instance bacteria in closed granulomas or bacteria replicating intracellularly are inaccessible. This is illustrated by the fact that even though TSCC happens after approximately 2 months of treatment, patients still have to be treated for the full 6 months in order to avoid relapse.

Finally, bacteria in the sputum may also not represent the full diversity within host [10,90] and culturing it can also reduce the genotypic diversity [10–12] which can only be mitigated via sub-culturing it or via whole genome sequencing [131] (which are either time-consuming or expensive). As a result, while based on bacterial numbers and trends it may be possible to infer what is happening within a patient, it may be very difficult to confirm it by tying it to specific subpopulations of bacteria.

When evaluating trials, linking trends in bacterial elimination rates to regimens come with an additional set of challenges. Patients are usually divided into dosing groups, for example 10, 20, 30 and 40 mg/kg bodyweight rifampicin groups. However there is a nonlinear relationship between bodyweight and pharmacokinetic parameters which may change affect drug plasma levels. This is also the reason why there are concerns regarding weight banded recommendations for treatments: some patients, may be underdosed [132,133]. In trials, this can be partially circumvented by measuring drug concentrations in plasma, however due to distribution patters these may be inaccurate indicators of tissue concentrations. For instance, moxifloxacin reaches higher concentrations in tissues than in the plasma [42].

Approaches in evaluating clinical trials can also be further optimized, one of the best examples of this came from the reanalysis of three fluoroquinolone tuberculosis trials. Individually, these trials failed to show non-inferiority for the 4-month long regimens after promising initial results. The reanalysis showed that by stratifying patients into groups the short regimen can be viable for patients with specific characteristics (for example HIV negative, low bacterial burden) [43].

1.3.5 Aims

The aim of this thesis is to explore the effects of heteroresistance on antibiotic treatments. I do this by modeling antibiotic action within cells, modelling how different levels of heterogeneities in bacterial populations can affect the overall elimination of bacteria, and analyzing a clinical trial to understand how a heteroresistance affects the treatment of patients.

2 Materials and Methods

2.1 Mathematical models

The pharmacodynamic models in this work rely partly on chemical reaction kinetics based models [134] and partly on dose-response curves based on experimental data available in the literature. The comparison and description of the different pharmacokinetic models is contained in paper #1, which is a review on drug-target kinetics based pharmacodynamic models [134].

The mathematical models in paper #2 and #3 are extensions and approximations of the mathematical model by Abel zur Wiesch et al. [135]. This model uses the master equations form of the binding kinetics between antibiotics and their targets to describe antibiotic action. By modeling multiple subpopulations, this model shows that relatively small variations in the model parameters can cause a distinct slowdown in elimination. Thereby it gives one possible mechanistic explanation for heteroresistant behavior.

The pharmacokinetic model in paper #4 and #5 is based on a recent pharmacokinetic model by Strydom et al. [93] published in early 2019. It model is a fitted mathematical model to measurements from tuberculosis patients undergoing lung resection surgery. It is a compartmental pharmacokinetics model with most major TB drugs (isoniazid, rifampicin, pyrazinamide, kanamycin, linezolid, clofazimine, moxifloxacin) and it models 9 relevant lesion types in the lungs. To my knowledge, currently this is the most detailed model on pharmacokinetics in tuberculosis patients.

The mathematical model of paper #5 is a compartmental model similar to those used in epidemiology. It simulates the spread of bacteria from infected sites (tissues) to susceptible sites within the same patient. This model is based on the SEIS (susceptible – exposed – infected – susceptible) model extended with an extra “persisting” compartment in order to capture the effects of heteroresistance when clearing individual infected sites.

2.2 Datasets

In paper #2, I used the experimental dataset published by Bergmiller et al. [136] to demonstrate the use of the mathematical approach. That dataset showed that in *E.coli* the inheritance of efflux pumps is biased towards the mother cells during the replication process and as a result it leads to an accumulation of efflux pumps in older cells.

For the analysis in paper #4 and #5, I used the clinical trial NCT01392911 [28], an early bactericidal activity (EBA) dose ranging trial on tuberculosis patients. In this trial, patients were randomized into 10, 20, 25, 30, 35 or 40 mg doses per kg bodyweight of rifampicin dosing groups. They have received rifampicin first as a monotherapy for the initial seven days, after which standard doses of isoniazid, pyrazinamide, and ethambutol were added for the next seven days of the trial.

In paper #4, I also used a multi arm multi stage (MAMS) trial NCT01785186 [27]. Here, participants were randomized into five experimental regimens, including arms on high rifampicin doses. From these, I only used the control (HRZE, standard regimen) and high rifampicin (HR35ZE, standard regimen but with 35mg/kg rifampicin) treatment arms. During the course of the trial, patients received the experimental regimens for 12 weeks, after which they received the standard continuation phase regimen (rifampicin and isoniazid) for another 14 weeks.

3 Results

3.1 Paper 1: Review on state of the art in modelling antibiotic action

This is a review on pharmacodynamic and pharmacokinetic models that include drug-target binding, with a focus on antibiotic pharmacodynamics. Approaches in modeling antibiotic action including modeling drug-target kinetics have been gaining traction in microbiology and provide an alternative to approaches that are based on dose-response/pharmacodynamic curves. This is because drug target kinetics, can also model and include phenomena that would be difficult with models only using dose-response curves. For example, the (i) post antibiotic effect: a delayed bacterial regrowth after antibiotic exposure, the (ii) off-target binding, or (iii) the synergistic or antagonistic action of drugs.

In addition to the scientific discussions, my contribution to this paper was the part titled “Illustration of mechanistic antibiotic models”. This part is on how the mechanistic antibiotic action models are related to pharmacodynamic functions that describe the relationship between external antibiotic concentrations and the net population change in bacteria. Pharmacodynamic functions combine bacterial replication and elimination which means that at the MIC where the net growth of the population is zero there can still be replication and elimination within the bacterial colony.

3.2 Characterizing heteroresistance

3.2.1 Paper 2: Estimating treatment length in mathematical models of slowdown in bacterial elimination

Note: this paper was published before the new definitions on persistence and heteroresistance, and as a result both are referred to as “persistence” in the publication.

The precursor for this thesis is Abel zur Wiesch et al.’s [135] work on heteroresistance. It uses a master equations based approach to model antibiotic binding to their targets in cells. It shows how smaller cell-to-cell variations the parameters of the drug-target kinetics (for example number of targets) can result

in a slowdown in bacterial elimination. Therefore, it showed that an observed slowdown is not necessarily caused by persistence (dormant state model), but can be due to other different mechanisms as well.

Here, I expand on this work. First, via an approximation I show how the master equations-based model works and how it can be related back to a simple reaction-kinetics based model. This allowed me to compare it to other heteroresistance (and persistence) models. For example, how and to what extent variations in binding rates, number of molecules, or antibiotic concentrations can slow down the elimination of a given subpopulation.

To demonstrate the use of the approach, I used experimental data from Bergmiller et al.'s 2015 paper on the inheritance of efflux pumps [136]. It demonstrated that the inheritance of efflux pumps in *E.coli* is biased towards mother cells which results an accumulation of efflux pumps in older cells which may be a contributing cause to an observable slowdown in elimination. I have shown that the difference between mother and daughter cells can create a mild slowdown in elimination rates, however it is not sufficient to explain the total slowdown when exposing all the bacteria to antibiotics in the dataset. This suggests that heteroresistance (and persistence [137]) mechanisms may not be mutually exclusive, and multiple small mechanisms can add up creating more pronounced slowdown in elimination.

One of the main advantages of this approach is that it allows a quick evaluation on whether certain cell-to-cell variations would cause discernible slowdown in elimination and whether this is observable on all antibiotic concentrations or just a subset of them.

3.2.2 Paper 3: Modeling the effects of heterogeneity in multi-step antibiotic action using Gillespie simulations

Current methods of modeling antibiotic action usually describe single step processes, i.e. when the binding of antibiotic molecules to their targets leads directly to the elimination of the cell. This is a simplifying assumption [57], however modeling multi-step processes is cumbersome with the current mathematical tools used in the field.

In the literature, reaction kinetics of drug-target binding usually modelled with a simple differential equations based approach, or a master equations. Simpler models however cannot give accurate results when modeling low number of molecules, as they model continuous values instead of discrete ones (i.e. the models return 0.5 molecules instead of 0 or 1). This poses a problem in cases where there are a low number of targets, for example gyrase which has a 100 copies per cell approximately [138]. The use of master equations can circumvent this issue, however that approach requires one differential equation per each possible combination in the number of antibiotic, target, and bound target molecules. This makes the use of master equations cumbersome in multi-step processes as it can quickly inflate the number of equations.

Here, I show that the Gillespie stochastic simulation algorithm can sufficiently capture the dynamics of multi-step processes. The Gillespie stochastic simulation algorithm is well known in computational biology and chemistry, however it has not been used before to model antibiotic action before. With a Gillespie simulation based approach, I demonstrate that mutations in any stage of the multi-step processes can affect antibiotic susceptibility, and therefore can lead to heteroresistant behavior (biphasic time-kill curves). This is supported by studies showing that heterogeneity in gene expression levels can lead to heteroresistance [80]

The models of multi-step processes also show that changes in susceptibility to antibiotics can be more than just an increase and decrease in the effective antibiotic concentration and the shape of the pharmacodynamic curve may also change. This shows that while experimentally, the variations in MIC within the population may be a useful tool to show susceptibility levels, the MIC itself only captures part of it.

3.3 Tuberculosis treatments

3.3.1 Paper 4: Characterizing a slowdown in bacterial elimination and its effects on the treatment in a clinical trial on tuberculosis patients.

In tuberculosis treatments there is often an observed slowdown in elimination of bacteria. In this work, I analyzed an early bactericidal activity clinical trial on high rifampicin doses on tuberculosis patients (NCT01392911, [28]). The primary aim was to characterize the slowdown in elimination via a statistical approach and compare it to definitions and mathematical models of both persistence and heteroresistance in order to distinguish between the two. The secondary aim was to connect the results to a different clinical trial in a later phase in order to evaluate the impact of the slowdown in elimination on treatments.

Based on the statistical analysis of the trial, I have found that there is a slowdown in elimination of bacteria in the timeframe of the clinical trial (2 weeks) and therefore the elimination of bacteria can be separated into (at least) two distinct quick and slow phases. Both depended on antibiotic concentrations. Here, the quick phase was better predicted by the total drug exposure (AUC), which was expected as rifampicin has been shown to be more dependent on it previously [139]. However, the slow phase were better predicted by the peak drug concentrations (C_{max}) which was unknown so far. This is because the behavior of the slow phase depends on the mechanism causing it: in persistence the slow phase should be independent of antibiotic concentrations, and in heteroresistance it should be dependent on antibiotic concentrations, particularly on peak drug concentrations [135,140]. Therefore, based on both mathematical models as well as the definitions of heteroresistance and persistence, the statistical analysis indicates that the slowdown is more likely to be caused by heteroresistance rather than persistence. For the mathematical models I have used a simplified model as well as a more detailed, PK-PD based approach. I have shown that in both models the slow phase should not only depend on external antibiotic concentrations, but also that for the slow phase the peak drug concentrations should be better predictors than the total drug exposure.

Next, I combined the results from the statistical analysis, PK-PD based mathematical models, and the approach to assess the slowdown in elimination (paper #2) to estimate an effective susceptibility distribution for bacteria. It is the “effective” distribution, as it encompasses multiple factors that affect elimination rates: susceptibility, accessibility by antibiotics, and differential susceptibility due to environmental effects. The distribution showed that there should be a small fraction of the bacterial population (approx. 1%) with at least 8x the MIC when compared to the majority of the population (with a range of susceptibilities in between). This fits the definition of heteroresistance [84,85]. The caveat here is that the calculated distribution of susceptibility only reflect the effective susceptibility (susceptibility of bacteria within their environments as measured by sputum samples) and not the susceptibility of the bacteria in *in vitro* conditions.

Finally, I have also estimated the time to sputum culture conversion (TSCC) based on the statistical analysis, and found that by taking the slowdown in elimination into account, it is possible to link the results from the clinical trial to a similar clinical trial in the next phase (that measured TSCC). TSCC has been shown to be (moderately) indicative of treatment success [130], therefore this demonstrate that the slowdown in elimination (therefore heteroresistance) may have an impact on treatment success rates.

3.3.2 Paper 5: Modeling the effects of heteroresistance with multiple infected sites

In diseases such as tuberculosis, *Staphylococcus aureus* infections, and salmonella, there can be multiple infected sites. It is thought that in these cases, the bacteria can evade immune clearance from the body by infecting new, susceptible tissues where there is no active immune response yet, even if the immune system is capable of clearing most of the individual infected sites [115]. This is also true in tuberculosis, where immune system itself is often capable of sterilizing or containing individual sites [56,120,121] and it has also been shown that there may be new lesions with ongoing inflammation during and after curative treatments as well [9]. In this work, I was interested whether heteroresistance has an impact on

treatment lengths when bacteria infect multiple distinct sites. Here, the goal was to assess whether heteroresistance has an impact on disease dynamics rather than capturing the dynamics of tuberculosis, therefore I used a compartmental epidemiological model that models the spread of bacteria from infected sites (tissues) to susceptible sites. The parametrization is based on the results and estimates paper 4, extended with a hypothetical immune elimination of infected sites. This rate was chosen based on the differences between the predicted TSCC by the PK PD model and the predictions based on the statistical analysis in paper 4.

Heteroresistance (and a slowdown in elimination in general) is often assumed to prolong treatments as it is assumed that the surviving bacteria may cause relapse after treatments. In this work, I have shown that even if the immune system can clear the remaining bacteria, heteroresistance can still extend the necessary treatment length, by allowing individual sites to survive and stay infectious longer during treatments. This is relevant in assessing tuberculosis clinical trials where the underlying dynamics of the cannot be measured directly, and the total bacterial burden is assessed via the sputum which originates from only a subset of infected sites. This can be investigated in follow-up work, with the same model the model extended with more types of infected sites to better capture the dynamics of tuberculosis, for example compartments that produce sputum or closed, necrotic granulomas that may harbor viable bacteria but are normally contained.

This approach allowed to model the immune clearance of bacteria in a more abstract way when compared to other approaches investigating the interplay between the immune system, heteroresistance, and antibiotic treatments [8,106,112,113]. This abstraction allows us to avoid making assumptions on how to best capture the effects of the immune system at the cost of losing information and predictive power in the model. Compared to other approaches, this model describes multiple infected sites rather than one, as a result it is possible to model relapse with it without making the assumption that the immune system may allow the regrowth of a bacterial population at a site that was almost sterilized previously.

Even though the model is a more abstract model and therefore cannot capture the dynamics of tuberculosis, it provides a way to directly compare simulation results to clinical and qualitative observations. For instance, relapse rates after treatments, spontaneous cure rates for untreated cases, whether new lesions appear during and after treatments, or whether the immune system can clear infected sites. Additionally, while similarly to other models, the parameters may be still be difficult to measure, most of them can be directly tied to observable phenomena, for example the approximate length of time it takes granulomas to grow after infection.

4 Discussion

The slowdown in elimination of bacteria can be observed both *in vitro* and *in vivo*, however the *in vitro* and *in vivo* causes are not necessarily related to each other. *In vitro*, according to the latest definitions, the mechanisms can be separated into two groups: heteroresistance and persistence. *In vivo* it is often observed in various diseases, for instance staphylococcus aureus infections, salmonella, and tuberculosis [102,103,123,141–143]. It is often assumed that the slowdown increases the necessary treatment length by allowing the surviving bacteria to reinfect patients and thereby cause relapse, however this is yet to be shown definitively.

In this thesis, I mainly focus on heteroresistance and its role in tuberculosis treatments. The discussion is mainly on the latter as the pharmacodynamic aspects are covered in paper #1 which is a review on this topic. The overarching hypothesis of this thesis is that it may be possible to aid in the process of developing and optimizing antibiotic treatments by improving our understanding of the slowdown in elimination. I worked on both expanding the mathematical toolbox for investigating heteroresistance, analyzed the slowdown in bacterial elimination in a tuberculosis clinical trial (NCT01392911, [28]), and finally I also I linked these results to a different clinical trial (NCT01785186 [27]).

Heteroresistance is an emerging area of microbiology and antibiotic research. Currently, there are still many open questions within the field and the appropriate mathematical tools are also yet to be

established. Therefore, the first part of this thesis was on tailoring methods of modelling on antibiotic action to be better suited for modeling heteroresistance and providing tools for assessing whether different assumptions can lead to heteroresistant behavior. Here, the main objective was not to develop the optimize mathematical tools, but to provide clarity and to improve our ability to compare assumptions on mechanisms of heteroresistance. The secondary objective was to start a conversation by highlighting how limitations in modeling antibiotic action (for instance, multistep processes) limits our ability to investigate heteroresistance.

In paper #2, [140], I used data on the asymmetric inheritance of efflux pumps from [136] to illustrate the use of my model. There, I have also shown that the differences between daughter and mother cells can only partially explain the observed slowdown in elimination in those experiments. Therefore, it is likely that other bacterial heterogeneities (and/or persistence [137]) also contributes to the slowdown. This is related to paper #3, [144], on multi-step processes, where I demonstrate that changes in almost anywhere within the multi-step processes can affect the susceptibility to antibiotics. As a result, multiple small differences may add up (or negate each other [137]) and therefore may create a more substantial decrease in the susceptibility to antibiotics.

Both of these works were conceptualized before and around the time persistence and heteroresistance were not separated clearly in the literature. One of the reasons for this was that on the surface both look the same: they cause a slowdown in the elimination of bacteria. As a consequence, the nature of persistence as well as heteroresistance (which was still referred to as “persistence”) was hotly debated. Having two incompatible explanations for the slowdown meant that publishing in the field became cumbersome (both from the author and reviewer side): one had to be careful on what papers to use, and explain why other papers describing the “same phenomenon” were excluded. In my opinion this is partly what has led to the mathematical toolbox in the field to not be as developed as it can be. Therefore, large parts of this thesis is aimed at expanding this toolbox.

Shortening treatments and/or increasing treatment success rates is a long and expensive process in general. This is particularly true for tuberculosis, where even the drug susceptible case requires a 6 months of treatments with a combination of 4 different antibiotics. As a result, clinical trials take also a long time to complete and there can often be a disconnect between the different stages of clinical trials. For example, in the phase 2A trials, early bactericidal activity (EBA) trials that last for 2 weeks the different treatment arms are often evaluated by bacterial counts in the sputum [15]. Based on the bacterial count measurements, it is necessary to make a decision on what treatment arms to include in the following trials, even though it is not fully established how the decline in bacterial burdens affect the overall treatments [15,54]. The next possible endpoint is in approximately 2 months (sputum culture conversion), which is only moderately indicative of treatment success [130]. The end of the treatment and the follow-up to establish clinical treatment success rates come much later on. Therefore, drawing conclusions when moving on from one trial to the next is difficult and requires a lot of assumptions [130]. As a result, there have been calls to improve the current approaches in clinical trial design and the use of more quantitative/translational methods [15,54]. Some of the recently implemented approaches (for example, stratifying patients into treatment groups [145]) have been successful and show a promising start in advancing tuberculosis treatments even further [146].

In an analysis of a tuberculosis clinical trial on high rifampicin doses, I have shown that heteroresistance rather than persistence was the more likely cause for an observed slowdown in bacterial elimination. I confirmed these results using mathematical modeling of heteroresistance. These models were based on models of rifampicin pharmacokinetics in tuberculosis patients which only recently became available in the literature [93]. Finally, I connected these results from the statistical analysis to a different clinical trial on high rifampicin doses that measured the time to sputum conversion. Here, being able to connect the PK-PD model to it as well would have been ideal, however this was not possible due to the due to the gaps in our knowledge in the interaction between *M. tb* bacteria and the immune system.

To be able parameterize the PK-PD model with a susceptibility distribution I developed an approach in estimating the susceptibility distribution of bacteria based on bacterial count measurements. It is

intended to be used in the cases where we may not have access to the bacteria directly and therefore can only derive the susceptibility distribution based on trends in bacterial elimination. The method itself is based on the method I used for estimating treatment length in paper #2 and it returns the “effective” susceptibility distribution of bacteria from the fitted biphasic curves (if the slowdown is in fact caused by heteroresistance).

In the mathematical models, due to the lack of other data I made the assumption that heteroresistance only increases the MIC by decreasing the effective antibiotic concentrations. While this worked well in the model, in paper #3 I have also shown that this assumption does not necessarily hold true, however there was no data available in the literature justifying the use anything other than the basic approach to model a change in susceptibility.

The results of paper #4 results links a phase 2A (EBA) clinical trial and a trial in the subsequent phase by demonstrating that the TSCC can be approximated based on sputum colony counts. This was done by taking the slowdown in elimination of bacteria into account. Conversely, I have also shown that by neglecting to take it into account, the TSCC will be underestimated. Here, detecting the slowdown in elimination reliably required pooling data from multiple patients as well as detecting the patterns in it required combining data from all treatment arms in the dose ranging trial. This argues against reducing the frequency of bacteriological assessments over time in EBA trials (as it was done in this trial as well) as it hinders our ability to characterize the slow phase of bacterial elimination.

Finally, via the statistical analysis I have shown that the slow phase of bacterial elimination depends on pharmacokinetic profiles in the clinical trial. Furthermore, I have also demonstrated that the observed dependence is consistent the mathematical models of heteroresistance. Even though with the current mathematical models is it not possible to predict the ideal pharmacokinetic profiles, these results demonstrate that different dosing regimens as well as drug formulations can impact on all phases of bacterial elimination and therefore probably treatment success as well.

To my knowledge there are no current definitions on heteroresistance *in vivo*. Therefore, in this work, the classification as heteroresistance is somewhat subjective. The slowdown in elimination caused the different subpopulations may be caused by disjoint populations at different sites of infection with different environmental effects (susceptibility, drug distribution). When considering the treatment effects or the total bacterial burden in a patient, this is arguably still related to heteroresistance. However when considering individual sites of infection (for example probability of resistance emergence), this is different from both the mono and polyclonal heteroresistance. Paper #5 aims at exploring these questions. There I show that an observed slowdown in elimination in the total bacterial burden can correspond to both cases and is difficult to disentangle based on the trends in bacterial elimination. I used an epidemiological model to describe the infected sites (tissues) spreading bacteria to susceptible sites where there is no active immune response yet. While this particular model is parametrized with the results from paper #4, the dynamics themselves are thought to occur in other diseases as well, for example in *Staphylococcus aureus* infections and in salmonella [115]. Finally, my intention with some parts of paper #5 was to provide an alternative to the standard approaches, similarly to paper #2 and #3. I show that in this model the results from the different simulations and scenarios can be evaluated based on the probability of relapse after treatments. This way, the models can be compared to observations made in clinical trials and clinical practice. While both the model and the definition of relapse is abstracted, the goal here was to show an approach that allows us to use relevant data that can rarely be used directly in other modeling approaches.

Here, relapse is defined as the appearance of new infected sites that in turn may infect other susceptible tissues and therefore keep the disease from cleared from the body. With this definition, it is possible to calculate the probability of this event over time and therefore express the results in terms of probability of adverse events after the end of treatments. While there may be better tools and definitions to define relapse in models, my intention here was to demonstrate an approach that can create a bridge between mathematical models and how clinical trials are evaluated. For instance, this opens up the avenue of using non-inferiority when simulating different treatments and therefore ask the questions whether we

would see a difference in hypothetical trials or not. Additionally, while non-inferiority trials have been developed in order to find treatments that are “equivalent” (within a margin of error) or better than the standard of care, it also allows investigating how to improve different aspects of treatments such as tolerability, dosing, or costs. Noninferiority trials come with their own set of ethical problems [147,148], can be subjective in defining what is an acceptable difference from the standard of care [49,50,148], and is unsustainable, however they are still widely used in clinical trial design and are useful approaches [46]. Therefore, having this kind of relapse definition in the mathematical modeling toolbox can be valuable.

This thesis demonstrates the role of translational methods in clinical trials and drug development. For instance, they can shed light on why one treatment arm work better than other treatment arms or show new possible ways of optimizing treatments (in this case via different pharmacokinetic profiles). These kind of insights can eventually aid in designing clinical trials and treatments as well as provide further support to regimens that are in the process of being established. This thesis is part of the accumulating evidence supporting for high dose rifampicin for tuberculosis treatments as well as the evidence for the clinical significance of heteroresistance. More generally, this work represents a small step forward in modeling antibiotic action and the field of heteroresistance by showing its clinical significance, and by demonstrating the use of new tools that can aid in investigating heteroresistance.

The collection of methods in this thesis also demonstrates that no single method that is appropriate for all situations. For example, in ambiguous where not all the parameters/processes are known or measurable, simplified and more abstract approaches (paper #2 and #5) are easier to use than more detailed approaches (paper #3). In other cases, these roles are reversed.

At the time of writing this thesis, quantitative methods in biology and medicine have come far enough to be able to aid and advise in drug development. While the predictive ability of mathematical approaches is still lacking, they can eventually be improved with a better understanding of the immune system, bacteria, bacterial heterogeneity and antibiotic action. Additionally, with the improvement of microbiological and pharmacokinetic assessments in clinical trials mathematical models and estimates based on these models can be further improved.

5 References

1. World Health Organization. Global tuberculosis report 2019. 2019; Available at: <https://apps.who.int/iris/handle/10665/329368>.
2. Nordstoga I, Drage M, Steen TW, Winje BA. Wanting to or having to – a qualitative study of experiences and attitudes towards migrant screening for tuberculosis in Norway. *BMC Public Health* **2019**; 19:796.
3. Udwardia Z, Furin J. Quality of drug-resistant tuberculosis care: Gaps and solutions. *J Clin Tuberc Mycobact Dis* **2019**; 16:100101.
4. Isaakidis P, Rangan S, Pradhan A, Lodomirska J, Reid T, Kielmann K. ‘I cry every day’: experiences of patients co-infected with HIV and multidrug-resistant tuberculosis. *Trop Med Int Health* **2013**; 18:1128–1133.
5. Grobbelaar M, Louw GE, Sampson SL, van Helden PD, Donald PR, Warren RM. Evolution of rifampicin treatment for tuberculosis. *Infect Genet Evol* **2019**; 74:103937.
6. van Ingen J, Aarnoutse RE, Donald PR, et al. Why Do We Use 600 mg of Rifampicin in Tuberculosis Treatment? *Clin Infect Dis* **2011**; 52:e194–e199.
7. Seijger C, Hoefsloot W, Bergsma-de Guchteneire I, et al. High-dose rifampicin in tuberculosis: Experiences from a Dutch tuberculosis centre. *PLOS ONE* **2019**; 14:e0213718.
8. Levin BR, Baquero F, Ankomah PP, McCall IC. Phagocytes, Antibiotics, and Self-Limiting Bacterial Infections. *Trends Microbiol* **2017**; 25:878–892.

9. the Catalysis TB–Biomarker Consortium, Malherbe ST, Shenai S, et al. Persisting positron emission tomography lesion activity and Mycobacterium tuberculosis mRNA after tuberculosis cure. *Nat Med* **2016**; 22:1094–1100.
10. Shamputa IC, Jugheli L, Sadradze N, et al. Mixed infection and clonal representativeness of a single sputum sample in tuberculosis patients from a penitentiary hospital in Georgia. *Respir Res* **2006**; 7. Available at: <http://respiratory-research.biomedcentral.com/articles/10.1186/1465-9921-7-99>. Accessed 7 April 2019.
11. Metcalfe JZ, Streicher E, Theron G, et al. Mycobacterium tuberculosis Subculture Results in Loss of Potentially Clinically Relevant Heteroresistance. *Antimicrob Agents Chemother* **2017**; 61. Available at: <http://aac.asm.org/lookup/doi/10.1128/AAC.00888-17>. Accessed 7 April 2019.
12. Shockey AC, Dabney J, Pepperell CS. Effects of Host, Sample, and in vitro Culture on Genomic Diversity of Pathogenic Mycobacteria. *Front Genet* **2019**; 10:477.
13. Horsburgh CR, Barry CE, Lange C. Treatment of Tuberculosis. *N Engl J Med* **2015**; 373:2149–2160.
14. Lawn SD, Zumla AI. Tuberculosis. *The Lancet* **2011**; 378:57–72.
15. Davies G, Boeree M, Hermann D, Hoelscher M. Accelerating the transition of new tuberculosis drug combinations from Phase II to Phase III trials: New technologies and innovative designs. *PLOS Med* **2019**; 16:e1002851.
16. Behr MA, Edelstein PH, Ramakrishnan L. Revisiting the timetable of tuberculosis. *BMJ* **2018**; :k2738.
17. Sensi P, Margalith P, Timbal MT. Rifomycin, a new antibiotic; preliminary report. *Il Farm Ed Sci* **1959**; 14:146–147.
18. Gyselen A, Cosemans J, Lacquet LM, Vandenberghe E, Verbist L. Five years of clinical experience with rifampicin. *Acta Tuberc Pneumol Belg* **1971**; 62:289–307.
19. Batten J. Rifampicin in treatment of experimental tuberculosis in mice. *Tubercle* **1969**; 50:294–298.
20. Poole G, Stradling P, Worlledge S. Potentially serious side effects of high-dose twice-weekly rifampicin. *Br Med J* **1971**; 3:343–347.
21. Houk AN. Rifampin: its role in the treatment of tuberculosis. *Chest* **1972**; 61:518–519.
22. Lester W. Rifampin: a semisynthetic derivative of rifamycin--a prototype for the future. *Annu Rev Microbiol* **1972**; 26:85–102.
23. Controlled clinical trial of short-course (6-month) regimens of chemotherapy for treatment of pulmonary tuberculosis. *Lancet Lond Engl* **1972**; 1:1079–1085.
24. Fox W, Ellard GA, Mitchison DA. Studies on the treatment of tuberculosis undertaken by the British Medical Research Council tuberculosis units, 1946-1986, with relevant subsequent publications. *Int J Tuberc Lung Dis Off J Int Union Tuberc Lung Dis* **1999**; 3:S231-79.
25. Fox W, Nunn AJ. The cost of antituberculous drug regimens. *Am Rev Respir Dis* **1979**; 120:503–509.
26. Constans P, Baron A, Parrot R, Coury C. A study of 200 cases of active, recent pulmonary tuberculosis treated with rifampin-isoniazid. A follow-up history of one and one-half to three years. *Chest* **1972**; 61:539–549.
27. Boeree MJ, Heinrich N, Aarnoutse R, et al. High-dose rifampicin, moxifloxacin, and SQ109 for treating tuberculosis: a multi-arm, multi-stage randomised controlled trial. *Lancet Infect Dis* **2016**; 17:39–49.
28. Boeree MJ, Diacon AH, Dawson R, et al. A dose-ranging trial to optimize the dose of rifampin in the treatment of tuberculosis. *Am J Respir Crit Care Med* **2015**; 191:1058–1065.

29. Favez G, Chioléro R, Willa C. Rifampin-isoniazid compared with streptomycin-isoniazid in the original treatment of infectious pulmonary tuberculosis. Results of a controlled study. *Chest* **1972**; 61:583–586.
30. Acocella G, Pagani V, Marchetti M, Baroni GC, Nicolis FB. Kinetic studies on rifampicin. I. Serum concentration analysis in subjects treated with different oral doses over a period of two weeks. *Chemotherapy* **1971**; 16:356–370.
31. Curci G, Bergamini N, Delli Veneri F, Ninni A, Nitti V. Half-life of rifampicin after repeated administration of different doses in humans. *Chemotherapy* **1972**; 17:373–381.
32. Kreis B, Pretet S, Birenbaum J, et al. Two three-month treatment regimens for pulmonary tuberculosis. *Bull Int Union Tuberc* **1976**; 51:71–75.
33. Drlica K, Zhao X. Mutant selection window hypothesis updated. *Clin Infect Dis Off Publ Infect Dis Soc Am* **2007**; 44:681–688.
34. Jayaram R, Gaonkar S, Kaur P, et al. Pharmacokinetics-pharmacodynamics of rifampin in an aerosol infection model of tuberculosis. *Antimicrob Agents Chemother* **2003**; 47:2118–2124.
35. Peloquin C. What is the ‘right’ dose of rifampin? *Int J Tuberc Lung Dis Off J Int Union Tuberc Lung Dis* **2003**; 7:3–5.
36. Mitchison DA. Role of individual drugs in the chemotherapy of tuberculosis. *Int J Tuberc Lung Dis Off J Int Union Tuberc Lung Dis* **2000**; 4:796–806.
37. Diacon AH, Patientia RF, Venter A, et al. Early bactericidal activity of high-dose rifampin in patients with pulmonary tuberculosis evidenced by positive sputum smears. *Antimicrob Agents Chemother* **2007**; 51:2994–2996.
38. Omansen TF, Almeida D, Converse PJ, et al. High-Dose Rifamycins Enable Shorter Oral Treatment in a Murine Model of *Mycobacterium ulcerans* Disease. *Antimicrob Agents Chemother* **2018**; 63:e01478-18.
39. Hu Y, Liu A, Ortega-Muro F, Alameda-Martin L, Mitchison D, Coates A. High-dose rifampicin kills persisters, shortens treatment duration, and reduces relapse rate in vitro and in vivo. *Front Microbiol* **2015**; 6.
40. Burnier M, Wuerzner G, Struijker-Boudier H, Urquhart J. Measuring, analyzing, and managing drug adherence in resistant hypertension. *Hypertens Dallas Tex 1979* **2013**; 62:218–25.
41. Park S, Sentissi I, Gil S, et al. Medication Event Monitoring System for Infectious Tuberculosis Treatment in Morocco: A Retrospective Cohort Study. *Int J Environ Res Public Health* **2019**; 16:412.
42. Dartois V. The path of anti-tuberculosis drugs: from blood to lesions to mycobacterial cells. *Nat Rev Microbiol* **2014**; 12:159–167.
43. Imperial MZ, Nahid P, Phillips PPJ, et al. A patient-level pooled analysis of treatment-shortening regimens for drug-susceptible pulmonary tuberculosis. *Nat Med* **2018**; 24:1708–1715.
44. de Vos M, Ley SD, Wiggins KB, et al. Bedaquiline Microheteroresistance after Cessation of Tuberculosis Treatment. *N Engl J Med* **2019**; 380:2178–2180.
45. Kruk ME, Gage AD, Arsenault C, et al. High-quality health systems in the Sustainable Development Goals era: time for a revolution. *Lancet Glob Health* **2018**; 6:e1196–e1252.
46. Lienhardt C, Nahid P. Advances in clinical trial design for development of new TB treatments: A call for innovation. *PLOS Med* **2019**; 16:e1002769.
47. Kendall EA, Shrestha S, Cohen T, et al. Priority-Setting for Novel Drug Regimens to Treat Tuberculosis: An Epidemiologic Model. *PLOS Med* **2017**; 14:e1002202.
48. Clinical trial of six-month and four-month regimens of chemotherapy in the treatment of pulmonary tuberculosis. *Am Rev Respir Dis* **1979**; 119:579–585.

49. Nunn AJ, Phillips PPJ, Gillespie SH. Design issues in pivotal drug trials for drug sensitive tuberculosis (TB). *Tuberculosis* **2008**; 88:S85–S92.
50. Olliaro PL, Vaillant M. Designing noninferiority tuberculosis treatment trials: Identifying practical advantages for drug regimens with acceptable effectiveness. *PLOS Med* **2019**; 16:e1002850.
51. Connolly LE, Edelstein PH, Ramakrishnan L. Why Is Long-Term Therapy Required to Cure Tuberculosis? *PLoS Med* **2007**; 4:e120.
52. Lan AJ, Colford JM, Colford JM. The impact of dosing frequency on the efficacy of 10-day penicillin or amoxicillin therapy for streptococcal tonsillopharyngitis: A meta-analysis. *Pediatrics* **2000**; 105:E19.
53. Chastre J, Wolff M, Fagon J-Y. Randomized Trial Ventilator-Associated Pneumonia in Adults: A Comparison of 8 vs 15 Days of Antibiotic Therapy for. *Jama* **2003**; 290:29019:2588–2598.
54. Dooley KE, Hanna D, Mave V, Eisenach K, Savic RM. Advancing the development of new tuberculosis treatment regimens: The essential role of translational and clinical pharmacology and microbiology. *PLOS Med* **2019**; 16:e1002842.
55. Bartelink I, Zhang N, Keizer R, et al. New Paradigm for Translational Modeling to Predict Long-term Tuberculosis Treatment Response: Translational Modeling Predicts TB Treatment Response. *Clin Transl Sci* **2017**; 10:366–379.
56. Torrelles JB, Schlesinger LS. Integrating Lung Physiology, Immunology, and Tuberculosis. *Trends Microbiol* **2017**; 25:688–697.
57. Stokes JM, Lopatkin AJ, Lobritz MA, Collins JJ. Bacterial Metabolism and Antibiotic Efficacy. *Cell Metab* **2019**; 30:251–259.
58. Lopatkin AJ, Stokes JM, Zheng EJ, et al. Bacterial metabolic state more accurately predicts antibiotic lethality than growth rate. *Nat Microbiol* **2019**; Available at: <http://www.nature.com/articles/s41564-019-0536-0>. Accessed 13 November 2019.
59. Baeder DY, Yu G, Hozé N, Rolff J, Regoes RR. Antimicrobial combinations: Bliss independence and Loewe additivity derived from mechanistic multi-hit models. *Philos Trans R Soc Lond B Biol Sci* **2016**; 371. Available at: <http://www.ncbi.nlm.nih.gov/pubmed/27160596>.
60. Katzir I, Cokol M, Aldridge BB, Alon U. Prediction of ultra-high-order antibiotic combinations based on pairwise interactions. *PLOS Comput Biol* **2019**; 15:e1006774.
61. Mouton JW, Muller AE, Canton R, Giske CG, Kahlmeter G, Turnidge J. MIC-based dose adjustment: facts and fables. *J Antimicrob Chemother* **2018**; 73:564–568.
62. Brown MR, Collier PJ, Gilbert P. Influence of growth rate on susceptibility to antimicrobial agents: modification of the cell envelope and batch and continuous culture studies. *Antimicrob Agents Chemother* **1990**; 34:1623–1628.
63. Evans DJ, Allison DG, Brown MRW, Gilbert P. Susceptibility of *Pseudomonas aeruginosa* and *Escherichia coli* biofilms towards ciprofloxacin: effect of specific growth rate. *J Antimicrob Chemother* **1991**; 27:177–184.
64. Chmara H, Ripa S, Mignini F, Borowski E. Bacteriolytic effect of teicoplanin. *J Gen Microbiol* **1991**; 137:913–919.
65. Mascio CTM, Alder JD, Silverman JA. Bactericidal Action of Daptomycin against Stationary-Phase and Nondividing *Staphylococcus aureus* Cells. *Antimicrob Agents Chemother* **2007**; 51:4255–4260.
66. Ocampo PS, Lázár V, Papp B, et al. Antagonism between Bacteriostatic and Bactericidal Antibiotics Is Prevalent. *Antimicrob Agents Chemother* **2014**; 58:4573–4582.

67. McCall IC, Shah N, Govindan A, Baquero F, Levin BR. Antibiotic Killing of Diversely Generated Populations of Nonreplicating Bacteria. *Antimicrob Agents Chemother* **2019**; 63. Available at: <http://aac.asm.org/lookup/doi/10.1128/AAC.02360-18>. Accessed 21 July 2019.
68. Avican K, Fahlgren A, Huss M, et al. Reprogramming of *Yersinia* from Virulent to Persistent Mode Revealed by Complex In Vivo RNA-seq Analysis. *PLOS Pathog* **2015**; 11:e1004600.
69. Sandberg A, Hessler JHR, Skov RL, Blom J, Fridodt-Moller N. Intracellular Activity of Antibiotics against *Staphylococcus aureus* in a Mouse Peritonitis Model. *Antimicrob Agents Chemother* **2009**; 53:1874–1883.
70. Daryae F, Chang A, Schiebel J, et al. Correlating drug–target kinetics and in vivo pharmacodynamics: long residence time inhibitors of the FabI enoyl-ACP reductase. *Chem Sci* **2016**; 7:5945–5954.
71. Walkup GK, You Z, Ross PL, et al. Translating slow-binding inhibition kinetics into cellular and in vivo effects. *Nat Chem Biol* **2015**; 11:416–423.
72. Daryae F, Zhang Z, Gogarty KR, et al. A quantitative mechanistic PK/PD model directly connects Btk target engagement and in vivo efficacy. *Chem Sci* **2017**; 8:3434–3443.
73. Bigger Joseph W. TREATMENT OF STAPHYLOCOCCAL INFECTIONS WITH PENICILLIN BY INTERMITTENT STERILISATION. *The Lancet* **1944**; 244:497–500.
74. Balaban NQ, Merrin J, Chait R, Kowalik L, Leibler S. Bacterial persistence as a phenotypic switch. *Science* **2004**; 305:1622–1625.
75. Pu Y, Zhao Z, Li Y, et al. Enhanced Efflux Activity Facilitates Drug Tolerance in Dormant Bacterial Cells. *Mol Cell* **2016**; 62:284–294.
76. Bergmiller T, Andersson AMC, Tomasek K, et al. Biased partitioning of the multidrug efflux pump AcrAB-TolC underlies long-lived phenotypic heterogeneity. *Science* **2017**; 356:311–315.
77. Rego EH, Audette RE, Rubin EJ. Deletion of a mycobacterial divisome factor collapses single-cell phenotypic heterogeneity. *Nature* **2017**; 546:153–157.
78. Abel zur Wiesch P, Abel S, Gkatzis S, et al. Classic reaction kinetics can explain complex patterns of antibiotic action. *Sci Transl Med* **2015**; 7:287ra73.
79. Eilertson B, Maruri F, Blackman A, Herrera M, Samuels DC, Sterling TR. High Proportion of Heteroresistance in *gyrA* and *gyrB* in Fluoroquinolone-Resistant Mycobacterium tuberculosis Clinical Isolates. *Antimicrob Agents Chemother* **2014**; 58:3270–3275.
80. Nicoloff H, Hjort K, Levin BR, Andersson DI. The high prevalence of antibiotic heteroresistance in pathogenic bacteria is mainly caused by gene amplification. *Nat Microbiol* **2019**; 4:504–514.
81. Balaban NQ, Gerdes K, Lewis K, McKinney JD. A problem of persistence: still more questions than answers? *Nat Rev Microbiol* **2013**; 11:587–91.
82. Balaban NQ, Helaine S, Lewis K, et al. Definitions and guidelines for research on antibiotic persistence. *Nat Rev Microbiol* **2019**; Available at: <http://www.nature.com/articles/s41579-019-0196-3>. Accessed 18 April 2019.
83. El-Halfawy OM, Valvano MA. Antimicrobial Heteroresistance: an Emerging Field in Need of Clarity. *Clin Microbiol Rev* **2015**; 28:191–207.
84. Dewachter L, Fauvart M, Michiels J. Bacterial Heterogeneity and Antibiotic Survival: Understanding and Combatting Persistence and Heteroresistance. *Mol Cell* **2019**; 76:255–267.
85. Andersson DI, Nicoloff H, Hjort K. Mechanisms and clinical relevance of bacterial heteroresistance. *Nat Rev Microbiol* **2019**; Available at: <http://www.nature.com/articles/s41579-019-0218-1>. Accessed 1 July 2019.
86. Band VI, Weiss DS. Heteroresistance: A cause of unexplained antibiotic treatment failure? *PLOS Pathog* **2019**; 15:e1007726.

87. Ding Y, Onodera Y, Lee JC, Hooper DC. NorB, an Efflux Pump in *Staphylococcus aureus* Strain MW2, Contributes to Bacterial Fitness in Abscesses. *J Bacteriol* **2008**; 190:7123–7129.
88. Barry CE, Boshoff HI, Dartois V, et al. The spectrum of latent tuberculosis: rethinking the biology and intervention strategies. *Nat Rev Microbiol* **2009**; 7:845–855.
89. Liu Q, Via LE, Luo T, et al. Within patient microevolution of *Mycobacterium tuberculosis* correlates with heterogeneous responses to treatment. *Sci Rep* **2015**; 5. Available at: <http://www.nature.com/articles/srep17507>. Accessed 7 April 2019.
90. Lieberman TD, Wilson D, Misra R, et al. Genomic diversity in autopsy samples reveals within-host dissemination of HIV-associated *Mycobacterium tuberculosis*. *Nat Med* **2016**; 22:1470–1474.
91. Ley SD, de Vos M, Van Rie A, Warren RM. Deciphering Within-Host Microevolution of *Mycobacterium tuberculosis* through Whole-Genome Sequencing: the Phenotypic Impact and Way Forward. *Microbiol Mol Biol Rev* **2019**; 83. Available at: <http://mmbr.asm.org/lookup/doi/10.1128/MMBR.00062-18>. Accessed 7 April 2019.
92. Dheda K, Lenders L, Magombedze G, et al. Drug-Penetration Gradients Associated with Acquired Drug Resistance in Patients with Tuberculosis. *Am J Respir Crit Care Med* **2018**; 198:1208–1219.
93. Strydom N, Gupta SV, Fox WS, et al. Tuberculosis drugs' distribution and emergence of resistance in patient's lung lesions: A mechanistic model and tool for regimen and dose optimization. *PLOS Med* **2019**; 16:e1002773.
94. Prideaux B, Via LE, Zimmerman MD, et al. The association between sterilizing activity and drug distribution into tuberculosis lesions. *Nat Med* **2015**; 21:1223–1227.
95. Lafleur MD, Qi Q, Lewis K. Patients with long-term oral carriage harbor high-persister mutants of *Candida albicans*. *Antimicrob Agents Chemother* **2010**; 54:39–44.
96. Mulcahy LR, Burns JL, Lory S, Lewis K. Emergence of *Pseudomonas aeruginosa* strains producing high levels of persister cells in patients with cystic fibrosis. *J Bacteriol* **2010**; 192:6191–6199.
97. Torrey HL, Keren I, Via LE, Lee JS, Lewis K. High Persister Mutants in *Mycobacterium tuberculosis*. *PLOS ONE* **2016**; 11:e0155127.
98. Yee R, Yuan Y, Shi W, et al. Infection with persister forms of *Staphylococcus aureus* causes a persistent skin infection with more severe lesions in mice: failure to clear the infection by the current standard of care treatment. *Discov Med* **2019**; 28:7–16.
99. Boshoff HIM, Barry CE. Tuberculosis - Metabolism and respiration in the absence of growth. *Nat Rev Microbiol* **2005**; 3:70–80.
100. Chao MC, Rubin EJ. Letting Sleeping *dos* Lie: Does Dormancy Play a Role in Tuberculosis? *Annu Rev Microbiol* **2010**; 64:293–311.
101. Cadena AM, Fortune SM, Flynn JL. Heterogeneity in tuberculosis. *Nat Rev Immunol* **2017**; 17:691–702.
102. Mandal S, Njikan S, Kumar A, Early JV, Parish T. The relevance of persisters in tuberculosis drug discovery. *Microbiology* **2019**; 165:492–499.
103. Barr DA, Kamdolozi M, Nishihara Y, et al. Serial image analysis of *Mycobacterium tuberculosis* colony growth reveals a persistent subpopulation in sputum during treatment of pulmonary TB. *Tuberculosis* **2016**; 98:110–115.
104. Band VI, Crispell EK, Napier BA, et al. Antibiotic failure mediated by a resistant subpopulation in *Enterobacter cloacae*. *Nat Microbiol* **2016**; 1. Available at: <http://www.nature.com/articles/nmicrobiol201653>. Accessed 11 June 2019.

105. Band VI, Hufnagel DA, Jaggavarapu S, et al. Antibiotic combinations that exploit heteroresistance to multiple drugs effectively control infection. *Nat Microbiol* **2019**; Available at: <http://www.nature.com/articles/s41564-019-0480-z>. Accessed 18 July 2019.
106. Ankomah P, Levin BR. Exploring the collaboration between antibiotics and the immune response in the treatment of acute, self-limiting infections. *Proc Natl Acad Sci U S A* **2014**; 111:8331–8338.
107. Iwasaki A, Medzhitov R, Akiko I, Ruslan M. Control of adaptive immunity by the innate immune system. *Nat Immunol* **2015**; 16:343–353.
108. Pilyugin S. Modeling Immune Responses with Handling Time. *Bull Math Biol* **2000**; 62:869–890.
109. Eftimie R, Gillard JJ, Cantrell DA. Mathematical Models for Immunology: Current State of the Art and Future Research Directions. *Bull Math Biol* **2016**; 78:1–44.
110. Price I, Mochan-Keef ED, Swigon D, et al. The inflammatory response to influenza A virus (H1N1): An experimental and mathematical study. *J Theor Biol* **2015**; 374:83–93.
111. Kaiser P, Regoes RR, Dolowschiak T, et al. Cecum Lymph Node Dendritic Cells Harbor Slow-Growing Bacteria Phenotypically Tolerant to Antibiotic Treatment. *PLoS Biol* **2014**; 12:e1001793.
112. Gjini E, Brito PH. Integrating Antimicrobial Therapy with Host Immunity to Fight Drug-Resistant Infections: Classical vs. Adaptive Treatment. *PLoS Comput Biol* **2016**; 12:1–34.
113. D’Agata EMC, Dupont-Rouzeyrol M, Magal P, Olivier D, Ruan S. The impact of different antibiotic regimens on the emergence of antimicrobial-resistant bacteria. *PLoS ONE* **2008**; 3:4–12.
114. Mikkaichi T, Yeaman MR, Hoffmann A, MRSA Systems Immunobiology Group. Identifying determinants of persistent MRSA bacteremia using mathematical modeling. *PLOS Comput Biol* **2019**; 15:e1007087.
115. Bumann D. Heterogeneous host-pathogen encounters: Act locally, think globally. *Cell Host Microbe* **2015**; 17:13–19.
116. Lenaerts A, Barry CE, Dartois V. Heterogeneity in tuberculosis pathology, microenvironments and therapeutic responses. *Immunol Rev* **2015**; 264:288–307.
117. Prajsnar TK, Hamilton R, Garcia-Lara J, et al. A privileged intraphagocyte niche is responsible for disseminated infection of *Staphylococcus aureus* in a zebrafish model. *Cell Microbiol* **2012**; 14:1600–19.
118. Tuchscher L, Medina E, Hussain M, et al. *Staphylococcus aureus* phenotype switching: an effective bacterial strategy to escape host immune response and establish a chronic infection. *EMBO Mol Med* **2011**; 3:129–41.
119. Furin J, Cox H, Pai M. Tuberculosis. *The Lancet* **2019**; 393:1642–1656.
120. Lin PL, Ford CB, Coleman MT, et al. Sterilization of granulomas is common in active and latent tuberculosis despite within-host variability in bacterial killing. *Nat Med* **2014**; 20:75–79.
121. Russell DG. Tuberculosis Progression Does Not Necessarily Equate with a Failure of Immune Control. *Microorganisms* **2019**; 7:185.
122. Putrinš M, Kogermann K, Lukk E, Lippus M, Varik V, Tenson T. Phenotypic heterogeneity enables uropathogenic *Escherichia coli* to evade killing by antibiotics and serum complement. *Infect Immun* **2015**; 83:1056–1067.
123. Helaine S, Cheverton AM, Watson KG, Faure LM, Matthews SA, Holden DW. Internalization of *Salmonella* by Macrophages Induces Formation of Nonreplicating Persisters. *Science* **2014**; 343:204–208.
124. Saliba A-E, Li L, Westermann AJ, et al. Single-cell RNA-seq ties macrophage polarization to growth rate of intracellular *Salmonella*. *Nat Microbiol* **2016**; 2:16206.

125. Martínez-Ramos I, Mulet X, Moyá B, Barbier M, Oliver A, Albertí S. Overexpression of MexCD-OprJ Reduces *Pseudomonas aeruginosa* Virulence by Increasing Its Susceptibility to Complement-Mediated Killing. *Antimicrob Agents Chemother* **2014**; 58:2426–2429.
126. Manina G, Dhar N, McKinney JD. Stress and host immunity amplify mycobacterium tuberculosis phenotypic heterogeneity and induce nongrowing metabolically active forms. *Cell Host Microbe* **2015**; 17:32–46.
127. Baronti A, Lukinovich N. A pilot trial of rifampicin in tuberculosis. *Tubercle* **1968**; 49:180–186.
128. Murray JF, Schraufnagel DE, Hopewell PC. Treatment of Tuberculosis. A Historical Perspective. *Ann Am Thorac Soc* **2015**; 12:1749–1759.
129. Palaci M, Dietze R, Hadad DJ, et al. Cavitary Disease and Quantitative Sputum Bacillary Load in Cases of Pulmonary Tuberculosis. *J Clin Microbiol* **2007**; 45:4064–4066.
130. Horne DJ, Royce SE, Gooze L, et al. Sputum monitoring during tuberculosis treatment for predicting outcome: systematic review and meta-analysis. *Lancet Infect Dis* **2010**; 10:387–94.
131. Genestet C, Hodille E, Westeel E, et al. Subcultured *Mycobacterium tuberculosis* isolates on different growth media are fully representative of bacteria within clinical samples. *Tuberculosis* **2019**; 116:61–66.
132. Muliaditan M, Della Pasqua O. How long will treatment guidelines for TB continue to overlook variability in drug exposure? *J Antimicrob Chemother* **2019**; :dkz319.
133. Court R, Chirehwa MT, Wiesner L, et al. Quality assurance of rifampicin-containing fixed-drug combinations in South Africa: dosing implications. *Int J Tuberc Lung Dis Off J Int Union Tuberc Lung Dis* **2018**; 22:537–543.
134. Clarelli F, Liang J, Martinecz A, Heiland I, Abel zur Wiesch P. Multi-scale modeling of drug binding kinetics to predict drug efficacy. *Cell Mol Life Sci* **2019**; Available at: <http://link.springer.com/10.1007/s00018-019-03376-y>. Accessed 7 January 2020.
135. Abel zur Wiesch P, Abel S, Gkotz S, et al. Classic reaction kinetics can explain complex patterns of antibiotic action. *Sci Transl Med* **2015**; 7:287ra73.
136. Bergmiller T, Andersson AMC, Tomasek K, et al. Biased partitioning of the multidrug efflux pump AcrAB-TolC underlies long-lived phenotypic heterogeneity. *Science* **2017**; 356:311–315.
137. Pu Y, Zhao Z, Li Y, et al. Enhanced Efflux Activity Facilitates Drug Tolerance in Dormant Bacterial Cells. *Mol Cell* **2016**; 62:284–294.
138. Malmström J, Beck M, Schmidt A, Lange V, Deutsch EW, Aebersold R. Proteome-wide cellular protein concentrations of the human pathogen *Leptospira interrogans*. *Nature* **2009**; 460:762–5.
139. Gumbo T, Louie A, Deziel MR, et al. Concentration-Dependent *Mycobacterium tuberculosis* Killing and Prevention of Resistance by Rifampin. *Antimicrob Agents Chemother* **2007**; 51:3781–3788.
140. Martinecz A, Abel zur Wiesch P. Estimating treatment prolongation for persistent infections. *Pathog Dis* **2018**; 76.
141. Johnson PJT, Levin BR. Pharmacodynamics, Population Dynamics, and the Evolution of Persistence in *Staphylococcus aureus*. *PLoS Genet* **2013**; 9.
142. Lechner S, Lewis K, Bertram R. *Staphylococcus aureus* Persists Tolerant to Bactericidal Antibiotics. *J Mol Microbiol Biotechnol* **2012**; 22:235–244.
143. Claudi B, Spröte P, Chirkova A, et al. Phenotypic variation of salmonella in host tissues delays eradication by antimicrobial chemotherapy. *Cell* **2014**; 158:722–733.
144. Martinecz A, Clarelli F, Abel S, Abel zur Wiesch P. Reaction Kinetic Models of Antibiotic Heteroresistance. *Int J Mol Sci* **2019**; 20:3965.

145. Churchyard GJ. A stratified approach to tuberculosis treatment. *Nat Med* **2018**; 24:1639–1641.
146. Phillips PPJ, Mitnick CD, Neaton JD, Nahid P, Lienhardt C, Nunn AJ. Keeping phase III tuberculosis trials relevant: Adapting to a rapidly changing landscape. *PLOS Med* **2019**; 16:e1002767.
147. Noninferiority Trials. *N Engl J Med* **2018**; 378:303–305.
148. Mauri L, D’Agostino RB. Challenges in the Design and Interpretation of Noninferiority Trials. *N Engl J Med* **2017**; 377:1357–1367.

Paper 1



Multi-scale modeling of drug binding kinetics to predict drug efficacy

Fabrizio Clarelli¹ · Jingyi Liang¹ · Antal Martinecz¹ · Ines Heiland² · Pia Abel zur Wiesch^{1,3}

Received: 6 November 2019 / Revised: 6 November 2019 / Accepted: 12 November 2019 / Published online: 25 November 2019
© The Author(s) 2019

Abstract

Optimizing drug therapies for any disease requires a solid understanding of pharmacokinetics (the drug concentration at a given time point in different body compartments) and pharmacodynamics (the effect a drug has at a given concentration). Mathematical models are frequently used to infer drug concentrations over time based on infrequent sampling and/or in inaccessible body compartments. Models are also used to translate drug action from in vitro to in vivo conditions or from animal models to human patients. Recently, mathematical models that incorporate drug-target binding and subsequent downstream responses have been shown to advance our understanding and increase predictive power of drug efficacy predictions. We here discuss current approaches of modeling drug binding kinetics that aim at improving model-based drug development in the future. This in turn might aid in reducing the large number of failed clinical trials.

Keywords Pharmacodynamics · Pharmacokinetics · Binding kinetics · Antimicrobial activity · Mathematical biology · Differential equations

Introduction

Over the last 50 years, mathematical models describing drug pharmacokinetics (PK) and pharmacodynamics (PD) developed from the first concepts of simple relationships between drug concentration and its effects in the 1960 s [1–5] to advanced models that substantially improve our comprehension of the drug action mechanisms [6–10]. Advances in computational power and the improved accuracy and availability of experimental data have further fuelled model development.

We discuss mathematical modeling approaches that connect drug binding kinetics with its downstream effects across different scales for a multitude of different applications such as treatments for bacterial and viral diseases,

tumors, hypertension and mental illnesses. In this review, we will exemplarily highlight modeling approaches at different scales, starting with pharmacokinetic models including drug-target binding (“[Pharmacokinetic models](#)”), over traditional pharmacodynamic models (“[Traditional pharmacodynamic models](#)”) to various mechanistic pharmacodynamic drug-target binding models (“[Mechanistic pharmacodynamic models](#)”). We will conclude with a guide on how to select appropriate models for the system under investigation (“[How to select the appropriate model](#)”). An overview of the approaches discussed here is given in Fig. 1.

This review is not aiming at being a comprehensive description of all possible applications. We instead want to provide an overview of how mathematical models are used to describe PD and PK in a wide range of diseases, and more comprehensively describe PD models of drug-target binding in infectious diseases. Traditional pharmacodynamic models were introduced 50–100 years ago (e.g. the E_{\max} model and its derivative, the Hill function or sigmoidal E_{\max} model) [5, 11, 12]. Starting from these models, we discuss the evolution of target binding models and the underlying assumptions that determine in which scenarios those models can be used. At all scales, model complexity can vary considerably depending on the existing knowledge and details required to answer the pharmacological question to be addressed. We describe what can be gained by using more complex

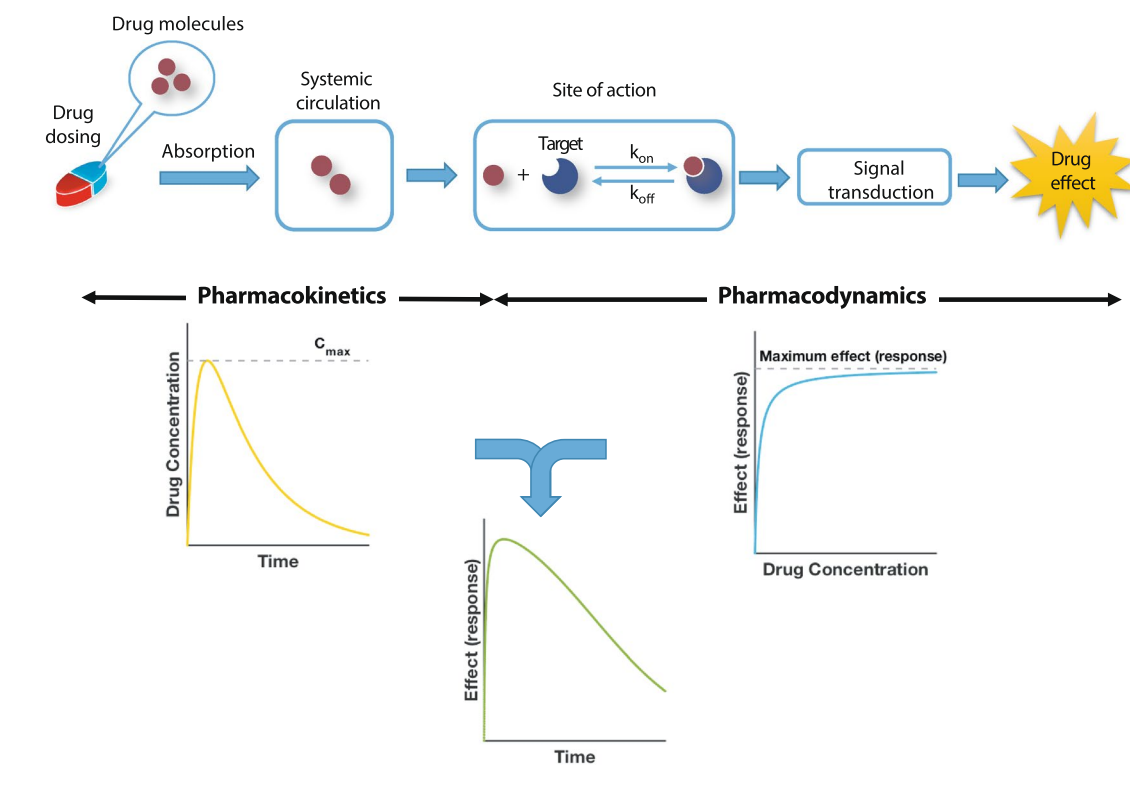
Fabrizio Clarelli and Jingyi Liang contributed equally to this work.

✉ Pia Abel zur Wiesch
pia.z.wiesch@uit.no

¹ Department of Pharmacy, Faculty of Health Sciences, UiT The Arctic University of Norway, 9037 Tromsø, Norway

² Department of Arctic and Marine Biology, UiT The Arctic University of Norway, 9037 Tromsø, Norway

³ Centre for Molecular Medicine Norway, Nordic EMBL Partnership, Blindern, P.O. Box 1137, 0318 Oslo, Norway



Section "Pharmacokinetic models"

- "Drug concentration affected by drug-target binding"
- "Binding kinetics to plasma proteins"

Section "Pharmacodynamic models"

- "Traditional pharmacodynamic models"
- "Mechanistic pharmacodynamic models"
- "Illustration of mechanistic antibiotic PD models"

Section "How to select the appropriate model"

Fig. 1 Schematic overview of PK/PD modeling and review outline. The process from drug administration to the emergence of effects consists of PK and PD components. PK describes the drug concentration profile in blood or at the site of action, i.e., the movement of drugs within the body after administration. PD describes how the given drug concentration in its target tissue elicits its effects. Mech-

anistically, this involves that drug molecules bind to their targets after reaching the desired site of action and induce various signaling transduction pathways, which ultimately, leads to biological effects/responses. Integrated PK/PD models allow us to investigate the drug efficacy over time under different dosing regimens

modeling approaches and which experimental data need to be available to parametrize those models. Of note, while the models we focus on describe antibacterial action, many of them may be applicable to other scenarios, for example tumor cells.

Pharmacokinetics and pharmacodynamics

PK describes the drug concentration profile in blood or at the site of action, i.e., the movement of drugs within the body after administration. PD describes how the given drug concentration in its target tissue elicits its effects. While multi-scale models that describe both PK and PD in

mechanistic detail have been developed [13], we discuss PK and PD approaches separately for clarity.

PK describes the "movement" of the drug in the human body, often subdivided in compartments. The different drug concentrations in different body compartments are governed by absorption, distribution, metabolism and elimination or excretion [14]. As soon as the drug enters the bloodstream, it can potentially be delivered to the site of action. Often, the target tissue in which the drug action occurs is inaccessible or not practical for routinely measuring local concentrations. Reliable estimates of the relationship between drug concentration in plasma and the target tissue are difficult to obtain and typically involve sophisticated models. While a detailed PK model has been successfully applied to tuberculosis to

describe local drug concentrations in the target tissue [10], the data used to validate the model came from an extremely invasive procedure (lung resection). As a result, data on local drug concentrations are rarely available and it is therefore estimated by other means, such as using a linear relationship.

Once the drug reaches the site of action, PD describes the relationship between drug concentration and its efficacy. It is important to decide which effect we are interested in, and how this is related to target occupancy. In some cases, such as virus neutralization by antibodies, the observable endpoint that defines efficacy can be easily ascribed to molecular mechanisms. Direct drug efficacy can be predicted by solely using binding kinetic models. In other therapeutic areas, the observable effects are very complex, such as behavioral changes in mental illnesses. These complex processes are presumed to be related to target occupancy, which in turn leads to an inhibition or activation of downstream signaling pathways. Indirect drug efficacy is therefore mathematically described as a function of the amount of bound target, $E = f(AT)$. This function can be either completely mechanistic when all contributing molecular pathways are known, or only partly mechanistic, such as when modeling drug-target binding and subsuming downstream mechanisms in a dose–response function.

Sometimes, the boundaries between modeling PK and PD are not well defined. It may, for example, depend on whether one defines an entire bacterium or the molecules that bind to the antibiotic inside the bacterial cell as the “target”. In the former case, diffusion across the bacterial cell envelope would be described by a pharmacodynamic model, and in the latter by a pharmacokinetic model. For the purpose of this review, we define mathematical models describing the drug penetration in a host’s target tissue as pharmacokinetics describing drug penetration into foreign organisms (e.g. bacteria) as pharmacodynamics, even though this distinction is somewhat arbitrary. Ultimately, these distinctions may be of secondary importance since the mathematical terms describing drug penetration into a body compartment or a bacterial cell can be part of either PK and PD model and both together are used to predict a drug’s effect-time profile for various dosing regimens (Fig. 1).

Binding kinetics

For our purposes, drug binding kinetics describes the interactions between a drug molecule A (ligand) and a specific or unspecific binding partner B (target or receptor), which form the ligand–receptor complex AB : $A + B \xrightleftharpoons[k_{\text{off}}]{k_{\text{on}}} AB$. In this reaction, k_{on} (units $\text{M}^{-1} \text{s}^{-1}$) is the association (binding) rate and k_{off} (units s^{-1}) is the dissociation rate per second. The dissociation constant K_D (unit M , $\text{M} = \text{mol per liter}$) is defined

as $K_D = \frac{k_{\text{off}}}{k_{\text{on}}}$. It describes the molar concentration at which half of the total binding partner molecules are occupied at equilibrium and is a measure of the binding affinity. The half-life of the complex AB is given by $t_{1/2} = \frac{\ln(2)}{k_{\text{off}}}$.

Pharmacokinetic models

Pharmacokinetic models are mostly used in the pre-clinical and clinical drug development to calculate required drug concentrations and treatment schedules. They usually describe drug absorption, distribution, processing and elimination but not the molecular mechanisms at the drug target site. Drug binding can affect local and global drug concentrations in various ways.

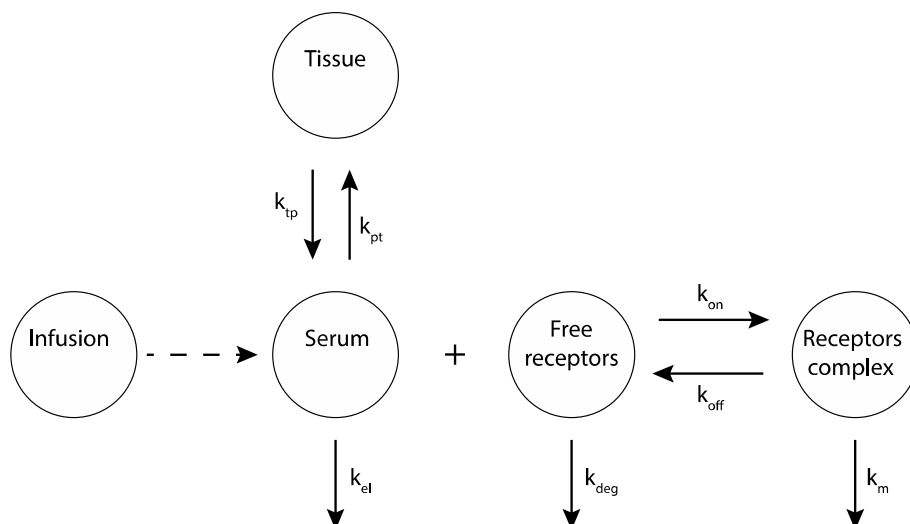
Drug concentration affected by drug-target binding

Mager and Sugiyama [15–18], combined PK and PD models to describe drugs that bind with high affinity, using the term “Target Mediated Drug Disposition” (TMDD, introduced by Levy [19]). TMDD refers to drug molecules that “bind with high affinity” to their targets [15], and a substantial amount of target is present and may exhibit a nonlinear PK behavior. To describe such behavior, the researchers introduced a two-compartment PK model with a PD target binding model [15]. The drug concentration in the central compartment (C_p) binds (k_{on}) with its targets to form a complex (DR) that has a total binding capacity R_{max} . The complex DR can dissociate (k_{off}) and degrade with a rate constant, k_m . In the central compartment (Serum), the drug can be eliminated (k_{el}) or can bind with non-specific targets in tissue (DT), see Fig. 2. Here, targets are assumed to be homogeneous, equivalent and independent. Traditional pharmacodynamic approaches (Hill-functions) are used to describe drug efficacy of the resulting local concentrations. The models consist of systems of ordinary differential equations, and they are used (with appropriate adjustments) to describe several examples like angiotensin-converting-enzyme inhibitor (ACE inhibitor), imirestat, warfarin, bosentan, monoamine oxidase type B inhibitors and natalizumab [17].

Binding kinetics to plasma proteins

Drugs taken up through the gastrointestinal system are transported in the blood. It should be noted that many drugs in the blood are bound to transport proteins, which is strongly influencing their free and thus effective concentration. As blood transport proteins un-specifically bind to small molecules, several drugs applied in combination, competitively affect their respective binding and release and thus the effective drug concentration. The effective drug concentration

Fig. 2 PK/PD model. The drug can be infused in the central compartment (Serum) and it can bind to non-specific targets in the tissue compartment. Also, the drug can be eliminated from the central compartment with a rate k_{el} , or bind to free targets (free receptors) to form a drug-target complex (receptor complex) with an association rate k_{on} and a dissociation rate k_{off} . The complex can degrade with a rate k_m , while free receptors can degrade with a rate k_{deg} . Modified from [15]



is often approximated as a constant percentage of plasma protein binding. However, this can be highly misleading as drug binding to either the targets or unspecific molecules decreases the free drug concentration [20]. The lower free drug concentration, in turn, shifts the equilibrium of drug-plasma protein binding and leads to a release of drug. Depending on the drug, modeling the kinetics of protein plasma binding can, therefore, be crucial [21]. As, furthermore, nutritional components as well as other drugs administered at the same time can be bound by the same transport proteins, other drugs as well as nutrition can affect free drug concentration and thus efficacy [22].

Pharmacodynamic models

Traditional pharmacodynamic models

Traditional PD models, i.e., E_{max} or Hill-functions can be derived using simplifying assumptions based upon the kinetics of drug-target binding. The effect of a drug at an observed site is related to the drug's concentration and time since administration. The relationship between the drug concentration and its effect is not linear [5], and the Hill function has been used to describe this relationship. The model is based on the idea that under certain assumptions (discussed below and in Fig. 3), the rate of change of the drug-target complex AT is given by the following equation:

$$\frac{dAT}{dt} = k_{on}(T_0 - AT(t))A - k_{off}AT(t), \quad (1)$$

where k_{on} is the association rate, k_{off} is the dissociation rate, T_0 is the initial number of targets and A is the drug concentration. At the equilibrium, Eq. (1) becomes

$$AT = \frac{T_0 A}{k_D + A}, \quad (2)$$

where $K_D = k_{off}/k_{on}$.

In its simplest form, E_{max} models are proportional to the concentration of the drug-target complex AT : $E = E_0 + \frac{E_{max}A}{EC_{50} + A}$. Here, E is the effect of the drug at a given concentration of drug A , E_{max} is the maximum effect, EC_{50} is the concentration of drug that produces the 50% of E_{max} and E_0 is the effect when $A=0$ (additional details in [1]). In 1910, Hill investigated the shape of the oxygen-hemoglobin saturation relationship [11, 23]. The shape of the curve was steeper than the predictions obtained with the steady-state solution (Eq. 2). To solve this issue, Hill added an exponential parameter to the model, the Hill exponent γ [23]. Thus, Eq. (2) can be easily transformed into the Hill function (Eq. (3) and Eq. A in Fig. 3):

$$E = E_0 + \frac{E_{max}A^\gamma}{EC_{50}^\gamma + A^\gamma}. \quad (3)$$

For drugs that show a steeper relationship between drug exposure and effect than the predictions with the E_{max} model, a Hill-function (also called sigmoidal E_{max} model, even though simple E_{max} models are also sigmoidal) can be used. The simplicity of E_{max} models results in their frequent application when little is known about the mechanisms of action for a given drug. However, it is important to realize that these models rely on a large number of assumptions (many of which are likely invalid in reality):

1. The number of target molecules is constant. In the case of intracellular targets, the number of targets per cell, i.e., the concentration is constant. If binding is modeled

- as a multistep process to a macromolecule, the number of binding sites per macromolecule is constant.
2. Independence of receptors. The probability of a receptor to bind a drug molecule is not affected by the number of other bound complexes. This implies that it is not important in which order they bind.
 3. The distribution of receptors is homogeneous. The intracellular space and diffusion are not included in these models, and for this reason, each receptor has the same probability of contact and therefore binding with the ligand.
 4. Reversible binding has biologically reversible consequences. This assumption is violated when cells, such as bacteria or cancer cells, die due to the effect of bound targets. Even if the drug afterwards dissociates from its target, the cell death is irreversible.
 5. No changes in the number of target molecules in the entire system, e.g., in a bacterial population or in a tumor. This precludes cellular growth or death.
 6. All targets or receptors are equivalent. This means that all the targets that bind the drug with the same rate elicit the same response to the drug.
 7. The time required to pass through the cell envelope is negligible. Under this assumption, the drug concentration outside the cell is equal to the drug concentration inside the cell.
 8. The drug concentration is constant during the time required to reach the equilibrium. This ensures that we can consider only the steady-state for each value of drug concentration, and it is sufficient to know only the rate $k_D = k_{\text{off}}/k_{\text{on}}$ (see Eq. 2).
 9. The rates of drug-target association and dissociation are very fast. Since the equilibrium happens when the derivative is zero (no more variation in time), one of the assumptions is that the association and the dissociation rates have to be fast enough so that the time to reach the equilibrium can be neglected. It is important to remember that, if the reaction rates are not fast enough, we need to use the full Eq. (1) instead of using only its equilibrium approximation in Eq. (2).

Mechanistic pharmacodynamic models

To overcome the limitations of empirical PD models, more and more detailed mechanistic models of drug binding and response have been developed in recent years. We start out with discussing approaches of increasing complexity that describe drug-target binding

Modeling drug-target binding

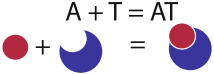
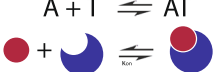

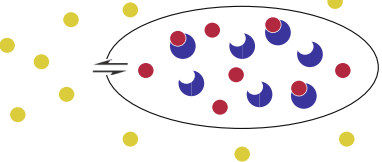
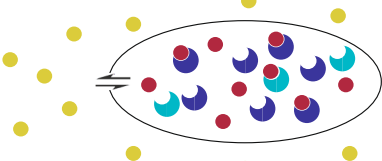
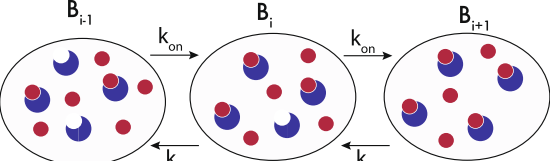
The use of mechanistic PD models for describing antibacterial action was pioneered by Hedges in 1966 [24]. In this work,

the authors describe the adsorption kinetics of a lethal amount of the bacterial toxin colicin by bacteria (e.g. *E. coli*). In this model, by analogy with photons in radiation, the targets are hit (and not bound) by the drug molecules. The model includes assumptions 1–9, which are listed above. The model describes two phases, in the first one the colicin is absorbed by receptors, and, in the second one, the lethal effect happens after the completion of phase 1 [4]. Finally, the lethal effect is defined once r targets (the threshold) are occupied ($r < n$).

Since then, models of increasing complexity have been employed. Figure 3 summarizes the main developments in the modeling of drug-target binding kinetics, starting from traditional Hill functions and successively relaxing assumptions, culminating with the equations describing the entire population dynamics of bacteria in response to drug-target binding.

The role of drug-target residence time Both traditional PD models and the earliest mechanistic PD model by Hedges [24] assume that the binding equilibrium is instantaneously reached. This makes the implicit assumption that only the equilibrium constant $K_D = k_{\text{off}}/k_{\text{on}}$ determines drug efficacy. The magnitude of the association rate k_{on} and dissociation rate k_{off} , and thereby binding kinetics, is assumed to have negligible influence. This has been challenged by Copeland et al. [25], who develop a concept from Ehrlich [26]: “a drug is efficacious only so long as it is bound to, and modulating the action of, its physiological target(s)”. The focus is, therefore on the crucial role played by the drug-target complex. In other words, the residence time ($t_{\text{red}} = 1/k_{\text{off}}$, which depends on the dissociation rate) of the drug-target complex is more important than the simple affinity. For the authors (see [25, 27]), the dissociation rate k_{off} is more important than k_{on} , due to several constraints acting on k_{on} (it can range considerably), while the dissociation rate k_{off} is entirely dependent on the reaction kinetics between the drug molecules and their targets. They, therefore argue that the optimization of the dissociation rate is of primary importance. The authors applied this modeling concept to viruses, inhibitors of steroid 5 β -reductase, inhibitors of purine nucleoside phosphorylase (PNP) and angiotensin II type 1 receptor (ATR1). Other interesting studies modeling the kinetics of drug-target binding rather than instantaneous equilibria include Tonge [28], Shimada [29] and Walkup [30].

Models describing multimer targets The majority of models assume that the target is one molecule with one single binding site. Many drug targets are homo- or hetero-multimers with multiple binding sites. One example is homotrimeric spikes on the surface of HIV virions that enable the virion to enter host cells. This has been modeled by Magnus et al. [31–33]: the authors estimate the number of antibodies (called stoichiometries) required for neutralizing a sin-

<ul style="list-style-type: none"> ● Extracellular drug ● Intracellular drug ☾ Free target ● ☾ Bound target ☾ Free unspec. target ● ☾ Bound unspec. target 	<p>A Section "Traditional pharmacodynamic models"</p> $A + T = AT$  $E = E_0 + \frac{E_{max}AY}{EA_{50}^Y + AY}$																					
<p>B Section "The role of drug-target residence time"</p> <p>Release assumption 9</p> $A + T \rightleftharpoons AT$  $\frac{dAT}{dt} = k_{on}(T_0 - AT(t))A - k_{off}AT(t)$	<p>C Section "Drug concentration affected by drug-target binding"</p> <p>Release assumptions 8+9</p>  $\begin{cases} \frac{dAT}{dt} = k_{on}(T_0 - AT(t))A(t) - k_{off}AT(t) \\ \frac{dA}{dt} = -k_{on}(T_0 - AT(t))A(t) + k_{off}AT(t) \end{cases}$																					
<p>D Section "Drug-target binding with a diffusion barrier"</p> <p>Release assumptions 7+8+9</p>  $\begin{cases} \frac{dA_e}{dt} = -p \left(A_e \frac{V_i}{V_e} - A_i \right) \\ \frac{dA_i}{dt} = p \left(A_e \frac{V_i}{V_e} - A_i \right) - k_{on}A_iT + k_{off}AT \\ \frac{dT}{dt} = -k_{on}A_iT + k_{off}AT \\ \frac{dAT}{dt} = k_{on}A_iT - k_{off}AT \end{cases}$	<p>E Section "Unspecific binding"</p> <p>Release assumptions 7+8+9</p> <p>With unpecific binding</p>  $\begin{cases} \frac{dA_e}{dt} = -p \left(A_e \frac{V_i}{V_e} - A_i \right) \\ \frac{dA_i}{dt} = p \left(A_e \frac{V_i}{V_e} - A_i \right) - k_{on}A_iT + k_{off}AT - k_{uf}A_iU + k_{ur}AU \\ \frac{dT}{dt} = -k_{on}A_iT + k_{off}AT \\ \frac{dAT}{dt} = k_{on}A_iT - k_{off}AT \\ \frac{dU}{dt} = -k_{uf}A_iU + k_{ur}UT \\ \frac{dUT}{dt} = k_{uf}A_iU - k_{ur}UT \end{cases}$																					
<p>F Section "Changes in the numbers of target molecules"</p> <p>Release assumptions 5+6+8+9</p>  $\begin{cases} \frac{dB_x}{dt} = k_{on}(n-x+1)AB_{x-1} - k_{off}xB_x - k_{on}(n-x)AB_x \\ \dots + k_{off}(x+1)B_{x+1} + \rho_x - r_xB_x \frac{K - \sum_{j=0}^n B_j}{K} - d_xB_x \\ \frac{dA}{dt} = -k_{on} \sum_{x=0}^{n-1} (n-x)AB_x + k_{off} \sum_{x=1}^n xB_x \\ \text{where: } \rho_x = 2 \sum_{i=x}^n f_{i,x} r_i B_i \frac{K - \sum_{j=0}^n B_j}{K} \end{cases}$	<p style="text-align: center;">Parameters</p> <table style="width: 100%; border-collapse: collapse;"> <tr> <td style="width: 33%;">E_0 Effect for $A=0$</td> <td style="width: 33%;">k_{on} Association rate</td> <td style="width: 33%;">U Unspecific free target</td> </tr> <tr> <td>EC_{50} Conc. for 50% E_{max}</td> <td>k_{off} Dissociation rate</td> <td>UT Unspecific drug-target complex</td> </tr> <tr> <td>E_{max} Max effect</td> <td>V_i Internal volume</td> <td>B_x Bacteria with i bound targets</td> </tr> <tr> <td>A Drug concentration</td> <td>V_e External volume</td> <td>r_x Growth rate with x bound targets</td> </tr> <tr> <td>AT Drug-target complex</td> <td>A_i Internal drug conc.</td> <td>d_x Death rate with x bound targets</td> </tr> <tr> <td>T_{max} (or n) Total # targets</td> <td>A_e External drug conc.</td> <td>K Carrying capacity</td> </tr> <tr> <td>T Free targets</td> <td>p Coefficient of permeation</td> <td>f_{ix} Hypergeometric distribution</td> </tr> </table>	E_0 Effect for $A=0$	k_{on} Association rate	U Unspecific free target	EC_{50} Conc. for 50% E_{max}	k_{off} Dissociation rate	UT Unspecific drug-target complex	E_{max} Max effect	V_i Internal volume	B_x Bacteria with i bound targets	A Drug concentration	V_e External volume	r_x Growth rate with x bound targets	AT Drug-target complex	A_i Internal drug conc.	d_x Death rate with x bound targets	T_{max} (or n) Total # targets	A_e External drug conc.	K Carrying capacity	T Free targets	p Coefficient of permeation	f_{ix} Hypergeometric distribution
E_0 Effect for $A=0$	k_{on} Association rate	U Unspecific free target																				
EC_{50} Conc. for 50% E_{max}	k_{off} Dissociation rate	UT Unspecific drug-target complex																				
E_{max} Max effect	V_i Internal volume	B_x Bacteria with i bound targets																				
A Drug concentration	V_e External volume	r_x Growth rate with x bound targets																				
AT Drug-target complex	A_i Internal drug conc.	d_x Death rate with x bound targets																				
T_{max} (or n) Total # targets	A_e External drug conc.	K Carrying capacity																				
T Free targets	p Coefficient of permeation	f_{ix} Hypergeometric distribution																				

gle virion and a whole virion population. The number of (HIV) spikes necessary for cell entry, combined with the minimal number of antibodies able to neutralize one spike (or trimer), permits to estimate how many antibodies are needed to neutralize a single virion and an entire population of virions. However, this estimation is not trivial as Fig. 4 illustrates: if there are more binding sites per trimer than needed for neutralization, a substantial fraction of antibod-

ies will bind "unnecessarily" to already neutralized trimers, thereby reducing efficacy.

Here, the assumption of equivalent receptors (assumption 6 on the list in "Traditional pharmacodynamic models") is invalid, because the same number of bound targets, combined differently, can have different outcomes.

Fig. 3 Overview of the main developments in modeling PD. In this figure, we give an overview of modeling approaches with increasing complexity that are commonly used to describe the molecular mechanisms of anti-infective drugs. The left column refers to the respective section in the text that describes the model as well a list of assumptions that are relaxed compared to a traditional Hill function. A drawing in the central column illustrates the model. Finally, the column on the right gives the respective equations. The parameters are described in the table below. In **a**, we describe the reaction at the equilibrium (E_{\max} , Hill), i.e., the time to reach the equilibrium of the reaction is neglected (“Traditional pharmacodynamic models”). In **b**, we relax the assumption 9 of the instantaneous equilibrium, i.e., we have the complete kinetic equation to describe the variation in time of the drug-target complex (see “The role of drug-target residence time”). In **c**, we release assumption 8 of constant drug concentrations, i.e., we add an equation describing a variable drug concentration. This can be a PK model added to our binding kinetics equation (“Drug concentration affected by drug-target binding”). In **d**, we release assumption 7. In this way, the internal drug concentration is not equal to the external drug concentration, i.e., we need an equation for the external and one for the internal drug concentration (“Drug-target binding with a diffusion barrier”). In **e**, we add unspecific targets with their own equations, and drug molecules can associate/dissociate to unspecific targets. Thus, fewer drug molecules are available for drug action (“Unspecific binding”). In **f**, we introduce the replication and death of bacteria, which leads to changes in the number of target molecules, i.e., we relax assumption 4 and 5, but not 6 and 7. To do so, bacteria are classified in compartments according to the number of bound target molecules. Each compartment is described by separate equation. (“Changes in the numbers of target molecules”)

Drug-target binding with a diffusion barrier In some cases, we need to extend the model to include the diffusion throughout the bacterial cell envelope for a variable drug concentration. Notably, the influx and efflux of drug molecules across the cell envelope are regulated by multiple mechanisms, which depends on the structure of the cell envelope and characteristics of drug molecules. Mathematical models on how drug molecules cross the cell envelope have been developed with different complexity levels (e.g. [7, 34]). However, the modeling approach can be limited due to lack of knowledge on the specific mechanisms. Assuming that the drug molecules only enter into the cell by diffusion, as shown in Fig. 3d (passive diffusion), we consider drug molecules outside bacterial cells that need to traverse the cell membrane by diffusion.

$$\begin{aligned}
 \frac{dA_e}{dt} &= -p \left(A_e \frac{V_i}{V_e} - A_i \right) \\
 \frac{dA_i}{dt} &= p \left(A_e \frac{V_i}{V_e} - A_i \right) - k_{\text{on}} A_i T + k_{\text{off}} AT \\
 \frac{dT}{dt} &= -k_{\text{on}} A_i T + k_{\text{off}} AT \\
 \frac{dAT}{dt} &= k_{\text{on}} A_i T - k_{\text{off}} AT.
 \end{aligned}
 \tag{4}$$

Here, A_e is the external number of antibiotic molecules, A_i is the intracellular number of antibiotic molecules, T is

the number of free targets, AT is the number of drug-target complexes, p is proportional to the permeability.

Unspecific binding An additional step involves the inclusion of unspecific binding by adding terms that describe how a drug A binds to an unspecific binding site U to form an unspecific complex AU (see Fig. 3e). Unspecific binding partners are often assumed to be ubiquitous, such that binding never saturates and therefore the number of free binding sites U does not change (i.e., does not need to be modeled explicitly). The unspecific binding rate is denoted as k_{uf} and the unspecific dissociation rate as k_{ur} . This model can be expressed as follows [7]:

$$\begin{aligned}
 \frac{dA_e}{dt} &= -p \left(A_e \frac{V_i}{V_e} - A_i \right) \\
 \frac{dA_i}{dt} &= p \left(A_e \frac{V_i}{V_e} - A_i \right) - k_{\text{on}} A_i T + k_{\text{off}} AT - k_{\text{uf}} A_i U + k_{\text{ur}} AU \\
 \frac{dT}{dt} &= -k_{\text{on}} A_i T + k_{\text{off}} AT \\
 \frac{dAT}{dt} &= k_{\text{on}} A_i T - k_{\text{off}} AT \\
 \frac{dU}{dt} &= -k_{\text{uf}} A_i U + k_{\text{ur}} UT \\
 \frac{dUT}{dt} &= k_{\text{uf}} A_i U - k_{\text{ur}} UT.
 \end{aligned}
 \tag{5}$$

Changes in the numbers of target molecules For antibiotics and anti-cancer drugs, the number of targets can change over time, because cancer cells or bacteria replicate (violating assumption 5). At the same time, bacteria or cancer cells die due to the effect of bound targets. This violates assumption 4, i.e., that a chemically reversible process is also biologically reversible: Let us assume that n bound targets kill a bacterial or cancer cell and that exactly n targets are currently bound to a dead cell. One drug-target complex may dissociate such that only $n-1$ targets are bound, but this will not lead to a resurrection of the dead cell. Thus, if the desired pharmacological effect means minimizing a cell population and that cell population replicates and dies, the binding kinetics will be affected by the dynamics of that cell population. This can only be neglected when the action of the drug is sufficiently fast such that the cells neither replicate nor die until the chemical reaction has reached equilibrium.

To incorporate both bacterial growth and death into the model, living bacteria can be classified into compartments based on the number of bound target molecules x [6], out of a total of n target molecules per bacterium. Here, bacterial cells with n target molecules are equivalent to molecules with n independent binding sites. The association

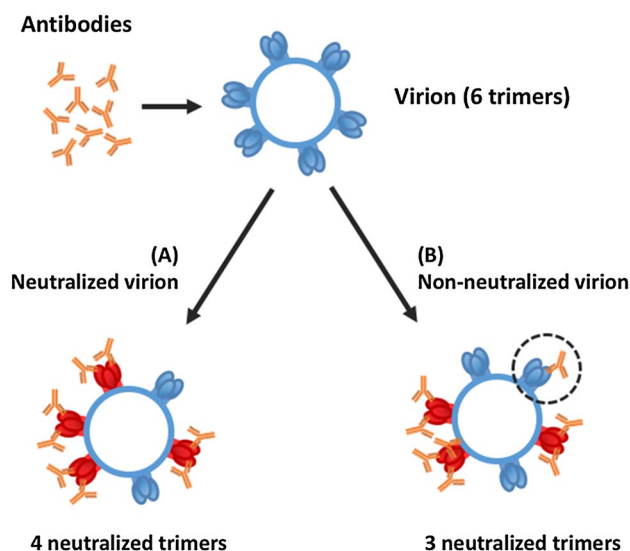


Fig. 4 Virion neutralization. An example of how random antibody binding can have different effects. Here, eight antibodies bind in two different ways to a virion with six trimers. In this example, the minimum number of bound trimers to neutralize a virion is four with at least two antibodies each. In (A), the virion is neutralized, four different trimers are bound to two antibodies. In (B), one trimer is bound to three antibodies and one trimer is bound with only one antibody (dashed circle), then there are only three trimers neutralized. Modified from [31]

and dissociation of the target and antibiotic molecules are described by the following system of differential equations.

$$\begin{aligned} \frac{dB_x}{dt} &= k_{\text{on}}(n-x-1)AB_{x-1} - k_{\text{off}}xB_x - k_{\text{on}}(n-x)AB_x + k_{\text{off}}(x+1)B_{x+1} + \rho_x - r_xB_x \frac{K - \sum_{j=0}^n B_j}{K} - d_xB_x \\ \frac{dA}{dt} &= -k_{\text{on}} \sum_{x=0}^{n-1} (n-x)AB_x + k_{\text{off}} \sum_{x=1}^n xB_x \\ \rho_x &= 2 \sum_{i=x}^n f_{i,x} r_i B_i \frac{K - \sum_{j=0}^n B_j}{K}, \end{aligned} \quad (6)$$

where living bacteria replicate at a rate r_x , a function of the number of bound target molecules x , as well as they die at a rate d_x , a function of the bound targets x . K is the carrying capacity of the total bacterial population.

The number of targets per bacterium is constant, i.e., it doubles when bacteria duplicate, but the number x of bound targets in the mother cells remains constant during the duplication and it is distributed in the two daughter cells following the hypergeometric distribution $f_{i,x}$ (see Fig. 3f).

Linking target occupancy to drug efficacy

Drug efficacy is the capacity of a drug to produce an effect after binding to its target. Various measures are used to quantitatively evaluate the drug efficacy in *in vitro*, *ex vivo* and *in vivo* studies. Binding kinetics and the residence time

of the drug-target complex gain more and more attention and are recognized as reliable indicators for drug efficacy. The traditional PK/PD approach to predict drug efficacy by correlating an observable drug effect to measures of drug exposure such as peak concentration (C_{max}) or average concentration (area under the curve, AUC) is based on assumptions of a rapid equilibrium between the free and bound drug (Fig. 3a). PK/PD models that incorporate the complete kinetic scheme of drug-target binding (Fig. 3b–f) enable us to predict drug efficacy from target occupancy under non-equilibrium conditions, which is more likely to occur in an open systems such as the human body [19]. For drugs that slowly dissociate from their targets, the free drug and drug-target will not be in rapid equilibrium. In this case, the traditional PK/PD model may underpredict the drug effect [22], whereas models with time-dependent drug-target binding will be more mechanistic and suitable for analyzing the relationship between drug concentration and efficacy [21].

However, it is challenging to estimate the relationship (i.e., define the function effect $E=f(AT)$, see “[Pharmacokinetics and pharmacodynamics](#)”) between target occupancy and drug effects. Here we summarize models incorporating a detailed kinetic scheme of drug-target binding and a function f for various diseases in Table 1.

The simplest approach (and the implicit assumption in most PD models) is to assume a linear relationship between target occupancy and drug effects. For example, models of calcium channel blocker in essential hypertension patients [29], gastric acid secretion in dogs [39], antiplatelet effects

of aspirin and ibuprofen in human [35] and inhibition of DPP-4 activity in patients with type 2 diabetes [40], use positive or negative linear functions to convert the level of drug-target complex to the corresponding pharmacological responses. When the total number of targets at the site of action is uncertain or impossible to be measured, apparent fractional receptor occupancy can be used by setting the receptor level to one unit [36]. Some models define a linear correlation with certain conditions. In a model of paLpxC inhibitor in animal studies of *Pseudomonas* infection, Walkup et al. [30] assume a saturation limit of the drug-induced killing of bacteria that the killing rate is linearly increased to target occupancy between the minimum and maximum target occupancy required for the antibacterial effects. Similarly, we earlier defined [6] that the replication

Table 1 Mathematical models with different drug efficacy functions by which drug efficacy is defined as a function of the target occupancy

Function type	Drug (A)	Target (T)	Effect (E)	Function description	References
Linear function	Calcium channel antagonists	Calcium channel	Antihypertensive effect	$\frac{dE}{dt} = k_{on}A(E_{max} - E) - k_{off}E$	[29]
Linear function	Two drugs: aspirin and NSAIDs (e.g. ibuprofen (A_{ibu}))	Platelet cyclooxygenase-1	Inhibition on platelet aggregation (aspirin: irreversible acetylation; ibuprofen: reversible inhibition)	$E = (T + A_{ibu}T)(1 - \alpha A_{ibu})$ α : coefficient for ibuprofen efficacy	[35]
Linear function	Buprenorphine	μ -Opioid receptor in the brain	Respiratory depressant and antinociceptive effects	Respiratory depressant effect $E = E_{baseline}(1 - \alpha\rho_{app})$ Antinociceptive effects $E = \frac{E_{baseline}}{1 - \rho_{app}}$ ρ_{app} : apparent fractional receptor occupancy E_0 : baseline response α : intrinsic activity of the drug	[36]
Linear function (with condition)	Translation inhibiting antibiotics (e.g. tetracycline)	Ribosomes	Bacteriostatic action	Growth rate of bacteria is $r_{growth}(f_c) = \begin{cases} 0 & f_{free} < f_c \\ \frac{1}{1-f_c}f_{free} - f_c & f_{free} > f_c \end{cases}$ f_{free} : the fraction of unbound drug f_c : critical threshold	[27]
Linear function (with condition)	LpxC inhibitors	LpxC enzyme	Killing of <i>Pseudomonas aeruginosa</i>	The killing rate of bacteria $k_{kill} \cdot AT$ (k_{kill} is the maximum killing rate constant) when AT is between the minimum and maximum target occupancy required for the antibacterial effects	[22]
Sigmoid function (Hill equation)	Antipsychotic drugs	Dopamine D_2 receptor	Cellular cAMP response for competition binding between antagonists (A_0) and dopamine (A_d) to D_2 receptor	Overall effect on the rate of cAMP production by receptor antagonists and dopamine is $\left(k_0 + K_{max} \frac{(A_0T)^n}{(A_0T_0)^n + (A_0T)^n} \right) \left(1 - \frac{(A_dT)^n}{(A_dT_0)^n + (A_dT)^n} \right)$	[37]
Sigmoid function (Hill equation)	Trastuzumab-valine-citrulline-monomethyl auristatin E	Tubulin	Killing of tumor cell	Killing rate $r(AT) = K \max \frac{AT^m}{AT_0^m + AT^m}$	[38]

rate of bacteria linearly depends on the uninhibited ribosomes above a critical threshold.

For some cases, experimental evidence also suggests a nonlinear relationship between observed receptor occupancies and effects [41], and several models that use sigmoid functions to define the relationship between the level of drug-target complex and the pharmacological effects [37, 38]. For instance, a recent *in vitro* and *in silico* combined model consists of competitive binding between D_2 receptor antagonist and endogenous dopamine as well as the downstream response of cellular cyclic adenosine monophosphate (cAMP) [37]. The production rate of cAMP is oppositely affected by the concentration of D_2 -receptor-antagonist complex and receptor-dopamine complex, using a combination of Hill equations.

Alternatively, PD/PK models that incorporate explicit mechanistic simulation of downstream processes initiated by drug-target binding is possible. With increasing knowledge about the molecular mechanisms of diseases, we can develop increasingly complex models of intracellular drug responses. This approach is especially useful when the direct relationship between target occupancy and response is complicated and uncertain. Models demonstrate that the binding of drug-target can induce downstream signal transduction and feedback mechanisms, therefore, affect the drug efficacy at a network level [42].

Illustration of mechanistic antibiotic PD models

Figure 5 illustrates the observable endpoints of antibiotic efficacy *in vitro* and crucial aspects of antibiotic action that can be described by mechanistic PD models.

The aim of antibiotic treatment is to reduce the number of bacteria in a patient's body. The efficacy of antibiotics to do so is typically assessed by so-called time-kill curves (Fig. 5a), where bacterial counts are measured over time after exposure to antibiotics at increasing concentrations. These can be used to estimate the PD curves for a given drug-bacteria combination in a given environment (Fig. 5b). It is important to note that PD curves measure the net population change rather than the replication (Fig. 5c) and death of bacteria (Fig. 5d) separately. As a result, a zero-net change in the population size at the minimal concentration at which bacterial growth stops, i.e., when the net change in the population is exactly zero (minimal inhibitory concentration or MIC) does not necessarily mean that there is no replication of bacteria in a given sample, a very high replication and death rate that neutralize each other would yield the same observation. Figure 5c, d also demonstrate mechanisms that can alter the effects of antibiotic action: upon the replication of bacteria, the bound targets in cells are distributed (randomly) among the daughter cells. If drug-target association and dissociation are on a comparable timescale to

replication rates, this can affect the efficiency of the given antibiotic (“Changes in the numbers of target molecules”). Furthermore, after a cell dies, its targets do not immediately disappear, and these targets can leak into the extracellular space. Therefore, even replication and death can eventually lower the free extracellular antibiotic concentrations, which in turn can affect the antibiotic action on other cells.

How to select the appropriate model

Traditional PD models have substantial advantages, such as their simplicity and the fact that a relatively moderate amount of experimental data is needed to parametrize them. However, traditional PD models are typically unable to capture a variety of PD effects. When such effects are observed, an explicit, mechanistic model may be a better choice because “tweaking” traditional approaches may result in equally complex mathematical models that, in addition to their complexity, have no mechanistic basis and are challenging to parametrize with experimental data. Table 2 provides an overview of PD effects (with a focus on antibiotics, but similar effects have been observed in other systems) that can be easily described using mechanistic models.

Post-antibiotic effect

Sometimes, after antibiotic exposure, bacterial regrowth is delayed. This is called “post-antibiotic effect” (PAE). The reason is that the drug-target complex requires some time to dissociate and free the targets, as well as the drug molecules to leave the intracellular space. To explain this effect, we need models with explicit association and dissociation terms, but also a growth rate and a death rate as a function of the number of bound targets are helpful. Models with the association and dissociation rates can explain this effect as demonstrated by Walkup [30] and Abel zur Wiesch [6, 7].

Inoculum effect

A second challenge is to determine reliable drug dosing able to clear an infection. Predictions for optimal drug concentrations can be distorted by the initial bacterial concentration, i.e., increased initial bacterial concentration can imply a decreased antibiotic efficacy [43]. A useful review of the inoculum effect *in vivo* and *in vitro* with beta-lactams (where this effect is pronounced) is given in [44]. One explanation for this effect relates to the fact that the change in the drug availability after binding can be a function of the drug affinity. This effect can be explained by a kinetic model of binding—intuitively, drug molecules that are already bound to their targets cannot kill more bacteria [6, 8].

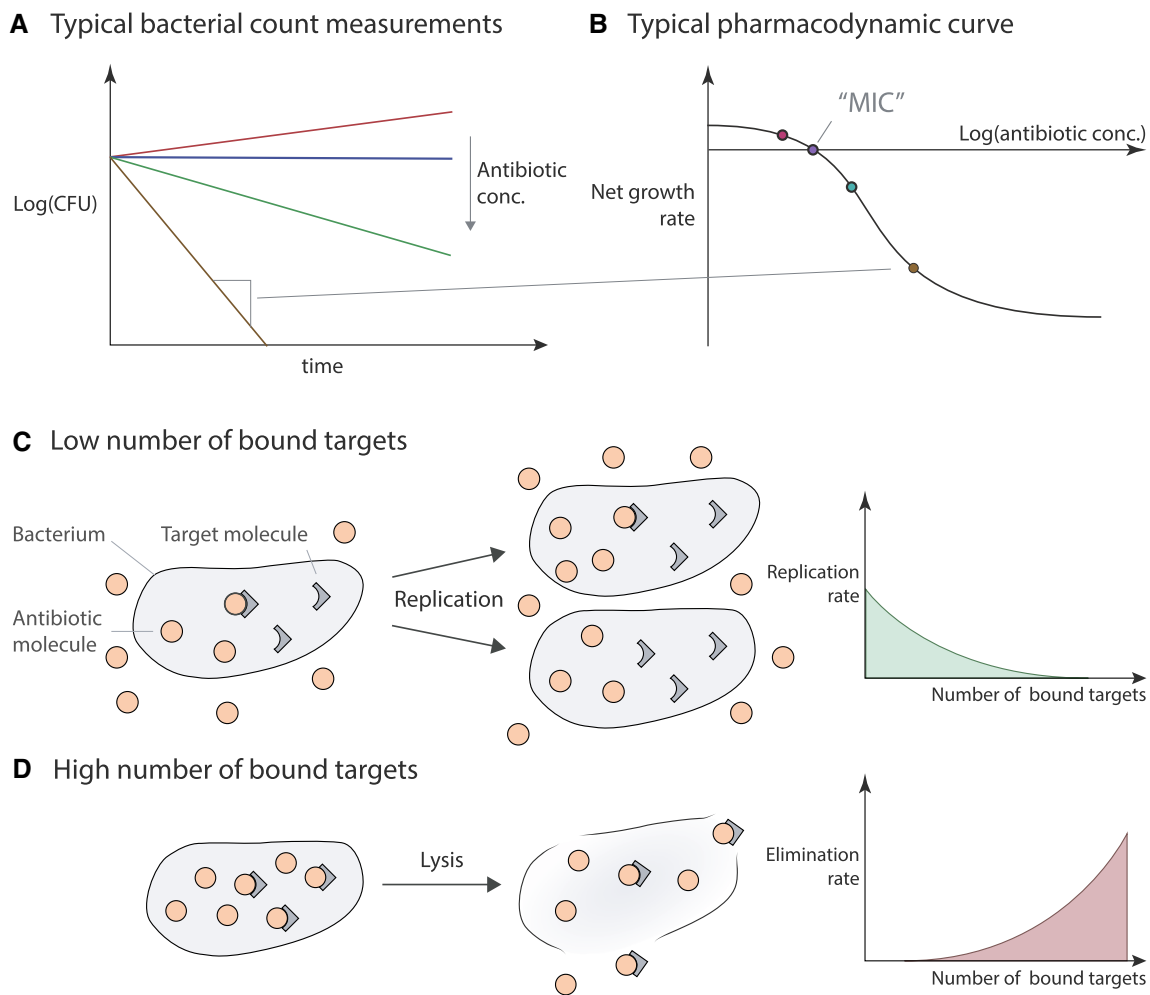


Fig. 5 Illustration of the modeled antibiotic action—**a** illustrates typically measured bacterial count measurements over time. These measurements are often used to create “pharmacodynamic curves” (**b**) that define the relationship between the net growth of bacteria (the total replication minus death) at a given antibiotic concentration. In this framework, the minimal inhibitory concentration (MIC) is the concentration when the net growth rate predicted by pharmacodynamic curve is zero. In drug-target binding models, the number of bound

targets (at a given intracellular antibiotic concentration) affects either bacterial replication, death, or both (**c**, **d**). **c** Illustrates the replication part, in addition, it also illustrates the assumption that during this process the bound targets are distributed randomly among daughter cells [6]. **d** Illustrates the bacterial elimination part, it also illustrates the possibility that upon elimination, bacteria lyse and release their contents into the extracellular space. This, in turn, may eventually reduce the free antibiotic concentrations

Heterogeneous population

In reality, the bacterial population can be heterogeneous. Several parameters can change, and this has consequences on the behavior of the bacterial population. For example, parameters can include the minimum inhibitory concentration or the minimum bactericidal concentration, the total number of target molecules, the permeability of the cell membrane, the minimum threshold of bound targets to kill bacteria and the growth rate and the death rates described as a function of the number of bound targets. All of these parameters and functions are important in determining the efficacy of a drug and can be easily incorporated into

mechanistic models [6] by using distributions rather than fixed parameter values to inform a model.

Synergistic and antagonistic action of drugs

It is crucial to determine when multiple antibiotics can have synergistic or antagonistic effects. Understanding how bacterial populations react to multi-drug treatment can be surprisingly complex. In particular, it is unclear what the “null-hypothesis” for an independent action of two antibiotics should be, and this precludes determining synergy or antagonism. Several models describe the independent action of two drugs, for example, Loewe additivity and Bliss

Table 2 Summary of effects explained by the models in the last column

Effect	Description	Models including this effect
Post-antibiotic effect (PAE)	PAE is a delayed bacterial regrowth after antibiotic exposure	[6, 7, 30]
Inoculum effect	The efficacy of a drug concentration can be a function of the initial bacterial concentration. Increased initial bacterial concentration can imply decreased antibiotic efficacy	[6, 8, 43, 44]
Heterogeneous population	The bacterial population can be heterogeneous, i.e. with different values in: (a) Minimum inhibitory concentration (b) Minimum bactericidal concentration (c) Total number of target molecules (d) Permeability of the cell membrane (e) Minimum threshold of bound targets to kill bacteria (f) Growth rate as a function of bound targets (g) Death rate as a function of bound targets. All of these parameters and functions are important in the efficacy of the drug.	[6]
Off-target binding	Unspecific targets that can bind to the drug molecules. This implies that the total amount of drug molecules available to bind to main targets (action of the drug) can be smaller	[6]
Synergistic and antagonistic action of drugs	Loewe additivity and Bliss independence are compared. Bliss independence is suggested in the presence of different targets. Loewe additivity when the antimicrobials target the same component	[9]

independence. Baeder et al. [9] described a multi-hit model (following the idea of Hedges [24]) in which bacteria die when a given number of targets are “hit” by antimicrobials. Bliss independence assumes that there is no interaction between antimicrobials. While, Loewe additivity represents a measure of antimicrobials interaction, i.e., if there is synergy or antagonism. The authors suggest which model is best, based on the antimicrobials. In particular, Bliss independence is the best choice in the presence of different targets, while Loewe additivity is recommended when the two antimicrobials target the same component.

Conclusions

Over the last 50 years, PK and PD modeling have shifted toward mechanistic approaches. In particular, the development of mechanistic PD modeling allows a deeper understanding of drug action, implying a broad array of future applications [45], such as antivirals, antibiotics, hypertension, inhibitors and any application that involves target binding. Here, we have discussed mathematical models describing molecular mechanisms of the drug action, and how these models can be applied to several diseases, which underlying assumptions we need and which phenomena can be captured. It is important to be aware of these assumptions.

For example in viruses, which neither replicate independently or can irreversibly die, the dynamics of the viral population can be neglected and viruses can be idealized as macromolecules with multiple binding sites [46]. Bacteria and cancer cells continuously divide and thereby reproduce the drug target. The chemically reversible processes

(binding) are coupled to biologically irreversible processes (death). Depending on the speed of population turnover, a simplified model of a bacterium as a macromolecule will fail to adequately capture drug efficacy. It is also important to consider which parameters have been experimentally determined and to judge how much confidence one can have in those parameters. When choosing a more complex model, one should always be aware of the dangers of overparametrization if the parameters are not well known. However, when model and parameter choices match the biological systems, it has been repeatedly shown that both quantitative predictions, as well as biological understanding, can be vastly improved by the use of mechanistic models.

Acknowledgements This work was funded by Bill and Melinda Gates Foundation Grant OPP1111658 (P.AzW.), Research Council of Norway (NFR) Grant 262686 (to P.AzW.), European Union’s Horizon 2020 research and innovation programme grant agreement No 73307 (P.AzW.) and 75468 (I.H.).

Author contributions PAzW and IH designed the review. FC, JL, IH and PAzW identified relevant literature. FC wrote the first draft, FC, JL, AM and PAzW designed figures and FC, JL, AM, IH and PAzW wrote the manuscript.

Compliance with ethical standards

Conflict of interest The authors declare no competing interests.

Open Access This article is distributed under the terms of the Creative Commons Attribution 4.0 International License (<http://creativecommons.org/licenses/by/4.0/>), which permits unrestricted use, distribution, and reproduction in any medium, provided you give appropriate credit to the original author(s) and the source, provide a link to the Creative Commons license, and indicate if changes were made.

References

- Gesztelyi R, Zsuga J, Kemeny-Beke A, Varga B, Juhasz B, Tosaki A (2012) The Hill equation and the origin of quantitative pharmacology. *Arch Hist Exact Sci* 66(4):427–438. <https://doi.org/10.1007/s00407-012-0098-5>
- Levy G (1964) Relationship between elimination rate of drugs and rate of decline of their pharmacologic effects. *J Pharm Sci* 53:342–343. <https://doi.org/10.1002/jps.2600530325>
- Levy G (1966) Kinetics of pharmacologic effects. *Clin Pharmacol Ther* 7(3):362–372. <https://doi.org/10.1002/cpt196673362>
- Reynolds BL, Reeves PR (1963) Some observations on the mode of action of colicin F. *Biochem Biophys Res Commun* 11:140–145
- Wagner JG (1968) Kinetics of pharmacologic response. I. Proposed relationships between response and drug concentration in the intact animal and man. *J Theor Biol* 20(2):173–201
- Abel Zur Wiesch P, Abel S, Gkotz S, Ocampo P, Engelstadter J, Hinkley T, Magny C, Waldor MK, Udekwu K, Cohen T (2015) Classic reaction kinetics can explain complex patterns of antibiotic action. *Sci Transl Med* 7(287):287ra273. <https://doi.org/10.1126/scitranslmed.aaa8760>
- Abel Zur Wiesch P, Clarelli F, Cohen T (2017) Using chemical reaction kinetics to predict optimal antibiotic treatment strategies. *PLoS Comput Biol* 13(1):e1005321–e1005321. <https://doi.org/10.1371/journal.pcbi.1005321>
- Baeder DY, Regoes RR (2019) Pharmacodynamic inoculum effect from the perspective of bacterial population modeling. *bioRxiv*. <https://doi.org/10.1101/550368>
- Baeder DY, Yu G, Hoze N, Rolff J, Regoes RR (2016) Antimicrobial combinations: Bliss independence and Loewe additivity derived from mechanistic multi-hit models. *Philos Trans R Soc Lond Ser B Biol Sci*. <https://doi.org/10.1098/rstb.2015.0294>
- Strydom N, Gupta SV, Fox WS, Via LE, Bang H, Lee M, Eum S, Shim T, Barry CE III, Zimmerman M, Dartois V, Savić RM (2019) Tuberculosis drugs' distribution and emergence of resistance in patient's lung lesions: a mechanistic model and tool for regimen and dose optimization. *PLoS Med* 16(4):e1002773. <https://doi.org/10.1371/journal.pmed.1002773>
- Hill AV (1910) The possible effects of the aggregation of the molecules of haemoglobin on its dissociation curves. *J Physiol* 40:iv–vii
- Langmuir I (1918) The adsorption of gases on plane surfaces of glass, mica and platinum. *J Am Chem Soc* 40(9):1361–1403. <https://doi.org/10.1021/ja02242a004>
- Kalra P, Brandl J, Gaub T, Niederalt C, Lippert J, Sahle S, Küpfer L, Kummer U (2019) Quantitative systems pharmacology of interferon alpha administration: a multi-scale approach. *PLoS One* 14(2):e0209587. <https://doi.org/10.1371/journal.pone.0209587>
- Wagner JG (1981) History of pharmacokinetics. *Pharmacol Ther* 12(3):537–562. [https://doi.org/10.1016/0163-7258\(81\)90097-8](https://doi.org/10.1016/0163-7258(81)90097-8)
- Mager DE, Jusko WJ (2001) General pharmacokinetic model for drugs exhibiting target-mediated drug disposition. *J Pharmacokin Pharmacodyn* 28(6):507–532
- Mager DE, Wyska E, Jusko WJ (2003) Diversity of mechanism-based pharmacodynamic models. *Drug Metab Dispos* 31(5):510–518
- Mager DE (2006) Target-mediated drug disposition and dynamics. *Biochem Pharmacol* 72(1):1–10. <https://doi.org/10.1016/j.bcp.2005.12.041>
- Sugiyama Y, Hanano M (1989) Receptor-mediated transport of peptide hormones and its importance in the overall hormone disposition in the body. *Pharm Res* 6(3):192–202
- Levy G (1994) Pharmacologic target-mediated drug disposition. *Clin Pharmacol Ther* 56(3):248–252. <https://doi.org/10.1038/clpt.1994.134>
- Talbert AM, Tranter GE, Holmes E, Francis PL (2002) Determination of drug—plasma protein binding kinetics and equilibria by chromatographic profiling: exemplification of the method using L-tryptophan and albumin. *Anal Chem* 74(2):446–452. <https://doi.org/10.1021/ac010643c>
- Li P, Fan Y, Wang Y, Lu Y, Yin Z (2015) Characterization of plasma protein binding dissociation with online SPE-HPLC. *Sci Rep* 5:14866. <https://doi.org/10.1038/srep14866>
- Maheshwari V, Thijssen S, Tao X, Fuerstinger DH, Kappel F, Kotanko P (2019) In silico comparison of protein-bound uremic toxin removal by hemodialysis, hemodiafiltration, membrane adsorption, and binding competition. *Sci Rep* 9(1):909. <https://doi.org/10.1038/s41598-018-37195-1>
- Holford N (2017) Pharmacodynamic principles and the time course of immediate drug effects. *Transl Clin Pharmacol* 25(4):157–161
- Hedges AJ (1966) An examination of single-hit and multi-hit hypotheses in relation to the possible kinetics of colicin adsorption. *J Theor Biol* 11(3):383–410
- Copeland RA, Pompliano DL, Meek TD (2006) Drug-target residence time and its implications for lead optimization. *Nat Rev Drug Discov* 5(9):730–739. <https://doi.org/10.1038/nrd2082>
- Ehrlich P (1913) Address in Pathology on chemotherapeutics: scientific principles, methods, and results. *Lancet* 182(4694):445–451
- Copeland RA (2016) The drug-target residence time model: a 10-year retrospective. *Nat Rev Drug Discov* 15(2):87–95. <https://doi.org/10.1038/nrd.2015.18>
- Tonge PJ (2018) Drug-target kinetics in drug discovery. *ACS Chem Neurosci* 9(1):29–39. <https://doi.org/10.1021/acscchemneu.7b00185>
- Shimada S, Nakajima Y, Yamamoto K, Sawada Y, Iga T (1996) Comparative pharmacodynamics of eight calcium channel blocking agents in Japanese essential hypertensive patients. *Biol Pharm Bull* 19(3):430–437
- Walkup GK, You Z, Ross PL, Allen EK, Daryaei F, Hale MR, O'Donnell J, Ehmann DE, Schuck VJ, Buurman ET, Choy AL, Hajec L, Murphy-Benenato K, Marone V, Patey SA, Grosser LA, Johnstone M, Walker SG, Tonge PJ, Fisher SL (2015) Translating slow-binding inhibition kinetics into cellular and in vivo effects. *Nat Chem Biol* 11(6):416–423. <https://doi.org/10.1038/nchembio.1796>
- Magnus C, Regoes RR (2011) Restricted occupancy models for neutralization of HIV virions and populations. *J Theor Biol* 283(1):192–202. <https://doi.org/10.1016/j.jtbi.2011.06.004>
- Magnus C, Regoes RR (2012) Analysis of the subunit stoichiometries in viral entry. *PLoS One* 7(3):e33441. <https://doi.org/10.1371/journal.pone.0033441>
- Magnus C (2013) Virus neutralisation: new insights from kinetic neutralisation curves. *PLoS Comput Biol* 9(2):e1002900. <https://doi.org/10.1371/journal.pcbi.1002900>
- Nichols WW (2017) Modeling the kinetics of the permeation of antibacterial agents into growing bacteria and its interplay with efflux. *Antimicrob Agents Chemother* 61(10):e02576-02516. <https://doi.org/10.1128/AAC.02576-16>
- Hong Y, Gengo FM, Rainka MM, Bates VE, Mager DE (2008) Population pharmacodynamic modelling of aspirin- and ibuprofen-induced inhibition of platelet aggregation in healthy subjects. *Clin Pharmacokinet* 47(2):129–137. <https://doi.org/10.2165/00003088-200847020-00006>
- Yassen A, Olofson E, Kan J, Dahan A, Danhof M (2007) Animal-to-human extrapolation of the pharmacokinetic and pharmacodynamic properties of buprenorphine. *Clin Pharmacokinet* 46(5):433–447. <https://doi.org/10.2165/00003088-200746050-00005>

37. de Witte WEA, Versfelt JW, Kuzikov M, Rolland S, Georgi V, Gribbon P, Gul S, Huntjens D, van der Graaf PH, Danhof M, Fernandez-Montalvan A, Witt G, de Lange ECM (2018) In vitro and in silico analysis of the effects of D2 receptor antagonist target binding kinetics on the cellular response to fluctuating dopamine concentrations. *Br J Pharmacol* 175(21):4121–4136. <https://doi.org/10.1111/bph.14456>
38. Singh AP, Guo L, Verma A, Wong GG, Shah DK (2019) A cell-level systems PK-PD model to characterize in vivo efficacy of ADCs. *Pharmaceutics*. <https://doi.org/10.3390/pharmaceutics11020098>
39. Abelo A, Holstein B, Eriksson UG, Gabrielsson J, Karlsson MO (2002) Gastric acid secretion in the dog: a mechanism-based pharmacodynamic model for histamine stimulation and irreversible inhibition by omeprazole. *J Pharmacokinet Pharmacodyn* 29(4):365–382
40. Landersdorfer CB, He YL, Jusko WJ (2012) Mechanism-based population pharmacokinetic modelling in diabetes: vildagliptin as a tight binding inhibitor and substrate of dipeptidyl peptidase IV. *Br J Clin Pharmacol* 73(3):391–401. <https://doi.org/10.1111/j.1365-2125.2011.04108.x>
41. Haraguchi K, Ito K, Kotaki H, Sawada Y, Iga T (1997) Prediction of drug-induced catalepsy based on dopamine D1, D2, and muscarinic acetylcholine receptor occupancies. *Drug Metab Dispos* 25(6):675–684
42. Yin N, Pei J, Lai L (2013) A comprehensive analysis of the influence of drug binding kinetics on drug action at molecular and systems levels. *Mol BioSyst* 9(6):1381–1389. <https://doi.org/10.1039/c3mb25471b>
43. Udekwi KI, Parrish N, Ankomah P, Baquero F, Levin BR (2009) Functional relationship between bacterial cell density and the efficacy of antibiotics. *J Antimicrob Chemother* 63(4):745–757. <https://doi.org/10.1093/jac/dkn554>
44. Lenhard JR, Bulman ZP (2019) Inoculum effect of β -lactam antibiotics. *J Antimicrob Chemother*. <https://doi.org/10.1093/jac/dkz226>
45. Csajka C, Verotta D (2006) Pharmacokinetic-pharmacodynamic modelling: history and perspectives. *J Pharmacokinet Pharmacodyn* 33(3):227–279. <https://doi.org/10.1007/s10928-005-9002-0>
46. Shen L, Rabi SA, Sedaghat AR, Shan L, Lai J, Xing S, Siliciano RF (2011) A critical subset model provides a conceptual basis for the high antiviral activity of major HIV drugs. *Sci Transl Med* 3(91):91ra63. <https://doi.org/10.1126/scitranslmed.3002304>

Publisher's Note Springer Nature remains neutral with regard to jurisdictional claims in published maps and institutional affiliations.

Paper 2

RESEARCH ARTICLE

Estimating treatment prolongation for persistent infections

Antal Martinecz^{1,*},† and Pia Abel zur Wiesch^{1,2}

¹Department of Pharmacy, Faculty of Health Sciences, UiT The Arctic University of Norway, 9037 Tromsø and
²Centre for Molecular Medicine Norway, Nordic EMBL Partnership, P.O. Box 1137, Blindern, 0318 Oslo, Norway

*Corresponding author: Department of Pharmacy, Faculty of Health Sciences, UiT The Arctic University of Norway, 9037 Tromsø.

E-mail: antal.martinecz@uit.no

One sentence summary: This study shows a generalized mathematical framework applicable for most persistence mechanisms that can be used to estimate treatment length in persistent infections.

Editor: Olivier Restif

†Antal Martinecz, <http://orcid.org/0000-0001-6539-6358>

ABSTRACT

Treatment of infectious diseases is often long and requires patients to take drugs even after they have seemingly recovered. This is because of a phenomenon called persistence, which allows small fractions of the bacterial population to survive treatment despite being genetically susceptible. The surviving subpopulation is often below detection limit and therefore is empirically inaccessible but can cause treatment failure when treatment is terminated prematurely. Mathematical models could aid in predicting bacterial survival and thereby determine sufficient treatment length. However, the mechanisms of persistence are hotly debated, necessitating the development of multiple mechanistic models. Here we develop a generalized mathematical framework that can accommodate various persistence mechanisms from measurable heterogeneities in pathogen populations. It allows the estimation of the relative increase in treatment length necessary to eradicate persisters compared to the majority population. To simplify and generalize, we separate the model into two parts: the distribution of the molecular mechanism of persistence in the bacterial population (e.g. number of efflux pumps or target molecules, growth rates) and the elimination rate of single bacteria as a function of that phenotype. Thereby, we obtain an estimate of the required treatment length for each phenotypic subpopulation depending on its size and susceptibility.

Keywords: persistence; antimicrobial; treatment length; mathematical model; bacteria; antibiotic

INTRODUCTION

Antibacterial treatments can be lengthy for certain diseases. An extreme example is tuberculosis, where the treatment lasts between 6 and 24 months (Lawn and Zumla 2011; Horsburgh, Barry and Lange 2015). As the treatment length increases, patient adherence can dramatically drop (Burnier et al. 2013), which in turn can increase the treatment length even further while also inflating its costs. A major barrier in reducing treatment length is the risk of relapse: if bacterial populations are below detection

limit but not eliminated, bacteria may regrow resulting in treatment failure (Fig. 1). This can be due to various different mechanisms, for example bacteria hiding in 'sanctuary sites' (Claudi et al. 2014; Kaiser et al. 2014), in cells (Prajsnar et al. 2012), granulomas (Monack, Bouley and Falkow 2004; Lawn and Zumla 2011) or the phenomenon of persistence in a single bacterial population (Balaban et al. 2004; Lewis 2007; Ankomah and Levin 2014; Abel zur Wiesch et al. 2015; Bergmiller et al. 2017). In this work we focus on the latter, specifically in bacterial populations.

Received: 28 February 2018; Accepted: 8 August 2018

© FEMS 2018. This is an Open Access article distributed under the terms of the Creative Commons Attribution License (<http://creativecommons.org/licenses/by/4.0/>), which permits unrestricted reuse, distribution, and reproduction in any medium, provided the original work is properly cited.

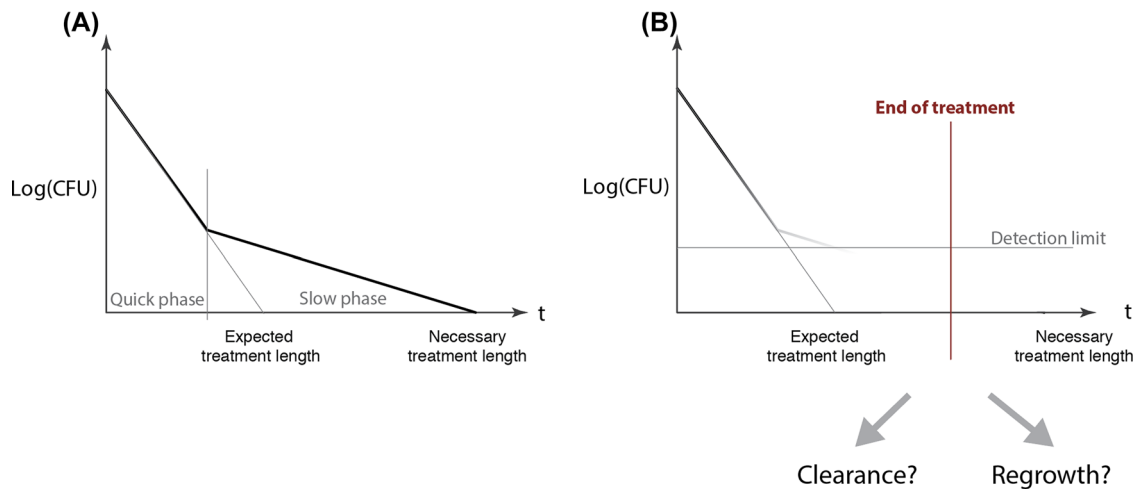


Figure 1. Persistence lengthens treatment. A and B, Shows the change in the number of bacteria (colony forming units, CFU) over time. The curve is a typical biphasic kill-curve associated with persistence. In these cases, a fraction of the population may be below the detection limit. Therefore, if the treatment is terminated at the expected treatment length based on only initial elimination rates; a fraction of the population might survive. As these bacteria are still viable, they might regrow and cause relapse. As the Y-axis is logarithmic, exponential decays are straight lines that cross the X-axis at one individual bacterium. We assume that at this time point the population is eliminated. B, Illustrates how persisters below the detection limit can complicate treatments by making it difficult to assess whether it is safe to end a treatment.

Persistent bacteria survive prolonged exposure to antibiotics, despite being genetically susceptible. This phenomenon is often characterized by bi- or multi-phasic kill-curves: after the initial rapid elimination of bacteria, the rate of elimination slows down. Therefore, as depicted in Fig. 1, bacteria can survive for a longer time than one would expect based on the initial elimination rates.

The nature and cause of bacterial persistence during antibiotic therapy is hotly debated (Balaban *et al.* 2013). Antibiotic persistence models can be divided into two (nonexclusive) groups. First, the ‘classical’ models that assume a distinct phenotype or state that causes persistence. Here, the minority of persister cells and the majority of normal cells are clearly distinct (Balaban *et al.* 2004; Lewis 2007) and antibiotic susceptibility in the bacterial population follows a bimodal distribution (in the extreme case no antibiotic susceptibility for persisters and full susceptibility for ‘normal’ cells). Second, ‘heterogeneity’ based models that assume a (unimodal) distribution in bacterial susceptibility. Here, persisting bacteria are not distinct, but are at the tail of the susceptibility distribution (Wakamoto *et al.* 2013; Fridman *et al.* 2014; Abel zur Wiesch *et al.* 2015). We have previously demonstrated that minor heterogeneities in drug-target binding are sufficient to explain multiphasic kill-curves and thus persistence as we currently understand it (Abel zur Wiesch *et al.* 2015). Moreover, our work made the prediction that a larger variance in molecular heterogeneity increases persister-like behavior that has now been confirmed experimentally (Rego, Audette and Rubin 2017).

The purpose of this work is to estimate the impact of persistence on the time required until all bacteria are cleared by antibiotics. Specifically, we develop a generalized framework that can be used on various mechanisms of persistence, including persistence against antimicrobial peptides or other agents of the host’s immune system. While the principles can be applied to all types of distributions of persister phenotypes, we focus on bacterial persistence due to heterogeneity in susceptibility that follows a Gaussian distribution. Having a common framework allows the comparison of various mechanisms, as well as ap-

plying them in the same model, and consequently investigating their combined effects on treatment length. While persistence against antibiotics in bacteria has received most attention, there is also evidence that elimination by the immune system can also result in bi- or multi-phasic kill-curves. For example, the dynamics of antibodies binding to the epitopes of HIV virions (Magnus and Regoes 2011; Magnus *et al.* 2013), cell-to-cell variability in the apoptosis of cancer cells (Spencer *et al.* 2009), persisters’ tolerance towards serum-complement mediated killing (Putrinš *et al.* 2015), or local adaptation to-, and heterogeneity in the immune clearance of bacterial colonies (Bumann 2015).

Here, we present a mathematical modeling framework that allows translating population heterogeneity in antibiotic susceptibility (uni-, bi- or multi-modal) into time-kill curves and the required treatment time to eradicate a bacterial population. This modeling framework consist of two parts: first, a simplified model that allows translating drug target binding in homogeneous bacterial subpopulations into elimination rates. The simplified model is applicable to any mechanism of pathogen killing where step-wise binding or molecular recognition is involved. Second, estimating prolongation of treatment length in bacterial populations with heterogeneities in elimination rates. This part of the modeling framework is independent of the mechanism responsible for the heterogeneity in elimination rates and can be used to infer the heterogeneities’ effects on treatment prolongation. We also show this with an experimental dataset as an example on how to use our methodology.

MATERIALS AND METHODS

In the following, we first describe the response of a single bacterium to successive binding of a killing agent and then the response of a bacterial population (elimination rate) to an increasing number of mean bound target molecules. Finally, we show how heterogenous elimination rates of individual subpopulations can be used to estimate the increase in treatment length caused by persisters.

Inferring bacterial elimination rates from drug-target binding

Response of single bacteria to antibiotic binding

Whether bacteria are killed by antibiotics, the immune system or even viruses by antivirals, molecular binding and recognition is arguably involved in all cases. Therefore, models that incorporate subsequent binding events are useful for understanding the response to drugs or the immune system (Magnus and Regoes 2011; Shen et al. 2011; Magnus et al. 2013). Previously, we have demonstrated (Abel zur Wiesch et al. 2015), that bacterial populations with heterogeneity in the number of targets can show persistent behavior. The first aim here is to generalize and simplify this model.

In (Abel zur Wiesch et al. 2015), we set up a mathematical model, where we calculated the following for multiple subpopulations with different number of targets (Fig. 2, and Equation 1): first, number of antibiotic molecules inside each cell based on external antibiotic concentrations. Second, the number of bacteria with x bound targets (within each subpopulation), and finally the replication and elimination for bacteria with x bound targets (for each x in each subpopulation). In that model, we assumed that the antibiotic concentration is the same inside and outside the cells. Therefore, the number of antibiotic molecules inside each bacterium can be estimated based on the average volume of a bacterium and the external concentration.

Our model describes successive binding steps, meaning that each compartment/differential equation (B_x) contains and keeps track of the number of bacteria with the given number of bound targets (x) (see Fig. 2).

The differential equations of the binding kinetics are:

$$\frac{dB_x}{dt} = k_f^* A(t) B_{x-1} (n - (x - 1)) - k_r x B_x - k_f^* A(t) B_x (n - x) + k_r (x + 1) B_{x+1}, \quad (1)$$

where:

- $k_f^* = \frac{k_f}{V_i \cdot n_A}$ is the adjusted forward reaction rate to accommodate working with the number molecules inside the cells instead of concentrations. Here, k_f is the forward reaction rate, $V_i = 10^{-15}$ [l] is the average cell volume, and $n_A = 6 \cdot 10^{23}$ is the Avogadro number,
- k_r is the reverse reaction rate,
- $A(t)$ is the concentration of antibiotics in or around the bacterium,
- x is the number of bound targets,
- n is the number of targets,
- B_x is the number of bacteria with x bound targets.

All the models mentioned above (Magnus and Regoes 2010; Shen et al. 2011; Abel zur Wiesch et al. 2015) assume for simplicity that the elimination rate function for a single bacterium is a step function. Once a threshold in the number of bound targets is reached, the bacterium dies or, in the case of virions, becomes noninfectious.

The model gets significantly simpler if it is sufficient to calculate the mean number of bound targets instead of calculating the full reaction kinetics model (Equation 1). This can be done if the binding kinetics and bacterial replication/elimination rates can be separated from each other. The condition for this is that the binding rates have to be at least a magnitude faster than the change of external antibiotic concentrations or the replication/elimination rates. In other words, they have to be on dif-

ferent time-scales. In these cases, the reaction kinetics will always reach steady state before any new replication/elimination 'event' happens, and the changes in antibiotic concentration is also closely followed by the reaction kinetics due to the differences in the timescales the two are acting on. Consequently, when calculating the binding kinetics, the two other processes can be regarded as 'constant'. This is the case for slow growing bacteria (e.g. *Mycobacterium tuberculosis*) and when antibiotic concentrations are well above the minimum inhibitory concentration (MIC), as we have shown in (Abel zur Wiesch, Clarelli and Cohen 2017). For other cases, this depends on the binding rates and concentrations of the antibiotics, as well as the replication of rates of the given bacterium. As we assume that there is no change in the number of target molecules through bacterial death, our model would also be applicable in cases where dead bacteria or at least their target molecules are not degraded and continue participating in drug binding.

With this simplification, the time course of the mean number of bound targets (\bar{x}) can be determined by using classical reaction kinetics ($A + T \rightleftharpoons AT$, Equation 2) between the free targets ($n - \bar{x}$) and the antibiotics (A):

$$\frac{d\bar{x}}{dt} = k_f A(t) (n - \bar{x}) - k_r \bar{x} \quad (2)$$

If $A(t)$ fluctuates slowly compared to the settling time of the reaction, the equilibrium of this time course is at:

$$v = n \frac{A(t)}{\frac{k_r}{k_f} + A(t)} \quad (3)$$

After separation of reaction kinetics from the replication and elimination processes, the binding kinetics reduced to a problem of calculating the number of bound targets at a constant antibiotic concentration. Therefore, the number of mean bound targets can be determined using Equations (2) or (3) and the distribution of bound targets around it (as depicted on Fig. 2C) can be approximated with a Gaussian distribution (van Kampen 2007).

In the following, we will investigate how a population of bacteria responds to an increasing number of bound targets, which in turn is dependent on the antibiotic concentration (Equations 2 and 3).

Response of bacterial population to successive drug binding (i.e. dose-response curves)

On a population-level, we expect a step function in single cell response to result in a sigmoidal elimination curve: the random binding and unbinding of antibiotics and their targets creates a dynamic equilibrium around the mean number of bound targets (\bar{x}). Consequently, the number of bound targets will occasionally reach the threshold for elimination long before the mean number of bound target reaches it (see Fig. 2). The frequency with which bacteria reach that threshold by chance and are therefore killed increases with the antibiotic concentration and this results in a sigmoidal curve, as has been observed in experimental data (Regoes et al. 2004).

Based on the distribution around the mean bound targets, it is possible to estimate an effective elimination rate curve for a homogeneous population of bacteria (see Fig. 2D, and Equation 4). As a result, the only input necessary for the effective elimination rate curve is now the mean number of bound targets.

$$\delta^*(\bar{x}) = \sum_x \delta(x) B(x, \bar{x}), \quad (4)$$

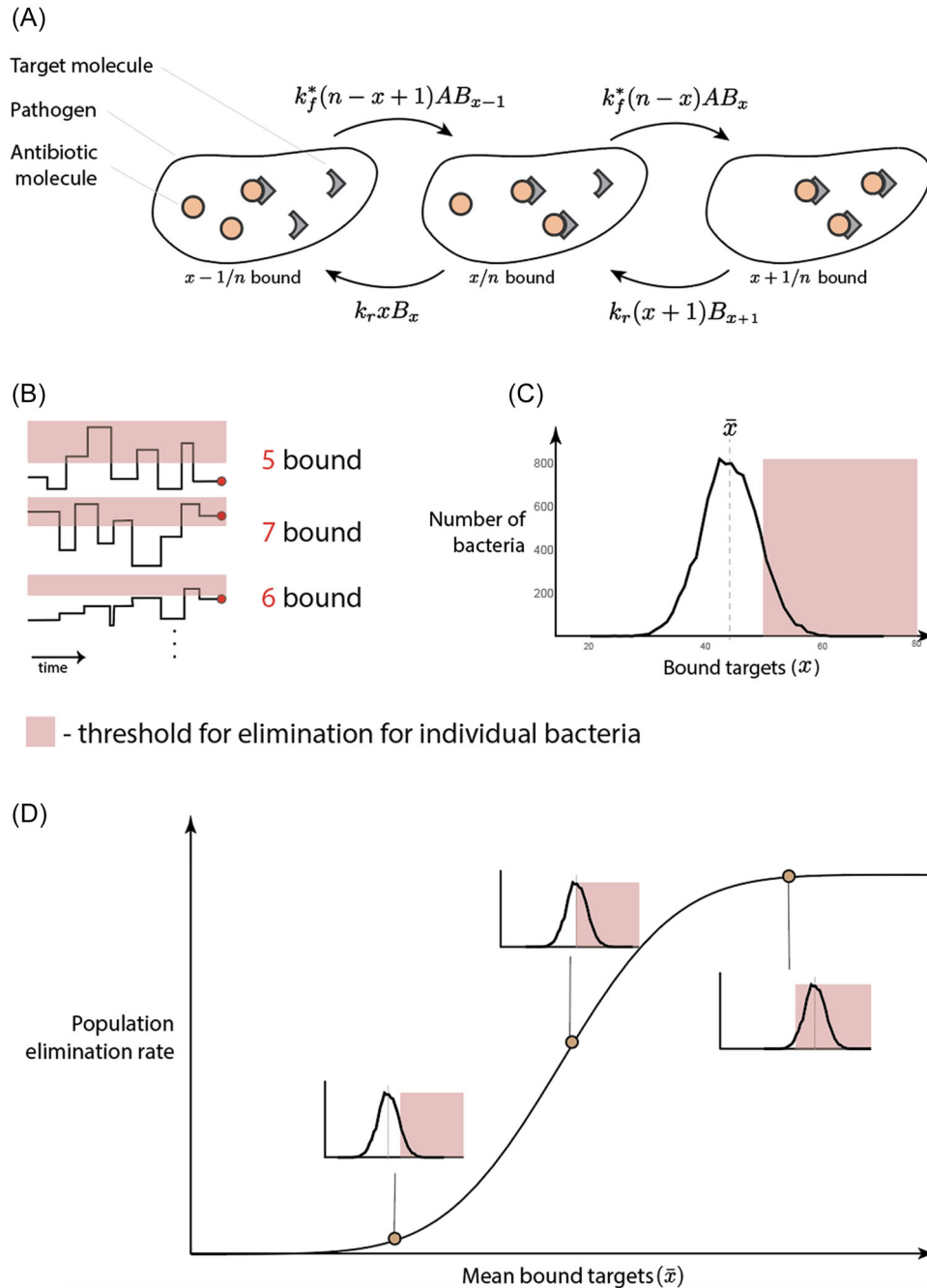


Figure 2. Overview of the mathematical model describing successive binding steps. A, Illustrates how the binding kinetics are calculated (Equation 1). Here, k_f^* is the adjusted forward reaction rate (see below), k_r is the reverse reaction rate, A is the concentration of antibiotics inside the bacterium, x is the number of bound targets, n is the number of targets and B_x is the number of bacteria with x bound targets. B, Shows how the random binding and unbinding of targets causes a variance in the number of bound targets around the mean and how this causes the individual bacterium to cross the number of bound targets required for elimination. C, Gillespie simulation of Equation (1). This plot shows the distribution around the mean. The parameters used are $k_d = 10^{-5}$ (ciprofloxacin, (Spratt 1975; Terrak et al. 1999)), number of targets $n = 100$ (gyrase, (Malmström et al. 2009; Maier et al. 2011)). D, Shows how the random binding and unbinding (Figure B and C) will cause a fraction of population to die earlier than expected that results in a net elimination rate. The curve on Figure D was obtained using Equation (4).

where:

- $B(x, \bar{x})$ is the distribution of bound targets around the mean \bar{x} (Fig. 2B and C)
- $\delta(x)$ is the elimination rate depending on the number of bound targets (Fig. 2B and C)
- $\delta^*(\bar{x})$ is the effective, population-wide elimination rate, only depends on the mean bound targets (Fig. 2D).

Integrating population heterogeneity on dose-response curves

Bacterial populations often contain various heterogeneities that can cause heterogeneities in elimination rates, for example the numbers of efflux pumps (Pu et al. 2016; Bergmiller et al. 2017), or sizes of bacteria and therefore the intracellular target

concentrations (Abel zur Wiesch et al. 2015; Rego, Audette and Rubin 2017) can vary from cell to cell.

In (Abel zur Wiesch et al. 2015) among others, we have demonstrated that the effects of small heterogeneities in the number of targets can lead to biphasic time–kill curves. Here, heterogeneity in the number of targets can be included the following way: the relationship between the number of targets (n) and mean bound targets (\bar{x}) is an exponential function and therefore locally linear. The effects of small changes can thus be approximated as linear: $\bar{x}(c \cdot n, A) = c \cdot \bar{x}(n, A)$ for small changes: $c \approx 1$. For example, a 5% decrease in the maximum number of targets will result in 5% decrease in bound targets. Therefore, it is not necessary to calculate the mean number of bound targets for each subpopulation with different molecular content. As a result, elimination rates can be more effectively calculated at a given antibiotic concentration A , if we already know one representative subpopulation $\bar{x}(n, A)$, where the heterogeneity in the population can be measured with the parameter n (for example, number of efflux pumps or number of targets).

$$\delta^*(\bar{x}(c \cdot n, A)) = \delta^*(c \cdot \bar{x}(n, A)) \quad (5)$$

Finally, the time–kill curves of all subpopulations (e.g. with n target molecules, but more generally with a given phenotype i) have to be summed up to yield a time–kill curve of the entire bacterial population:

$$B_{\text{total}}(t) = \sum_i B_i(0) e^{\delta_i t} \quad (6)$$

In order to be able to compare the effects of persistence on treatment length (described below), we are assuming that the net growth rate for all subpopulations is negative. Otherwise the increase in treatment lengths will be infinite when some subpopulations have a positive net growth. This makes the comparison of different mechanisms difficult. However, as antibiotics are generally administered at multiples of the MIC this is often a reasonable assumption.

RESULTS

We first set out to investigate how different degrees of population heterogeneity in the number of target molecules affect persistence, defined as a slowdown in bacterial killing at a constant drug concentration. If we assume the same threshold (absolute number of bound targets, not percentages) for elimination, all subpopulations will have the same effective elimination curve. The heterogeneity in target molecules results, in a first approximation, in the same degree of heterogeneity in the number of bound targets for each subpopulation. This places the subpopulations at different points on the effective elimination rate curves. (see Fig. 3A). Therefore, small heterogeneities within the number of targets (1%–5% standard deviation around the mean) can lead to persistent behavior in the population of bacteria.

The same approach can be used for having different elimination rates while having the same number of mean bound targets as a different mechanism for persistence (see Fig. 3B). Finally, these two can be combined to account for more general cases. For example, when the subpopulations with different numbers of targets also differ from each other in the threshold of bound targets required to eliminate a single cell (i.e. different susceptibilities). The interplay between the change in susceptibility and

bound targets can still cause persistent behavior, depending on their relationship (see Fig. 3C and D).

Estimating treatment length

In this work, we have defined treatment length as the time point where all bacterial subpopulations are eliminated. We calculate the time to extinction for each individual subpopulation of bacteria and determine which is longest one. However, this necessitates the simplification that the eliminations of subpopulations are independent of each other: upon lysing the cells do not release their targets to the extracellular space. Furthermore, we neglect the decrease in extracellular antibiotic concentrations due to the uptake by cells. The goal of approximating the effects of heterogeneity and binding kinetics was to be able to reduce persistence models into two parts: the elimination rate as a function of a certain persistence mechanism and the distribution of subpopulations exhibiting various degrees of this persistence mechanism. This way, the treatment length for each subpopulation can be estimated by dividing the two functions (Equation 7). The resulting function shows the time points where the given subpopulations drop below one bacterium. This is best demonstrated by Fig. 1: as the Y-axis is logarithmic, exponential decays are straight lines that cross the X-axis at one individual bacterium. Therefore, (at constant antibiotic concentrations) dividing the logarithm of subpopulation size at $t = 0$ with their corresponding elimination rates will give us the time point the given subpopulation will go below one bacterium. We assume that at this time point they are eliminated, see Fig. 1.

$$t_{\text{survival}}(\bar{x}) = \frac{\text{Log}[B_{\text{total}}(\bar{x})]}{\delta^*(\bar{x})}, \quad (7)$$

where $B_{\text{total}}(\bar{x})$ is the size of the subpopulation that has the mean of \bar{x} bound targets (as depicted on the bottom left subplots on Fig. 3).

If we normalize Equation (7) with time it takes to eliminate the largest subpopulation (the median of the population distribution, Fig. 4A), we get the fold-increase in time it takes to eliminate each subpopulation compared to the majority (see Fig. 4 and Equation 8).

$$t^*_{\text{survival}}(\bar{x}) = t_{\text{survival}}(\bar{x}) / t_{\text{survival}}(\bar{x}_{\text{majority}}) \quad (8)$$

In Fig. 5, to demonstrate the estimation of treatment length and to reproduce the results of (Abel zur Wiesch et al. 2015), we have plotted increase in treatment length for 1%, 2%, 3% and 4% heterogeneity in bound targets, meaning that the different subpopulations show a normal distribution in the number of (mean) bound targets, with the standard deviation of $\sigma = 0.02 \bar{x}$ (for a 2% heterogeneity). This can be due to the same heterogeneity in the number of targets among the subpopulations of bacteria as discussed above. Here, above a 2% heterogeneity, persistent bacteria take substantially longer to eliminate than the majority of the population. This is consistent with our results in (Abel zur Wiesch et al. 2015), where we have shown that a 2% heterogeneity in bound targets is sufficient to show persistent behavior. The parameters used are $k_d = 10^{-5}$, number of targets $n = 100$ (gyrase, (Malmström et al. 2009; Maier et al. 2011)); the cells are eliminated when more than 50 of their targets are bound (independently of the number of targets, n). The distribution around the mean (used in Equations 7 and 8, see Fig. 2C) was obtained by simulating the reaction kinetics using Gillespie simulations for

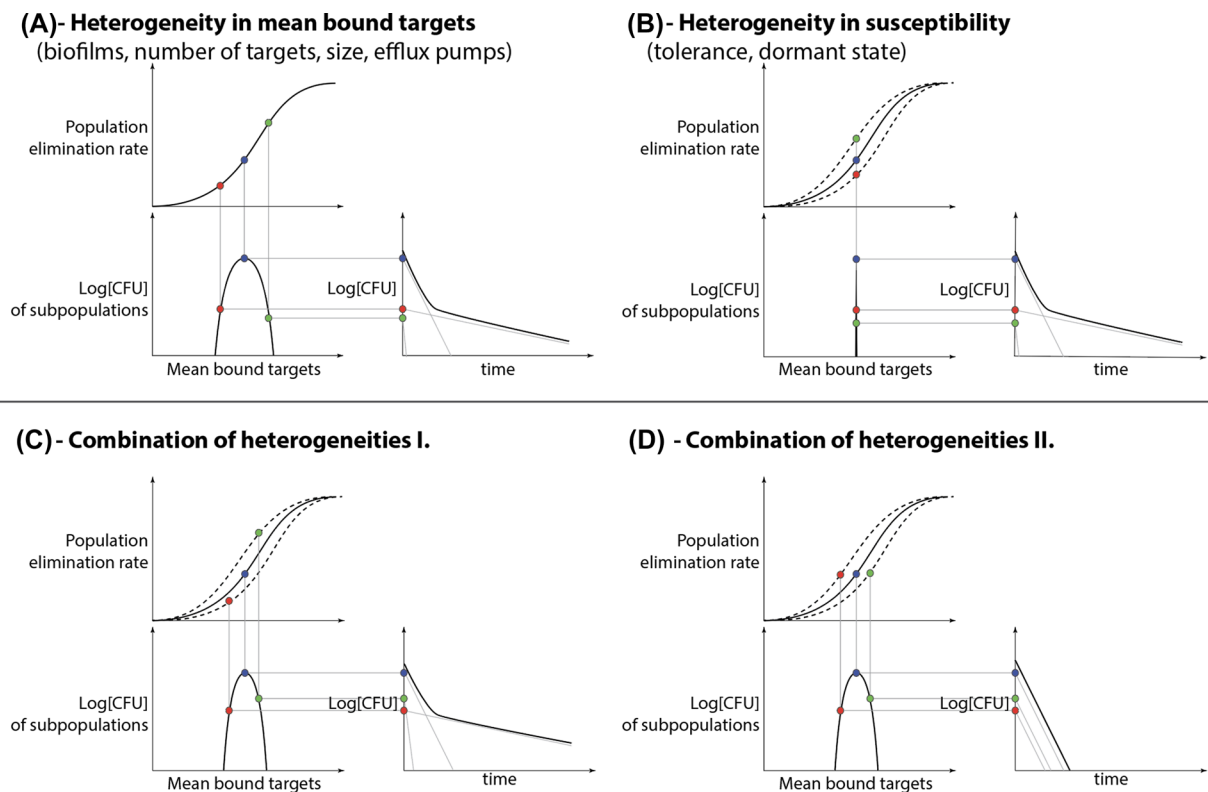


Figure 3. Bacterial populations with heterogeneities can show persistent behavior. These plots demonstrate how the model can be applied to various heterogeneities in the population. A, Shows the case where the assumed persistence mechanism causes a heterogeneity (only) in the number of bound targets. B, Where the assumed persistence mechanism causes a heterogeneity (only) in the susceptibility to the killing agent. C and D, Shows the combination of the two: whether heterogeneity results in persistent behavior depends on the relationship between the two heterogeneities within the population.

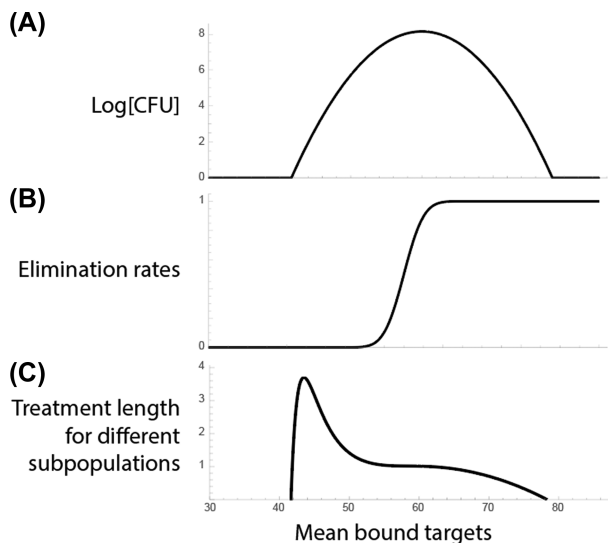


Figure 4. Estimation of treatment length. This plot demonstrates how treatment length for different subpopulations (C) can be estimated from the heterogeneity in the population (A) and the elimination rate function (B). A, Shows the heterogeneity in the mean bound targets within the population, here the majority of the population is simply the median of this distribution. B, It is the elimination rate function for the population, here we assume that the subpopulations only differ from each other in the mean number of bound targets. C, It shows the assumed treatment length for each subpopulation (obtained with Equation 8), assuming that each of the subpopulations are independent of each other and the treatment length can be calculated as the time point where the given subpopulation goes below 1 bacterium.

the given k_d and n . It is a normal distribution with the standard deviation of $\sigma = 4$.

Using experimental data in our model

In this subsection, we demonstrate how to use an experimental dataset in our model. As the purpose of this subsection is to demonstrate a workflow, for the sake of brevity, we present a hypothetical and idealized scenario. We use the measurements of (Bergmiller *et al.* 2017) which measured the distribution of growth rates in cells exposed to the bacteriostatic antibiotic tetracycline with single cell microscopy and thereby the heterogeneity in treatment response. They have also quantified a trait that contributes to this heterogeneity, the number of efflux pumps. This heterogeneity arises from biased partitioning during the replication of bacteria, which results in the daughter cells' having fewer efflux pumps and therefore an efflux activity of 85–90% of the mother cells' (measured dye uptake).

To illustrate how to investigate such a dataset, we first obtain dose response curves for mother and daughter cells. Here, we assume that the only difference between the two generations is the number and activity of efflux pumps. Therefore, we take the median of both population growth rates to acquire a difference between the two generations (Fig. 6A and B). Next, we estimate the reduced (relative) drug concentrations affecting the mother cells by multiplying the external drug concentrations with the measured difference in efflux activity (dye uptake) between daughter and mother cells. While a proper analysis is outside the scope of this paper, in Fig. 6 we demonstrate that after the adjustment of drug concentrations the growth rate curves of

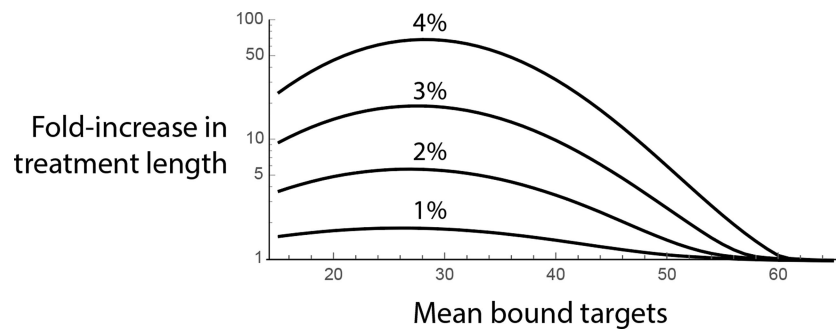


Figure 5. Increase in treatment length caused by persistence. This figure shows the fold-increases in treatment length (using Equation 8) for antibiotic concentrations that bind to 15%–70% of targets (threshold of elimination is 50 bound targets). The different curves are for different levels of heterogeneities in the number of maximum targets within the population. As the plot demonstrates, even small heterogeneities can cause a substantial increase in the required treatment length.

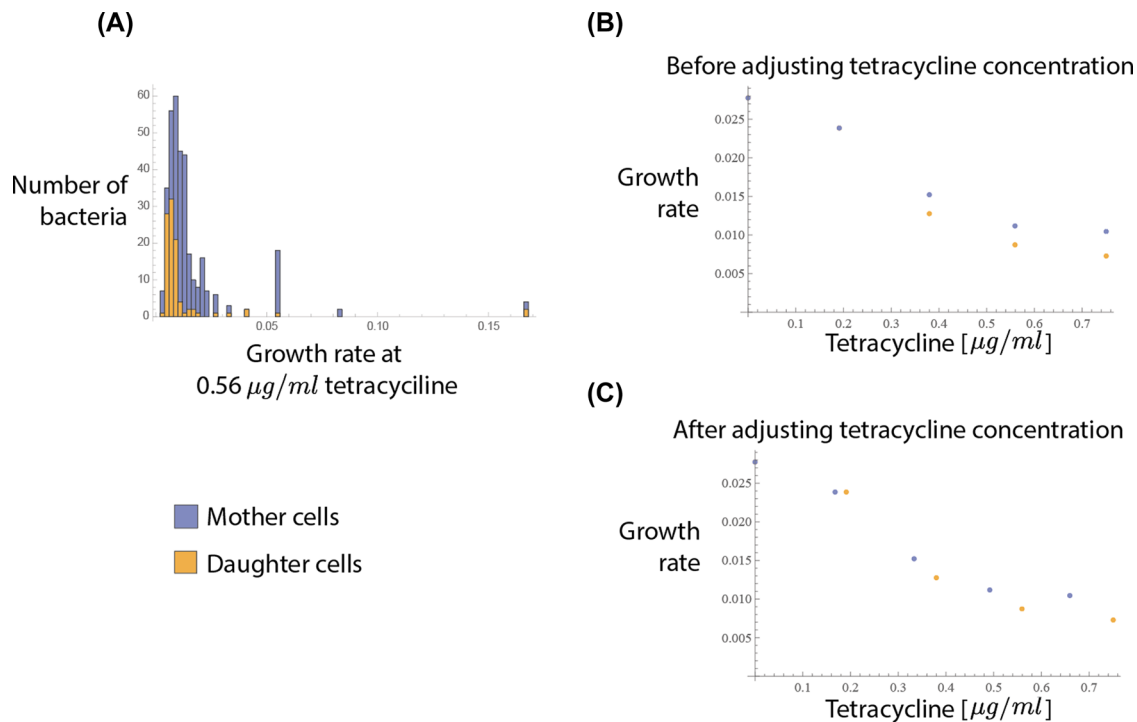


Figure 6. Using an experimental data set in the model. This plot illustrates the workflow of using an experimental dataset (taken from (Bergmiller et al. 2017)) in the model. The dataset describes the change in replication rates under tetracycline exposure due to the biased partitioning of efflux pumps between mother and daughter cells. **A**, Shows the histogram of measured growth rates at a specific antibiotic concentration for both the mother and daughter cells. **B**, Plots the medians of all the measured distributions at various antibiotic concentrations. In **(C)** the antibiotic concentrations for the mother cells have been adjusted to account for the increased efflux activity measured in the dataset that shows that the mother cells have 10% less dye taken up due to the higher numbers of efflux pumps. Here we have only used small part of the dataset, just to demonstrate the workflow from the experimental data to our model, in this case Fig. 3A.

the daughter and mother cells get close to each other and intersect.

In this analysis, we can directly go to the step to estimate time–kill curves and the required treatment length because bacterial response to antibiotics (i.e. replication rate) was measured directly (Equations 5 and 6). The antibiotic used is tetracycline, a bacteriostatic antibiotic that mainly affects bacterial growth and is thought to act together with the immune system to clear infections. In order to create time–kill curves and calculate the time until the last bacterium would be eliminated, we generated a dataset by adding a constant elimination rate (caused by the immune system or an additional drug) to the available measured generation times. As a result, we get a distribution of eliminations rates for both mother and daughter cells. First, as within one generation we also have a distribution of growth (now elimi-

nation) rates (Fig. 6A), even mother or daughter cells in isolation should show biphasic kill-curves (Fig. 7A and B). This is possibly due to other persistence mechanisms as well as heterogeneity in efflux pumps within both the mother and daughter cell populations.

Next, in order to show the difference in the two generations, on Fig. 7C we have plotted the ratio of median elimination rates for the mother and daughter cells. We have opted to do this as the kill-curves would also depend on the steady state ratio of daughter and mother cells within a population (Figs. 3A and 4). This ratio or elimination rates can be used as a proxy to measure how biphasic a kill-curve is: the closer it gets to one, the smaller the difference is in the slopes for biphasic kill-curves. Fig. 7C demonstrates that if there is only one generation difference within the population, only low background killing rates

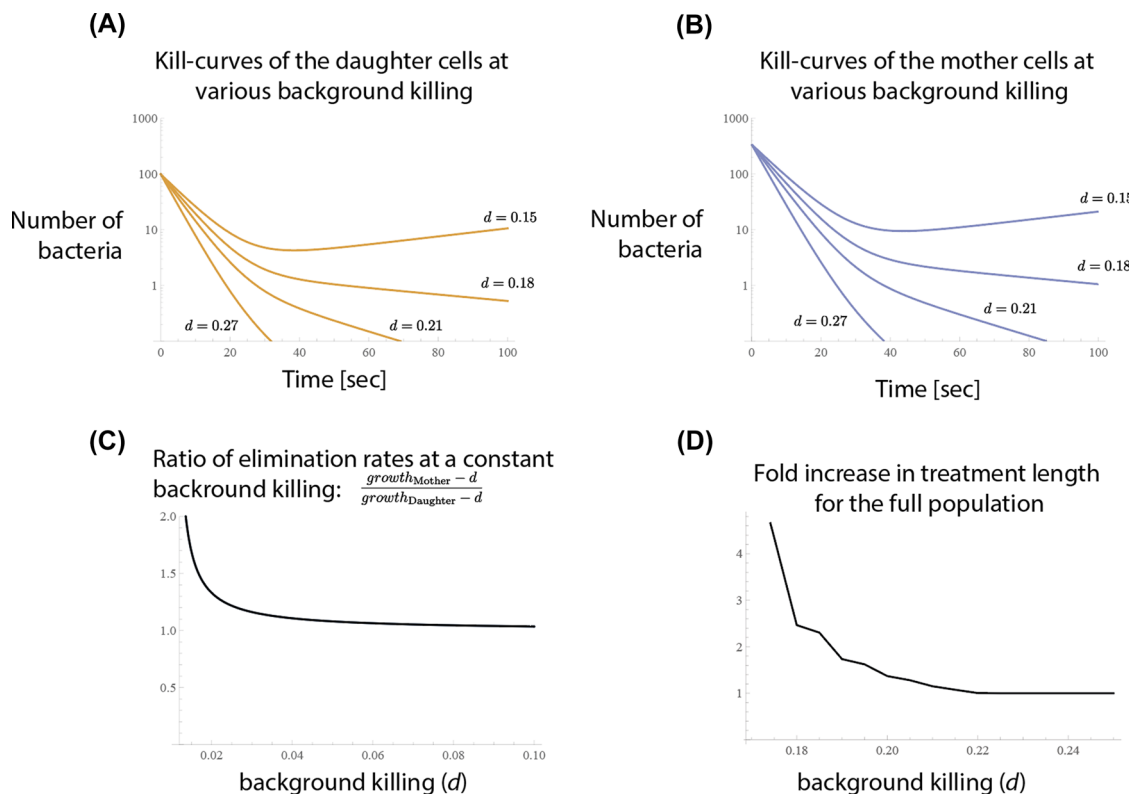


Figure 7. Separating persistence mechanisms with the model. This figure shows that the model can be used to separate different persistence mechanisms. To produce these plots, we have used the experimental data of (Bergmiller et al. 2017). On (A and B) we have plotted the theoretical kill-curves based on the distribution of bacteria on Fig. 6A for mother and daughter cells respectively (using Equation 6). As the measurements were taken with a bacteriostatic drug (tetracycline), we have added a constant background killing to the population in order to create kill-curves from growth curves. It is important to note here that the heterogeneity that gives rise to the biphasic kill-curves are present in both the mother and daughter cells (see Fig. 6A). C, Shows the ratio of the median elimination rates for the mother and daughter cells. We have opted to show this as a measure of persistence instead of kill-curves as the kill-curves would also depend on the steady state population-sizes of the mother and daughter cells. This plot demonstrates we can expect biphasic kill-curves only at low background killing, provided that there are only two generations in a population. D, Shows the increase in time it takes to eliminate the whole population at different background killings due to the heterogeneity in growth rates. This curve is obtained similarly to Fig. 5 and Equation (8).

(< 0.02 [1/s]) would result in biphasic kill-curves. This is significantly different from Fig. 7A or B, where just for mother or daughter cells alone even at higher background killing (0.27 [1/s]) we saw biphasic kill-curve, indicating that only one generation difference in mother and daughter cells explains only a part of the heterogeneity in treatment response in this dataset. As shown in (Bergmiller et al. 2017) natural bacterial populations have multiple generations present and consequently the mother cells in the experimental data might not have been from the same generation. Therefore, the differences in the number of efflux pumps might explain a larger part of heterogeneity in treatment response in this dataset, however investigating this is out of the scope of this work.

Taken together, Figs. 6 and 7 demonstrate how one can use our model with experimental data, separate mechanisms of persistence from others, and quickly estimate the parameter ranges where we would see biphasic curves with the given assumptions.

DISCUSSION

The purpose of this work is to develop a mathematical model that can be used to estimate the increase in treatment length caused by persisters. At the same time, it should be general enough to encompass most proposed persistence mechanisms. We have demonstrated how the model presented in this paper

can be used to describe persistence mechanisms that cause heterogeneities in either the susceptibility to the killing agent or the number of bound targets. Using a dataset from (Bergmiller et al. 2017), we have demonstrated how our framework can be used to infer time-kill curves as well as the increase in necessary treatment length from measured heterogeneities in bacterial populations. We have also shown how this approach can help shedding light on the relative contributions of different persistence mechanisms.

Our mathematical framework can accommodate many different molecular mechanisms of bacterial persistence. These mechanisms can be separated into two different groups: they either affect the number of bound targets or the elimination rates. Examples for mechanisms that affect the number of bound targets are: (i) heterogeneity in the number of efflux pumps as it affects the concentration of antibiotics within the cells, but probably does not have a great impact on susceptibility to a given intracellular antibiotic concentration (Bergmiller et al. 2017). (ii) Heterogeneity in cell volumes: if the relationship between cell volumes and number of targets is not linear, it will affect concentration of targets and therefore the number of bound targets (Rego, Audette and Rubin 2017). (iii) Biofilms: the antibiotic concentration is lower around bacteria that are deeper into the biofilms due to the imperfect penetration of antibiotics into biofilms, consequently the internal antibiotic concentrations in these cells will be lower as well (Lewis 2008). Examples of

heterogeneities in how bacteria respond to a given number of bound targets include: (i) dormancy and (ii) increased lag time before replication if antibiotics only act on bacteria when they are actively replicating (Balaban et al. 2004; Lewis 2007; Fridman et al. 2014).

Moreover, as the model only describes heterogeneity in susceptibility to the killing agent and/or the number of bound targets subpopulation, the model can also be applied to immune-system mediated killing: AMPs, antibodies (Magnus and Regoes 2010), heterogeneity in the elimination of bacterial colonies by the immune system (Bumann 2015) or the elimination of cancer cells (Spencer et al. 2009).

Our model is applicable when the bacterial population constantly declines, either because the antimicrobial concentrations are constantly above MIC or because the action of an antibiotic together with e.g. the immune system eliminates bacteria. Different types of models have to be employed in order to be able to investigate the effects of multiple-doses that are spaced far out or the effects of nonadherence. Furthermore, in our theoretical work we have only demonstrated how to work with unimodal distributions of persistence mechanisms. However, the application of our framework to skewed and not clearly unimodal experimental data demonstrates that it can be easily used to describe bi- or multi-modal distributions as well.

In summary, our approach allows the comparison and combination of multiple mechanisms within the same model that allows us to eliminate the inconsistencies when comparing different mechanisms, especially when it comes to fitting mathematical models describing different mechanisms of persistence to experimental or clinical data in different frameworks. Our work presents a simple and tractable way for estimating the effects of heterogeneities in bacterial populations, how they may result in persistent behavior, and how much they can increase the time until all subpopulations are eliminated. Ultimately, such models may aid decision making when it is safe to stop antibiotics without risking relapse due to remaining bacteria below detection limit.

SUPPLEMENTARY DATA

Supplementary data are available at [FEMSPD](https://femspd.cup.com/femspd/article-abstract/76/6/fly/065/5068691) online.

ACKNOWLEDGEMENTS

We thank Sören Abel for comments that greatly improved the manuscript. Furthermore, we thank Călin C. Guet and Anna M. C. Andersson for their comments on the manuscript and discussions on their experimental data (Bergmiller et al. 2017).

FUNDING

This work was supported by a Norwegian Research Council Young Research Talents grant to PzW [grant number 271 176] as well as by a PhD fellowship to AM by UiT- The Arctic University of Norway. These funding sources had no role in the design of this study, its execution, analyses, interpretation of the data, or decision to submit results.

Conflicts of interest. None declared.

REFERENCES

Abel zur Wiesch P, Abel S, Gkatzis S et al. Classic reaction kinetics can explain complex patterns of antibiotic action. *Sci Transl Med* 2015;7:287ra73.

- Abel zur Wiesch P, Clarelli F, Cohen T. Using chemical reaction kinetics to predict optimal antibiotic treatment strategies. *PLoS Comput Biol* 2017;13:1–28.
- Ankomah P, Levin BR. Exploring the collaboration between antibiotics and the immune response in the treatment of acute, self-limiting infections. *Proc Natl Acad Sci* 2014;111:8331–8.
- Balaban NQ, Gerdes K, Lewis K et al. A problem of persistence: still more questions than answers? *Nat Rev Micro* 2013;11:587–91.
- Balaban NQ, Merrin J, Chait R et al. Bacterial persistence as a phenotypic switch. *Science* 2004;305:1622–5.
- Bergmiller T, Andersson AMC, Tomasek K et al. Biased partitioning of the multidrug efflux pump AcrAB-TolC underlies long-lived phenotypic heterogeneity. *Science* 2017;356:311–5.
- Bumann D. Heterogeneous host-pathogen encounters: act locally, think globally. *Cell Host Microbe* 2015;17:13–19.
- Burnier M, Wuerzner G, Struijker-Boudier H et al. Measuring, analyzing, and managing drug adherence in resistant hypertension. *Hypertension* 2013;62:218–25.
- Claudi B, Spröte P, Chirkova A et al. Phenotypic variation of salmonella in host tissues delays eradication by antimicrobial chemotherapy. *Cell* 2014;158:722–33.
- Fridman O, Goldberg A, Ronin I et al. Optimization of lag time underlies antibiotic tolerance in evolved bacterial populations. *Nature* 2014;513:418–21.
- Horsburgh CR, Barry CE, Lange C. Treatment of tuberculosis. *N Engl J Med* 2015;373:2149–60.
- Kaiser P, Regoes RR, Dolowschiak T et al. Cecum lymph node dendritic cells harbor Slow-Growing bacteria phenotypically tolerant to antibiotic treatment. *PLoS Biol.* 2014;12:e1001793.
- van Kampen NG. *Stochastic Processes in Physics and Chemistry*. 3rd edn. Elsevier, 2007.
- Lawn SD, Zumla AI. Tuberculosis. *Lancet* 2011;378:57–72.
- Lewis K. Persister cells, dormancy and infectious disease. *Nat Rev Micro* 2007;5:48–56.
- Lewis K. Multidrug tolerance of biofilms and persister cells. *Curr Top Microbiol Immunol* 2008;322:107–31.
- Magnus C, Brandenburg OF, Rusert P et al. Mathematical models: a key to understanding HIV envelope interactions? *J Immunol Methods* 2013;398–399:1–18.
- Magnus C, Regoes RR. Estimating the stoichiometry of HIV neutralization. *PLoS Comput Biol* 2010;6:e1000713.
- Magnus C, Regoes RR. Restricted occupancy models for neutralization of HIV virions and populations. *J Theor Biol* 2011;283:192–202.
- Maier T, Schmidt A, Güell M et al. Quantification of mRNA and protein and integration with protein turnover in a bacterium. *Mol Syst Biol* 2014;7:511.
- Malmström J, Beck M, Schmidt A et al. Proteome-wide cellular protein concentrations of the human pathogen *Leptospira interrogans*. *Nature* 2009;460:762–5.
- Monack DM, Bouley DM, Falkow S. Salmonella typhimurium persists within macrophages in the mesenteric lymph nodes of chronically infected Nrpmp1 + / + mice and can be reactivated by IFN γ neutralization. *J Exp Med* 2004;199:231–41.
- Prajsnar TK, Hamilton R, Garcia-Lara J et al. A privileged intraphagocyte niche is responsible for disseminated infection of *Staphylococcus aureus* in a zebrafish model. *Cell Microbiol* 2012;14:1600–19.
- Pu Y, Zhao Z, Li Y et al. Enhanced efflux activity facilitates drug tolerance in dormant bacterial cells. *Mol Cell* 2016;62:284–94.
- Putrinš M, Kogermann K, Lukk E et al. Phenotypic heterogeneity enables uropathogenic *Escherichia coli* to evade killing by

- antibiotics and serum complement. *Infect Immun* 2015;**83**:1056–67.
- Rego EH, Audette RE, Rubin EJ. Deletion of a mycobacterial divi-some factor collapses single-cell phenotypic heterogeneity. *Nature* 2017;**546**:153–7.
- Regoes RR, Wiuff C, Zappala RM *et al.* Pharmacodynamic functions: a multiparameter approach to the design of antibiotic treatment regimens. *Antimicrob Agents Chemother* 2004;**48**:3670–6.
- Shen L, Rabi SA, Sedaghat AR *et al.* A critical subset model provides a conceptual basis for the high antiviral activity of major HIV drugs. *Sci Transl Med* 2011;**3**:91ra63-.
- Spencer SL, Gaudet S, Albeck JG *et al.* Non-genetic origins of cell-to-cell variability in TRAIL-induced apoptosis. *Nature* 2009;**459**:428–32.
- Spratt BG. Distinct penicillin binding proteins involved in the division, elongation, and shape of *Escherichia coli* K12. *Proc Natl Acad Sci* 1975;**72**:2999–3003.
- Terrak M, Ghosh TK, van Heijenoort J *et al.* The catalytic, glycosyl transferase and acyl transferase modules of the cell wall peptidoglycan-polymerizing penicillin-binding protein 1b of *Escherichia coli*. *Mol Microbiol* 1999;**34**:350–64.
- Wakamoto Y, Dhar N, Chait R *et al.* Dynamic persistence of antibiotic-stressed mycobacteria. *Science* 2013;**339**:91–5.

Paper 3



Article

Reaction Kinetic Models of Antibiotic Heteroresistance

Antal Martinecz ¹, Fabrizio Clarelli ¹, Sören Abel ^{1,2} and Pia Abel zur Wiesch ^{1,2,*}

¹ Department of Pharmacy, Faculty of Health Sciences, UiT—The Arctic University of Norway, 9037 Tromsø, Norway

² Centre for Molecular Medicine Norway, P.O. Box 1137, Blindern, 0318 Oslo, Norway

* Correspondence: pia.z.wiesch@uit.no; Tel.: +47-776-461-65

Received: 12 July 2019; Accepted: 13 August 2019; Published: 15 August 2019



Abstract: Bacterial heteroresistance (i.e., the co-existence of several subpopulations with different antibiotic susceptibilities) can delay the clearance of bacteria even with long antibiotic exposure. Some proposed mechanisms have been successfully described with mathematical models of drug-target binding where the mechanism's downstream of drug-target binding are not explicitly modeled and subsumed in an empirical function, connecting target occupancy to antibiotic action. However, with current approaches it is difficult to model mechanisms that involve multi-step reactions that lead to bacterial killing. Here, we have a dual aim: first, to establish pharmacodynamic models that include multi-step reaction pathways, and second, to model heteroresistance and investigate which molecular heterogeneities can lead to delayed bacterial killing. We show that simulations based on Gillespie algorithms, which have been employed to model reaction kinetics for decades, can be useful tools to model antibiotic action via multi-step reactions. We highlight the strengths and weaknesses of current models and Gillespie simulations. Finally, we show that in our models, slight normally distributed variances in the rates of any event leading to bacterial death can (depending on parameter choices) lead to delayed bacterial killing (i.e., heteroresistance). This means that a slowly declining residual bacterial population due to heteroresistance is most likely the default scenario and should be taken into account when planning treatment length.

Keywords: reaction kinetics; antibiotics; pharmacodynamics; Gillespie algorithm; antibiotic resistance; bacterial persistence; stochastic simulation

1. Introduction

When bacteria are exposed to antibiotics *in vitro* or *in vivo*, the elimination rate often changes dramatically over time. Typically, an initial phase of rapid decline is followed by a phase where bacterial killing is very slow or even absent. However, the bacteria that survive the rapid decline are not genetically different from those that were killed. When the bacteria are recultured from the surviving population and exposed to antibiotics at the same concentration again, they exhibit the same bi- or multiphasic killing as in the first experiment. This sets delayed bacterial killing apart from stable resistance mutations (antibiotic resistance). Just like antibiotic resistance, multiphasic bacterial killing has clinical implications: it is thought to complicate treatments, as it allows fractions of bacterial populations to survive extended exposure to antibiotics [1,2].

The characteristic slowdown of bacterial elimination after antibiotic exposure can be due to various mechanisms. According to a recent consensus statement [3], these mechanisms can be divided into either antibiotic persistence or heteroresistance. In this work we focus on the latter: in heteroresistance, the observation is that not all cells in a bacterial population are equally susceptible to antibiotics. It can be defined as the coexistence of multiple subpopulations of bacteria with varying levels of

susceptibility to antibiotics. In these mixed populations, the more resistant subpopulations should have a significantly different susceptibility. In practice, this means that the so-called minimum inhibitory concentration (MIC; antibiotic concentration where the net growth of the population is zero) should show an at least eightfold increase when compared to the majority of the population [3–5]. There are multiple mechanisms that can contribute to this phenomenon, such as unstable resistance mutations [6]. In addition to mutations, it has also been shown that diversity among cells that result in slight variations in susceptibility to antibiotics can also lead to heteroresistance, including differences in the number of intracellular targets [7,8], differences in cell sizes and therefore diversity in the intracellular concentration of targets [9], or cell-to-cell differences in the number of efflux pumps that affect the intracellular antibiotic concentrations [10,11]. Currently, there is great interest surrounding heteroresistance; however, due to its by definition transient nature, it is difficult to investigate [1,4,5]. To find potential mechanisms that lead to heteroresistance and therefore guide experiments, mathematical modeling of antibiotic action can be helpful.

Indeed, models that include both intracellular drug-target binding and its effect on a bacterial population have been successfully employed to model heteroresistance [7]. Such drug-target binding models are becoming increasingly popular [12–14]. Modeling the reaction kinetics of drug-target binding can be challenging because it often involves low numbers of molecules; for example, the common antibiotic target gyrase has a 100 copies per cell [15,16]. In these cases, differential equations do not give accurate results, as they do not allow modeling discrete values instead of continuous values. This is a problem when the modeled process is sensitive to the changes in molecular numbers, for example, toxic byproducts and the model gives the result of half a molecule instead of 0 or 1. To circumvent this issue, approaches based on master equations can be employed [7]. For simplicity and the purpose of this paper, we call deterministic systems of differential equations “master equations” even if they are not necessarily linear. These deterministic equations model entire bacterial populations and classify bacteria into compartments according to how many target molecules are bound. However, these are often cumbersome to design and use, as they require a differential equation per “state” of the system, for example, one equation per possible number of bound targets.

Master equations have several advantages, among them the ability to incorporate bacterial growth and death with the subsequent changes in target molecule content and occupancy. As deterministic models, they do not need to be run many times to get representative averages. However, these current mathematical approaches have limitations in terms of the complexity of the molecular mechanisms that lead to bacterial death or suppress bacterial replication. When antibiotics bind to their intracellular targets, they interfere with essential functions of cells and thereby inhibit bacterial replication (bacteriostatic effect) or kill the cells (bactericidal effect). Both the bactericidal and bacteriostatic effects can be multi-step processes, for example the binding of antibiotics to their target can lead to the production of toxic byproducts that eventually kill the cells in, for example, kanamycin or norfloxacin [17]. In master equations-based approaches, the additional number of processes quickly inflates the required number of equations, as it would need one equation for each combination of molecule numbers, for example toxic byproducts and bound targets. The approaches used in [7] for example employ $n+1$ equations for n target molecules, with n ranging from 10^2 to 10^5 . Modeling an additional step in the molecular cascade leading to bacterial death would then require 10^4 to 10^{10} equations. Therefore, the current mathematical tools bar us from quickly testing and evaluating models of multi-step intracellular processes, thereby making it difficult to test theories on mechanisms that can lead to heteroresistance. As a result, while it is suspected that changes in the production of toxic byproducts or diversity in other parts in intracellular kinetics can lead to heteroresistant behavior, it is yet to be shown by modeling.

In this work, we use Gillespie simulations—stochastic simulations of the reaction kinetics in single bacterial cells [18,19]—to model multi-step intracellular processes and show that diversity in the rates in these processes at different levels can lead to heteroresistance. Thereby, we also demonstrate that Gillespie simulations are an effective tool in investigating population dynamics of bacteria, particularly

when modeling multi-step processes. While Gillespie simulations have been an invaluable tool in computational biology, they are yet to be used in the context of modeling the response of bacterial populations to antibiotics.

2. Results

When bacteria are exposed to antibiotics, the elimination of bacteria can slow down dramatically over time. Figure 1a shows a schematic of a so-called time-kill curve (measured bacterial numbers over time after antibiotic exposure)—and thereby gives an example of how multiple subpopulations can result in a slowdown of elimination. If this phenomenon is caused by heteroresistance, the underlying mechanism is a coexistence of multiple subpopulations with varying degrees of susceptibility to antibiotics. The susceptibility to antibiotics can be captured with pharmacodynamic curves that describe the net population growth (replication minus death, or the slope of the time-kill curve) at a given antibiotic concentration. The antibiotic concentration at zero net growth is called the minimum inhibitory concentration (MIC). Figure 1b illustrates how multiphasic killing of bacterial populations can lead to different pharmacodynamic curves, one for quickly and one for slowly declining bacteria. Here, we model single- (Figure 1c) and multi-step processes (Figure 1d) that result in the elimination of bacteria and obtain pharmacodynamic curves. We assess whether hypothetical variations in the parameters of the multistep processes involved in bacterial drug-susceptibility can result in bi- or multiphasic time-kill curves. We employ Gillespie simulations, demonstrating that they can be an effective tool in modeling antibiotic action in bacteria.

First, we show the relationship among Gillespie simulations and the already established methods—master equations and simple reaction kinetics. This relationship is well studied in the literature modeling other processes [19,20], and our goal here is to provide a starting point for comparing the models that are built upon them. Figure 2 illustrates that all methods model the same process, therefore yielding similar results. Simple reaction kinetics describe the mean (Figure 2a,b), and master equations describe the probability of observing a given state of the system (given number of bound targets) (Figure 2c,d). Gillespie simulations are stochastic simulations that describe one possible time-course of the observed number of bound targets over time (Figure 2e,f). When repeated sufficiently often, the average of the Gillespie simulations should yield the same result as the other two approaches.

We aimed to illustrate that modeling based on Gillespie algorithms predicts the same time-kill curves resulting from reaction kinetics as the already established heteroresistance model based on master equations [7]. To this end, we chose a setting where bacterial growth is negligible over the observed time period (easily modeled with classical Gillespie algorithms) and where bacterial death is caused by a single reaction step (easily modeled with master equations). We furthermore assume that when bacteria die, target degradation is negligible in the period we observe. This may mean either that the entire cellular structure remains intact for a while or that targets that are released by bacterial lysis into the medium are not degraded quickly. For the sake of clarity, we simulated the binding kinetics of a fictive situation with only few targets. The time course of target occupancy is shown in Figure 3a. The predictions of target occupancy are the same for a deterministic master equation model and the Gillespie algorithm, in line with the large body of literature showing that Gillespie algorithms are useful tools to describe reaction kinetics [19,23,24]. Based on these simulations of target occupancy, we predict time-kill curves of a bacterial population with multiple subpopulations having the same number of targets, but the thresholds for killing follow a normal distribution, that is, varying susceptibility or heteroresistance. In Figure 3, we demonstrate that both master equations and the Gillespie algorithm give essentially the same result.

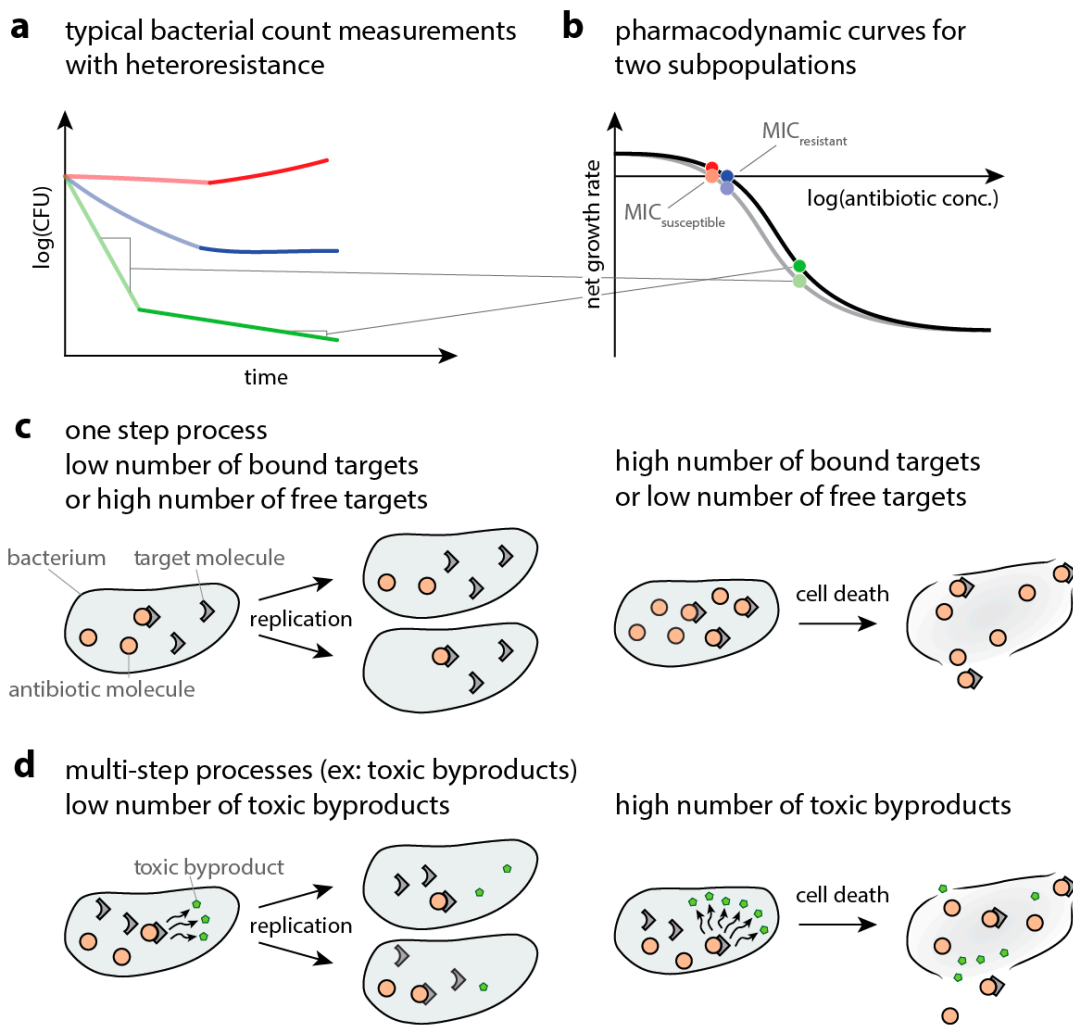


Figure 1. Schematic explanation of observed data and underlying processes. (a) Schematic drawing of a time–kill curve, where bacterial numbers are followed over time after exposure to different antibiotic concentrations (increasing from red to blue to green). The initial fast decline is depicted in pale, the subsequent slow decline in dark colors. (b) Schematic of a pharmacodynamic curve showing how increasing antibiotic concentrations (different colors) affect bacteria. The x-axis shows logarithm of the antibiotic concentrations. The y-axis shows the resulting net growth rate, that is., bacterial replication minus death, as measured by the slope of bacterial decline. The gray line depicts the quickly declining population (more susceptible), the black line represents the population declining more slowly. The gray lines between (a) and (b) illustrate how to translate the slope of time–kill curves to the pharmacodynamic curves. The pale and dark points illustrate the slopes of the time–kill curves in the corresponding colors in (a). (c) Schematic representation of the events leading to bacterial death if the drug–target complex itself is toxic. Bacteria can still replicate when few target molecules are bound by the antibiotic (left panel) but die when a high number of target molecules that exceed the killing threshold are bound (right panel). (d) Schematic representation of the events leading to bacterial death if the drug–target complex causes the accumulation of a toxic metabolite. Bacteria can still replicate when only a few metabolite molecules are present and die when too much metabolite has accumulated.

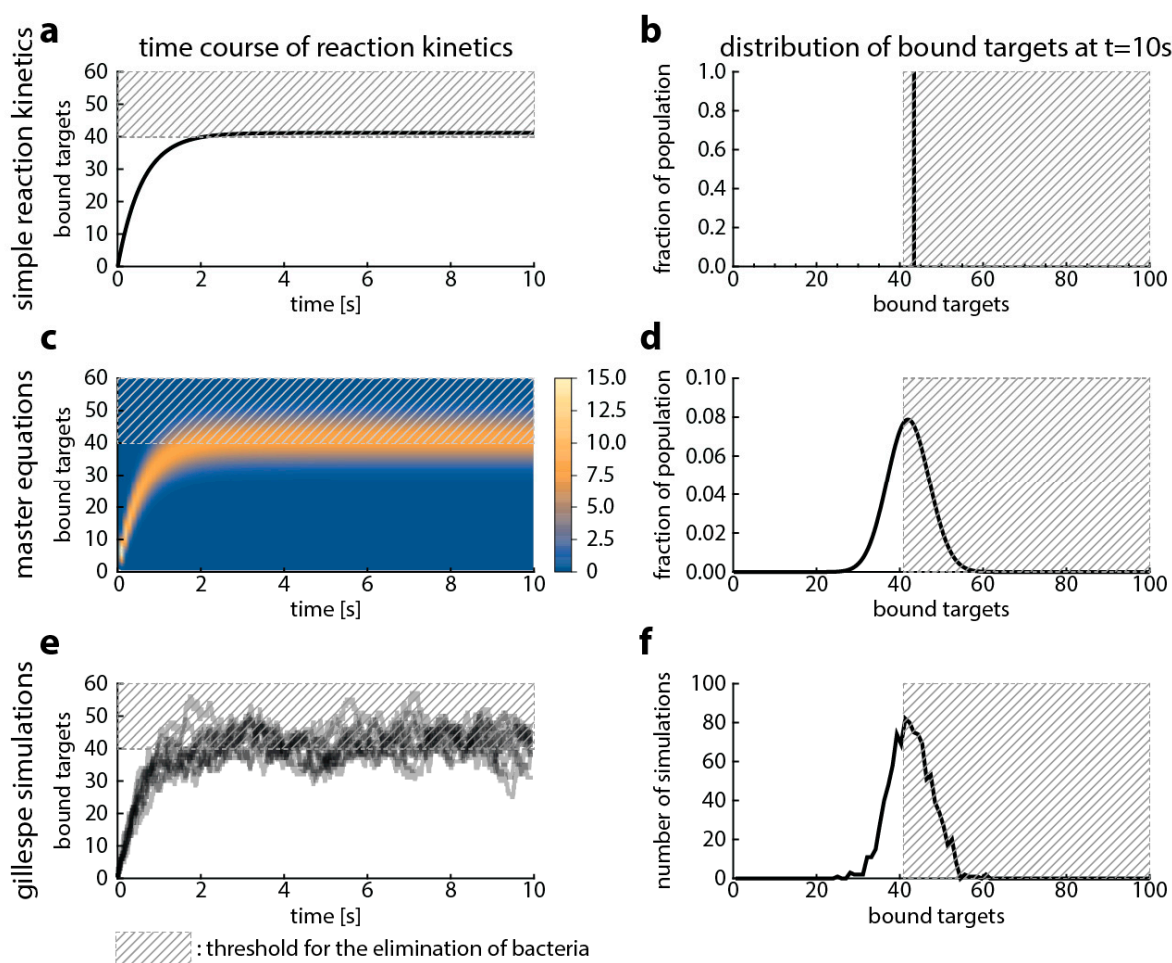


Figure 2. Comparison of modeling approaches that follow the reaction kinetics of antibiotic target-binding. In this figure, we compare three approaches: simple reaction kinetics (a,b), master equations (c,d) and Gillespie simulations (e,f). We used the following parameters: $k_f = 10^5 \text{ M}^{-1}\text{s}^{-1}$ and $k_r = 1 \text{ s}^{-1}$ (based on $K_D = \frac{k_r}{k_f} = 10^{-5} \text{ M}$ for ciprofloxacin [21,22]), number of targets: 100 molecules (gyrase, [15,16]), and the antibiotic concentration is $116 \mu\text{M}$. The left column shows the time course of antibiotic target-binding. The x-axis shows the time, the y-axis shows the percentage bound target and the dashed grey area illustrates an arbitrary threshold of bound target when we presume bacterial killing would occur. The legend for the heat map in (c) is given next to the figure and shows the percentage of the bacterial population in a given state. The right column shows the distribution of target occupancies (x-axis) in the upper panel for the corresponding modeling approach well after steady state has been reached (plateau in left column, at 10 s).

We thereby established that both methods, as expected, are equivalent under the condition that bacterial replication can be neglected. Next, we set out to investigate how these dynamics are changed by bacterial replication: the production of new (unbound) target molecules and the inheritance of bound target molecules from the mother cell.

To illustrate under which conditions bacterial replication can be neglected, we now compare target occupancy predicted with master equation-based simulations for fast (doubling time 20 min, e.g., *Escherichia coli*) and slow (doubling time 24 h, e.g., *Mycobacterium tuberculosis*) bacterial replication rates. Figure 4 shows the differences between simulations where we kept the difference of bacterial replication and elimination constant (“same” net growth), but we changed the ratio of the two (i.e., high replication and elimination at the same time, or low bacterial elimination and low replication). While the assumption that bacterial replication does not affect target occupancy has been made elsewhere [13,26], we find that neglecting replication gives substantially different results for a doubling time of 20 min.

However, we also find that there are relatively minor differences when replication only occurs every 24 h.

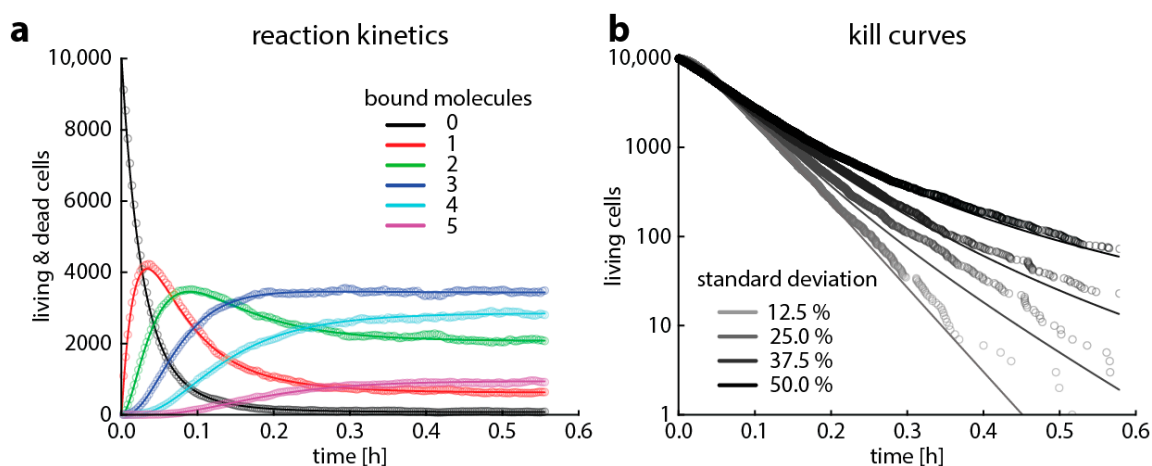


Figure 3. Comparison of the output of a Gillespie algorithm and simulations based on master equations. This is a simplified case for clarity, where a cell only contains five target molecules and dies on average within one second when more than two target molecules are bound. The binding rate k_f is $1.2 \times 10^6 \text{ M}^{-1}\text{s}^{-1}$, the unbinding rate k_r is 1.2×10^{-3} (for rifampicin, [25]), and the antibiotic concentration is 1.7 nM (10^{15} molecules/liter). (a) Shows the predicted average target occupancy: the number of bacteria with 0 (black), 1 (red), 2 (green), 3 (blue), 4 (turquoise), and 5 (purple) bound targets for 10,000 Gillespie simulations (dots) or the master equation approach (lines). (b) Shows the predicted time–kill curves when modeling 10,000 bacterial cells with Gillespie simulations (dots) or the master equation approach (lines) for bacterial populations where the threshold for killing follows a normal distribution with 12.5%, 25%, 37.5%, or 50% standard deviation.

Finally, to show the flexibility of the approach and to investigate potential sources of heteroresistance, we modelled four different scenarios that lead to bacterial death (Table 1 in Materials and Methods shows the events and their rates modeled in the Gillespie algorithm):

- A high proportion of bound versus unbound target is toxic (i.e., “relative toxicity”). In this case, we assume a bacterium is dead once the ratio of bound target and total target molecules exceeds a threshold. Here, we introduce heterogeneity by assuming that the number of target molecules is normally distributed around its mean.
- The target has an “essential” function (i.e., the cell dies when less than a certain amount of target is free). In this case, we assume a bacterium is dead once the number of free target falls below a threshold. Here, we introduce heterogeneity by assuming that the threshold for killing is normally distributed around its mean.
- The antibiotic-target complex is “primary toxic” (i.e., the cell is immediately damaged by bound targets). In this case, we assume a bacterium is dead once the number of bound targets exceeds a threshold. Here, we introduce heterogeneity by assuming that the number of target molecules is normally distributed around its mean.
- The antibiotic-target complex is “secondary toxic” (i.e., triggers the accumulation of toxic metabolites that ultimately kill the cell). In this case, we assume a bacterium is dead once the number of toxic metabolites exceeds a threshold. Here, we introduce heterogeneity by assuming that the rate of toxic metabolite production is normally distributed around its mean.

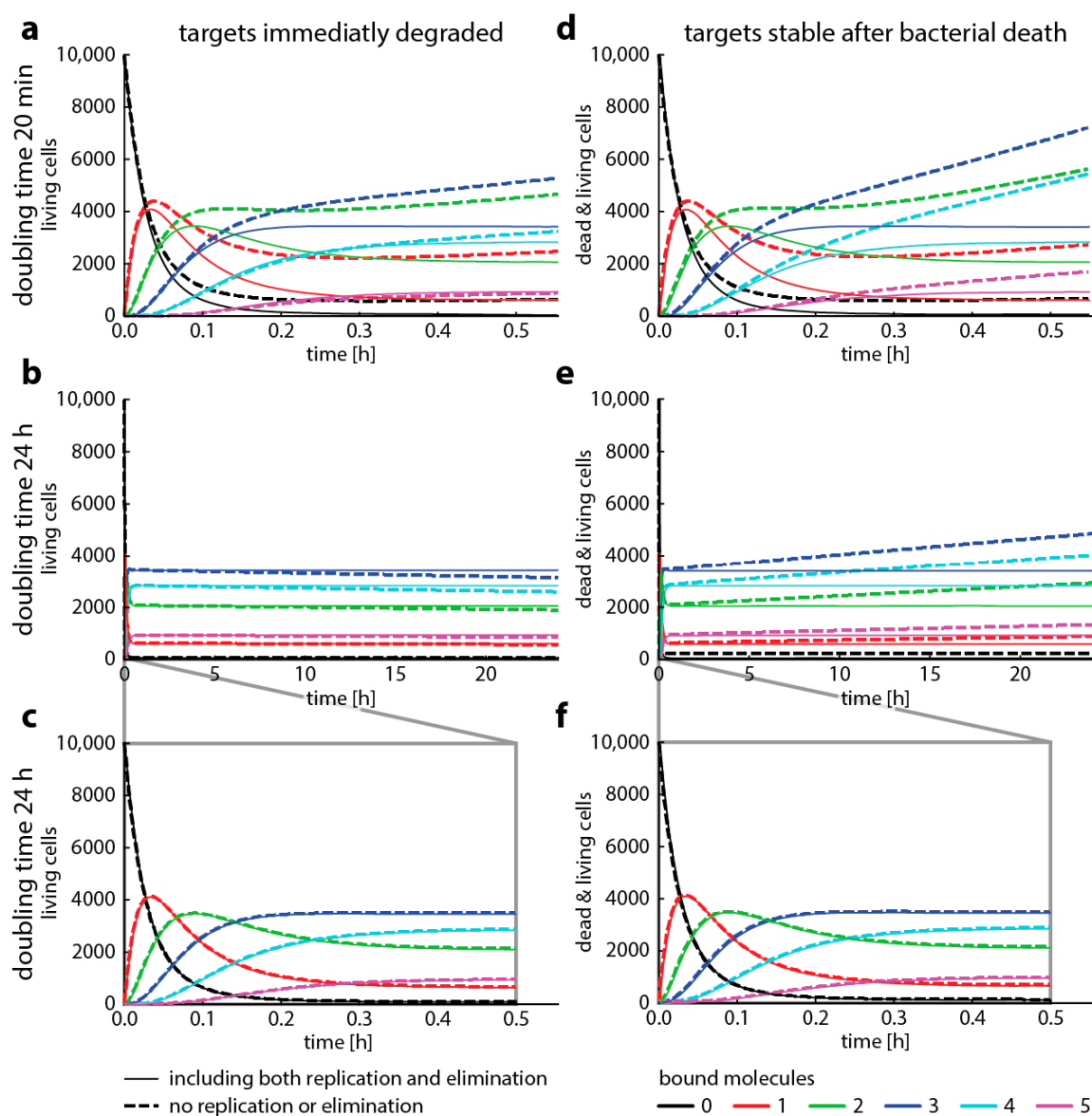


Figure 4. Bacterial replication changes target occupancy. This graph shows how target occupancy with replication and death (dashed lines) changes compared to target occupancy without replication or death (solid lines, compare to Figure 2) for two different cases. Cases, where the drug targets are immediately degraded after bacterial death (left column) or remain stable after bacterial death (right column). All parameters are the same as in Figure 3, with added replication and adjusted death rates. We assume that replication immediately ceases when more than two target molecules are bound and that cell die immediately when there are at least 4 bound target molecules. The doubling time ($\frac{\ln(2)}{\text{replication rate}}$) is either 20 min (top panel) or 24 h (mid and bottom panels). The bottom panel highlights the first 30 min of the mid panel time course. The death rate is always 2 x the replication rate. (a–c) show the number of living bacteria only, (d–f) show both living and dead cells.

As demonstrated previously for variances in target molecule content, normally distributed population variances in the binding kinetics of any of the steps leading to bacterial killing leads to multiphasic kill curves (or heteroresistance) (Figure 5). In our case, this occurred when the variation in the population was above 4–10% (Figure A2).

Table 1. Event table and parameter descriptions for Gillespie simulations.

Model	Reactions	Description	Rate
Single step model	$A + T \rightarrow AT$	Forward reaction	$\hat{k}_f AT$
	$AT \rightarrow A + T$	Backward reaction	$k_r AT$
Multi-step model	$A + T \rightarrow AT$	Forward reaction	$\hat{k}_f AT$
	$AT \rightarrow A + T$	Backward reaction	$k_r AT$
	$AT \rightarrow AT + M_{tox}$	Toxic metabolite production	$k_{tox} AT$

Using the results from each simulation, we implemented the elimination of bacteria taking place after the number of bound targets (single-step case) or toxic metabolites (multi-step case) cross a threshold. In a simplified case, the first time-point where the simulations cross this threshold, we consider the cell to be dead. However, in single-step processes, (computationally) there is no upper limit to the elimination rates as it is defined only by the speed of the reaction. Therefore, it is best implemented after as “time above the threshold” instead: after a cell spends more than a given amount of time above the threshold, we consider the cell dead.

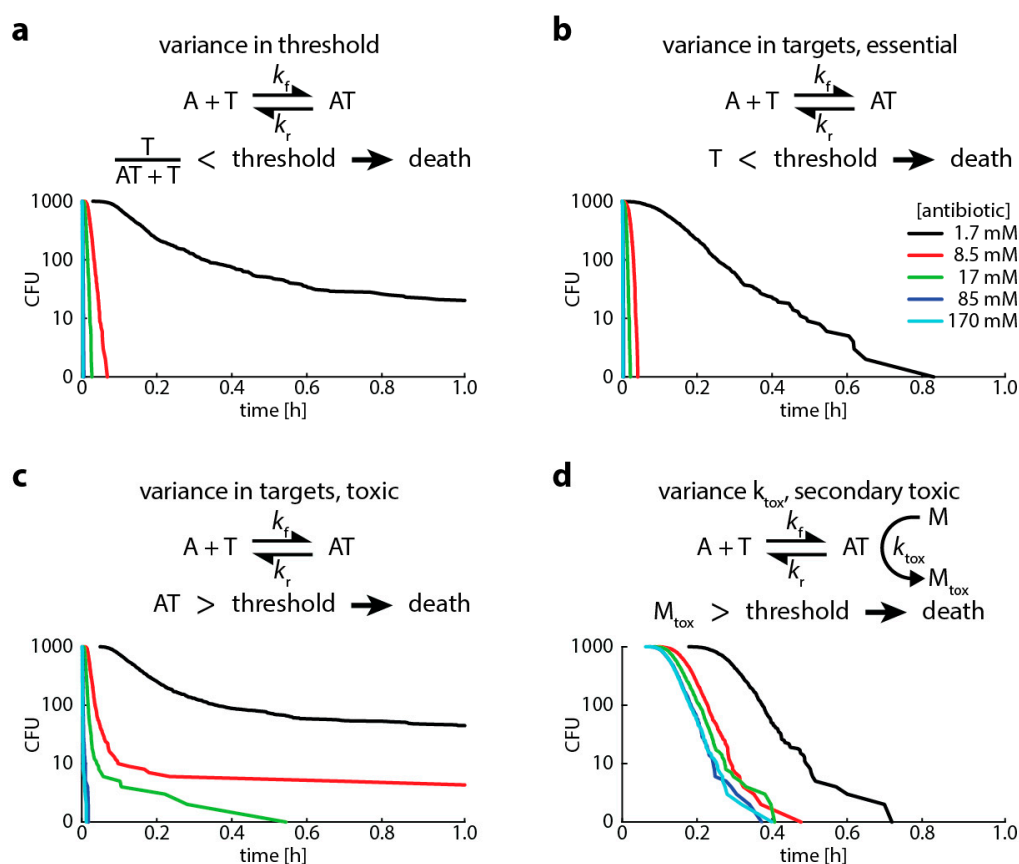


Figure 5. Variances in any step that causes bacterial killing: binding kinetics or killing threshold leads to multiphasic kill curves. This graph shows Gillespie simulations of four different scenarios of bacterial killing (see explanation in text). In all simulations, we assume (i) 100 target molecules, (ii) a binding rate k_f of $1.2 \times 10^6 \text{ M}^{-1}\text{s}^{-1}$, (iii) an unbinding rate k_r of 1.2×10^{-3} (for rifampicin, [25]), and (iv) an intracellular volume of 10^{-15} . We vary the antibiotic concentration from 1.7 (black), 8.5 (red), 17 (green), 85 (blue) to 170 (turquoise) mM. (a) “Relative toxicity” (point 1 in main text above), threshold for killing 50%, threshold normally distributed with 20% standard deviation (SD). (b) “Essential target function” (point 2 in main text above), threshold for killing 50 free target molecules, target number normally distributed with 20% SD. (c) “Primary toxic” (point 3 in main text above), threshold for killing 50 bound target molecules, target number normally distributed with 20% SD. (d) “Secondary toxic” (point 4 in main text above), threshold for killing 500 accumulated toxic metabolites, rate of metabolite production k_{tox} is $1.2 \times 10^6 \text{ M}^{-1}\text{s}^{-1}$, k_{tox} normally distributed with 20% SD.

3. Discussion

The aim of this paper is to extend the toolbox for modeling the intracellular processes that kill bacteria and to illustrate how these tools can be used to describe bacterial heteroresistance. Traditionally, antibiotic efficacy was mainly described by a single value, the minimal inhibitory concentration (MIC, see points in Figure 1B). While there is often a correlation between treatment success and MIC [27,28], there is limited predictive power, since not all patients infected with bacteria that are classified as susceptible by their MIC are successfully treated with antibiotics [6]. More importantly, up to two thirds of patients infected with bacteria that are classified as resistant to the prescribed antibiotic based on MIC measurements are successfully treated (despite the infection per se being serious) [29]. This has led to calls for more sophisticated approaches where the entire dose-response curve (entire curve in Figure 1B) is taken into account, which is described by pharmacodynamic models [30]. Currently used pharmacodynamic models (E_{max} /Hill-models) originated in 1910 [31,32] and make a large number of simplifying assumptions. Therefore, novel models including drug-target binding have been developed to overcome the limitations of traditional models.

Previously, established deterministic antibiotic-target binding models classify bacterial populations in compartments based on drug occupancy. Here, we use the Gillespie stochastic simulation algorithm that focuses on the reaction kinetics in single cell and model bacterial populations by running simulations as many times as there are cells in the population. This means that a bacterial population of e.g., 1000 cells is modeled by running 1000 individual simulations. The Gillespie algorithm is a well-established computational method in computational biology [24], chemistry [19], and epidemiology [33]. However, it has not been used to model the effects of antibiotics on bacterial populations. Gillespie simulations fill the niche of modeling multi-step intracellular processes, as the use of current modeling approaches make this cumbersome.

We have modeled bacterial death as an event that is triggered by spending a specific amount of time spent above a threshold of bound targets or toxic byproducts. This approximation is only valid for one generation of bacteria because it does not allow taking into account the fact that the bound targets of the mother cells are distributed to the daughter cells. This means that for the daughter cells, the simulations should not start at 0 bound targets. To accurately model this, it would be necessary to stop the simulation after the cell is supposed to replicate, dividing the bound targets randomly between the daughter cells, increase the total number of target to reflect target synthesis during growth, and then start new simulations with the daughter cells. This would greatly increase the complexity of the model and shows the central difference in the biological population aspects, that is, bacterial replication. In approaches based on master equations, this can be easily done for each compartment of bound target molecules with well-established biological population equations (e.g., logistic or exponential growth). Therefore, to demonstrate the how this approximation on growth changes bacterial dynamics, we modelled it with an established master equations-based approach [7].

In Figure 4, we presented four cases where we modeled how fast and how slow bacterial growth combined with different assumptions about target stability after cell death affects the dynamics of the system. Our aim here is to illustrate how and when to use different modeling approaches to describe antibiotic action on a molecular scale. We highlight how a major assumption, that antibiotic target occupancy is independent of bacterial replication, can fundamentally change model predictions. While this assumption has been made elsewhere [13,26], our results indicate that Gillespie simulations neglecting bacterial replication are not suited for modeling organisms with fast growth such as *E. coli*.

However, Gillespie algorithms seem to yield similar results as master equations for slow replication. When we assume that bacterial death results in immediate target degradation, the total amount of target binding is slightly underestimated. Conversely, when we assume the other extreme, that targets are stable after bacterial death, the total amount of target binding is overestimated. Therefore, if realistic target degradation rates were available to inform models with replication, they would probably result in an even better concordance between Gillespie simulations and master equations. However, the results presented here are strongly dependent on the parameter setting we chose. Before making a decision

to neglect replication (and therefore making modeling complex reactions possible), it is advisable to compare one-step simulations parametrized with corresponding binding rates (e.g., the first step, a composite binding rate, or the binding rates of the rate-limiting step) with and without the replication rates of the bacterial organism to be studied. Figure A1 gives a more comprehensive overview of the dynamics when we change assumptions about growth and death. In summary, neglecting replication warrants careful checking for the specific bacteria–drug pair and is most applicable to slow bacterial replication rates as for example found in *M. tuberculosis*.

The intended uses of this approach are in vitro studies that investigate antibiotic effects on bacteria. For instance, the expression of genes involved in the bacterial response to antibiotics may vary in a bacterial population thereby leading to heteroresistance [6]. These measured heterogeneities can be used to parametrize the presented multistep models in order to predict how these may affect time–kill curves. They can be used to assess whether the measured heterogeneities are sufficient to explain response to antibiotics (as there could be a multitude of processes contributing to changes in time–kill curves). Additionally, in vivo gene expression levels may be measured [34], but it might be difficult to obtain time–kill curves. In these cases, our approach might help to better understand bacterial responses. Our and other drug-target binding models can also easily replace traditional pharmacodynamic E_{\max} - or Hill functions when modeling antibiotic action in patients. Moreover, they can be easily incorporated in mixed effect pharmacokinetic/pharmacodynamic (PK/PD) models where the drug concentration is supplied by a PK model, and drug-target binding models are used to describe fixed pharmacodynamic effects with additional stochastic effects [35].

Using our Gillespie-based approach, we have run simulations for both single-step processes as well as multi-step processes and demonstrated (Figure 5) that normally distributed population variances in the binding kinetics of any of the steps involving bacterial killing can lead to multiphasic kill curves (or heteroresistance). This means that heteroresistant behavior can emerge in response to minor changes in the processes leading to bacterial death. As we have shown previously in [7,8], this behavior can be expected at concentrations where the pharmacodynamic curves for the majority and minority subpopulations (for example, Figure 1b) are further apart from each other. This mainly happens at the steeper parts of the pharmacodynamic curves (i.e., around inflection point), where a shift in the pharmacodynamic curves caused by the changes in binding kinetics can create a large enough difference thereby producing multiphasic time–kill curves.

We would therefore caution not to interpret the criterion of a substantially different MIC in heteroresistant subpopulations too strictly, in concordance with [6,36]. An eightfold change in MIC as an experimental criterion is sensible because of the low accuracy of testing MICs (fourfold changes are regarded as the same result [36]). However, our models show that minor changes in binding kinetics, which do not necessarily lead to an 8-fold change in MIC, can lead to multiphasic time–kill curves (i.e., heteroresistance). In addition, our work highlights that one should expect multiphasic kill curves in almost all settings even in the absence of specific bacterial subpopulations, because it is extremely unlikely that the content of all molecules involved in bacterial killing is exactly the same in all cells of a population. Therefore, all antibiotic treatment should take residual, slowly killed bacterial populations into account.

4. Materials and Methods

4.1. Simple Reaction Kinetics (Excluding Bacterial Replication and Death)

For modelling simple reaction kinetics between antibiotic molecules and their target molecules, we used the following differential equations:

$$\frac{dAT(t)}{dt} = A \cdot T(t)\hat{k}_f - AT(t)k_r \quad (1)$$

$$\frac{dT(t)}{dt} = -A \cdot T(t)\hat{k}_f + AT(t)k_r, \quad (2)$$

where:

- $\hat{k}_f = \frac{k_f}{V_i \cdot n_A}$ is the adjusted forward reaction rate to accommodate working with the number molecules inside the cells instead of concentrations. Here, k_f is the forward reaction rate, $V_i = 10^{-15}$ l is the average cell volume, and $n_A = 6 \cdot 10^{23}$ is the Avogadro number.
- k_r is the reverse reaction rate.
- A is the number of antibiotic molecules inside the cell.
- $T(t)$ is the number of free target molecules inside the cell.
- $AT(t)$ is the number of bound target molecules inside the cell.

For all simulations we used the binding parameters of ciprofloxacin: the parameters used are $K_D = \frac{k_r}{k_f} = 10^{-5}$ M (ciprofloxacin [21,22]), number of targets $n = 100$ (gyrase, [15,16]).

We only used the simple reaction kinetics for illustrating the connection among the different ways to model chemical reaction kinetics, therefore this model does not include bacterial replication or death.

4.2. Master Equations (Including Bacterial Replication and Death)

An approach based on systems of ordinary differential equations fully described in [7] combines a modeling the chemical reaction kinetics of antibiotics binding to their targets, and bacterial population dynamics (i.e., bacterial growth and death). Here, each equation describes bacteria with a given number of bound targets. However, in addition to the reaction kinetics model providing the connection between the equations, upon replication the mother cells distribute their bound targets among the daughter cells randomly.

$$\begin{aligned} \frac{dB_x}{dt} &= \hat{k}_f(n-x+1)AB_{x-1} - k_rxB_x - \hat{k}_f(n-x)AB_x + k_r(x+1)B_{x+1} + \rho_x \\ &\quad - r_xB_x \frac{K - \sum_{j=0}^n B_j}{K} - d_xB_x, \quad \text{for } x \in [2 : n-1] \end{aligned} \quad (3)$$

$$\begin{aligned} \frac{dB_0}{dt} &= -\hat{k}_fnAB_0 + k_rB_1 + \rho_0 - r_0B_0 \frac{K - \sum_{j=0}^n B_j}{K} - d_0B_0, & \text{for } x = 0 \\ \frac{dB_n}{dt} &= \hat{k}_fAB_{n-1} - k_rnB_n + \rho_n - r_nB_n \frac{K - \sum_{j=0}^n B_j}{K} - d_nB_n, & \text{for } x = n \end{aligned}$$

where:

- x is the number of bound targets,
- n is the number of targets,
- B_x is the number of bacteria with x bound targets,
- d_x is the elimination rate of bacteria at x bound targets,
- $\rho_x = 2 \sum_{i=x}^n f_{i,x} r_i B_i \frac{K - \sum_{j=0}^n B_j}{K}$ —describes the inheritance of bound targets from the mother cells (“inflow”) using the hypergeometric distribution $f_{i,x}$ for the random distribution of targets.
- r_x is the replication rate of cells at x bound targets.

These systems of differential equations are not necessarily classical master equations because they are not linear. However, when assuming that bacterial replication is exponential and not logistic (i.e., there is no maximal bacterial density) and when assuming that the extracellular antibiotic concentration is constant, these systems become linear and therefore classical master equations. Similarly to [7,8], we also modeled heteroresistance with these equations, here we modeled multiple subpopulations with varying numbers of targets, threshold for elimination, or rate. Here we describe the frequency of subpopulations as a normal distribution around the mean. We varied the standard deviation to model different levels of heterogeneity.

4.3. Gillespie Simulations (Excluding Bacterial Replication And Including Bacterial Death)

The Gillespie stochastic simulation algorithm first published in 1977 is a general algorithm to simulate stochastic processes originally developed to capture the binding kinetics [18]. Starting from the initial conditions, the simulation is computed by repeating the following three steps. First, determining the rates of the next possible reactions based on the number of molecules and reaction rates (R_i) at the given time-point. Second, drawing two random numbers, one from an exponential distribution with a mean of $(\sum R_i)^{-1}$ to determine the time until the next time-step. In addition, we chose which reaction is going to happen, where reaction “ x ” taking place has the probability of $\frac{R_x}{\sum R_i}$. The third step involves updating the numbers of molecules and time accordingly to step two [19].

In this work, we use this algorithm to simulate chemical reaction kinetics within cells, modeling both systems with a single or two steps (Table 1).

4.4. Implementation

Codes for Figure 3, Figure 5, and S2 were implemented in statistical software package R (version 3.4.4, The R Foundation for Statistical Computing, Vienna, Austria). Codes for Figure 2 were implemented in Mathematica (Version 12.0, Wolfram Research, Inc., Champaign, IL, USA). Codes for Figure 4 and S1 were implemented in MATLAB (2019a, The MathWorks, Natick, MA, USA). All codes are available on www.abel-zur-wiesch-lab.com.

Author Contributions: Conceptualization, A.M. and P.A.z.W.; methodology, A.M. and P.A.z.W.; software, A.M., F.C. and P.A.z.W.; validation, P.A.z.W.; investigation, A.M., F.C. and P.A.z.W.; writing—original draft preparation, A.M.; writing—review & editing, S.A. and P.A.z.W.; visualization, A.M., F.C., S.A. and P.A.z.W.; supervision, P.A.z.W.; project administration, P.A.z.W.; funding acquisition, S.A. and P.A.z.W.

Funding: This work was funded by the Bill and Melinda Gates Foundation, grant number OPP1111658 (P.A.z.W.); the Research Council of Norway (NFR), grant number 262686 (to P.A.z.W.) and grant number 249979 (to S.A.); and Helse-Nord, grant number 14796 (to S.A.). The publication charges for this article have been funded by a grant from the publication fund of UiT—The Arctic University of Norway.

Conflicts of Interest: The authors declare no conflict of interest. The funders had no role in the design of the study; in the collection, analyses, or interpretation of data; in the writing of the manuscript, or in the decision to publish the results.

Appendix A

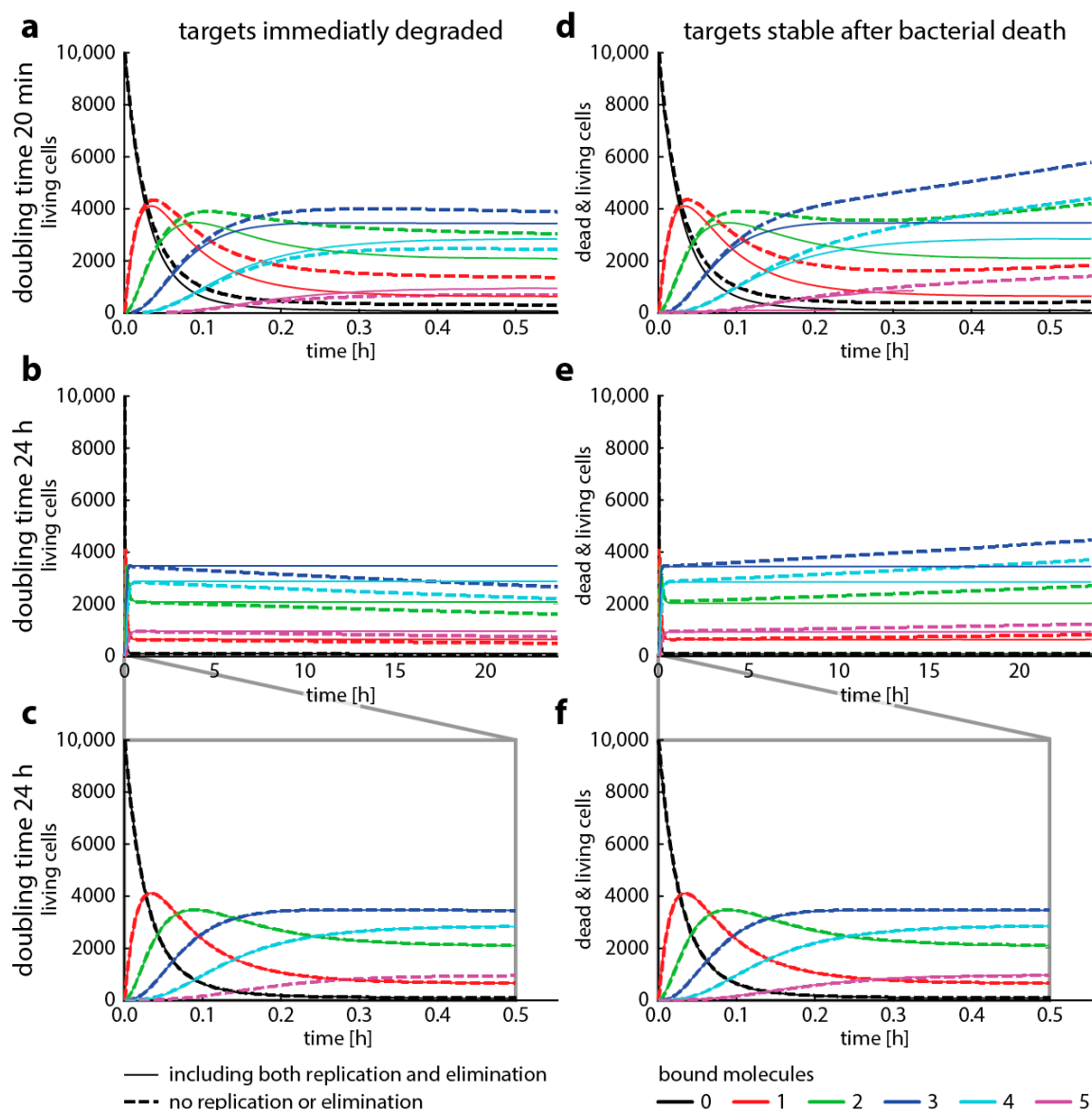


Figure A1. Bacterial replication changes target occupancy. This graph shows simulations of the same parameter sets as in Figure 4, but with different assumptions about how target occupancy changes bacterial replication. In Figure 4, we assume that the replication rate depending on target occupancy is a step function where replication suddenly ceases when more than two target molecules are bound. In this figure, we assume that the replication rate depends linearly on target occupancy. As in Figure 4, this graph shows how target occupancy with replication and death (dashed lines) changes compared to target occupancy without replication or death (solid lines) for two different cases where the drug targets are immediately degraded after bacterial death (left column) or remain stable after bacterial death (right column). All parameters are the same as in Figure 3 with added replication. We assume that replication immediately ceases when more than two target molecules are bound and that cell die immediately when there are at least four bound target molecules. The doubling time ($\frac{\ln(2)}{\text{replication rate}}$) is either 20 min (top panel) or 24 h (mid and bottom panels). The bottom panel highlights the first 30 min of the mid panel time course. The death rate is always 2x the replication rate. (a–c) show the number of living bacteria only, (d–f) show both living and dead cells.

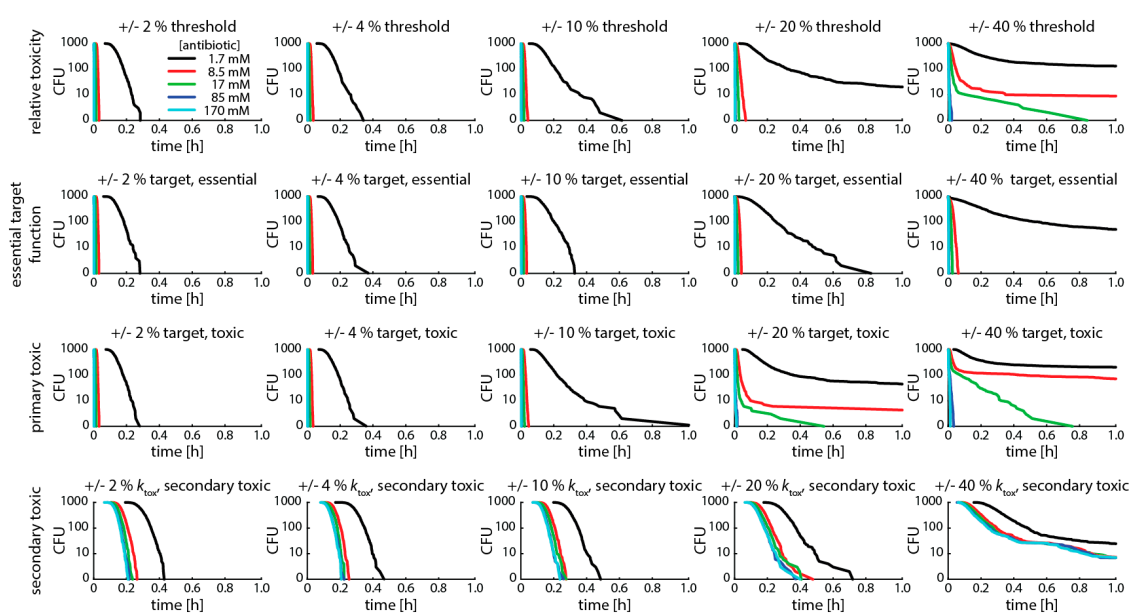


Figure A2. Variances in binding kinetics of any step causing bacterial killing leads to multiphasic kill curves. This graph shows simulations with the same parameter set as Figure 5, but different variances in bacterial populations. We show Gillespie simulations of four different scenarios of bacterial killing (see explanation in text) and different degrees of variance (columns). In all simulations, we assume (i) 100 target molecules, (ii) a binding rate k_f of $1.2 \times 10^6 \text{ M}^{-1}\text{s}^{-1}$, (iii) an unbinding rate k_r of 1.2×10^{-3} (for rifampicin, [25]), and (iv) an intracellular volume of 10^{-15} . We vary the antibiotic concentration from 1.7 (black), 8.5 (red), 17 (green), 85 (blue) to 170 (turquoise) mM. The top panel shows the “relative toxicity” scenario. Threshold for killing 50%, threshold normally distributed with standard deviation (SD) given in graph. The second panel shows the “essential target function” scenario. Threshold for killing 50 free target molecules, target number normally distributed with SD given in the graph. The third panel shows the “primary toxic” scenario. Threshold for killing 50 bound target molecules, target number normally distributed with SD given in the graph. The bottom panel shows the “secondary toxic” scenario. Threshold for killing 500 accumulated toxic metabolites, rate of metabolite production k_{tox} is $1.2 \times 10^6 \text{ M}^{-1}\text{s}^{-1}$, k_{tox} is normally distributed with SD given in the graph.

References

1. Band, V.I.; Weiss, D.S. Heteroresistance: A cause of unexplained antibiotic treatment failure? *PLoS Pathog.* **2019**, *15*, e1007726. [[CrossRef](#)] [[PubMed](#)]
2. Band, V.I.; Crispell, E.K.; Napier, B.A.; Herrera, C.M.; Tharp, G.K.; Vavikolanu, K.; Pohl, J.; Read, T.D.; Bosinger, S.E.; Trent, M.S.; et al. Antibiotic failure mediated by a resistant subpopulation in *Enterobacter cloacae*. *Nat. Microbiol.* **2016**, *1*, 16053. [[CrossRef](#)] [[PubMed](#)]
3. Balaban, N.Q.; Helaine, S.; Lewis, K.; Ackermann, M.; Aldridge, B.; Andersson, D.I.; Brynildsen, M.P.; Bumann, D.; Camilli, A.; Collins, J.J.; et al. Definitions and guidelines for research on antibiotic persistence. *Nat. Rev. Microbiol.* **2019**, *17*, 441–448. [[CrossRef](#)] [[PubMed](#)]
4. Andersson, D.I.; Nicoloff, H.; Hjort, K. Mechanisms and clinical relevance of bacterial heteroresistance. *Nat. Rev. Microbiol.* **2019**, *17*, 479–496. [[CrossRef](#)] [[PubMed](#)]
5. El-Halfawy, O.M.; Valvano, M.A. Antimicrobial Heteroresistance: An Emerging Field in Need for Clarity. *Clin. Microbiol. Rev.* **2015**, *28*, 191–207. [[CrossRef](#)] [[PubMed](#)]
6. Nicoloff, H.; Hjort, K.; Levin, B.R.; Andersson, D.I. The high prevalence of antibiotic heteroresistance in pathogenic bacteria is mainly caused by gene amplification. *Nat. Microbiol.* **2019**, *4*, 504–514. [[CrossRef](#)] [[PubMed](#)]
7. Abel zur Wiesch, P.; Abel, S.; Gkatzis, S.; Ocampo, P.; Engelstädter, J.; Hinkley, T.; Magnus, C.; Waldor, M.K.; Udekwu, K.; Cohen, T. Classic reaction kinetics can explain complex patterns of antibiotic action. *Sci. Transl. Med.* **2015**, *7*, 287ra73. [[CrossRef](#)] [[PubMed](#)]

8. Martinecz, A.; Abel zur Wiesch, P. Estimating treatment prolongation for persistent infections. *Pathog. Dis.* **2018**, *76*, fty065. [[CrossRef](#)]
9. Rego, E.H.; Audette, R.E.; Rubin, E.J. Deletion of a mycobacterial divisome factor collapses single-cell phenotypic heterogeneity. *Nature* **2017**, *546*, 153–157. [[CrossRef](#)]
10. Bergmiller, T.; Andersson, A.M.C.; Tomasek, K.; Balleza, E.; Kiviet, D.J.; Hauschild, R.; Tkačik, G.; Guet, C.C. Biased partitioning of the multidrug efflux pump AcrAB-TolC underlies long-lived phenotypic heterogeneity. *Science* **2017**, *356*, 311–315. [[CrossRef](#)]
11. Pu, Y.; Zhao, Z.; Li, Y.; Zou, J.; Ma, Q.; Zhao, Y.; Ke, Y.; Zhu, Y.; Chen, H.; Baker, M.A.B.; et al. Enhanced Efflux Activity Facilitates Drug Tolerance in Dormant Bacterial Cells. *Mol. Cell* **2016**, *62*, 284–294. [[CrossRef](#)] [[PubMed](#)]
12. Tonge, P.J. Drug-Target Kinetics in Drug Discovery. *ACS Chem. Neurosci.* **2018**, *9*, 29–39. [[CrossRef](#)] [[PubMed](#)]
13. Walkup, G.K.; You, Z.; Ross, P.L.; Allen, E.K.H.; Daryae, F.; Hale, M.R.; O'Donnell, J.; Ehmann, D.E.; Schuck, V.J.A.; Buurman, E.T.; et al. Translating slow-binding inhibition kinetics into cellular and in vivo effects. *Nat. Chem. Biol.* **2015**, *11*, 416–423. [[CrossRef](#)] [[PubMed](#)]
14. Daryae, F.; Tonge, P.J. Pharmacokinetic–pharmacodynamic models that incorporate drug–target binding kinetics. *Curr. Opin. Chem. Biol.* **2019**, *50*, 120–127. [[CrossRef](#)] [[PubMed](#)]
15. Malmström, J.; Beck, M.; Schmidt, A.; Lange, V.; Deutsch, E.W.; Aebersold, R. Proteome-wide cellular protein concentrations of the human pathogen *Leptospira interrogans*. *Nature* **2009**, *460*, 762–765. [[CrossRef](#)] [[PubMed](#)]
16. Maier, T.; Schmidt, A.; Güell, M.; Kühner, S.; Gavin, A.-C.; Aebersold, R.; Serrano, L. Quantification of mRNA and protein and integration with protein turnover in a bacterium. *Mol. Syst. Biol.* **2011**, *7*, 511. [[CrossRef](#)]
17. Belenky, P.; Ye, J.D.; Porter, C.B.M.; Cohen, N.R.; Lobritz, M.A.; Ferrante, T.; Jain, S.; Korry, B.J.; Schwarz, E.G.; Walker, G.C.; et al. Bactericidal Antibiotics Induce Toxic Metabolic Perturbations that Lead to Cellular Damage. *Cell Rep.* **2015**, *13*, 968–980. [[CrossRef](#)]
18. Gillespie, D.T. Exact stochastic simulation of coupled chemical reactions. *J. Phys. Chem.* **1977**, *81*, 2340–2361. [[CrossRef](#)]
19. Gillespie, D.T.; Hellander, A.; Petzold, L.R. Perspective: Stochastic algorithms for chemical kinetics. *J. Chem. Phys.* **2013**, *138*, 170901. [[CrossRef](#)]
20. Gillespie, D.T. A rigorous derivation of the chemical master equation. *Phys. Stat. Mech. Appl.* **1992**, *188*, 404–425. [[CrossRef](#)]
21. Spratt, B.G. Distinct penicillin binding proteins involved in the division, elongation, and shape of *Escherichia coli* K12. *Proc. Natl. Acad. Sci. USA* **1975**, *72*, 2999–3003. [[CrossRef](#)] [[PubMed](#)]
22. Terrak, M.; Ghosh, T.K.; van Heijenoort, J.; Van Beeumen, J.; Lampilas, M.; Aszodi, J.; Ayala, J.A.; Ghuysen, J.M.; Nguyen-Distèche, M. The catalytic, glycosyl transferase and acyl transferase modules of the cell wall peptidoglycan-polymerizing penicillin-binding protein 1b of *Escherichia coli*. *Mol. Microbiol.* **1999**, *34*, 350–364. [[CrossRef](#)] [[PubMed](#)]
23. Gillespie, D.T. Stochastic Simulation of Chemical Kinetics. *Annu. Rev. Phys. Chem.* **2007**, *58*, 35–55. [[CrossRef](#)] [[PubMed](#)]
24. Li, H.; Cao, Y.; Petzold, L.R.; Gillespie, D.T. Algorithms and Software for Stochastic Simulation of Biochemical Reacting Systems. *Biotechnol. Prog.* **2008**, *24*, 56–61. [[CrossRef](#)] [[PubMed](#)]
25. Wehrli, W. Kinetic Studies of the Interaction between Rifampicin and DNA-Dependent RNA Polymerase of *Escherichia coli*. *Eur. J. Biochem.* **1977**, *80*, 325–330. [[CrossRef](#)]
26. Baeder, D.Y.; Yu, G.; Hozé, N.; Rolff, J.; Regoes, R.R. Antimicrobial combinations: Bliss independence and Loewe additivity derived from mechanistic multi-hit models. *Philos. Trans. R. Soc. Lond. B. Biol. Sci.* **2016**, *371*. [[CrossRef](#)] [[PubMed](#)]
27. Goldstein, E.J.C.; Solomkin, J.S.; Citron, D.M.; Alder, J.D. Clinical Efficacy and Correlation of Clinical Outcomes with In Vitro Susceptibility for Anaerobic Bacteria in Patients with Complicated Intra-abdominal Infections Treated With Moxifloxacin. *Clin. Infect. Dis.* **2011**, *53*, 1074–1080. [[CrossRef](#)]
28. Colangeli, R.; Jedrey, H.; Kim, S.; Connell, R.; Ma, S.; Chippada Venkata, U.D.; Chakravorty, S.; Gupta, A.; Sizemore, E.E.; Diem, L.; et al. Bacterial Factors That Predict Relapse after Tuberculosis Therapy. *N. Engl. J. Med.* **2018**, *379*, 823–833. [[CrossRef](#)]
29. Doern, G.V.; Brecher, S.M. The Clinical Predictive Value (or Lack Thereof) of the Results of In Vitro Antimicrobial Susceptibility Tests. *J. Clin. Microbiol.* **2011**, *49*, S11–S14. [[CrossRef](#)]

30. Onufrak, N.J.; Forrest, A.; Gonzalez, D. Pharmacokinetic and Pharmacodynamic Principles of Anti-infective Dosing. *Clin. Ther.* **2016**, *38*, 1930–1947. [[CrossRef](#)]
31. Hill, A.V. The possible effects of the aggregation of the molecules of haemoglobin on its dissociation curves. *J. Physiol.* **1910**, *40*, iv–vii.
32. Holford, N. Pharmacodynamic principles and the time course of immediate drug effects. *Transl. Clin. Pharm.* **2017**, *25*, 157. [[CrossRef](#)]
33. Kouyos, R.D.; Abel zur Wiesch, P.; Bonhoeffer, S. On Being the Right Size: The Impact of Population Size and Stochastic Effects on the Evolution of Drug Resistance in Hospitals and the Community. *PLoS Pathog.* **2011**, *7*, e1001334. [[CrossRef](#)] [[PubMed](#)]
34. Avican, K.; Fahlgren, A.; Huss, M.; Heroven, A.K.; Beckstette, M.; Dersch, P.; Fällman, M. Reprogramming of *Yersinia* from Virulent to Persistent Mode Revealed by Complex In Vivo RNA-seq Analysis. *PLoS Pathog.* **2015**, *11*, e1004600. [[CrossRef](#)] [[PubMed](#)]
35. Thorsted, A.; Thygesen, P.; Agersø, H.; Laursen, T.; Kreilgaard, M. Translational mixed-effects PKPD modelling of recombinant human growth hormone-from hypophysectomized rat to patients: Translational PKPD model of rhGH. *Br. J. Pharm.* **2016**, *173*, 1742–1755. [[CrossRef](#)] [[PubMed](#)]
36. Mouton, J.W.; Muller, A.E.; Canton, R.; Giske, C.G.; Kahlmeter, G.; Turnidge, J. MIC-based dose adjustment: Facts and fables. *J. Antimicrob. Chemother.* **2018**, *73*, 564–568. [[CrossRef](#)] [[PubMed](#)]



© 2019 by the authors. Licensee MDPI, Basel, Switzerland. This article is an open access article distributed under the terms and conditions of the Creative Commons Attribution (CC BY) license (<http://creativecommons.org/licenses/by/4.0/>).

Paper 4

High peak rifampicin plasma concentrations accelerate the slow phase of bacterial elimination in tuberculosis patients: evidence for heteroresistance

Antal Martinecz¹, Martin J. Boeree², Andreas H. Diacon^{3,4}, Rodney Dawson^{5,6}, Rob E. Aarnoutse⁷, Pia Abel zur Wiesch^{1,8}

¹Department of Pharmacy, Faculty of Health Sciences, University of Tromsø;

²Department of Lung Diseases, Radboud Institute of Health Science, Radboud university medical center, Nijmegen, the Netherlands;

³Faculty of Medicine and Health Sciences, Stellenbosch University, Tygerberg, South Africa;

⁴TASK Applied Science, Cape Town, South Africa;

⁵Department of Respiratory Medicine, University of Cape Town, Cape Town, South Africa;

⁶The Lung Institute, Cape Town, South Africa;

⁷Department of Pharmacy, Radboud university medical center, Nijmegen, The Netherlands

⁸Centre for Molecular Medicine Norway, Nordic EMBL Partnership, Oslo, Norway

Abstract

Background: Antibiotic treatments are often associated with the slowdown in the elimination of bacteria over time. This slowdown separates the killing of bacteria into at least two distinct phases: an initial quick phase followed by a slower phase. *In vitro* the prevalent mechanistic explanations for the slowdown in elimination are either antibiotic persistence or heteroresistance. Persistence is defined as the switching back and forth between susceptible and non-susceptible states, while heteroresistance is defined as the coexistence of bacteria with heterogeneous susceptibilities. Both of these mechanisms are thought to also cause a slowdown in elimination in patients and therefore complicate and prolong the necessary antibiotic treatments. This is also the case in tuberculosis, however currently, the mechanistic reasons are unknown and therefore the strategies to mitigate it are also unknown.

Methods and Findings: Here, we analyse an early bactericidal activity, dose ranging trial on high rifampicin doses in tuberculosis patients (trial NCT01392911) and show that there is a slowdown in the elimination of bacteria as observed on sputum bacterial counts. Furthermore, the late phase of bacterial killing is not only dependent on both peak concentrations ($p=0.003$) and total drug exposure ($p=0.01$), but that peak concentrations have a stronger influence on elimination rates than the total drug exposure. We compare these results to mathematical models of both heteroresistance and persistence based on pharmacokinetic-pharmacodynamic models of rifampicin tissue distributions in tuberculosis patients. We find that the observation on the slow phase's dependence on pharmacokinetic parameters and its skew towards C_{max} are only compatible with the model of heteroresistance and incompatible with the model of persistence. Furthermore, the observed bacterial decline and the model predictions of heteroresistance show a strong agreement as well, allowing us to conclude that the heterogeneous elimination of bacteria in the sputum producing compartment may be the cause of the observed slowdown. We estimate the hypothetical susceptibility distribution that would lead to the heterogeneous elimination and find that it fits the definition of heteroresistance, making it to be the likely cause.

Finally, based on our analysis, we estimate the time to sputum culture conversion and compare the results to a different clinical trial on high rifampicin doses (trial NCT01785186). We demonstrate that by taking the a slowdown in elimination into account, we can get a better and more conservative estimate on the times to sputum culture conversion, thereby linking the two trials together. The times to sputum culture conversion which is moderately correlated with treatment success rates, these results indicate that the slowdown in elimination may contribute to adverse events after the end of treatments.

Conclusions: Our findings indicate that different pharmacokinetic profiles may be used to optimize treatments to accelerate killing in the slow phase and thereby possibly affecting treatment lengths or relapse rates. Our work adds to the growing body of literature supporting high rifampicin doses for TB

therapy and gives hope that high doses could allow shortening treatment as is currently investigated in ongoing clinical trials.

Introduction

Tuberculosis has been plaguing humanity for millennia. The standard treatment for antibiotic susceptible tuberculosis is a 6 month long combination therapy which still carries a significant risk of relapse: up to 15% [1,2]. Shortening these treatments is a public health priority, however, it is difficult to achieve due to the lack of insight into how antibiotic therapies affect bacterial populations *in vivo* in general, and especially in the case of tuberculosis.

In tuberculosis clinical trials, bacterial loads in patients are often assessed based via the sputum. In phase 2A, early bactericidal activity (EBA) trials, sputum bacterial counts are commonly used. In later phases, the time to sputum culture conversion (TSCC), i.e. the time when bacterial sputum cultures are repeatedly negative, is used instead [3,4]. TSCC has been shown to be correlated to the probability of relapse and later adverse events [5]. This indicates that bacterial burden in sputum may be indicative of the total bacterial burden in a patient, even if the sputum does not allow a complete quantification of the bacterial burden. This is because i) not all bacteria in sputum can be cultured [6–8], and ii) only bacteria in (micro)cavities connected to the airways are thought to be detected in sputum, and intracellular bacteria or bacteria in granulomas remain inaccessible. iii) Even though sputum culture conversion in after the first 2 months of treatment on average, patients still have to be treated for the full 6 months in order to avoid relapse.

In addition to imperfect quantification, even the rate at which culturable bacteria in sputum decline is difficult to determine. This is because bacterial killing follows a typical biphasic pattern with a fast initial and a slow late decline. Such biphasic bacterial killing has been observed both *in vivo* and *in vitro*. The nature and cause of these biphasic kill curves are a hotly debated subject in microbiology. The different explanations for this slowdown can be divided into two general groups: persistence (Figure 1A) and heteroresistance (Figure 1B) [9]. The persistence, contains mechanisms that rely on switching back and forth between an antibiotic susceptible and a non-susceptible state. Here the most commonly shown mechanisms are the switch between a replicating and a non-replicating state, and a switch between intracellular and extracellular lifestyles [10–12]. The other group, heteroresistance, contains mechanisms that rely on a diversity in the susceptibility to antibiotics within the population of bacteria [13–15]. While in tuberculosis research, heteroresistance usually refers to the coexistence of both susceptible and resistant strains, in microbiology it also refers to the observation that that not all bacteria in a clonal culture exhibit the same antibiotic susceptibility [16]. Both mechanisms have been shown to exist in tuberculosis bacteria when exposed to rifampicin *in vitro* and most probably both exist *in vivo* as well, although their clinical significance is unknown [11,17,18].

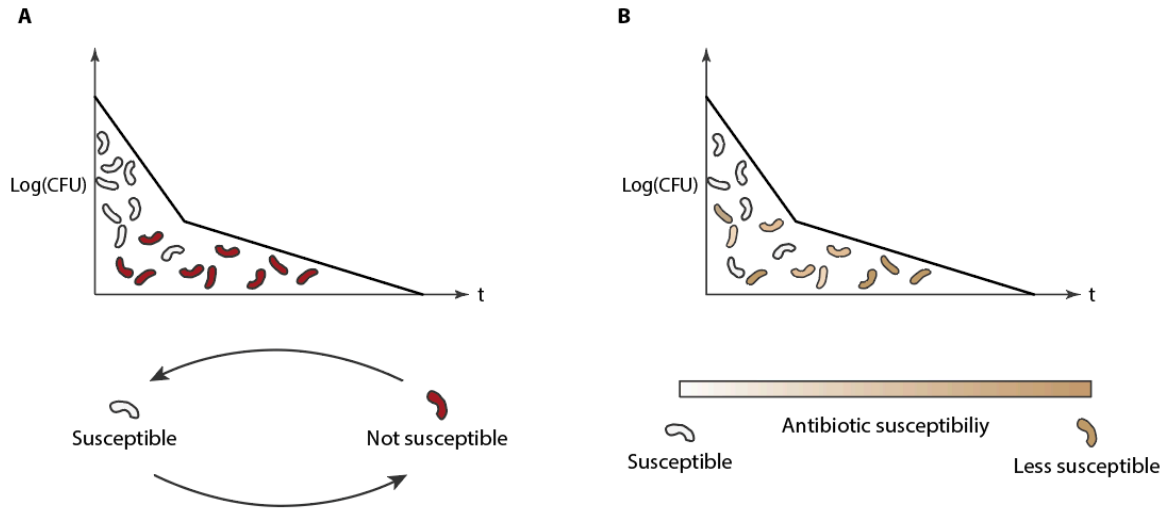


Figure 1 Mechanisms that can result in a slowdown in elimination. This figure illustrates the two main types of mechanisms that can slow down the elimination of bacteria. In both cases, X-axis is the time and the Y axis is the number of bacteria. **Figure A** shows that if bacteria switch back and forth between a susceptible and non-susceptible state, over time only the non-susceptible ones remain. These are only eliminated when they exit a non-susceptible state. **Figure B** shows that if there is a diversity within the susceptibility on antibiotics within the population of bacteria, some subpopulations will end up being eliminated at a slower pace.

We concentrate on rifampicin, which is one of the key drugs used in the treatment of drug susceptible tuberculosis. Previous studies have linked clinical trial based mathematical models of rifampicin exposure to the time to culture conversion or the increase in time to culture positivity measured over 14 days which is a way to quantify bacteria [19,20]. Additionally, another study with a limited number of patients linked higher rifampicin doses per bodyweight to the rate of late bacterial decline [13]. Animal models have also predicted a significant treatment shortening with higher rifampicin concentrations [21]. However, the results of these studies are difficult to use in mathematical models that would aid in designing optimal TB therapy. Time to positivity is challenging to convert into quantitative estimates of bacterial burden, and mathematical models are needed to convert time to positivity into bacteria per unit volume to calculate the rate of bacterial decline [22]. This means that a quantification necessitates the use of yet another model nested into a statistical analysis, which introduces potential inaccuracies. While rifampicin levels predicted with mathematical modelling offer an excellent starting point to investigate dose-response relationships, a direct statistical link between pharmacokinetic parameters directly measured in patients and treatment response is missing.

Currently, it is unclear which mechanisms contribute to the biphasic decline of bacteria in sputum. This is difficult to investigate experimentally, because of the inaccessible location of the bacteria in patients' lungs and because most microbiological characterizations require removing bacteria from the patients, thereby altering both the bacteria and their environment. However, a better quantitative link between antibiotic exposure and bacterial killing would allow us to compare clinical results to mathematical model predictions and thereby aid in investigating the nature of the slowdown in bacterial decline. Specifically, we investigate the effects of changing antibiotic time concentration profiles in models of persistence and heteroresistance and compare them to observed patterns in patients with different pharmacokinetic characteristics. Depending on the causes behind the biphasic behaviour, pharmacokinetic parameters have different impacts on the treatments and bacterial counts. In mathematical models of heteroresistance, we have shown previously that the slow phase can be only affected by higher drug doses if it is caused by a diversity in elimination rates, rather than switching between states [13,23].

Therefore, to find out the possible mechanisms behind the slowdown in elimination, we analyse the bacterial count measurements from a clinical trial (NCT01392911, [24]). Our mathematical models predict that the changes in the rates of early (day 1-4) and late (day 4-14) bacterial elimination depending on C_{max} and AUC depend on the biological mechanism underlying the biphasic killing. We therefore

correlate both peak drug concentrations (C_{max}) and total drug exposure (AUC) to the early and late rates of bacterial decline. We compared the statistical data analysis with mathematical models heteroresistance and persistence during treatments. Finally, based on the statistical analysis, we also estimated how TSCC may depend on C_{max} and AUC and compared the estimates to measured TSCCs in a different clinical trial (NCT01785186, [25]).

Results

In this work we investigated the possible mechanistic causes behind the observed slowdown in elimination in the clinical trial. We investigated the properties of the slowdown in elimination in response to different pharmacokinetic measures (AUC and C_{max}) via statistical analysis, as different behaviours hint at the mechanistic causes of the slowdown. To reduce the noise of in vivo measurements, we pooled data together from multiple participants. In order to avoid bias from the choice of group sizes, we have repeated the analysis with a wide range of group sizes. We formed these groups by dividing the measured range of pharmacokinetic parameters (either C_{max} or AUC) into 10-40 equal sized intervals. Unless otherwise indicated, we report the median values for all of statistical descriptors (e.g. R^2 , p-value), and estimated parameters (reported in Table 1).

For each group's pooled sputum bacterial count measurements (for all groupings), we fitted biphasic curves with different days of transition from the quick killing to the slow killing of the bacteria. We determined the most probably days of transition, day 3 or 4, based on the median R^2 (see Figure S 1) and median p-values of the fits (see Figure S 4). For the rest of the analyses, we use day 4 as the day of transition between the quick and the slow phase.

Based on the fitted curves, we find that both phases of elimination are dependent on antibiotic concentrations and therefore pharmacokinetic measures. This is demonstrated on Figure 2 which illustrates the dependence of kill rates in the slow phase on AUC or C_{max} as well the resulting smoothed time-kill curves based on the fits. Table 1 summarizes the properties of the fitted curves, Figure S 3 shows the all the determined fits for all different transition days, and Figure S 4 shows the corresponding of p-values. All the p-values reported in Table 1 and Figure S 4 has been corrected for multiple testing with the Benjamini-Hochberg method.

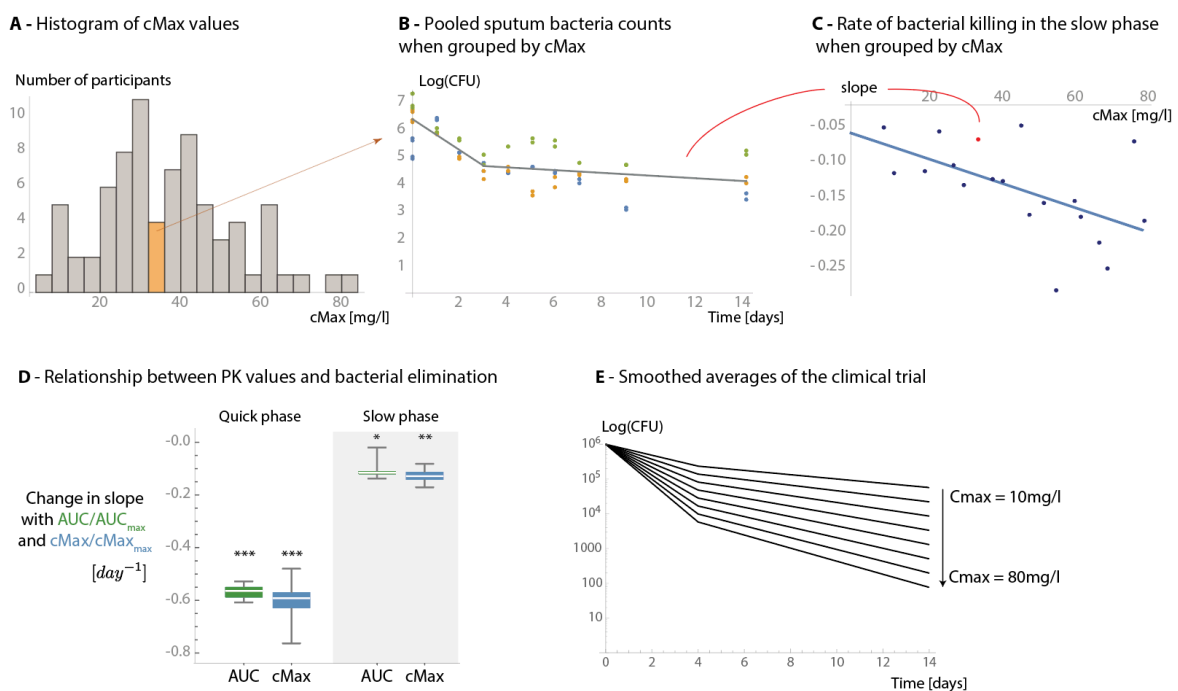


Figure 2 Overview of the fitting process and the relationship between the elimination rates of bacteria and pharmacokinetic measures. We have grouped participants (Figure A) based on their pharmacokinetic measurements. For each group, we

pooled the bacterial count measurements (Y-axis) of all participants (dots, here one colour corresponds to one participant) and fitted biphasic curves to them (solid line) (**Figure B**). Next, we analysed the relationship between the groups' mean pharmacokinetic measurements (X axis) and the properties of the fitted curves (Y axis) (**Figure C**). **Figure D** summarizes the dependence of the elimination rates in the quick and slow phases on $\frac{AUC}{AUC_{max}}$ and $\frac{cMax}{cMax_{max}}$. Here, we have normalized the values (by dividing with the maximum), in order to be able to show that both measures produce the same result but with different errors. **Figure E** demonstrates how this affects the bacterial count measurements (X-axis) over time (Y-axis). The curves were made with Eq (1), starting at 10^6 CFU/ml bacteria, using day 4 as the day of transition, with the obtained fits for elimination rates (see **Error! Reference source not found.**), and C_{max} values of 10, 20, 30...80 [mg/l] (in the dataset the C_{max} values range from 7.7 to 85.6 mg/ml).

Property	Grouped by	Intercept (SE)	Slope (SE)	Intercept p-value (corrected for multiple testing)	Slope p-value (corrected for multiple testing)	R ² (adjusted)	AIC (corrected)
Quick [day^{-1}]	AUC	-0.19 (± 0.038)	-0.0005 (± 0.00009)	0.0003	0.00007	0.67	-25
	C_{max}	-0.1 (± 0.057)	-0.0057 (± 0.001)	0.1	0.00016	0.54	-22
Slow [day^{-1}]	AUC	-0.075 (± 0.024)	-0.00015 (± 0.00005)	0.007	0.01	0.32	-43
	C_{max}	-0.043 (± 0.026)	-0.0018 (± 0.00051)	0.12	0.003	0.34	-57
Baseline Log(CFU) [-]	AUC	5.54 (± 0.18)	0.0012 (± 0.00044)	10^{-15}	0.0124	0.30	23
	C_{max}	5.27 (± 0.254)	0.016 (± 0.0052)	10^{-13}	0.0107	0.27	40
4 th day Log(CFU) [-]	AUC	4.77 (± 0.26)	-0.0009 (± 0.00063)	10^{-11}	0.163	0.30	23
	C_{max}	4.86 (± 0.307)	-0.008 (± 0.0064)	10^{-12}	0.23	0.27	40

Table 1 Summary of the median fitted values to the dataset across all groupings, with day 4 as the day of transition from quick phase to slow phase. All the P values reported are corrected for multiple testing with the Benjamini-Hochberg method. Here the overall elimination rates (used in Eq (1)) within each phase can be calculated as: $d_{quick} (cMax) = intercept [day^{-1}] + slope[\frac{day^{-1}}{mg/L}] \cdot cMax [mg/L]$.

We compared the predictive power of the pharmacokinetic measurements using the adjusted R2 (Figure S 1) and corrected AIC values (Figure S 2) of the fits. The quick phase was predicted better by the AUC rather than the C_{max} , while the slow phase was predicted by the C_{max} rather than the AUC. The dependence on pharmacokinetic measures of the quick phase this was expected as rifampicin is known to have dose dependent action [26] and is thought to be better predicted by the AUC [26]. However in case of the slow phase this was previously unknown as the behaviour of the slow phase is driven by its

mechanistic causes. We demonstrate this on Figure 3 where we have modelled the responses of the two main possible causes of the slowdown (persistence and heteroresistance) when *M. tuberculosis* is exposed to rifampicin. We used simplified exposure profiles where we kept the AUC constant: a sustained high concentration (C_{max}) for shorter duration of time and a low sustained concentration (C_{min}) for longer duration of time. We find that heteroresistance predicts that antibiotic concentrations affect the slope of the slow phase, while persistence predicts that antibiotic concentrations will have no effect on the slope of the slow phase. The simplified cases also demonstrate that a high C_{max} is required in order to eliminate the less susceptible subpopulations in heteroresistance. Therefore, our observations on the properties of the slow phase are consistent with the definitions and models of heteroresistance and are inconsistent with the definition and mathematical models of persistence [9].

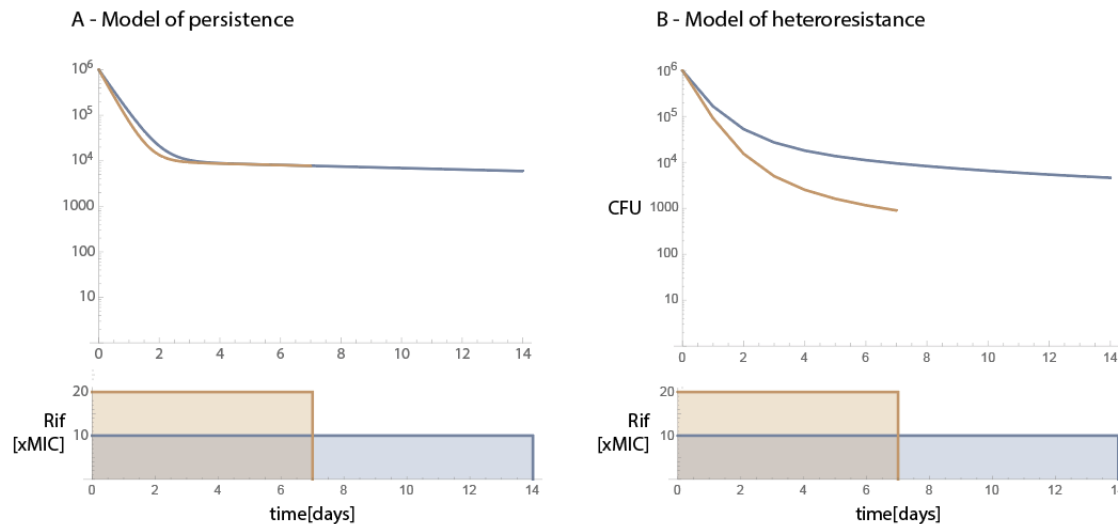


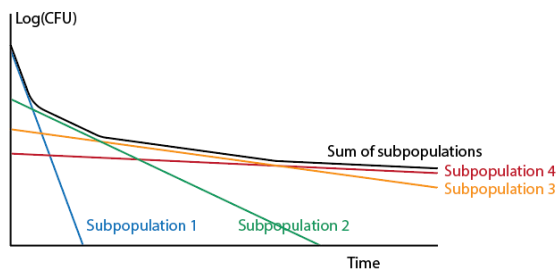
Figure 3 Predicted responses of the mathematical models of persistence and heteroresistance. This figure shows the qualitative difference between the causes behind the slowdown in elimination. The top row shows bacterial counts (Y-axis) over time (X-axis) for two different idealized dosing regimens (grey and black curves). The bottom row shows the two simplified exposure profiles: both have the same AUC but different C_{max} values. **Figure A** shows that if the slowdown in elimination is a result of switching between susceptible and non-susceptible states, then the slope of the slow phase is not dependent on C_{max} . On the other hand, **Figure B** shows that if the slowdown in elimination is the result of a diversity in the susceptibility to antibiotics, then a change in antibiotic concentrations should affect the slope of the slow phase as well.

Heteroresistance is defined as, and characterized by the coexistence of multiple subpopulations with different susceptibilities, where some (minority) subpopulations have at least 4 or 8x the MIC when compared to the majority of the population [9,27]. Therefore, to further assess whether the slowdown in elimination is caused by heteroresistance we calculated the hypothetical sensitivity distribution of bacteria based on the observed slowdown. Figure 4A and B illustrates the approach which is based on combining a PK-PD modelling with the results of the statistical analysis of the clinical trial. We calculated how subpopulations with different sensitivities would be eliminated from cavity walls with daily doses of rifampicin and compared this to the elimination rates of the slow phase in the clinical trial at each level of C_{max} . This allowed the identification the sensitivity of the subpopulation that dominates the elimination of the slow phase. We assigned the corresponding subpopulation size (based on the dataset Figure 4C) to each subpopulation which yielded the sensitivity distribution of bacteria (Figure 4D, purple dots). The resulting distribution shows a strong agreement with the definitions of heteroresistance (4-8x MIC subpopulations). In persistence the size of the slowly eliminated subpopulation should be independent of the antibiotic concentrations (i.e. Figure 4C would be different).

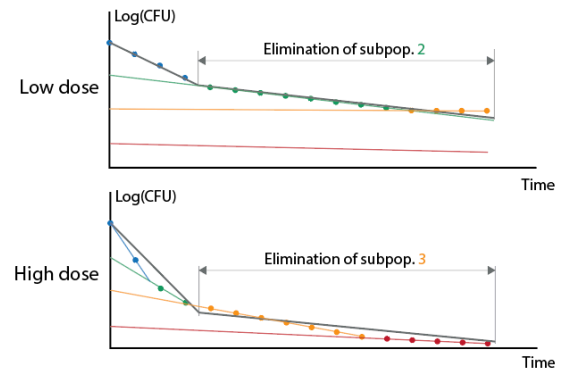
Next, we have also compared how well the mathematical model of heteroresistance in a PK PD mathematical model predicts the observed slowdown in elimination when compared to the smoothed averages of the clinical trial dataset. To do so, we have used the same model as for determining the sensitivity distributions. The parameters of the mathematical model are based on the literature: the pharmacokinetic model is based on [28] and the pharmacodynamic parameters are on [29]. The

sensitivity distribution in heteroresistance, which is fitted to the clinical trial dataset (assumed Gaussian distribution $\sigma = 1.3$ up to 16x MIC, see black line Figure 4D). Figure 5A B and C shows side by side the elimination of bacteria in the clinical trial, as well as the predicted elimination by heteroresistance and for a control by persistence. Figure 5D demonstrates that when compared, the difference between the observed elimination of bacterial in the clinical trial and the one predicted by heteroresistance stay within one log (see Figure S 6 for individual comparison of the curves). Therefore, we conclude that this model can sufficiently explain the observed slowdown on this timescale.

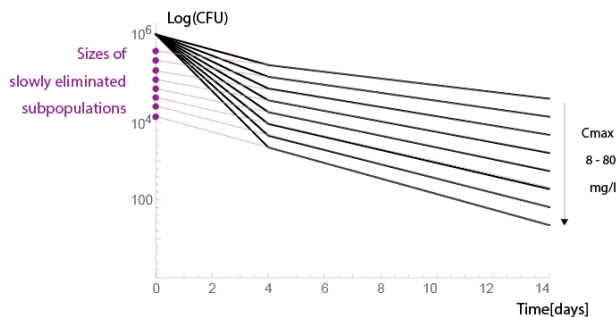
A - Assumption I: different parts of the time-kill curve are dominated by different subpopulations



B - Assumption II: after fitting biphasic curves, the slow phases are only representative of only a subset of the entire population, which can be identified based on its elimination rates (mathematical modeling)



C - Clinical trial dataset: the initial subpopulation sizes and elimination rates can be determined at each C_{max} value



D - Clinical trial dataset: based on C_{max}s, subpopulation sizes, and elimination rates we get the distribution of subpopulations

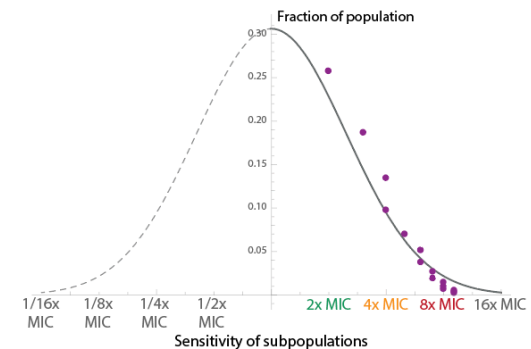


Figure 4 Estimating the sensitivity distribution of bacteria. This figure shows the method we used to estimate the sensitivity distribution of bacteria when the slowdown is caused by heteroresistance. **Figure A (illustration)** shows that different parts of the elimination curves (bacterial count (Y-axis) over time (X-axis)) represent the elimination of subpopulations with different MICs (different colours) [23]. In these cases, even after fitting biphasic curves on a multi-phasic elimination curves (**Figure B (illustration)**), the slow phase will represent a subset of subpopulations which can be identified based on the elimination rates at the given antibiotic concentration (C_{max} or AUC in case of PK based models). **Figure C** shows the parameters used obtained from clinical trial dataset: elimination rates in the slow phase and the corresponding “subpopulation sizes” at each C_{max}. **Figure D** shows the obtained sensitivity distribution and the fitted (assumed) normal distribution to it.

On Figure S 5 we demonstrate why there is a difference in the predictive power of C_{max} and AUC at different stages of the elimination when using PK based models instead of simplified exposure profiles. In the PK models, C_{max} and AUC both depend on multiple parameters and are only mildly correlated to each other. Because of this, when the C_{max}-es are close to the MIC (the elimination of less susceptible subpopulations in the slow phase), changes in pharmacokinetic parameters may increase AUC but decrease the C_{max} at the same time. As a result, the drug concentrations might not be high enough to overcome the MIC and the bactericidal action can decrease dramatically. On Figure S 5, we plotted the elimination of a subpopulation that has 8x MIC compared to the majority of the populations against the AUC and C_{max} measurements from multiple simulations. We modelled exposure to 10, 20, 30, 35, and 40 mg/kg of rifampicin, with variations ($\pm 20\%$) in absorption rates, drug elimination rates, and

bioavailability. The difference is mainly pronounced at peak drug concentrations close to the MIC, therefore at this particular MIC for all dosing groups the spearman's correlations are $\rho_{C_{max}} = 0.991$, $\rho_{AUC} = 0.979$, in other words the difference is small. For the 20 mg/kg dosing group however, the differences are more pronounced: $\rho_{C_{max}} = 0.988$, $\rho_{AUC} = 0.876$. Heteroresistance is characterised by a distribution subpopulations with different susceptibilities, we expect C_{max} to be a better predictor for other dosing groups as well. Based on these, we expect that in the slow phases of the slowdown, C_{max} should more reliably predict the slopes than the AUC.

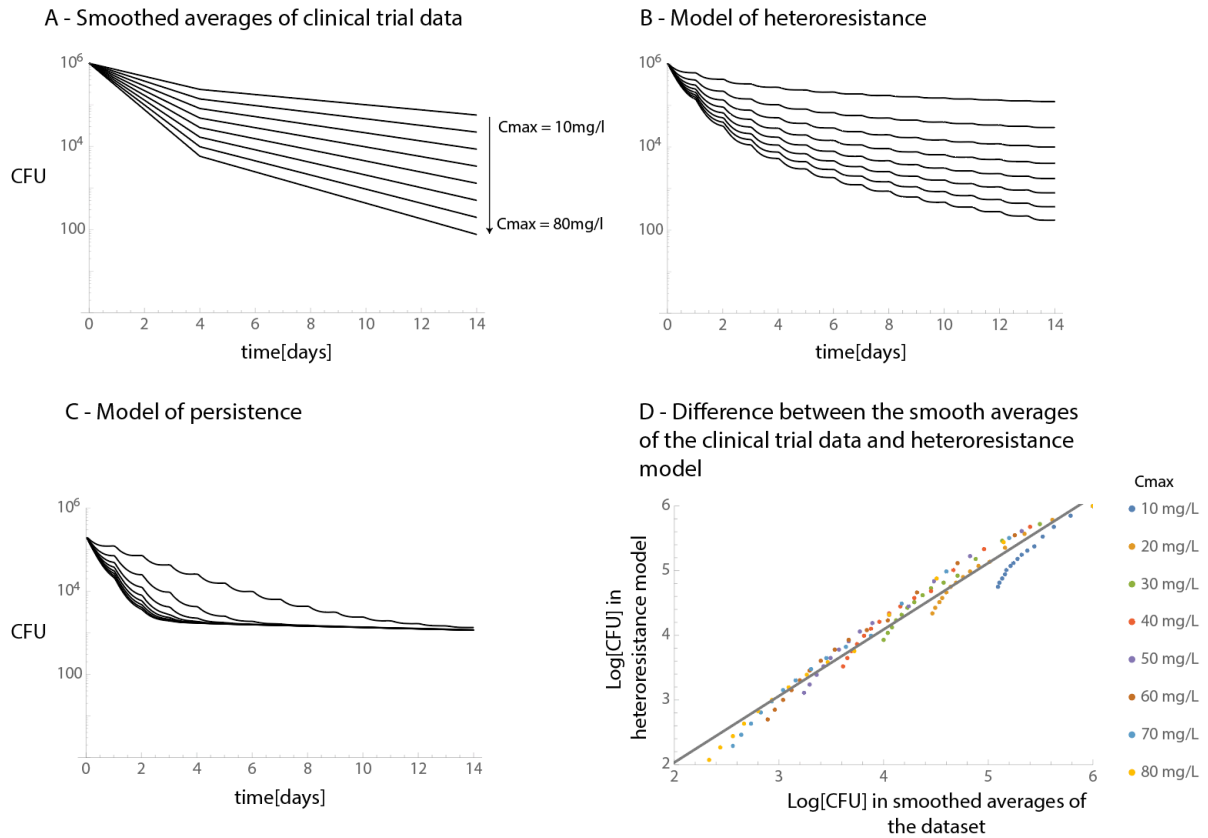


Figure 5 Comparison of the smoothed averages of the clinical trial and model predictions on sputum bacterial counts over time. This figure compares the smoothed averages of the clinical trial (Figure A, this is the same plot as in Figure 2E), the predicted decline of bacteria in cavity walls if the slowdown is caused by heteroresistance (Figure B) or persistence (Figure C). We generated these plots using pharmacokinetic models in the cavity wall with the same C_{max} values as in Figure A (10...80 mg/l). Finally, Figure D shows the difference between the curves on Figure A and B: on all days and C_{max} values combined, the X axis shows the model predictions and the Y axis shows the smoothed averages of the clinical trial ($R_{adj}^2 = 0.97$).

Finally, we estimated the expected time to sputum culture conversion based on the statistical analysis, assuming that there is no additional slowdown outside the timeframe of the clinical trial. We defined this as the timepoint where the fitted curves would go below 5 CFU, based on the estimated detection limits described in [30]. Figure 6 shows the expected time to culture conversion depending on C_{max} and AUC. We repeated the statistical analysis using monophasic kill curves (i.e. neglecting the possibility of a slowdown in elimination (see Table S1) and estimated TSCC that way as well. We compared both estimates to the measured times to sputum culture conversion of a multi-arm multi-stage (MAMS) clinical trial on high rifampicin doses (NCT01785186, [25]). From the MAMS trial, we used the control (HRZE, standard treatment with 10mg/kg rifampicin) and the high rifampicin (HR35ZE, standard treatment with an increased, 35mg/kg rifampicin dose) arms. In all cases, estimates that take the slowdown in elimination into account provide a more conservative estimate for the TSCC. For the HR35ZE treatment, estimates based on both PK parameters show an agreement with the clinical trial data. For the standard treatment however, only the estimates based on the AUC show an agreement with the data. This is because in the statistical analysis, the baseline rate of elimination in the slow phase was not statistically significant with C_{max} ($p=0.12$, see Table 1), only the dependence of elimination rates

with on changes of C_{max} were statistically significant ($p=0.003$). As a result, only at high rifampicin doses are estimates based on C_{max} reliable.

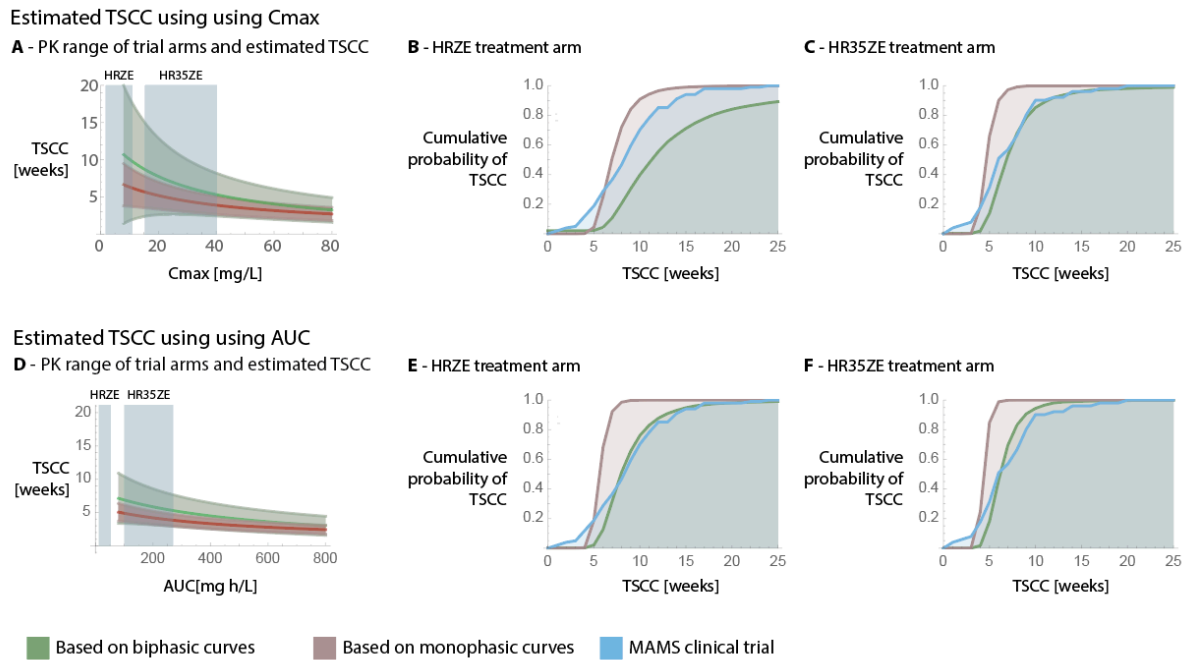


Figure 6 *Estimated TSCC based on the statistical analysis, and comparison to measured TSCCs in a multi arm multi stage (MAMS) clinical trial (NCT01785186, [25]). Here, the green curves show estimates based on biphasic curves (i.e taking the slowdown in elimination into account), while red shows estimation based on monophasic curves (i.e. neglecting the possibility of a slowdown in elimination). Blue always corresponds to data from the MAMS clinical trial. Figures A and D show the dependence of the predicted TSCC on the pharmacokinetic parameters (C_{max} and AUC respectively), as well as the measured pharmacokinetic ranges for the HRZE and HR35ZE treatment arms in the MAMS clinical trial used for comparison (blue boxes). Here, the area around the estimates signify the 95% confidence interval around our estimates. The estimates are only shown within the parameter ranges of the EBA clinical trial. Figures B,C,E, and F show the cumulative probability (Y-axis) of TSCC (X-axis) based on the estimates within the PK ranges of the MAMS trial as well as the data from the MAMS trial itself. This is shown for both C_{max} and AUC, as well as the HRZE, and HR35ZE treatment arms.*

Discussion

We analysed the measured sputum colony counts in an early bactericidal activity (EBA) trial and found that there is a slowdown in the bacterial killing rates, resulting in distinct quick (days 1-4) and slow phases (days 5-14). These phases correlated significantly with rifampicin levels measured in patient's plasma. In case of the slow phase, this was previously unclear as it can depend on the mechanism causing the slowdown. Therefore, it may or may not respond to increased antibiotic concentrations. Furthermore, we found that in the slow phase, the peak drug concentration (C_{max}) is a better predictor for bacterial killing than the overall exposure (AUC). We have done this by showing a direct statistical link between measured pharmacokinetic parameters and sputum colony counts at different stages of elimination.

Currently, the mechanistic reasons behind the slowdown in elimination are unknown and probably vary depending on the drug used and the observed timescales. In microbiology, there are two main explanations for a slowdown in elimination of bacteria: antibiotic persistence and heteroresistance. Both persistence and heteroresistance have been consistently shown to exist even in cultures of clonal bacterial populations, including *M. tuberculosis* [11,15,31,32]. While for both the clinical significances are unknown [9,27,33], both have been also shown to exist in tuberculosis patients [11,17,32,34–36]. Antibiotic persistence is characterised by bacteria occasionally switching between entirely non-susceptible and susceptible states. Here, the switch is commonly assumed to be independent of antibiotic concentrations. As the elimination of the non-susceptible population is solely dependent on the switch rate (as they reenter into a susceptible state), higher antibiotic concentrations would not accelerate the slow phase of elimination which is dominated by the persister subpopulation [9]. On the other hand, heteroresistance is defined as the coexistence of bacteria with different susceptibilities. Here, the

elimination of bacteria in the slow phase reflects the elimination of the less susceptible subpopulations, and as a result is dependent on antibiotic concentrations [9,13,23,27]. Our results are only compatible with the definitions of heteroresistance and not persistence, our observations are corroborated by the concentration dependences observed by others as well [30].

We compared these results to mathematical models of both persistence and heteroresistance parametrized with data available in the literature. The pharmacodynamics part is based on *in vitro* data of *M.tb* exposed to rifampicin [29,37–39]. The pharmacokinetic model (where applicable) is based on models of rifampicin tissue concentrations in TB patients [28], for the simulations we used cavity walls as open cavities are thought to be one of the sources of sputum. We found that the most probable cause of the slowdown in elimination on this time scale (in response to rifampicin) is heteroresistance rather than antibiotic persistence. An alternative hypothesis to this is the slowdown in elimination is caused by the heterogenous distribution of drugs in the lungs that which results in diverse elimination rates in bacteria [34,40,41]. In our case, this scenario is unlikely, as we have observed some subpopulations having 8x the MIC, the differences in exposure levels in the PK models we used cannot explain this large difference [28]. The different environments could result in different susceptibilities to antibiotics as well [34], however there are no available pharmacodynamic models on this that could be used for modelling. Arguably having a range of susceptibilities due to different environments is still a form heteroresistance when looking at a patient as a whole.

In the dataset, the quick phase of the elimination is better predicted by the AUC than C_{max} (Figure S 2). This is consistent with previous works showing the AUC dependence of rifampicin [26]. In the slow phase however we found that C_{max} is the better predictor for elimination when there is a discernible slowdown in elimination (higher rifampicin doses). Our models show that this is not a contradiction and is also expected in heteroresistance. The slow phase represents the elimination of the less susceptible subpopulations where an increased MIC has to be overcome. Increasing AUC can potentially decrease C_{max} which in turn may reduce the ability to overcome the higher MICs of some subpopulations.

The clinical significance of heteroresistance is still unknown [27,33]. By estimating the time to sputum culture conversion (TSCC) we show that the slowdown in elimination (and thereby heteroresistance) may have a clinical relevance. We estimated TSCC based on the statistical analysis using either biphasic curves or monophasic curves (i.e. fitting a straight line to the bacterial counts). As an earlier TSCC is mildly associated with treatment success and the lack of it is associated with later adverse events [5,42]. The estimates based on monophasic curves serve as a control to assess whether there is a slowdown in elimination or if it is introduced by the statistical analysis. Furthermore it also serves as a demonstration on the impact of neglecting the possibility of slowdown can have on the estimates. We compared both of the estimates to the measured TSCCs in a different clinical trial. We show that with the use of biphasic curves the estimates on TSCC are not only more conservative, but show a better agreement with the data used for comparison. The statistical analysis in the EBA trial are based on a treatment where patients received rifampicin monotherapy for the first week and a combination therapy for the second (with the same rifampicin dose). In the MAMS trial, the patients have received only a combination therapy. The estimates and the dataset are in agreement, which means that either the additional TB drugs contribute very little to the bactericidal activity in the treatment, or that the elimination in the slow phase is more impactful on TSCC than in the initial quick phase. The latter possibility argues against the practice of having more sparse bacteriological assessments in the second half EBA clinical trials (as it was done in this trial as well), because it makes investigating the possible slowdown in eliminations more difficult.

Our findings strengthen the connection between quantitative bacteriological assessments in EBA trials (sputum bacterial count measurements) and the TSCC which is used in subsequent phases of trials. The importance of strengthening this connection has been highlighted in the recent literature as one of the current challenges in tuberculosis clinical trial design [3,4]. We also identify a possible source of errors when evaluating EBA trials: not all drugs or drug combinations may result in the same slowdown in elimination. A slowdown may be outside of the timeframe of the two weeks of the trial, causing us to significantly underestimate TSCC. Conversely, some drug combinations may cause little to no slowdown – in EBA trials, these may appear inferior to other treatment arms that have a fast initial elimination of bacteria and a slowdown later on.

This work is not without limitations: first, we have observed an association between baseline bacterial loads and PK values. While it does not affect the calculation of elimination rates itself, it may be a confounder [43,44]. However, it was not possible to correct for this based on the dataset due to the number of participants. Second, all the participants in the study received rifampicin monotherapy for the first week of the study, then received additional TB drugs as well in standard doses. Here, as all groups received the same doses of the additional drugs, therefore it should not affect our conclusions and we have seen no changes in the dataset after day 7, the additional drugs may still have had an effect on our results. Furthermore it makes it difficult to assess whether our results are true for rifampicin monotherapy as well, or just for combination therapy. Third, the PK PD model of heteroresistance currently cannot be used to predict TSCC. This is because in the model there are some subpopulations with very low susceptibility (16x MIC compared to the majority of the population) that are eliminated extremely slowly by antibiotics. This differences between the model and measurements can be due to the following: (i) the real susceptibility distribution of bacteria may be different, and subpopulations with very low susceptibility may not exist. (ii) In the model, the less susceptible subpopulations are modelled as having a decreased effective antibiotic concentrations, however this is just an approximation and may not be the case [45]. (iii) The immune elimination of bacteria is not modelled as the elimination rates are unknown. However, there is evidence that the immune system also plays a role in controlling TB infections [46–49]. Omitting these from the PK PD models can affect the estimated TSCC in various ways.

In the study one drug formulation was used and therefore the C_{max} and AUC measurements are highly correlated. As a consequence, the analysis on the differences between the effects of C_{max} and AUC rely on the patient-to-patient variance in the drug absorption, elimination, and distribution rates. We expect the differences between C_{max} and AUC to be more pronounced in trials that vary drug formulations or dosing strategies as well as drug doses. Therefore, our results also highlight the possibility of further optimizing treatments with choosing different time-concentration profiles. Currently, it is difficult to predict which type of time-concentration profile would be ideal. First, it is unclear whether toxicity depends on AUC or C_{max} . Second, it has been argued that antibiotics should be matched with others that have similar half-lives to avoid only one drug being present (functional-monotherapy [28]) and thereby not facilitating the emergence of resistance.

Our results suggest that the bactericidal activity during the treatment can be enhanced by optimizing for treatment strategies and rifampicin formulations. This in turn may increase treatment success rates by reducing the time to sputum culture conversion: the time until no more bacteria are detected in the sputum. A shorter time to sputum conversion has been shown to be mildly correlated with treatment success [5]. This is supported by previous works on the same trial, which linked higher rifampicin exposures to an increased probability of earlier culture conversion [19], and increased time to positivity in liquid cultures [20]. Other studies have also shown that high doses of rifampicin shorten treatment durations in mouse models of both *Mycobacterium tuberculosis* [21] and *Mycobacterium ulcerans* [50]. Finally, with a limited number of patients, in a different study we linked higher rifampicin doses per bodyweight to the rate of late killing [13]. Therefore, our work adds to the growing body of literature supporting high rifampicin doses for TB therapy and gives hope that high doses could allow shortening treatment as is currently investigated in ongoing clinical trials (NCT02581527) ([24,50]).

Materials and Methods

Dataset

For the main analysis, we used the dataset of NCT01392911, an early bactericidal activity dose ranging trial on tuberculosis patients. Here, participants received 10, 20, 25, 30, 35 or 40 mg doses per kg bodyweight of rifampicin as a monotherapy for the initial seven days, after which isoniazid, pyrazinamide, and ethambutol were added in standard doses for the second seven days of the trial. The effects of this is discussed in the results. From this dataset, we only used the data of participants that had C_{max} , AUC, as well as sputum bacterial count measurements available (n=80).

We estimated TSCCs (time to sputum culture conversion) using the main analysis and compared the estimates to the measured TSCCs in trial NCT01785186 [27]. This trial is a multi-arm multi-stage

(MAMS) clinical trial on tuberculosis patients that included treatment arms on high rifampicin doses. During the course of the trial, the participants received 12 weeks of experimental treatments, followed by the standard continuation phase (rifampicin and isoniazid) treatment for another 14 weeks. Here, we only used data from the control (HRZE, standard regimen n=123) and high rifampicin (HR35ZE, standard regimen but with 35mg/kg rifampicin, n=63) treatment arms.

Statistical analysis

In each patient, we had access to bacterial count determinations on 10 days. Our aim was to have at least 4 data points each for the early and late phase to estimate the rates of decline. Due to missing data, it was not possible to get reliable estimates of biphasic kill rates in substantial fraction of single patients. Therefore, we pooled bacterial counts from sputum samples from patients with similar pharmacokinetic measures. This also allowed us to include participants into the analysis that would not have enough measurements for fitting i.e. less than three days' worth of measurements for the quick or the slow phase. We divided the range between the measured minimum and maximum pharmacokinetic measurements (either AUC or C_{max}) into equal intervals. Next, using the least squares method, we fitted biphasic curves to the pooled Log (CFU) measurements from all patients within each of the intervals (see Eq (1)) for the fitted function). Finally, each of the intervals were assigned to have the median of the AUC and C_{max} values of the patients within. We used these in univariable analyses, where we tested the relationships between pharmacokinetic measures and the quick phase, slow phase, estimated last day, Log(CFU) on days 0, day 14, and day of transition from quick phase to slow phase. Here, the estimated last day as the time point where the fitted curves go below 5 CFU, which is the estimated detection limit based on [30]. For the relationships between the pharmacokinetic parameters and the quick or the slow phases we used weighted fits, where the weights were determined using the standard errors of the fits to the quick or to the slow phase ($\frac{1}{s.error}^2$). This allowed us to give smaller weights to cases where we are more uncertain about our estimates. In order to account for multiple testing, we have corrected all the P-values using the Benjamini-Hochberg method.

$$(1) \quad B(t) = \begin{cases} B(0) + d_q t, & t < T \\ B(0) + d_q T + d_s (t - T), & t \geq T \end{cases}$$

Finally, we used the corrected Akaike information criterion (AIC) values as well as the adjusted R-squared values of the fits assessing whether the C_{max} or the AUC is a better predictor for the slope of the slow phase.

Mathematical models of the slowdown in elimination

Slowdown in the elimination can stem from a diversity in the elimination rates within populations of bacteria or switching back and forth between susceptible and non-susceptible states. While the two are not mutually exclusive, one or the other may dominate the response on a given timescale. In order to model this, we use mathematical models of antibiotic persistence and heteroresistance in populations of bacteria in order to be able to assess the response of the two different mechanisms to different pharmacokinetic measurements. We are using these as a reference as both of these mechanisms has been observed in mycobacteria previously [15,32]. Table 2 summarizes the parameters and values used in the equations.

Parameter	Description	Value	Unit	Ref
EC_{max}	Maximum elimination rate	1.82	day^{-1}	[29,37–39]
EC_{50}	Half-maximal effective concentration	0.51	$\frac{mg}{l}$	[29,37–39]

r	Growth rate of <i>M.tb</i> bacteria	0.8	day^{-1}	[37,51]
b	Switch rate of <i>M.tb</i> from a non-replicating state to a replicating state	0.0016	h^{-1}	[10,11]
$B_{total}(0)$	Total modelled population size	10^6	-	Based on the dataset: $B(0)_{median} = 10^{5.9}$ $B(0)_{mean} = 10^{6.11}$

Table 2 Summary of parameters used in the mathematical models of persistence and heteroresistance.

Elimination rate curves

For both of the models, we used the antibiotic concentration – net growth (elimination) rate relationship available in the literature in [37] that processed data of *in vitro* M.tb exposure to rifampicin measurements by [38,39]:

$$(2) \quad \delta(A) = -r + \frac{EC_{max} A}{EC_{50} + A},$$

where A is the antibiotic concentration in $\left[\frac{mg}{ml}\right]$.

Phenotypic switch

The most well-known example of switching back and forth between states is bacterial persistence caused by a dormant state [10]. Here, it is assumed that a subset of bacteria is in a non-replicating, dormant state that protects them from the effects of antibiotics that damage growing bacteria (for example rifampicin). Bacteria in their dormant state should be completely or highly tolerant to antibiotics, however once they switch back to a replicating state, they are swiftly eliminated by antibiotics. Mathematically this can be modelled as described in Eq (3) [10]. These equations describe the two subpopulations of bacteria, one that is susceptible (n) and one that is non-susceptible (p). Once the dormant state bacteria start replicating again, they become susceptible to antibiotics again (switching rate b in the equations).

$$(3) \quad \begin{cases} \frac{dp}{dt} = -bp \\ \frac{dn}{dt} = bp - \delta(A)n \end{cases}$$

$$(4) \quad b = \frac{r_{M.tb}}{r_{E.coli}} b_{E.coli}$$

In [10], they have determined the switch rate (b) from non-replicating state to a replicating state for *E.coli* (persisters) to be. We have scaled this value by the differences in replication rates between *E.coli* and *M.tb* (Eq (4)) in order to preserve the assumptions of the original model on the determined fraction of persisters. This is supported by the literature [11] that found > 20 day lag times for *M.tb* (compared to our estimate of $\frac{1}{26} day^{-1}$ switch rates)

We chose to model the non-replicating or slowly replicating *M.tb* as non-susceptible to antibiotics, based on the current definition of persistence [9]. This is also supported by the literature that reported 17x, 50x, and 200x decrease in susceptibility to rifampicin in a non- or slowly replicating state [18,52,53]. This makes the elimination rates of persisters negligibly small on the MIC ranges (1 – 16x MIC) we use the mathematical model on.

Heteroresistance

The other mechanism responsible for the slowdown in the elimination is heteroresistance [9,17]. The underlying assumption is that the bacteria in a population are not completely identical or may express unstable resistance genes that can result in a diversity in the susceptibility to external antibiotic concentrations. Additionally, there can also be a diversity in the expression of efflux pumps, targets, or cell sizes for example [13–15] which can be described by the same model.

Mathematically, this can be calculated using Eq (5) [13,23] that describe multiple subsets of bacteria each with a slightly different susceptibility to antibiotics.

$$(5) \quad B_{total}(t) = \sum_i B_i(0)e^{\delta_i t},$$

here $B_i(0)$ represents the initial size of the i -th subpopulation. Furthermore, δ_i are the corresponding elimination rates.

The model simulates 9 subpopulations where the middle one (5th) has the “average” susceptibility and in the majority.

$$(6) \quad B_i^*(0) = B_{total}(0) * D(i - 5|0, 1), \text{ where } i = 1 \dots 9,$$

where $D(x|\mu, \sigma)$, is the probability density function of the normal distribution, with the mean: μ and standard deviation σ of the distribution.

Due to the way this is calculated (by taking the value of the normal distribution at the given point), $\sum B_i^*$ will be less than B_{total} and therefore has to be rescaled:

$$(7) \quad B_i(0) = \frac{B_{total}(0)}{\sum B_i^*(0)} * B_i^*(0)$$

Here we simulate decrease susceptibility as changing the effective antibiotic concentrations (A_i). For the purposes of this paper the two are the same, but this approach is easier to compute [23].

$$(8) \quad \delta_i = \delta(A_i).$$

Therefore we use the following to simulate 9 subpopulations with MICs ranging from 1/16th, 1/8th ... to 8x and 16x of the average:

$$(9) \quad A_i = \left(2^i (i - 5)\right) A_{input}$$

For simulations, the parameters for the population distribution $D(x|\mu, \sigma)$ are the fits to the statistical analysis as shown in Figure 4 ($\mu = 0, \sigma = 1.3$).

Determining the day of transition from quick phase to slow phase

In vivo data is noisy, and the transition from quick phase to slow phase (based on mathematical models) is smooth rather than a sudden. Therefore, it is difficult to find the day of transition based on individual fits of the biphasic curves. We have opted for determining the day of transition based on all the available fits rather than optimizing fits in for each biphasic curve individually. Therefore we repeated the fitting procedure for all dosing groups with a different day of transition. We chose the day of transition where median R^2 for the fits of the slow and fast decline were highest. We got the same result when minimizing the P-values as well.

PK-PD models

The pharmacokinetic model used the published compartmental pharmacokinetic model of [28]. For the sake of simplicity we only used absorption (Eq (10)), plasma (Eq (12)), and tissue (Eq (11)) compartments and have not used a compartment chain for the absorption:

$$(10) \quad \frac{dA_{abs}}{dt} = input(t) - ka A_{abs}$$

$$(11) \quad \frac{dA_{plasma}}{dt} = ka A_{abs} - \frac{CL}{V} A_{plasma}$$

$$(12) \quad \frac{dA_{tissue}}{dt} = k_{pl-tissue} (R_{tissue} \frac{A_{plasma}}{V} - A_{tissue})$$

Here the parameters are:

- $input(t)$ is the input function, to simulate daily doses of rifampicin. It implemented as Dirac delta functions (Dirac comb) spaced 24h apart.
- A_{abs} , A_{tissue} , and A_{plasma} are antibiotic concentrations in the absorption, plasma and tissue compartments
- $ka = 1.55 [h^{-1}]$: absorption rates of the drug from absorption compartment
- $CL = 5.72 [\frac{L}{h}]$ are clearance rates of the drug from the plasma compartment
- $V = 52.3 [L]$ is the volume of distribution in litres
- R_{tissue} is the penetration coefficient into the given tissue, see Table 3.
- $k_{pl-tissue}$ rate of drug moving from plasma to tissue (h^{-1}), see Table 3.

Parameter	Lung	Necrotic nodule	Caseum closed nodule	Caseous fibrotic nodule	Caseum from cavity	Cavity wall	Fibrotic tissue	Small cellular nodule	Fungal ball
R	0.69	0.569	0.443	0.733	0.449	0.614	0.539	0.348	0.447
k	1.68	0.751	0.367	0.367	0.204	1.98	0.209	4.67	0.212

Table 3 This table details R_{tissue} and $k_{pl-tissue}$ parameters for used throughout this work [28]

For the pharmacodynamic models, we omitted bacterial replication from the mathematical model for the sake of simplicity as well as the lack of data on the progeny of the less susceptible subpopulations as well as the persistent bacteria. Arguably there is very little replication taking place over the modelled time period (14 days). This is due to antibiotic concentrations being close to or above MIC for the majority of time, post-antibiotic effect (lag time after antibiotic exposure before the replication restarts), and the slowness of replication in vivo environments. Here, the bacterial populations is calculated with Eq (13):

$$(13) \quad \frac{dB_i(t)}{dt} = -\delta(A) B_i(t)$$

Acknowledgements

We thank Christopher Fröhlich, Santiago Ramon Garcia, Jingyi Liang, for their comments and discussions on the manuscript.

References

1. Horsburgh CR, Barry CE, Lange C. Treatment of Tuberculosis. *N Engl J Med* **2015**; 373:2149–2160.
2. Lawn SD, Zumla AI. Tuberculosis. *The Lancet* **2011**; 378:57–72.
3. Dooley KE, Hanna D, Mave V, Eisenach K, Savic RM. Advancing the development of new tuberculosis treatment regimens: The essential role of translational and clinical pharmacology and microbiology. *PLOS Med* **2019**; 16:e1002842.
4. Davies G, Boeree M, Hermann D, Hoelscher M. Accelerating the transition of new tuberculosis drug combinations from Phase II to Phase III trials: New technologies and innovative designs. *PLOS Med* **2019**; 16:e1002851.
5. Horne DJ, Royce SE, Gooze L, et al. Sputum monitoring during tuberculosis treatment for predicting outcome: systematic review and meta-analysis. *Lancet Infect Dis* **2010**; 10:387–94.
6. Shamputa IC, Jugheli L, Sadradze N, et al. Mixed infection and clonal representativeness of a single sputum sample in tuberculosis patients from a penitentiary hospital in Georgia. *Respir Res* **2006**; 7. Available at: <http://respiratory-research.biomedcentral.com/articles/10.1186/1465-9921-7-99>. Accessed 7 April 2019.
7. Metcalfe JZ, Streicher E, Theron G, et al. Mycobacterium tuberculosis Subculture Results in Loss of Potentially Clinically Relevant Heteroresistance. *Antimicrob Agents Chemother* **2017**; 61. Available at: <http://aac.asm.org/lookup/doi/10.1128/AAC.00888-17>. Accessed 7 April 2019.
8. Shockey AC, Dabney J, Pepperell CS. Effects of Host, Sample, and in vitro Culture on Genomic Diversity of Pathogenic Mycobacteria. *Front Genet* **2019**; 10:477.
9. Balaban NQ, Helaine S, Lewis K, et al. Definitions and guidelines for research on antibiotic persistence. *Nat Rev Microbiol* **2019**; Available at: <http://www.nature.com/articles/s41579-019-0196-3>. Accessed 18 April 2019.
10. Balaban NQ, Merrin J, Chait R, Kowalik L, Leibler S. Bacterial persistence as a phenotypic switch. *Science* **2004**; 305:1622–1625.
11. Barr DA, Kamdolozi M, Nishihara Y, et al. Serial image analysis of Mycobacterium tuberculosis colony growth reveals a persistent subpopulation in sputum during treatment of pulmonary TB. *Tuberculosis* **2016**; 98:110–115.
12. Saliba A-E, Li L, Westermann AJ, et al. Single-cell RNA-seq ties macrophage polarization to growth rate of intracellular Salmonella. *Nat Microbiol* **2016**; 2:16206.
13. Abel zur Wiesch P, Abel S, Gkotzis S, et al. Classic reaction kinetics can explain complex patterns of antibiotic action. *Sci Transl Med* **2015**; 7:287ra73.
14. Bergmiller T, Andersson AMC, Tomasek K, et al. Biased partitioning of the multidrug efflux pump AcrAB-TolC underlies long-lived phenotypic heterogeneity. *Science* **2017**; 356:311–315.
15. Rego EH, Audette RE, Rubin EJ. Deletion of a mycobacterial divisome factor collapses single-cell phenotypic heterogeneity. *Nature* **2017**; 546:153–157.
16. El-Halfawy OM, Valvano MA. Antimicrobial Heteroresistance: an Emerging Field in Need of Clarity. *Clin Microbiol Rev* **2015**; 28:191–207.
17. Ley SD, de Vos M, Van Rie A, Warren RM. Deciphering Within-Host Microevolution of *Mycobacterium tuberculosis* through Whole-Genome Sequencing: the Phenotypic Impact and Way Forward. *Microbiol Mol Biol Rev* **2019**; 83. Available at: <http://mmlbr.asm.org/lookup/doi/10.1128/MMBR.00062-18>. Accessed 7 April 2019.
18. Sarathy J, Dartois V, Dick T, Gengenbacher M. Reduced Drug Uptake in Phenotypically Resistant Nutrient-Starved Nonreplicating Mycobacterium tuberculosis. *Antimicrob Agents Chemother* **2013**; 57:1648–1653.

19. Svensson EM, Svensson RJ, te Brake LHM, et al. The Potential for Treatment Shortening With Higher Rifampicin Doses: Relating Drug Exposure to Treatment Response in Patients With Pulmonary Tuberculosis. *Clin Infect Dis* **2018**; 67.
20. Svensson RJ, Svensson EM, Aarnoutse RE, et al. Greater Early Bactericidal Activity at Higher Rifampicin doses Revealed by Modeling and Clinical Trial Simulations. *J Infect Dis* **2018**; :1–9.
21. Hu Y, Liu A, Ortega-Muro F, Alameda-Martin L, Mitchison D, Coates A. High-dose rifampicin kills persisters, shortens treatment duration, and reduces relapse rate in vitro and in vivo. *Front Microbiol* **2015**; 6.
22. Bowness R, Boeree MJ, Aarnoutse R, et al. The relationship between mycobacterium tuberculosis mgit time to positivity and cfu in sputum samples demonstrates changing bacterial phenotypes potentially reflecting the impact of chemotherapy on critical sub-populations. *J Antimicrob Chemother* **2015**; 70:448–455.
23. Martinecz A, Abel zur Wiesch P. Estimating treatment prolongation for persistent infections. *Pathog Dis* **2018**; 76.
24. Boeree MJ, Diacon AH, Dawson R, et al. A dose-ranging trial to optimize the dose of rifampin in the treatment of tuberculosis. *Am J Respir Crit Care Med* **2015**; 191:1058–1065.
25. Boeree MJ, Heinrich N, Aarnoutse R, et al. High-dose rifampicin, moxifloxacin, and SQ109 for treating tuberculosis: a multi-arm, multi-stage randomised controlled trial. *Lancet Infect Dis* **2016**; 17:39–49.
26. Gumbo T, Louie A, Deziel MR, et al. Concentration-Dependent Mycobacterium tuberculosis Killing and Prevention of Resistance by Rifampin. *Antimicrob Agents Chemother* **2007**; 51:3781–3788.
27. Andersson DI, Nicoloff H, Hjort K. Mechanisms and clinical relevance of bacterial heteroresistance. *Nat Rev Microbiol* **2019**; Available at: <http://www.nature.com/articles/s41579-019-0218-1>. Accessed 1 July 2019.
28. Strydom N, Gupta SV, Fox WS, et al. Tuberculosis drugs' distribution and emergence of resistance in patient's lung lesions: A mechanistic model and tool for regimen and dose optimization. *PLOS Med* **2019**; 16:e1002773.
29. Aljayyousi G, Jenkins VA, Sharma R, et al. Pharmacokinetic-Pharmacodynamic modelling of intracellular Mycobacterium tuberculosis growth and kill rates is predictive of clinical treatment duration. *Sci Rep* **2017**; 7:1–11.
30. Magombedze G, Pasipanodya JG, Srivastava S, et al. Transformation Morphisms and Time-to-Extinction Analysis That Map Therapy Duration From Preclinical Models to Patients With Tuberculosis: Translating From Apples to Oranges. *Clin Infect Dis* **2018**; 67:S349–S358.
31. Pu Y, Zhao Z, Li Y, et al. Enhanced Efflux Activity Facilitates Drug Tolerance in Dormant Bacterial Cells. *Mol Cell* **2016**; 62:284–294.
32. Chao MC, Rubin EJ. Letting Sleeping *dos* Lie: Does Dormancy Play a Role in Tuberculosis? *Annu Rev Microbiol* **2010**; 64:293–311.
33. Band VI, Weiss DS. Heteroresistance: A cause of unexplained antibiotic treatment failure? *PLOS Pathog* **2019**; 15:e1007726.
34. Lenaerts A, Barry CE, Dartois V. Heterogeneity in tuberculosis pathology, microenvironments and therapeutic responses. *Immunol Rev* **2015**; 264:288–307.
35. Operario DJ, Koeppel AF, Turner SD, et al. Prevalence and extent of heteroresistance by next generation sequencing of multidrug-resistant tuberculosis. *PLOS ONE* **2017**; 12:e0176522.
36. Mandal S, Njikan S, Kumar A, Early JV, Parish T. The relevance of persisters in tuberculosis drug discovery. *Microbiology* **2019**; 165:492–499.

37. Cadosch D, Abel zur Wiesch P, Kouyos R, Bonhoeffer S. The Role of Adherence and Retreatment in De Novo Emergence of MDR-TB. *PLoS Comput Biol* **2016**; 12:1–19.
38. de Steenwinkel JEM, de Knecht GJ, ten Kate MT, et al. Time-kill kinetics of anti-tuberculosis drugs, and emergence of resistance, in relation to metabolic activity of *Mycobacterium tuberculosis*. *J Antimicrob Chemother* **2010**; 65:2582–2589.
39. Marcel N, Nahta A, Balganesch M. Evaluation of killing kinetics of anti-tuberculosis drugs on *Mycobacterium tuberculosis* using a bacteriophage-based assay. *Chemotherapy* **2008**; 54:404–411.
40. Dartois V. The path of anti-tuberculosis drugs: from blood to lesions to mycobacterial cells. *Nat Rev Microbiol* **2014**; 12:159–167.
41. Prideaux B, Via LE, Zimmerman MD, et al. The association between sterilizing activity and drug distribution into tuberculosis lesions. *Nat Med* **2015**; 21:1223–1227.
42. Imperial MZ, Nahid P, Phillips PPJ, et al. A patient-level pooled analysis of treatment-shortening regimens for drug-susceptible pulmonary tuberculosis. *Nat Med* **2018**; 24:1708–1715.
43. Diacon AH, van der Merwe L, Demers A-M, Von Groote-Bidlingmaier F, Venter A, Donald PR. Pre-treatment mycobacterial sputum load influences individual on-treatment measurements. *Tuberc Edinb Scotl* **2014**; 94:690–694.
44. De Jager V, van der Merwe L, Venter A, Donald PR, Diacon AH. Time Trends in Sputum Mycobacterial Load and Two-Day Bactericidal Activity of Isoniazid-Containing Antituberculosis Therapies. *Antimicrob Agents Chemother* **2017**; 61.
45. Martinecz A, Clarelli F, Abel S, Abel zur Wiesch P. Reaction Kinetic Models of Antibiotic Heteroresistance. *Int J Mol Sci* **2019**; 20:3965.
46. Torrelles JB, Schlesinger LS. Integrating Lung Physiology, Immunology, and Tuberculosis. *Trends Microbiol* **2017**; 25:688–697.
47. Furin J, Cox H, Pai M. Tuberculosis. *The Lancet* **2019**; 393:1642–1656.
48. the Catalysis TB–Biomarker Consortium, Malherbe ST, Shenai S, et al. Persisting positron emission tomography lesion activity and *Mycobacterium tuberculosis* mRNA after tuberculosis cure. *Nat Med* **2016**; 22:1094–1100.
49. Lin PL, Ford CB, Coleman MT, et al. Sterilization of granulomas is common in active and latent tuberculosis despite within-host variability in bacterial killing. *Nat Med* **2014**; 20:75–79.
50. Omansen TF, Almeida D, Converse PJ, et al. High-Dose Rifamycins Enable Shorter Oral Treatment in a Murine Model of *Mycobacterium ulcerans* Disease. *Antimicrob Agents Chemother* **2018**; 63:e01478-18.
51. Grosset J. Bacteriologic basis of short-course chemotherapy for tuberculosis. *Clin Chest Med* **1980**; 1:231–241.
52. Koul A, Vranckx L, Dendouga N, et al. Diarylquinolines Are Bactericidal for Dormant Mycobacteria as a Result of Disturbed ATP Homeostasis. *J Biol Chem* **2008**; 283:25273–25280.
53. Gengenbacher M, Rao SPS, Pethe K, Dick T. Nutrient-starved, non-replicating *Mycobacterium tuberculosis* requires respiration, ATP synthase and isocitrate lyase for maintenance of ATP homeostasis and viability. *Microbiology* **2010**; 156:81–87.

Supplementary Material

Adjusted R-squared values for different days of transition

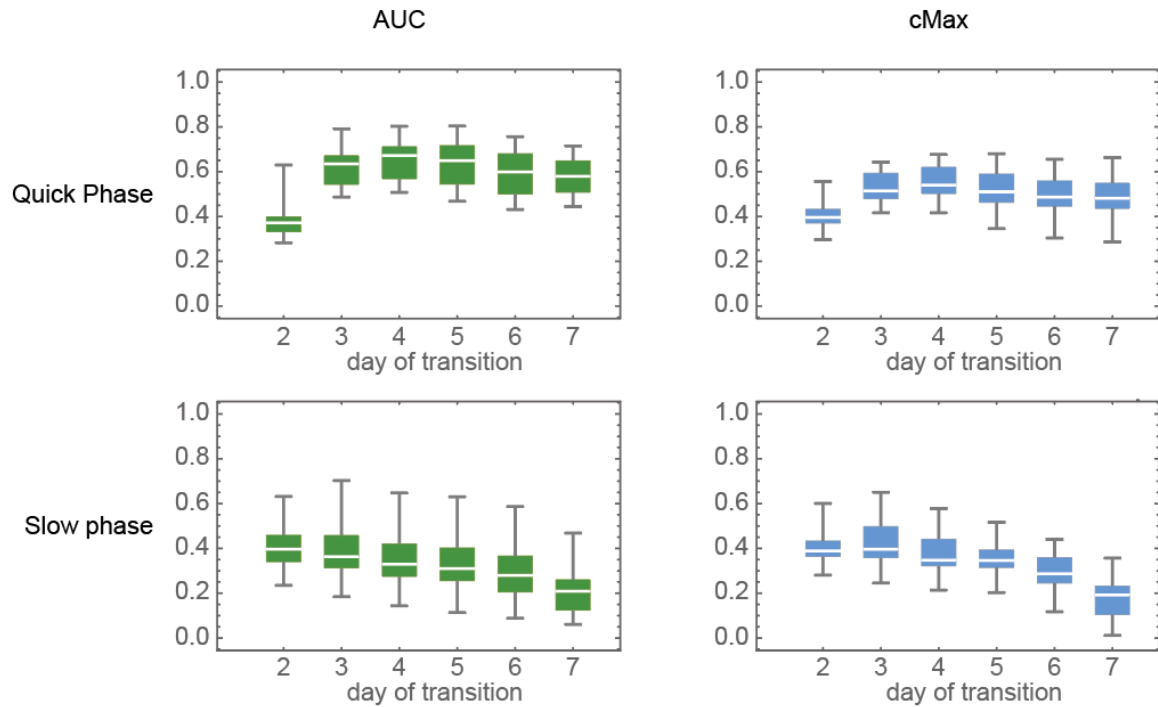


Figure S 1 Adjusted R squared values for the fits on the quick and slow phases' dependence on PK values. The different box-whisker plots in each figure correspond to a different set day of transition. These plots both show that values are consistently better predictors for the slope of the slow phase (based on adjusted R-squared values), as well as that we achieve the best fits for days 3 and 4.

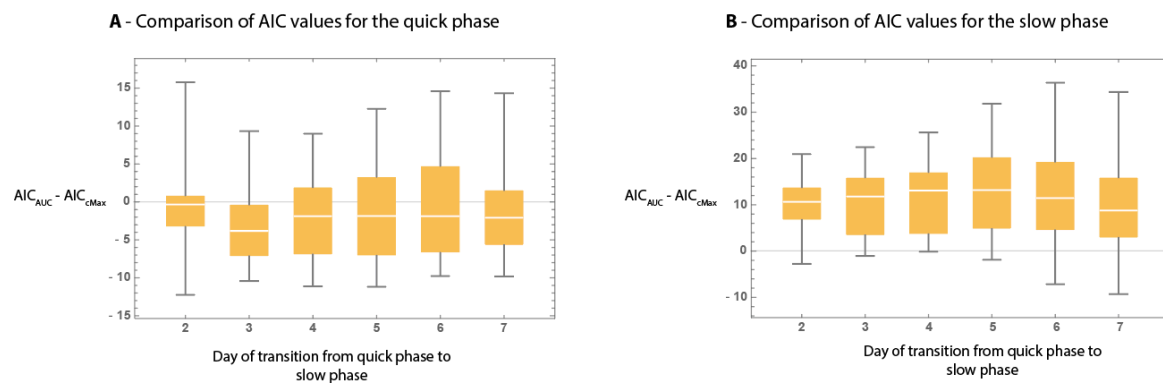


Figure S 2 Difference of corrected AIC values for the fits on the slow and quick phases for different days of transition. Here, the positive values indicate that C_{max} is a better predictor, while negative values would indicate that AUC is a better predictor for the given phase.

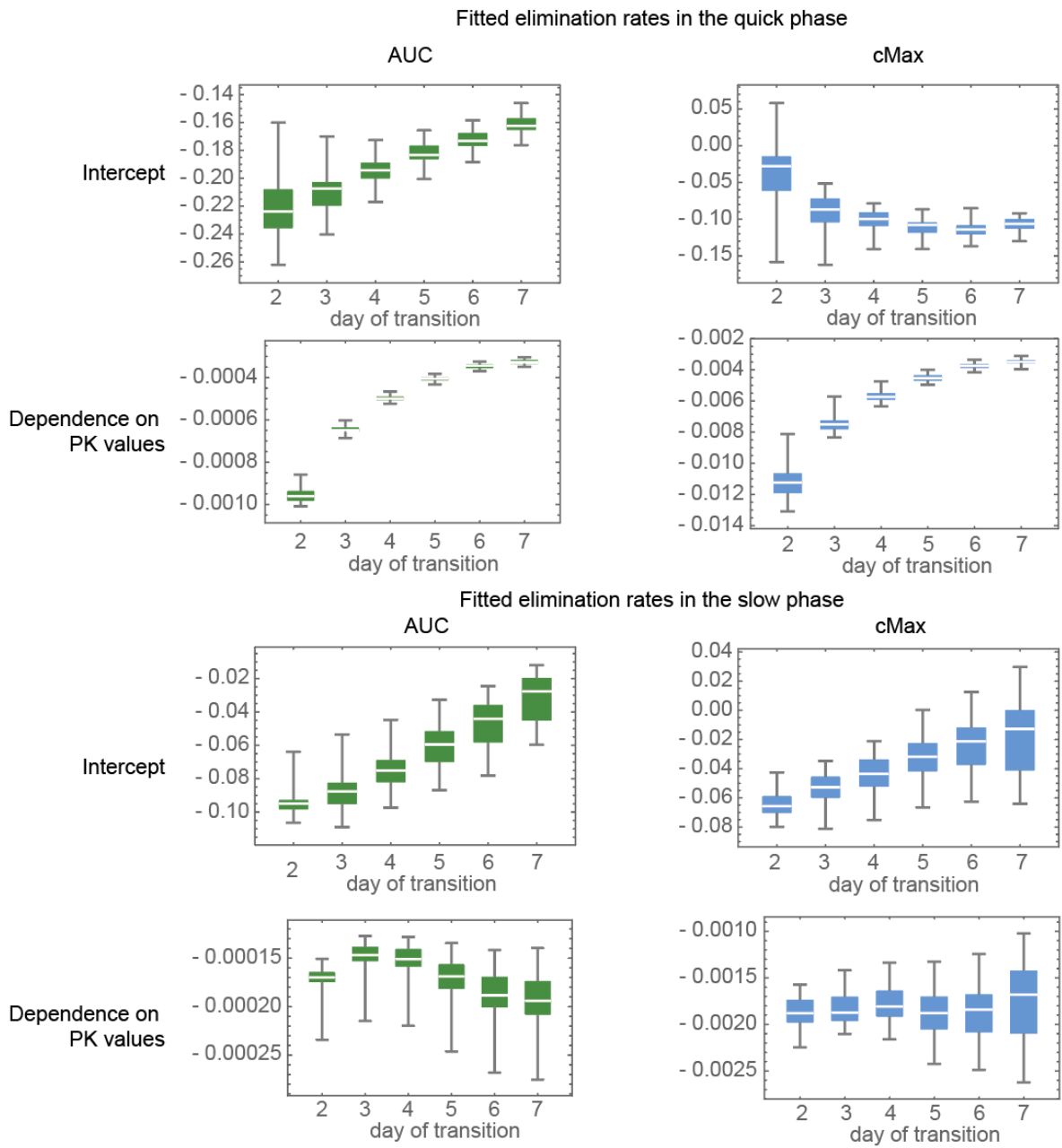


Figure S 3 The determined fits of the biphasic curves for different days of transition (days 2-7, Y-axis) from quick to slow phase. The box-whisker plots represent the results from groupings from dividing the range of PK values into 10 – 40 equal intervals.

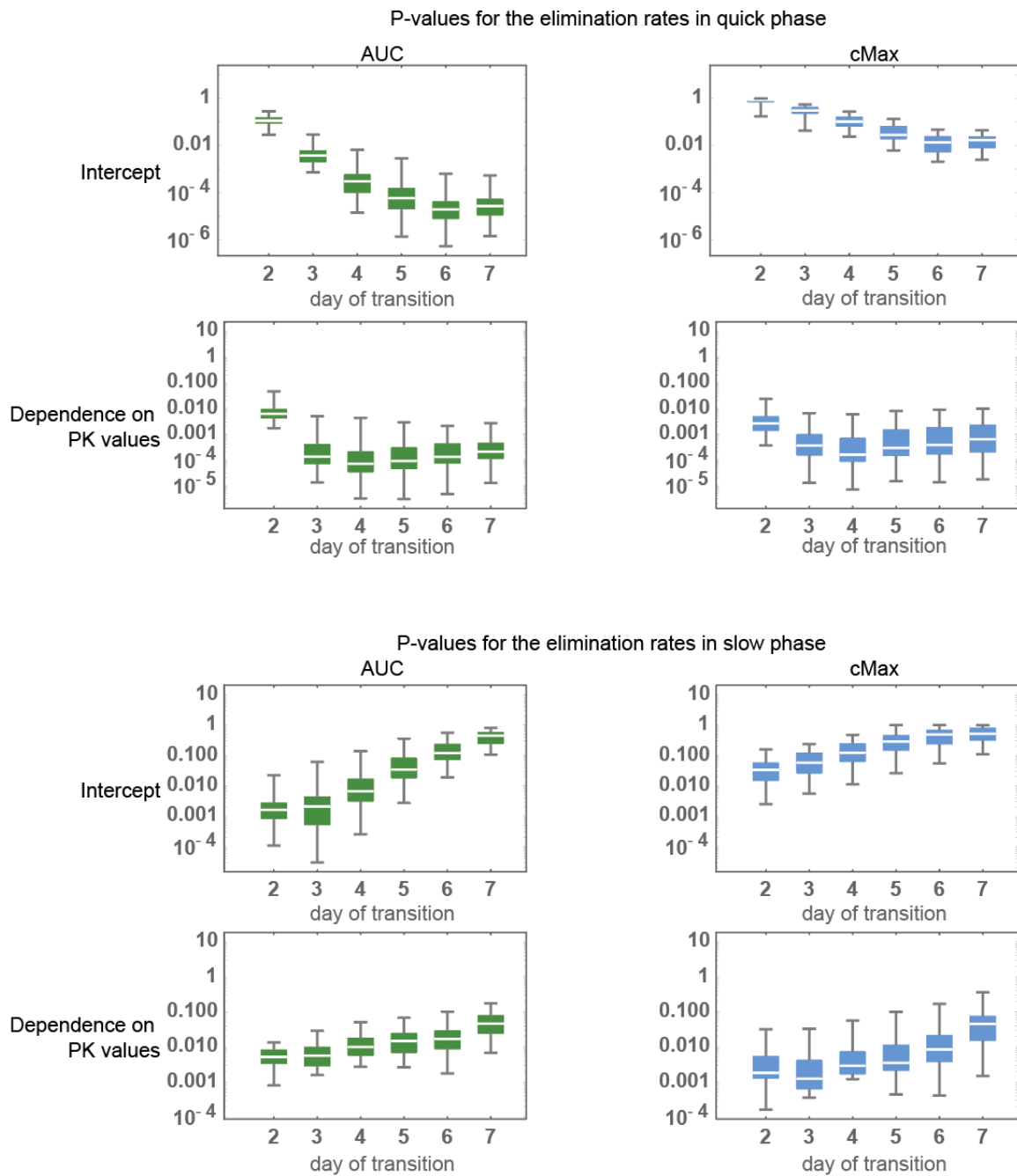


Figure S 4 P-values for the fitted data with different day of transition (days 2-7, Y-axis) from quick to slow phase. The box-whisker plots represent the results from groupings from dividing the range of PK values into 10 – 40 equal intervals. These plots show that if we get the best fits if the days of transition are set to day 3 or 4. Furthermore these also show that C_{max} is consistently a better predictor for the slope of the slow phase than the AUC.

Relationship between pharmacokinetic measurements at slight variations in parameters

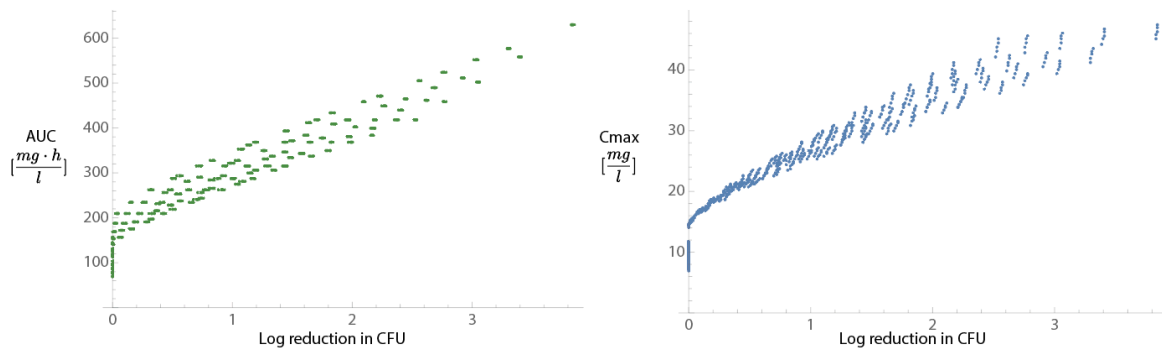


Figure S 5 Relationship between AUC, Cmax, and AUC above an increased MIC (8x the MIC of the majority). This plot demonstrates that when peak drug concentrations are close to the MIC, the Cmax has a stronger correlation with bactericidal action than the AUC. Here, a high MIC represents a resistant subpopulation in heteroresistance, therefore this plot also shows that in the slow phase of elimination where a higher MIC has to be overcome, Cmax will better predict the bactericidal activity than the AUC. We produced these plots using pharmacokinetic models of rifampicin in the cavity wall. We modelled 10, 20, 25, 30, 35 and 40 mg/kg of rifampicin, with variations ($\pm 20\%$) in absorption rates, drug elimination rates, and bioavailability.

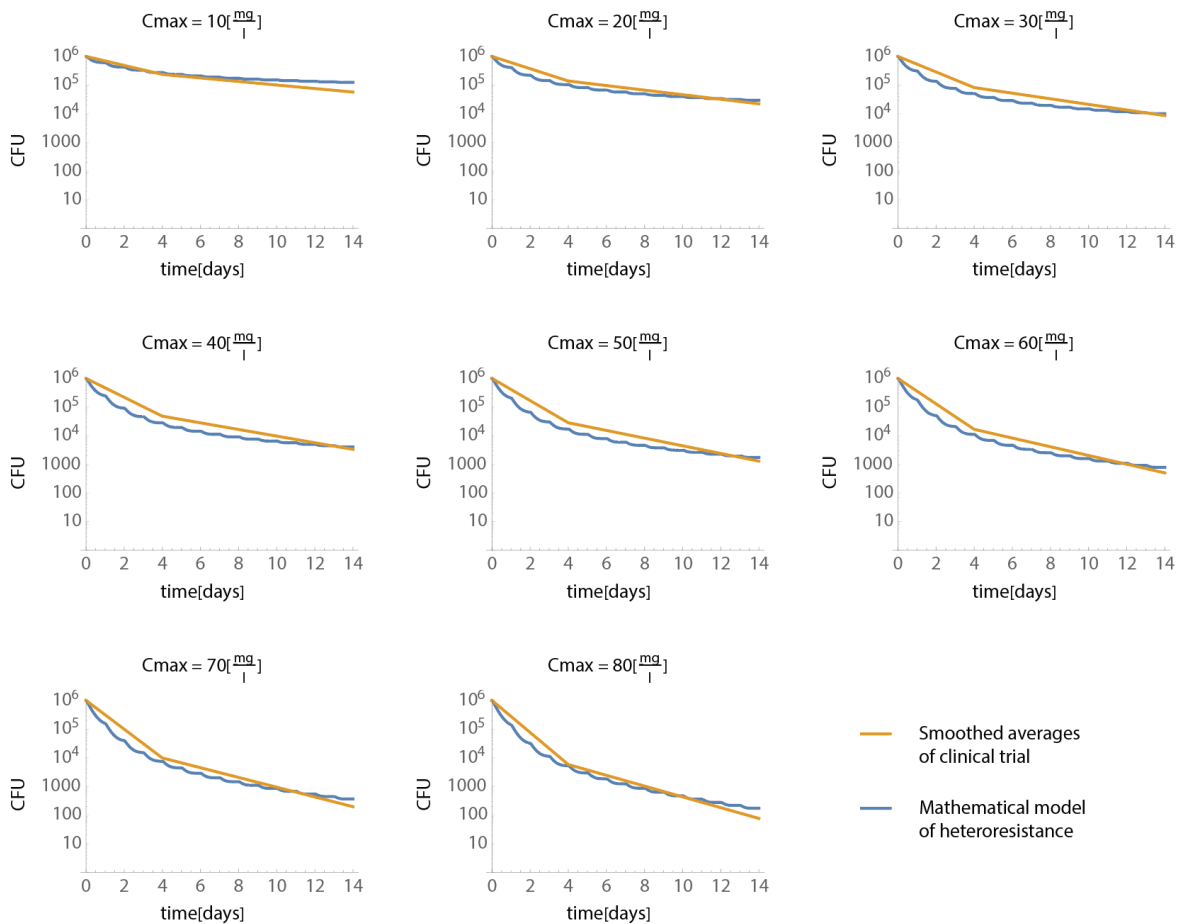


Figure S 6 Side by side comparison of the smoothed averages of the clinical trial dataset and the mathematical model of heteroresistance. All figures show the observed/predicted bacterial counts (Y-axis) over time (X-axis). Each figure shows the same at different Cmaxes. The Cmaxes were chosen to be at regular intervals within the range of the clinical trial dataset (10-80 mg/l), the inputs doses for the mathematical models were chosen to achieve the same Cmaxes within the model.

elimination rates (see **Error! Reference source not found.**), and C_{max} values of 10, 20, 30...80 [mg/l] (in the dataset the C_{max} values range from 7.7 to 85.6 mg/ml).

Property	Grouped by	Intercept (SE)	Slope (SE)	Intercept p-value (corrected for multiple testing)	Slope p-value (corrected for multiple testing)	R ² (adjusted)	AIC (corrected)
Elimination rates (monophasic)	AUC	-0.11 (±0.016)	-0.00026 (±0.00004)	10 ⁻⁶	10 ⁻⁵	0.68	-63
	C_{max}	-0.076 (±0.02)	-0.0026 (±0.0004)	0.0017	10 ⁻⁴	0.65	-73
Baseline (monophasic) Log(CFU) [-]	AUC	5.34 (±0.21)	0.001 (±0.00047)	10 ⁻¹⁴	0.05	0.15	30
	C_{max}	5.1 (±0.25)	0.0012 (±0.0005)	10 ⁻¹⁴	0.02	0.12	41

Table S1 Summary of the median fitted values to the dataset across all groupings, when assuming a monophasic elimination (fitting a straight line through the data). All the P values reported are corrected for multiple testing with the Benjamini-Hochberg method.

Paper 5

Heteroresistance increases the necessary treatment length in a within-host metapopulation model

Antal Martinecz, Pia Abel zur Wiesch*, Roland R. Regoes*

*These authors contributed equally to this work.

Abstract

Bacterial heterogeneity is thought to complicate antibiotic treatments. An example of this is heteroresistance which is defined as the coexistence of bacterial subpopulations with different susceptibilities to antibiotics. *In vitro*, heteroresistance has been shown to cause an apparent slowdown in the elimination of the bacterial populations, as some bacterial subpopulations may be less susceptible than others and therefore be eliminated more slowly. As a result, heteroresistance is often assumed to allow bacteria to survive antibiotic treatments *in vivo* and cause relapse if a treatment is terminated prematurely.

Heteroresistance may also complicate treatments in other ways as well. This is because *in vivo* bacterial population dynamics can differ greatly from *in vitro* observations. For instance, bacteria are eliminated by the immune system, which in some if not most cases may prevent bacterial regrowth at a given site of infection. At the same time, bacteria are also thought to spread to new sites of infection and establish colonies in tissues where immune response has not been elicited yet. This allows bacteria to avoid immune clearance from the body. Here, we focus on this scenario, and investigate whether heteroresistance can prolong antibiotic treatments by affecting the spread of bacteria within host during treatments.

To do so, we use a model similar to the SEIS model used in epidemiology. As tuberculosis involves spatially separated subpopulations, to parametrize the model with biologically relevant values, we use tuberculosis as an example. Where possible, we used data from our recent analysis of a clinical trial on high rifampicin doses in tuberculosis patients, as well as *in vitro* data available in the literature.

We demonstrate that heteroresistance can prolong antibiotic treatments even when the immune system can prevent relapse by regrowth at a given site. This is because delaying clearance at infected site presents opportunities to infect other sites. This highlights the fact that heteroresistance may affect treatments in multiple ways.

Introduction

In bacterial colonies individual cells have been shown to slightly differ from one another. This may be due to variations in cell sizes [1], number of efflux pumps [2], random (transient or stable) mutations [3], or gene amplification [4]. If these cell-to-cell heterogeneities cause a substantial diversity in the susceptibility to antibiotics, then these phenomena are often referred to as heteroresistance [3,5–7]. Heteroresistance itself can be further divided into two subcategories: monoclonal heteroresistance which encompasses transient causes of variations in susceptibility, and polyclonal heteroresistance, which encompasses stable resistance mutations [7]. When heteroresistant bacterial colonies are exposed to antibiotics, the elimination rates of the colony can slow down dramatically over time, reflecting the elimination of the bacterial subpopulations with decreased susceptibility [8].

As heteroresistant bacteria has shown to exist *in vivo* [9–11], it is often assumed that the slowdown in elimination rates caused by it can complicate antibiotic treatments. For instance, heteroresistance may allow fractions of bacterial colonies to survive prolonged exposure to antibiotics which may cause regrowth and therefore relapse if a treatment is terminated prematurely [9]. While this has not been shown conclusively yet, there is increasing evidence for it [9]. One of the major concerns is the possible emergence of resistance that follows relapse. This is arguably the case in polyclonal heteroresistance where regrowth from a stable resistant mutation may result in a colonies with only resistant mutants, It

is also often suspected in case of monoclonal heteroresistance as it may allow the eventual emergence of a resistant mutants [7]. In this work, we model on how the risk of relapse may extend the necessary length of treatments, rather than focusing on the resistance emergence aspect of it. Particularly, we are interested in heteroresistance in the context of tuberculosis.

In vivo, bacteria and therefore bacterial heterogeneity is not necessarily confined to a single bacterial colony. A recent systematic review [12] of the literature found that there may be a high diversity of the *Mycobacterium tuberculosis* (M.tb) genome within host, particularly with bacteria found at different infected sites within the same host [13,14]. It has been argued that this diversity may affect drug susceptibilities as well [13]. Additionally, in tuberculosis, M.tb can be found in a wide variety of sites within the lungs, for instance in granulomas, cavities, necrotic granulomas, as well as intracellularly within macrophages [15–17]. The different sites of infections have been shown to harbor different amounts of bacteria, and the pharmacokinetic properties may also be different type of sites as well as across lesions of the same type in the same organ of a patient [17]. Finally, the environments the bacteria are in can also affect their susceptibility to antibiotics. This can be due to the different environments can affect the growth and metabolic states of bacteria that in turn has shown to affect susceptibility [18], or different sites can also facilitate the microevolution of bacteria within the host [12].

This spatiality introduces additional dynamics in how bacterial heterogeneity may affect antibiotic treatments in addition to allowing individual colonies to survive antibiotic exposure. For example, it is possible to have individually homogeneous sites, but having differential susceptibilities across the different sites thereby acting similarly to heteroresistance when considering the patient as a whole. Here we refer to this as spatial heterogeneity. This raises the question of scale in the definition of heteroresistance and the possible differences between heteroresistance in individual colonies, and spatial heterogeneity.

Furthermore, in diseases that infect multiple sites it is thought that bacteria can evade immune clearance from the body by spreading bacteria to sites that have no active immune response yet [19,20]. This may be the case in tuberculosis as well, where the immune system has been shown to regularly sterilize or contain most infected sites and localized immune responses are thought to play an important role in controlling the disease [16,21–23]. The importance of immune clearance in tuberculosis treatments is demonstrated by the observation that viable M.tb bacteria can still be found in the lungs of patients 6 months after curative treatments [24]. These bacteria are either eventually sterilized or contained by the immune system without any additional exposure to antibiotics.

Mathematical modeling studies on the necessary lengths of antibiotic treatments (in order to avoid relapse) in the presence of the immune system often focus on modeling one individual site of infections. Therefore, relapse is often modelled as the regrowth of bacteria at a given site [25–28]. This requires the modeling assumption that there are conditions under which the immune system allows the regrowth of bacteria. However, it is unknown whether this is true or not. This also necessitates the assumption that within the mathematical models, there is an arbitrary population size above which the bacterial replication rates overwhelm the rate of the immune elimination. In other words, this is incompatible with the observation that the immune system often has the ability to sterilize individual infected sites without treatments. Without this modeling assumption, in single-site models, it is difficult to capture relapse in the sense of the bacterial populations fully recovering into their pre-treatment numbers.

Here we investigate the impact of bacterial heterogeneity (both heteroresistance and spatial) on the length of antibiotic treatments under the assumption that the immune system may be able to clear individual infected sites. Thereby evaluating previously untested scenarios on the possible role of spatiality during antibiotic treatments. Here, we focus on the question of whether heteroresistance can have a considerable impact in the dynamics of bacteria spreading from site-to-site during an antibiotic treatment. Additionally, we also investigate whether it is possible to distinguish between heteroresistance and spatial heterogeneity as observed on the total bacterial burden. To do so, we use a model similar to epidemiological models to capture the effects of bacteria spreading to site to site. We parametrize this model with data from our previous analysis of a clinical trial on high rifampicin doses

on tuberculosis patients where we have shown that there is slowdown in elimination of bacteria as observed on the colony counts of sputum samples. For the sake of consistency we focus on tuberculosis as an example, however these spatial dynamics are thought to occur in other diseases as well [19]. Therefore, we keep the model general in order to bring attention to the neglected aspect of spatiality in antibiotic treatments and heteroresistance.

Results

We focus on whether heteroresistance can affect the spread of bacteria from site to site during treatments within a patient. To this end, we use a model with susceptible, exposed, infected, and persisting compartments where the infected and persisting sites can spread bacteria to susceptible tissues. This model, while describing the within-host dynamics of a bacterial infection, has formal similarity to SEIR models in epidemiology.

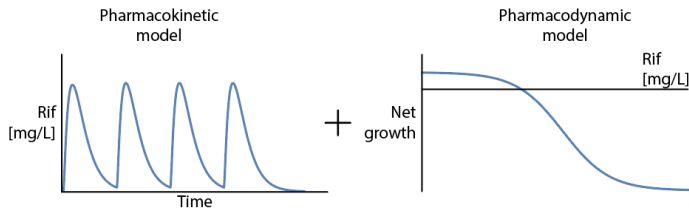
To parametrize the model, where possible, we used data from our previously published analysis on a clinical trial on high rifampicin doses in tuberculosis patients (*Note: paper #4 in the PhD thesis, has not been published yet*). There, we also used a PK-PD model to simulate a heteroresistant population of bacteria in the open cavities in the lungs of tuberculosis patients and demonstrated that the model showed a strong agreement with the observed bacterial decline in the clinical trial. Here, we use the same single site model (see Figure 1A), to estimate the elimination rates of bacterial populations (d , and d_p on Figure 1 C).

Where data was not available, we relied on other relevant data to have biologically plausible values. The growth rates of exposed sites (σ on Figure 1 C) were estimated based on *in vitro* growth rates of *M.tb*. The infection rates (spread of bacteria from infected sites to susceptible sites, β on Figure 1 C) are chosen in a way that the immune system without treatment can not clear the infection in the deterministic model. At the same time, in stochastic simulations it allows spontaneous cure in a fraction of cases, similarly to tuberculosis where the spontaneous recovery rate (for untreated cases) is up to 30% [29,30].

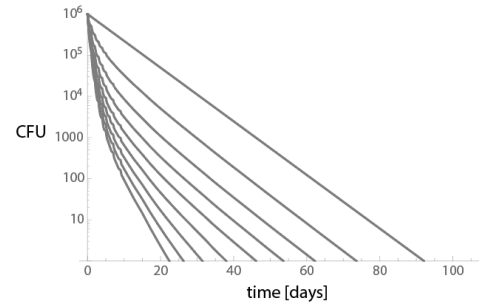
Using these parameters, we constructed the multi-site model. On Figure 1 we show that in the multi-site model, the total bacterial burden declines similarly to the single site model and therefore to the observed bacterial burden decline in the clinical trial. Figure 1A and B shows the single-site model, and Figure 1C and D shows the multi-site model. In the latter case, Figure 2 shows the dynamics of individual infected sites within the multi-site model.

Single-site model

A - Model

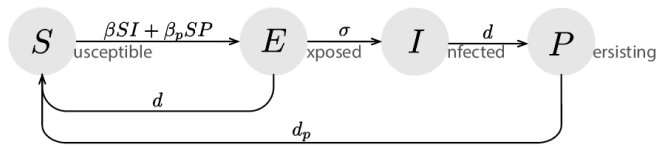


B - Simulations



Multi-site model

C - Model



D - Simulations

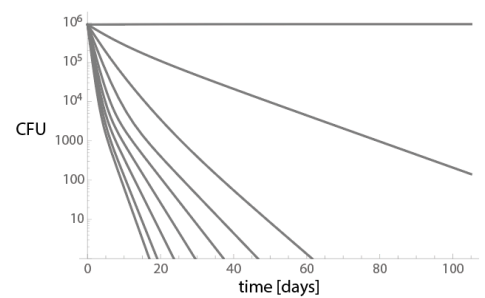
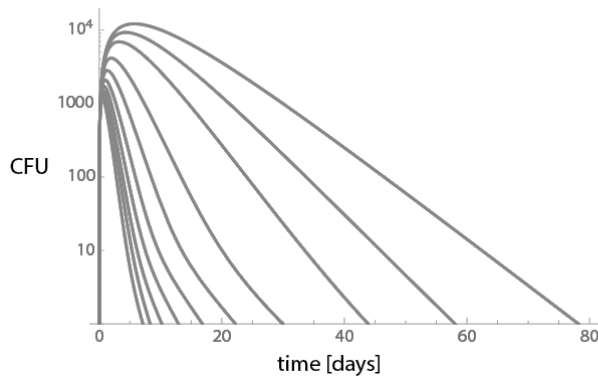


Figure 1 Comparison of trends in bacterial decline in the single- and multi-site model. Figures A and C show the schematics of the models while Figures B and D show the decline of bacteria at different dose (from left to right: 80...10 mg/kg rif, and “no treatment” cases).

A - With heteroresistance



B - Without heteroresistance

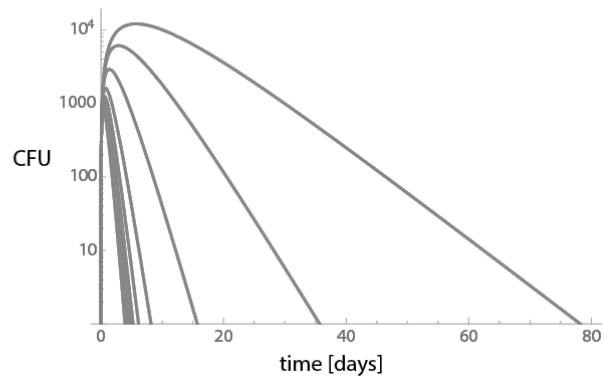


Figure 2 Dynamics of Individual infected sites within the multi-site model. The different curves belong to 0, 10, ..., and 80 mg/kg rifampicin doses. This figure shows that even though in the model bacterial populations are allowed to grow during treatment, their sizes are greatly reduced. Both of the figures were made by starting simulations at 1 exposed sites, and setting the spread of bacteria, β , to 0. Figure A shows the case with heteroresistance. Figure B shows the case without heteroresistance (homogeneous populations).

Next, we model relapse after the end of antibiotic treatments in order to be able to define the end of a treatment. Here, we defined relapse as developing a new infected site in the model after the end of treatment if it was modeled with stochastic simulations. This allows us to express relapse in terms of probabilities and therefore provide a more intuitive way to compare simulations. Figure 3 shows the treatment duration required for the relapse rates to go below 10%, with fully susceptible, heteroresistant bacteria, and moderately resistant bacteria (2x MIC). It shows, that heteroresistance prolongs the treatments the most, due to the occasional highly resistant (8x MIC: 1% of population, 16x MIC: 0.1%

of population) subpopulations. Here, the main difference was not at the end of the treatment, but during the treatment, where heteroresistance allowed more “infection events” (see Figure 4).

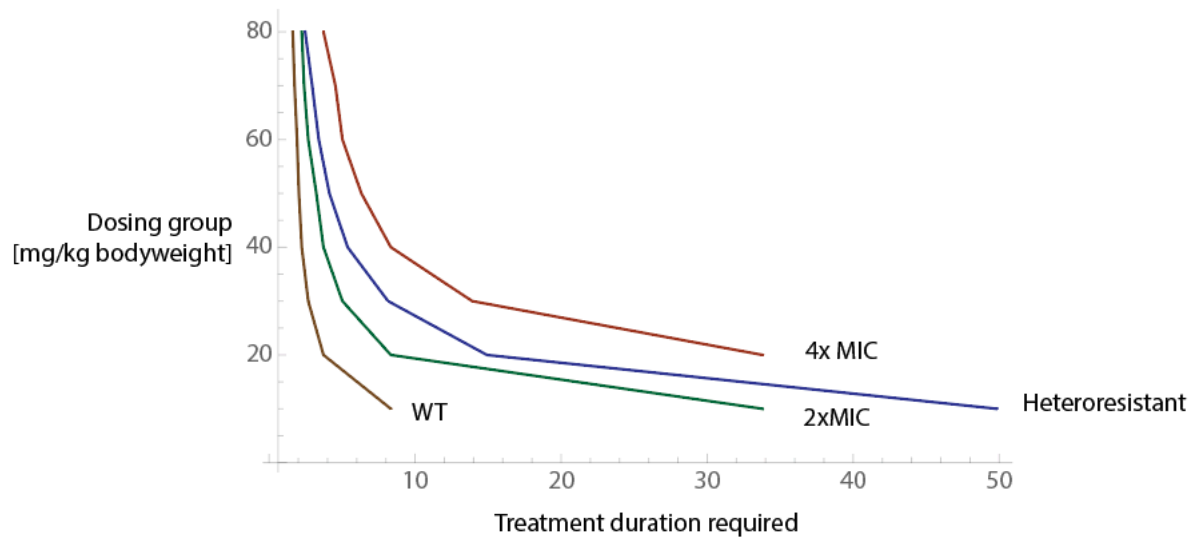


Figure 3 Comparison of the required length of treatment within the multi-site model with and without heteroresistance. Length of time (x axis) until the probability of infecting new sites decreases below 10% depending on dosing group (y axis). Here, we also plotted cases with homogeneous populations with mild resistant mutations (2x, and 4x MIC).

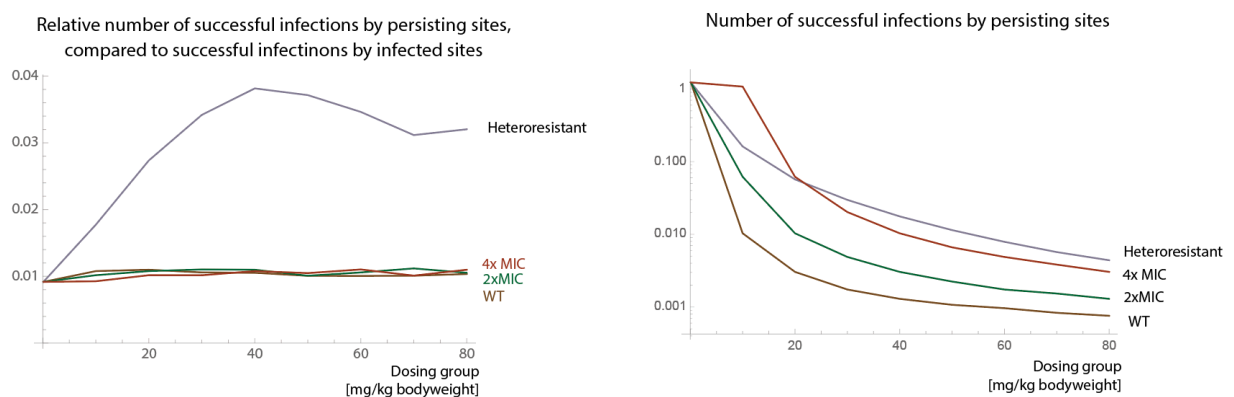


Figure 4 Contribution of persisting sites to the spread of bacteria. Figure A shows the relative infectivity compared to infected sites (Y axis) depending on the dosing group (X axis). Here, the homogeneous populations are always at 1% as they are 1% of the size of the infected sites. Figure B shows the total number of infections in the simulation (Y axis) depending on the dosing groups (X-axis). This number is a combination the ability to infect sites due to heteroresistance, as well as the number due to having more sites due to previous infection events.

Finally, Figure 5 shows that the same pattern on bacterial elimination can also be captured with a model where the slowdown is caused by individually homogeneous sites. Here, some sites are more slowly cleared than others due to either environmental factors that affect susceptibility, pharmacokinetics, mixed infections with resistant bacteria, or local microevolution.

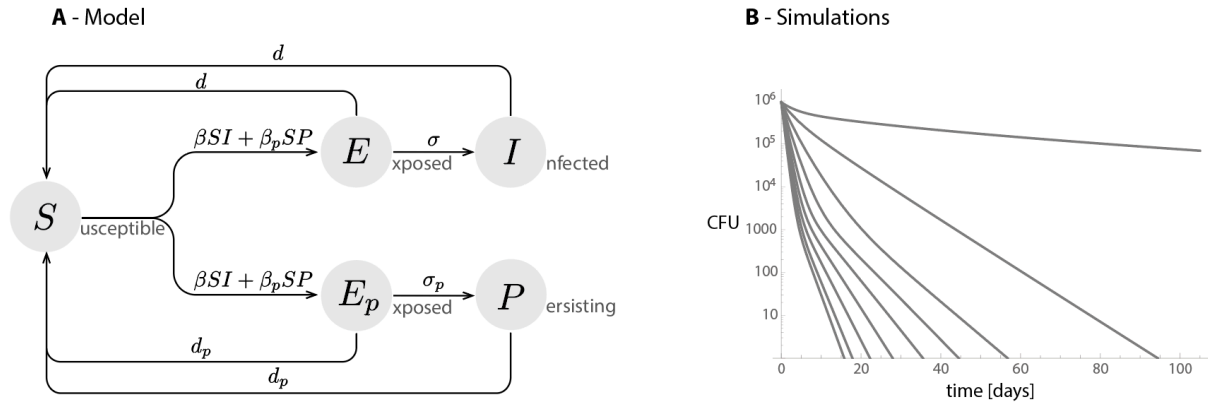


Figure 5 **Alternative explanation for a slowdown in elimination.** This figure shows that the same elimination curves can be achieved by modeling individually homogeneous sites with different susceptibilities to antibiotics rather than heterogeneous sites. **Figure A** shows the model and **Figure B** shows the resulting bacterial elimination.

Discussion

We set out to model the effects of bacterial heterogeneity on treatment lengths in the case where the bacteria can infect multiple sites within a host. We focus mainly on heteroresistance which is defined as the coexistence of bacteria with different susceptibilities [3,7]. We also investigate diversity in bacterial elimination rates due to bacteria residing at different locations in a patient which we refer to as spatial heterogeneity. We were particularly interested in the scenario, where the immune system can clear infected sites by itself, however the bacteria can also spread to new susceptible sites where there is no active immune response yet thereby evading clearance from the body without treatment. Even though this kind of multi-site dynamic is assumed to be case in a number of diseases, for instance tuberculosis, salmonella, and staphylococcus infections [19], it is a rarely investigated topic in the field of heteroresistance. In this work, we rely on tuberculosis as an example, therefore we parametrized the model with data from tuberculosis clinical trials, however the model is not intended to, and cannot capture the complex dynamics of tuberculosis.

Heteroresistance is often assumed to negatively impact antibiotic treatments. For instance, it may allow bacteria to survive prolonged exposure to antibiotics and causing relapse after an antibiotic treatment [9]. Here, we investigate whether heteroresistance can have an impact on antibiotic treatments in addition to these mechanisms, specifically whether it can affect the spread of bacteria from site-to-site during treatments. This is consistent with the observation that even during treatments there can be new infected sites that intensified in tuberculosis patients [24]. This may also be the case in other diseases as well such as *Staphylococcus aureus* infections where bacteria may use an intracellular niche to disseminate [31–33].

We set up a model similar to the SEIS model used in epidemiology to capture the spread of bacteria within host. In our model, all bacteria have the same susceptibility to the immune response, regardless of the size of the population, however we are assuming that the immune system takes time to respond to newly infected sites. This has also been observed in tuberculosis, where most infected sites can be sterilized or contained by the immune system by itself, however the bacteria can often spread to new sites preventing total clearance [20,23].

We show that if bacteria can establish new infected sites during treatments, heteroresistance can have a substantial impact on these dynamics and increase the ability of infected sites to spread bacteria to susceptible sites. When compared to the scenario to the mild resistance (2x MIC) case, heteroresistance increased the necessary treatment length more at higher antibiotic concentrations. This is because heteroresistance in these models acts as a bet-hedging strategy against a wider range of antibiotic concentrations.

We parametrized the model with results from our previous analysis (*paper #4 of the thesis*) of a clinical trial on high rifampicin doses in tuberculosis patients (trial NCT01392911, [34]). In that study, we showed that there is a slowdown in elimination rates over time, as observed on the sputum bacterial counts. Using mathematical models, we demonstrated that heteroresistance is a likely cause of the slowdown in elimination. However, as the sputum can originate from multiple sites, our more general conclusion was that the cause of the slowdown is the heterogeneous elimination of bacteria at the sputum producing compartments. In other words, it may be possible that there is no heteroresistance but due to spatial heterogeneity we observe similar dynamics. Both possibilities are supported by the literature, and therefore the cause of the slowdown is likely to be a mixture of the two. Heteroresistant bacteria has been shown to exist in *M.tb in vitro* [3], *in vivo* [10,11], and within host microevolution of *M.tb* bacteria has also show to occur within tuberculosis patients [12,13]. Recent pharmacokinetic studies have shown that there is a substantial variation in the pharmacokinetic properties not only across the different types of infected sites in TB patients but even across the same type of sites within the same organ in the same patient [17,35]. Furthermore, different sites are also different environments for the bacteria, which may affect bacterial susceptibility to antibiotics even further. The extreme case of this is the hypoxic environments in necrotic granulomas, which are shown to facilitate the switching to an entirely non-susceptible, dormant state (i.e. antibiotic persistence) of *M.tb* bacteria [36]. Disentangling the two possible causes is difficult via experimental approaches as well: the most common approach to assess bacterial burden is via sputum samples [37,38]. Sputum has been thought not the reflect the full diversity of bacteria within host [14,39], not only because intracellular bacteria or bacteria residing in closed granulomas are inaccessible, but also because the sampling and culturing methods can also affect bacterial diversity [39–42]. Finally, a study on mixed susceptible/resistant *M.tb* bacterial populations have shown that common antibiotic susceptibility testing methods in tuberculosis treatments cannot be used to detect heteroresistance [43].

Here we elaborate on this, and show that it is possible to observe the same slowdown in elimination with both heteroresistance and spatial heterogeneity. For spatial heterogeneity to produce the same behavior as heteroresistance, it is necessary for the model to have a specific constellation of bacterial numbers and susceptibility to antibiotics at different sites. Arguably, to observe a consistency across patients as the have seen in the clinical trial, the disease pathology would need to be conserved across patients as well. This makes heteroresistance a more likely cause of the slowdown in our previous study. The two possible causes of slowdown may also have implications in bacterial evolution and the possible emergence of resistance. For instance, the expression of certain antibiotic resistance mechanisms are dependent on environments [44], therefore some mutations may only emerge in spatial heterogeneity and not in heteroresistance. Conversely, heteroresistance is also thought to facilitate the emergence of resistant strains [7], which may be different in case of spatial heterogeneity. Finally, the two may be different diagnostically, heteroresistance may be detected with directed approaches [3,4,43], while spatial heterogeneity may not be detected depending on its mechanism of action (for instance, decreased susceptibility due to environmental effects).

In general, this highlights the question of scale in the definitions of heteroresistance, whether a patient can or should be described as heteroresistant as a whole when individual colonies in a patient are homogeneous. On one hand, on a patient level, the two cases may look similar, and may be mitigated by similar strategies (for example increased doses). On the other hand, the two may be different on a multi-patient level, as spatial heterogeneity may cause substantially larger inter-patient variability than heteroresistance, thereby requiring different general recommendations on treatment regimens. To disentangle the two, more studies are necessary in this topic.

Other, similar modeling studies in the literature mainly rely on modeling single sites of infection [25–28]. (*Note on references: heteroresistance was often referred to as “persistence” before the consensus statement on the definitions in 2019 [45]. Now the two are recognized as separate phenomena*). These models rely on modeling the immune system in a more mechanistic manner, however as a result use parameters that may be difficult to measure or observe. Here, we used a more a abstracted approach, which allowed us tie most parameters to observable phenomena, for instance the average time for an

exposed site to grow into a full-sized lesion (infected site). Additionally, this approach allowed us to express relapse or spontaneous recovery in terms of probabilities which in turn allowed us to compare the model to clinical observations and data that would be difficult to do so with other approaches. For example, in the model it was possible to choose parameters based on the fact that a small proportion (approx. 30% [29,30]) of untreated tuberculosis patients recover without treatment, while the majority won't. Modeling relapse this way can also open up the possibilities in comparing different simulations in a similar to the way clinical trials are assessed and designed: most treatments have a certain risk of unfavorable treatment outcome. New antibiotic treatments are often assessed based on their "non-inferiority" to the standard of care which allows considering trade-offs between different treatments. For example, shortening treatments while keeping the risk of relapse the same, or reducing the risk of relapse but keeping treatment lengths the same.

The abstracted nature of our model also means that it does not allow mechanistic investigations of heteroresistance. For instance the parameters used for bacterial elimination rates are estimates from the single-site models and therefore have to be used as is. As a result, the model does not allow changing the treatment regimen mid-treatment within the model. Additionally, our model is not set up in a way to capture the complex dynamics of tuberculosis as that would require more types of sites, for example not all sites may contribute to the sputum or the spatial dynamics of tuberculosis equally. Finally, our intention here was to demonstrate how heteroresistance can affect disease dynamics when bacteria can also spread from site to site rather than modeling a specific case. Therefore, some of the parameters in this model are hypothetical, therefore the model does not have a predictive power on tuberculosis treatments.

Taken together, our results show that heteroresistance may not only complicate antibiotic treatments after antibiotic treatments (by possibly causing relapse), but also during antibiotic treatments as well. We have also demonstrated that there is a grey area in the definition of heteroresistance, as the scale at which heteroresistance is considered in may matter. While we parametrized the model based on our knowledge of tuberculosis treatments, these results can be generalized into other diseases as well with similar multi-site dynamics. Finally, we have shown a modeling approach to antibiotic treatments that is more in line with experimental results, therefore facilitating more direct comparisons across disciplines.

Materials and methods

Single site model

The single site model is a pharmacokinetic-pharmacodynamic model. The pharmacokinetics part is based on a pharmacokinetics model fitted to data from tuberculosis patients undergoing lung resection surgery, published recently by Strydom et al. [17]. There, they have measured drug distribution patterns for most major TB drugs on multiple relevant lung lesion types. Here, we use the parameters for rifampicin pharmacokinetics in the open cavities of the lungs. We omitted the multiple absorption compartments for rifampicin, as modeling the lag time between dosing and drug absorption is not relevant for our simulations. The pharmacodynamics part is based on in vitro measurements on *M.tb* exposed to rifampicin available in the literature [46–49]. Here, we did not model the replication of *M.tb*, in between the daily doses when the drug concentrations dip below the MIC. The reason for this is that due to the post antibiotic effect, decreased replication rates in vivo when compared to in vitro, and the assumed presence of immune elimination there is arguably very little replication taking place. Additionally, modeling the random distribution of resistant traits (if they are not hereditary) would require additional assumptions and may affect the dynamics of the system [50]. Therefore, errors introduced by using inaccurate parameters and assumptions for this would be similar to errors introduced by omitting modelling replication in the model.

Previously, in an analysis of a clinical trial on high rifampicin doses on tuberculosis patients (*paper #4 in the thesis*) we have shown that heteroresistance is a likely cause for the slowdown in bacterial elimination. There, we estimated a hypothetical susceptibility distribution of bacteria and demonstrated

that the PK PD model showed a strong agreement with the data on the dynamics of bacterial decline observed over 14 days in a course of the clinical (trial NCT01392911, [34]) (see Figure S 2). Finally, there we also estimated time until no bacteria are detected in the sputum (time to sputum culture conversion, TSCC) based on the PK PD model as well as the statistical analysis of the clinical trial and compared these estimates to the measured times in a different clinical trial (trial NCT01785186, [51]). We found that while based on the statistical analysis we could get reasonable estimates, it was not possible to do so with the PK PD model. This could be rectified by adding an extra elimination term to the PK PD model ($\delta_{imm} = 0.15 \frac{1}{day}$, in Eq (5)). In this work, we use this value as a stand-in for the immune elimination of bacteria as it is an elimination term independent of the dosing groups (Figure S 1, 2 and 3). Note, that this did decrease the fit between the PK PD model and the clinical trial for the first 14 days (Figure S 4).

Pharmacokinetics model

We used compartmental pharmacokinetic model of [17]. From this model, we only used one absorption compartment as lag times are not relevant to our model:

$$(1) \quad \frac{dA_{abs}}{dt} = input(t) - ka A_{abs}$$

$$(2) \quad \frac{dA_{plasma}}{dt} = ka A_{abs} - \frac{CL}{V} A_{plasma}$$

$$(3) \quad \frac{dA_{tissue}}{dt} = k_{pl-tissue} \left(R \frac{A_{plasma}}{V} - A_{tissue} \right)$$

Here the parameters are the ones published by Strydom et al in [17]:

- $input(t)$ is the input function, to be able to implement daily doses of drugs into the absorption compartment. It implemented a Dirac comb function with the spikes spaced 24h apart.
- A_{abs} , A_{tissue} , and A_{plasma} are antibiotic concentrations in the absorption, plasma and tissue compartments
- $ka = 1.55 [h^{-1}]$: absorption rates of the drug from absorption compartment
- $CL = 5.72 [\frac{L}{h}]$ are clearance rates of the drug from the plasma compartment
- $V = 52.3 [L]$ is the volume of distribution in liters
- $R = 0.614$ is the penetration coefficient into the tissue (cavity wall).
- $k_{pl-tissue} = 1.98$ rate of drug moving from plasma to tissue (h^{-1}).

Elimination rate curves

We used the pharmacodynamic model available in the literature [46] on *in vitro* M.tb exposure to rifampicin:

$$(4) \quad \delta(A) = -r + \frac{EC_{max} A}{EC_{50} + A},$$

where A is the antibiotic concentration in $[\frac{mg}{ml}]$. In the model we do not allow replication, therefore in cases where it was negative (replication), it was replaced with $\delta(A) = 0$.

Table 1 summarizes the values used for this model. For the estimates, we simulated daily doses of rifampicin of 10...80 kg/kg bodyweight for a 60kg person, same as in our previous analysis.

Parameter	Description	Value	Unit	Ref
EC_{max}	Maximum elimination rate	1.82	day^{-1}	[46–49]
EC_{50}	Half-maximal effective concentration	0.51	$\frac{mg}{l}$	[46–49]

r	Growth rate of <i>M.tb</i> bacteria	0.8	day ⁻¹	[46,52]
$B_{total}(0)$	Total modelled population size	10 ⁶	-	Based on the dataset: B(0) _{median} = 10 ^{5.9} B(0) _{mean} = 10 ^{6.11}

Table 1 Summary of parameters used in the PD model.

Pharmacodynamic and heteroresistance model

The pharmacodynamic model is based on modeling individual subpopulations with the time-varying antibiotic concentrations (A, see Eq (3)) as an input with an added constant immune elimination rate (δ_{imm}):

$$(5) \quad \frac{dB_i(t)}{dt} = -(\delta(A) + \delta_{imm}) B_i(t)$$

$$(6) \quad B(t) = \sum_i B_i(t)$$

,where $B_i(0)$ is the size of each subpopulation and δ_i are the corresponding elimination rates.

Here we modelled 9 subpopulations where the 5th subpopulation is the ‘‘average’’ susceptibility and in the majority.

$$(7) \quad B_i^*(0) = B_{total}(0) * D(i - 5|0, 1), \text{ where } i = 1 \dots 9$$

As this function just takes portions of the normal distribution, the $\sum B_i^*$ will be less than B_{total} and therefore has to be rescaled:

$$(8) \quad B_i(0) = \frac{B_{total}(0)}{\sum B_i^*(0)} * B_i^*(0)$$

where $D(x|\mu, \sigma)$, is the probability density function of the normal distribution, with the mean: μ and standard deviation σ of the distribution.

For the purposes of this paper, a range of susceptibilities for different subpopulations is mathematically the same as having the same sensitivities but a varying effective antibiotic concentrations (A_i) [8]. However the latter is easier to compute. Therefore, we calculate the different elimination rates (δ_i), from Eq (9):

$$(9) \quad \delta_i = \delta(A_i).$$

With this, we rescaled the antibiotic input sizes (therefore the MIC) by a factor of 2 for each subpopulation:

$$(10) \quad A_i = \left(2^i (i - 5)\right) A_{input}$$

As a result in the model, there are 9 subpopulations ranging from 1/16th, 1/8th... to 8x and 16x the MIC of the average. For simulations, the parameters for the population distribution $D(x|\mu, \sigma)$ are the fits to the statistical analysis as shown in previously in (*paper #4*) ($\mu = 0, \sigma = 1.3$).

Multi-site model

To model the within-host infection dynamics, we use a compartmental epidemiological model with susceptible (S), exposed (E), infected (I), and persisting (P) compartments (see Figure 1). Here, all compartments are modeling tissues as (possible) sites of infection. The susceptible compartment keeps track of the available susceptible tissue, with no ongoing immune response yet (for example, inflammation, granuloma formation). The exposed compartment keeps track of tissues exposed to bacteria these colonies are in their exponential phase and will eventually be either cleared or turn into infecteds. For instance these can be interpreted as macrophages infected the *M.tb*. The infected compartment keeps track of tissues with full sized lesions (for example granulomas, or open cavities), within the model these are the main drivers of infecting susceptible tissues. Finally, the persisting compartment keeps track of former infected tissues that have been reduced to 1% of their original bacterial density. This is the assumed size of heteroresistant subpopulations [3,7,45], therefore this compartment allows us to model decreased elimination rates for the heteroresistant bacteria (or keep it the same for homogeneous bacterial populations). The model is described by Eqs (11)-(14) :

$$(11) \quad S = S_{max} - E - I - P,$$

$$(12) \quad \frac{dE}{dt} = (\beta I + \beta_p P) \frac{S}{S_{max}} - \sigma E - dE,$$

$$(13) \quad \frac{dI}{dt} = \sigma E - dI,$$

$$(14) \quad \frac{dP}{dt} = dI - d_p P,$$

where:

- $S_{max} = 100$ is the maximum number of susceptible sites (arbitrary)
- S, E, I, P are the numbers of susceptible, exposed, infected and persisting sites.
- $\beta = 0.9 \left[\frac{1}{day} \right]$ and $\beta_p = 0.01 \beta$ are rates of spreading bacteria from infected and persisting sites to susceptible sites, see below for the reason behind this value
- $\sigma = \frac{1}{17.3} \left[\frac{1}{day} \right]$, growth rates of exposed sites. At $r = 0.8 \left[\frac{1}{day} \right]$ (see Table 1), it takes 17.3 days for *M.tb* to grow from 1 to 10^6 bacteria *in vitro*. This is based on the choice to represent an infected site as $10^5 - 10^6$ bacteria (for plotting, to have comparable results with the clinical trial dataset on Figure 1, Figure S 2, and Figure S 4).
- d and d_p are the elimination rates of persisting sites. See below.

The rates for spreading bacteria were chosen in a way, that without treatment, the immune system by itself cannot clear the infection, however random, spontaneous cure is achieved in some fraction of the cases. Similarly to tuberculosis where spontaneous cure for untreated cases is around 30% [29,30]. Within the model this fraction was around 40% within 2 years at $\beta = 0.9 \left[\frac{1}{day} \right]$, in the Gillespie simulations of the system. This value was high enough to prevent cure without treatment in the majority of cases, but the treatments close to the standard dose were still effective and give similar results to standard treatments. 95% of the Gillespie simulations for the 5 [mg/kg] rifampicin case finished within 6 months, which is comparable to the treatment length of tuberculosis (6 months with 10 mg/kg rifampicin with combination therapy, and up to 15% relapse rate [53,54]).

The elimination rates d and d_p are determined by solving Eq (5) and (6) for τ and τ_p where: $B(\tau) = 0.01 \cdot B(0)$ and $B(\tau_p) = 0.01^2 \cdot B(0)$. I.e., calculating the time it takes for the single infected site to reach 1% and 0.01%. $d = \frac{4.6}{\tau}$, and $d_p = \frac{4.6}{\tau_p}$. This way, the two will correspond to an exponential decay rate where it takes the same amount of days to reach 1% of their original size (see Figure 1)

Note that this is not intended to capture the dynamics of tuberculosis, predicted treatment times for other dosing groups are significantly lower than the real ones. Our goal here is to demonstrate the flexibility of this approach in modeling as it allows us to translate results more easily to clinical observations.

The simulations start at 23 exposed, 9 infected and 9 persisting sites. These correspond to the composition to the steady state number of sites in the untreated case in the model. To have comparable results to the clinical trial dataset as well as the PK PD model, infected sites are plotted with 10^5 bacteria each, and persisting sites contain 10^3 bacteria each.

Relapse

We defined relapse of a new infected site appearing after the end of the treatment. In the model, we determined this by evaluating the probability of no new infected site appearing in the Gillespie stochastic simulation algorithm after that time point. The Gillespie algorithm have been used successfully to simulate epidemiological models and has a rich history in computational biology. Normally, it consists of three repeated steps: (i) calculating the time until the next event as well as

probabilities of all the events that may happen, (ii) picking an event randomly based on the probability of each event happening, and (iii) updating the parameters and returning to step (i). This results in a random chain of events that only contains integer numbers, for example it only works with 0,1,2,3 or 4 infected sites rather than 0.1 infected sites. The mean of many Gillespie simulations give approximately the same result as modeling the system with differential equations [5].

In our model, an simpler example for this would be to start with one exposed site, that may grow into an infected site or may be cleared by the immune system/antibiotics. The probability of each event is determined by the rates of growth and elimination (see Table 2). For calculating the probability of relapse, we are only interested in specific event chains. For example, “what is the probability of all exposed sites being eliminated rather than growing?”, or “what is the probability of an infected site (during its lifetime) spreading bacteria to at least one susceptible site (i.e. creating an exposed site), which subsequently grows into a new infected site?”. Table 2 summarizes this approach.

This allows us to assign a probability of relapsing if a treatment is terminated with a given combination of exposed (e), infected (i), and persisting (p) sites. The numbers of these sites are calculated with using differential equations (Eq (11)-(14)), therefore the numbers are not necessarily integers. We are making the assumption that the calculated probabilities for non-integers can be interpolated this way.

Eq (15) describes the probability is calculated for a given number of. The short derivation and expression for P_e , P_i , P_{i2} , and P_p are described in Table 2.

$$(15) \quad P_{infect} = (1 - P_e)^e (1 - P_p)^p (1 - P_i)^i (1 - P_{i2})^i$$

Scheme	Event (red route)	Probability
	Growth of exposed site	$P_e = \frac{\sigma}{\sigma + d}$
	No growth of n exposed sites	$(1 - P_e)^n$
	At least one growth from n exposed sites	$1 - (1 - P_e)^n$
	Persisting site exposing susceptible sites once	$P_p^* = \frac{\beta_p}{d_p + \beta_p}$
	Persisting site exposing susceptible sites n times before disappearing	$(1 - P_p^*)(P_p^*)^n$
	At least one successful infection from persisting site	$P_p = \sum_n (1 - P_p^*)(P_p^*)^n (1 - (1 - P_e)^n)$
	Infected site infecting once	$P_i^* = \frac{\beta}{d + \beta}$
	Infected site infecting n times then turning into persisting site	$(1 - P_i^*)(P_i^*)^n$

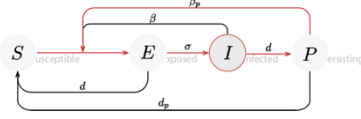
	At least one successful infection from infected sites infecting n times	$P_i = \sum_n (1 - P_i^*)(P_i^*)^n (1 - (1 - P_e)^n)$
	At least one successful infection from infected only after it turns to persisting	$P_{i2} = (1 - P_i)P_p$

Table 2 Equations describing the probability of event chains (taking the red route instead of the black) if one were to run a Gillespie simulation starting (red circle) from one exposed/persisting/infected site. The parameters for the equations are described along with the multi-site model above.

References

1. Rego EH, Audette RE, Rubin EJ. Deletion of a mycobacterial divisome factor collapses single-cell phenotypic heterogeneity. *Nature* **2017**; 546:153–157.
2. Bergmiller T, Andersson AMC, Tomasek K, et al. Biased partitioning of the multidrug efflux pump AcrAB-TolC underlies long-lived phenotypic heterogeneity. *Science* **2017**; 356:311–315.
3. Andersson DI, Nicoloff H, Hjort K. Mechanisms and clinical relevance of bacterial heteroresistance. *Nat Rev Microbiol* **2019**; Available at: <http://www.nature.com/articles/s41579-019-0218-1>. Accessed 1 July 2019.
4. Nicoloff H, Hjort K, Levin BR, Andersson DI. The high prevalence of antibiotic heteroresistance in pathogenic bacteria is mainly caused by gene amplification. *Nat Microbiol* **2019**; 4:504–514.
5. Martinecz A, Clarelli F, Abel S, Abel zur Wiesch P. Reaction Kinetic Models of Antibiotic Heteroresistance. *Int J Mol Sci* **2019**; 20:3965.
6. Abel zur Wiesch P, Abel S, Gkatzis S, et al. Classic reaction kinetics can explain complex patterns of antibiotic action. *Sci Transl Med* **2015**; 7:287ra73.
7. Dewachter L, Fauvart M, Michiels J. Bacterial Heterogeneity and Antibiotic Survival: Understanding and Combatting Persistence and Heteroresistance. *Mol Cell* **2019**; 76:255–267.
8. Martinecz A, Abel zur Wiesch P. Estimating treatment prolongation for persistent infections. *Pathog Dis* **2018**; 76.
9. Band VI, Weiss DS. Heteroresistance: A cause of unexplained antibiotic treatment failure? *PLOS Pathog* **2019**; 15:e1007726.
10. Eilertson B, Maruri F, Blackman A, Herrera M, Samuels DC, Sterling TR. High Proportion of Heteroresistance in *gyrA* and *gyrB* in Fluoroquinolone-Resistant *Mycobacterium tuberculosis* Clinical Isolates. *Antimicrob Agents Chemother* **2014**; 58:3270–3275.
11. Operario DJ, Koeppel AF, Turner SD, et al. Prevalence and extent of heteroresistance by next generation sequencing of multidrug-resistant tuberculosis. *PLOS ONE* **2017**; 12:e0176522.
12. Ley SD, de Vos M, Van Rie A, Warren RM. Deciphering Within-Host Microevolution of *Mycobacterium tuberculosis* through Whole-Genome Sequencing: the Phenotypic Impact and Way Forward. *Microbiol Mol Biol Rev* **2019**; 83. Available at: <http://mmlbr.asm.org/lookup/doi/10.1128/MMBR.00062-18>. Accessed 7 April 2019.
13. Liu Q, Via LE, Luo T, et al. Within patient microevolution of *Mycobacterium tuberculosis* correlates with heterogeneous responses to treatment. *Sci Rep* **2015**; 5. Available at: <http://www.nature.com/articles/srep17507>. Accessed 7 April 2019.

14. Lieberman TD, Wilson D, Misra R, et al. Genomic diversity in autopsy samples reveals within-host dissemination of HIV-associated *Mycobacterium tuberculosis*. *Nat Med* **2016**; 22:1470–1474.
15. Dartois V. The path of anti-tuberculosis drugs: from blood to lesions to mycobacterial cells. *Nat Rev Microbiol* **2014**; 12:159–167.
16. Barry CE, Boshoff HI, Dartois V, et al. The spectrum of latent tuberculosis: rethinking the biology and intervention strategies. *Nat Rev Microbiol* **2009**; 7:845–855.
17. Strydom N, Gupta SV, Fox WS, et al. Tuberculosis drugs' distribution and emergence of resistance in patient's lung lesions: A mechanistic model and tool for regimen and dose optimization. *PLOS Med* **2019**; 16:e1002773.
18. Stokes JM, Lopatkin AJ, Lobritz MA, Collins JJ. Bacterial Metabolism and Antibiotic Efficacy. *Cell Metab* **2019**; 30:251–259.
19. Bumann D. Heterogeneous host-pathogen encounters: Act locally, think globally. *Cell Host Microbe* **2015**; 17:13–19.
20. Russell DG. Tuberculosis Progression Does Not Necessarily Equate with a Failure of Immune Control. *Microorganisms* **2019**; 7:185.
21. Torrelles JB, Schlesinger LS. Integrating Lung Physiology, Immunology, and Tuberculosis. *Trends Microbiol* **2017**; 25:688–697.
22. Furin J, Cox H, Pai M. Tuberculosis. *The Lancet* **2019**; 393:1642–1656.
23. Lin PL, Ford CB, Coleman MT, et al. Sterilization of granulomas is common in active and latent tuberculosis despite within-host variability in bacterial killing. *Nat Med* **2014**; 20:75–79.
24. the Catalysis TB–Biomarker Consortium, Malherbe ST, Shenai S, et al. Persisting positron emission tomography lesion activity and *Mycobacterium tuberculosis* mRNA after tuberculosis cure. *Nat Med* **2016**; 22:1094–1100.
25. Levin BR, Baquero F, Ankomah PP, McCall IC. Phagocytes, Antibiotics, and Self-Limiting Bacterial Infections. *Trends Microbiol* **2017**; 25:878–892.
26. Ankomah P, Levin BR. Exploring the collaboration between antibiotics and the immune response in the treatment of acute, self-limiting infections. *Proc Natl Acad Sci U S A* **2014**; 111:8331–8338.
27. Gjini E, Brito PH. Integrating Antimicrobial Therapy with Host Immunity to Fight Drug-Resistant Infections: Classical vs. Adaptive Treatment. *PLoS Comput Biol* **2016**; 12:1–34.
28. D'Agata EMC, Dupont-Rouzeyrol M, Magal P, Olivier D, Ruan S. The impact of different antibiotic regimens on the emergence of antimicrobial-resistant bacteria. *PLoS ONE* **2008**; 3:4–12.
29. Tiemersma EW, van der Werf MJ, Borgdorff MW, Williams BG, Nagelkerke NJD. Natural History of Tuberculosis: Duration and Fatality of Untreated Pulmonary Tuberculosis in HIV Negative Patients: A Systematic Review. *PLoS ONE* **2011**; 6:e17601.
30. Caminero JA, Matteelli A, Loddenkemper R. Tuberculosis: are we making it incurable? *Eur Respir J* **2013**; 42:5–8.
31. Tuchscher L, Medina E, Hussain M, et al. *Staphylococcus aureus* phenotype switching: an effective bacterial strategy to escape host immune response and establish a chronic infection. *EMBO Mol Med* **2011**; 3:129–41.
32. Prajsnar TK, Hamilton R, Garcia-Lara J, et al. A privileged intraphagocyte niche is responsible for disseminated infection of *Staphylococcus aureus* in a zebrafish model. *Cell Microbiol* **2012**; 14:1600–19.
33. Löffler B, Tuchscher L, Niemann S, Peters G. *Staphylococcus aureus* persistence in non-professional phagocytes. *Int J Med Microbiol* **2014**; 304:170–176.

34. Boeree MJ, Diacon AH, Dawson R, et al. A dose-ranging trial to optimize the dose of rifampin in the treatment of tuberculosis. *Am J Respir Crit Care Med* **2015**; 191:1058–1065.
35. Cadena AM, Fortune SM, Flynn JL. Heterogeneity in tuberculosis. *Nat Rev Immunol* **2017**; 17:691–702.
36. Gengenbacher M, Rao SPS, Pethe K, Dick T. Nutrient-starved, non-replicating *Mycobacterium tuberculosis* requires respiration, ATP synthase and isocitrate lyase for maintenance of ATP homeostasis and viability. *Microbiology* **2010**; 156:81–87.
37. Dooley KE, Hanna D, Mave V, Eisenach K, Savic RM. Advancing the development of new tuberculosis treatment regimens: The essential role of translational and clinical pharmacology and microbiology. *PLOS Med* **2019**; 16:e1002842.
38. Davies G, Boeree M, Hermann D, Hoelscher M. Accelerating the transition of new tuberculosis drug combinations from Phase II to Phase III trials: New technologies and innovative designs. *PLOS Med* **2019**; 16:e1002851.
39. Shamputa IC, Jugheli L, Sadradze N, et al. Mixed infection and clonal representativeness of a single sputum sample in tuberculosis patients from a penitentiary hospital in Georgia. *Respir Res* **2006**; 7. Available at: <http://respiratory-research.biomedcentral.com/articles/10.1186/1465-9921-7-99>. Accessed 7 April 2019.
40. Metcalfe JZ, Streicher E, Theron G, et al. *Mycobacterium tuberculosis* Subculture Results in Loss of Potentially Clinically Relevant Heteroresistance. *Antimicrob Agents Chemother* **2017**; 61. Available at: <http://aac.asm.org/lookup/doi/10.1128/AAC.00888-17>. Accessed 7 April 2019.
41. Shockey AC, Dabney J, Pepperell CS. Effects of Host, Sample, and in vitro Culture on Genomic Diversity of Pathogenic *Mycobacteria*. *Front Genet* **2019**; 10:477.
42. Genestet C, Hodille E, Westeel E, et al. Subcultured *Mycobacterium tuberculosis* isolates on different growth media are fully representative of bacteria within clinical samples. *Tuberculosis* **2019**; 116:61–66.
43. Folkvardsen DB, Thomsen VO, Rigouts L, et al. Rifampin Heteroresistance in *Mycobacterium tuberculosis* Cultures as Detected by Phenotypic and Genotypic Drug Susceptibility Test Methods. *J Clin Microbiol* **2013**; 51:4220–4222.
44. Ding Y, Onodera Y, Lee JC, Hooper DC. NorB, an Efflux Pump in *Staphylococcus aureus* Strain MW2, Contributes to Bacterial Fitness in Abscesses. *J Bacteriol* **2008**; 190:7123–7129.
45. Balaban NQ, Helaine S, Lewis K, et al. Definitions and guidelines for research on antibiotic persistence. *Nat Rev Microbiol* **2019**; Available at: <http://www.nature.com/articles/s41579-019-0196-3>. Accessed 18 April 2019.
46. Cadosch D, Abel zur Wiesch P, Kouyos R, Bonhoeffer S. The Role of Adherence and Retreatment in De Novo Emergence of MDR-TB. *PLoS Comput Biol* **2016**; 12:1–19.
47. de Steenwinkel JEM, de Kneegt GJ, ten Kate MT, et al. Time-kill kinetics of anti-tuberculosis drugs, and emergence of resistance, in relation to metabolic activity of *Mycobacterium tuberculosis*. *J Antimicrob Chemother* **2010**; 65:2582–2589.
48. Marcel N, Nahta A, Balganesch M. Evaluation of killing kinetics of anti-tuberculosis drugs on *Mycobacterium tuberculosis* using a bacteriophage-based assay. *Chemotherapy* **2008**; 54:404–411.
49. Aljayyousi G, Jenkins VA, Sharma R, et al. Pharmacokinetic-Pharmacodynamic modelling of intracellular *Mycobacterium tuberculosis* growth and kill rates is predictive of clinical treatment duration. *Sci Rep* **2017**; 7:1–11.
50. Lee JA, Riazi S, Nemati S, et al. Microbial phenotypic heterogeneity in response to a metabolic toxin: Continuous, dynamically shifting distribution of formaldehyde tolerance in *Methylobacterium extorquens* populations. *PLOS Genet* **2019**; 15:e1008458.

51. Boeree MJ, Heinrich N, Aarnoutse R, et al. High-dose rifampicin, moxifloxacin, and SQ109 for treating tuberculosis: a multi-arm, multi-stage randomised controlled trial. *Lancet Infect Dis* **2016**; 17:39–49.
52. Grosset J. Bacteriologic basis of short-course chemotherapy for tuberculosis. *Clin Chest Med* **1980**; 1:231–241.
53. Horsburgh CR, Barry CE, Lange C. Treatment of Tuberculosis. *N Engl J Med* **2015**; 373:2149–2160.
54. Lawn SD, Zumla AI. Tuberculosis. *The Lancet* **2011**; 378:57–72.

Supplementary materials

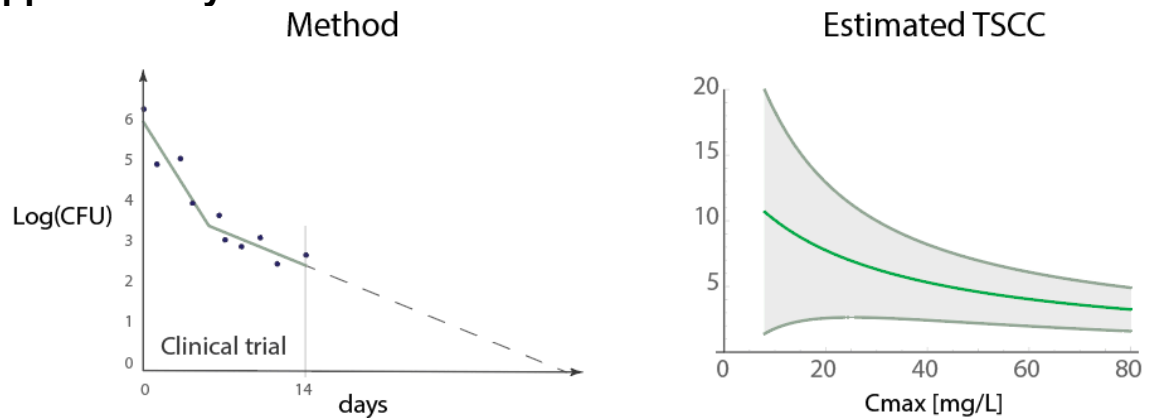


Figure S 1 The clinical trial we base the parameters on has only 14 days' worth of data. In a different manuscript we are working on we estimated (see Figure A for method) the timepoint where no bacteria should be detected in the sputum (Figure B, "time to culture conversion", "TSCC"). We compared these estimates to a different clinical trial where they have measured TSCCs (and not bacterial decline) and found that the two showed strong agreement.

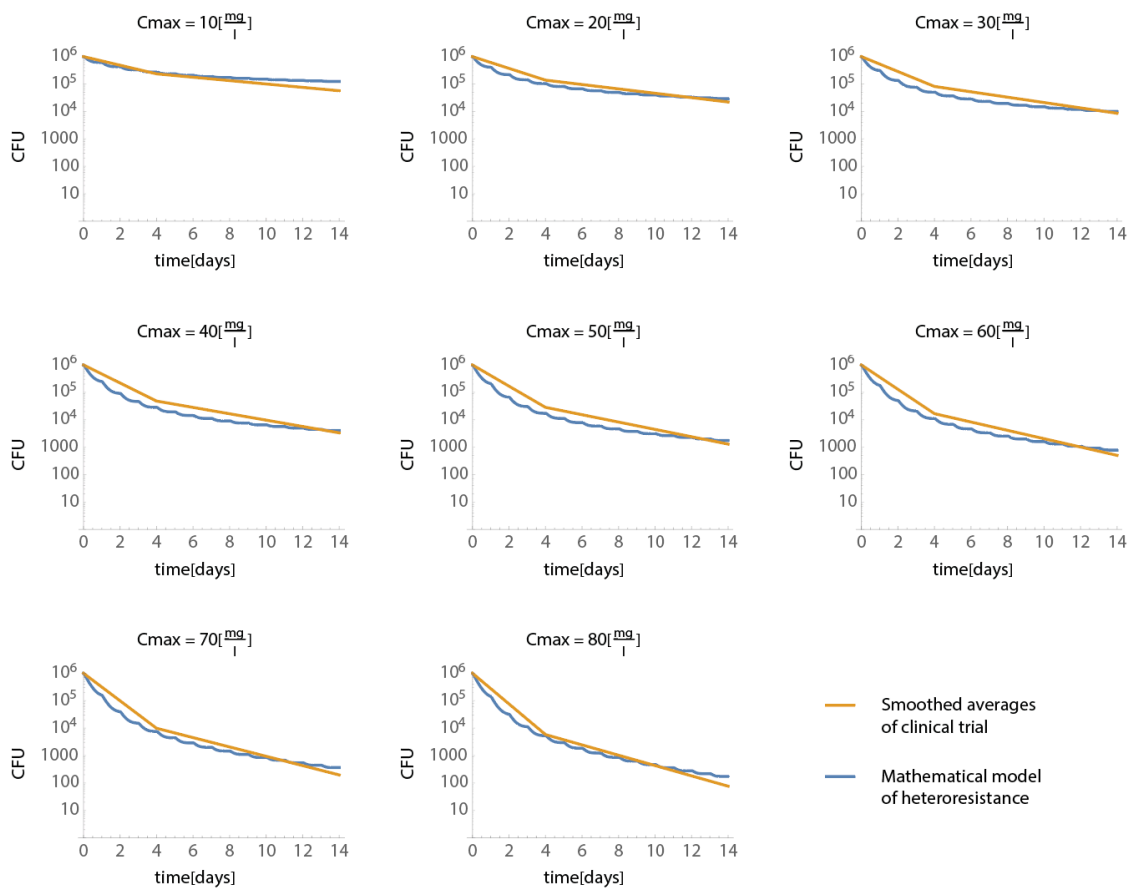


Figure S 2 comparison of smooth averages from a clinical trial (orange) and single site (PK-PD) model (blue). The single-site model curves up at the end of the 14 day period, and as a result, we cannot estimate the time until no bacteria should be detected in the sputum.

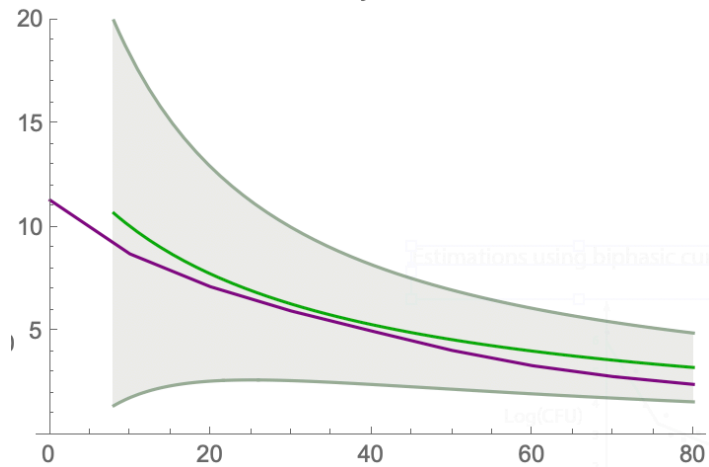


Figure S 3 This figure shows the same as Figure 4B, and the estimates based on the PK PD model if we add a constant elimination term, however it also decreases the fit to the first 14 days of treatments (see Figure below).

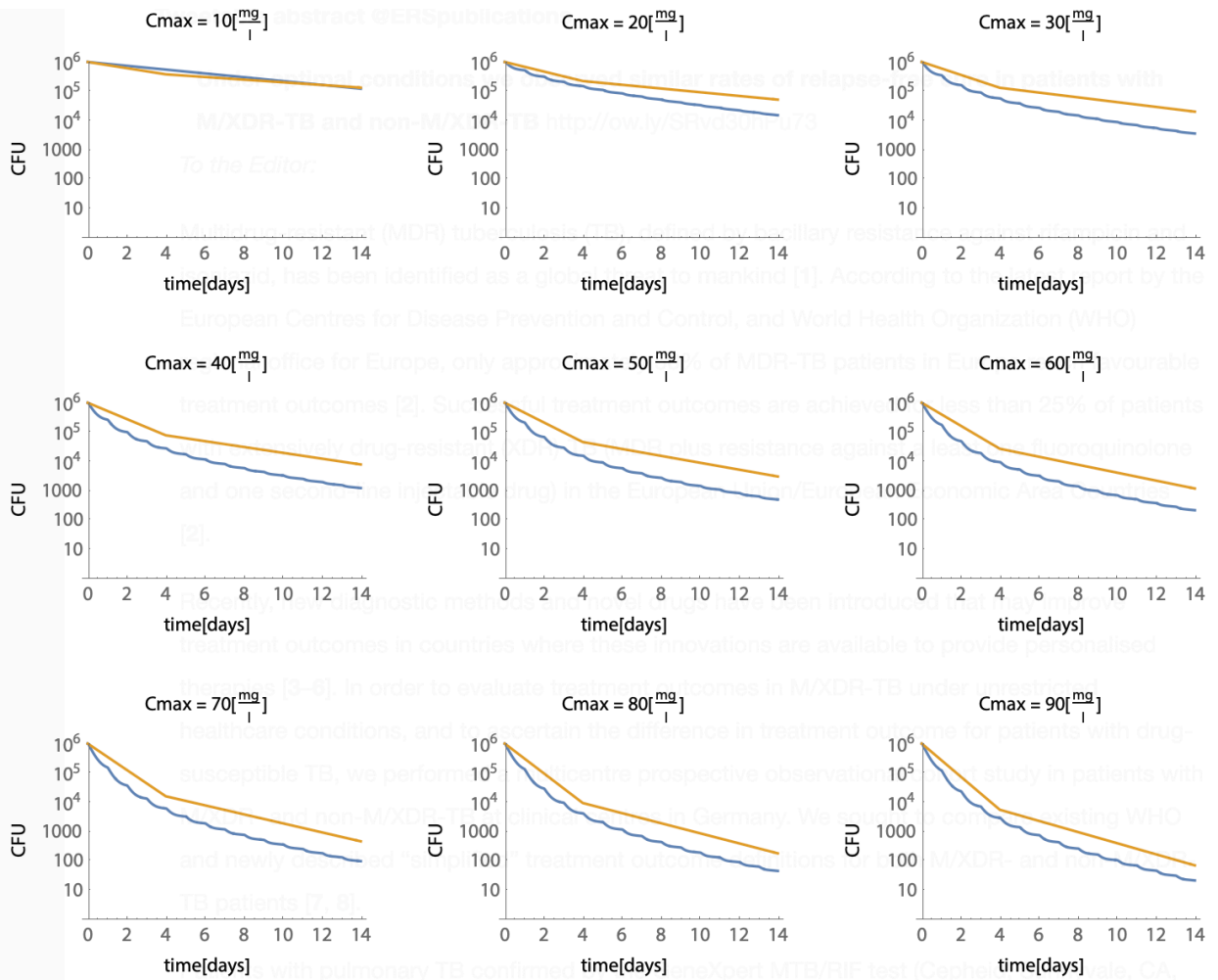


Figure S 4 Comparison of clinical trial data and PK/PD models with added "immune elimination".

